2015-04-06

Mechanisms of Synapse Formation and Synaptic Plasticity

Luk, Collin Chill-Fone

THE UNIVERSITY OF CALGARY

Mechanisms of Synapse Formation and Synaptic Plasticity

by

Collin Chill-Fone Luk

A DISSERTATION

SUBMITTED TO THE FACULTY OF GRADUATE STUDIES

IN PARTIAL FULFILMENT OF THE REQUIREMENTS FOR THE

DEGREE OF DOCTOR OF PHILOSOPHY

DEPARTMENT OF NEUROSCIENCE

CALGARY, ALBERTA

MARCH, 2015

Abstract

Synapses are the fundamental building blocks of the nervous system. Following target cell contact, they are formed through a process that requires the precise orchestration of both pre- and postsynaptic differentiation of synaptic machinery. However, the precise time course of synaptogenesis, and the role of extrinsic factors in synapse formation remains unclear.

To examine the time course of synaptogenesis, I developed a novel "growth ball" model to study synapse at the level of isolated growth cones. Specifically, I found that functional synapses can reform in isolated growth cones within minutes of contact with their synaptic partner. However, in the absence of the cell body, these synapses cannot be maintained**.**

To further investigate the importance of the cell body, I demonstrate that extrinsic trophic factors can "prime" postsynaptic neurons for synapse formation through the functional expression of excitatory acetylcholine receptors via activity dependent mechanisms. Specifically, trophic factor induced activity follows a specific pattern of progression, which I termed an activity "signature", that is necessary for proper expression of excitatory acetylcholine receptors.

Finally, I demonstrate and characterize a novel form of use-dependent short-term potentiation that is observed in the visceral dorsal 1/left pedal dorsal 1 synapse. This synaptic plasticity is induced rapidly by a short presynaptic tetanic pulse and remains potentiated until a subsequent action potential is triggered in a use- rather than time-dependent manner. I show that the molecular switch underlying this form of potentiation is calcium/calmodulin kinase II (CaMKII). Taken together, these studies demonstrate both intrinsic and extrinsic mechanisms of synapse formation and identify a novel role for CaMKII in a use-dependent form of synaptic plasticity.

Acknowledgements

"There is no wasted experiment."—Dr. Syed (2004).

When I started in the Syed lab as a young student coming out of high school, I would never have fathomed that over a decade later I would still be a part of the Syed lab. What an incredible journey it has been.

I think writing the acknowledgements is as daunting for me as the rest of the thesis because the amount of gratitude I have for all the people that have made this dissertation possible could not justifiably be expressed in a few short pages. It could easily be as long as the rest of the dissertation. In light of that, I would like to start off by saying thank-you, sincerely and genuinely, to all the people that have been a part of my academic journey.

Dr. Syed, there is an old Chinese saying that goes: "A day as a teacher, a lifetime as a father". I now understand this saying. In your lab, I have received much more than a PhD in neuroscience. I think back to when I walked into your lab as a young 17-year-old and now as I walk out at the "young" age of 29, I realize that you have trained me with a PhD in Life. You have taught me so much more than any manuscript or textbook could ever have. Your love and passion for science is contagious and never once in the past decade have I see it falter—even for one second. You continue to get me excited and allow me fall in love with science over and over again with every conversation I have with you. I would not be who I am today without your guidance and for that, thank-you.

Dr. Wali Zaidi. You are nothing short of a Master of all trades. Your work ethic, passion for life and your never ending support had me excited to get to the lab every single day—even on

the days that you made me feed snails. You are been an incredible teacher, friend and father figure to me.

Fenglian, I am so glad that I got to share the battlefield with you for so many years. Your genuine attitude towards science, the lab, family and friends is something I hope to see in myself as I go forward. You always made lunch time that much more enjoyable with your stories and laughter.

Svetlana and Jean for all the thankless work that you do in the background to make everything run smoothly, I am so grateful. I may not have said this enough when I was in the lab, but thank-you for all that you do.

Carolyn, I really do not know where I would be without you. Literally. Thank-you for always keeping me on track and getting things done before I even know that they need to be done.

To my many collaborators who have become my friends, thank-you for the wonderful ride and being as crazy as me to push the boundaries of what is possible. Geoff Mealing, Christophe Py, Marzia Martina, Dolores Martina, Tanya Comas and Robert Monette, because of you guys, I will always have fond memories of Ottawa. Bhavik Patel, you are right, the best science does occur when disciplines collide—thanks for showing me this and for allowing me to indulge in “Cowboy Science”. Lior Blockstein, thank-you for all the tireless Saturday mornings of work followed by what is almost surely a good lunch.

To my lab members, Pierre, Tara, Angie, Nichole, Joanie, Arthur and Noelle. It has been an incredible honour to have worked with all of you.

To my committee members, Dr. McFarlane and Dr. van Minnen, thank-you for spending hours on ends listening to me talk about my research, but at the end still coming up with constructive feedback to help guide me through my research.

To my examiners Dr. Dyck and Dr. Ali, I am grateful for your comments and for making my examination enjoyable.

To my family, who has supported me through all these years. To my grandparents, for making me soup and leaving food out for me whenever I got home late. To my Dad, who has always given me his unequivocal support no matter what I did. To my mom, who despite not knowing what I was working on, always told me to “finish quickly”. To my sister, who always loved to look on my computer screen while I was writing and say “that looks boring” but then would follow it up with a “well at least you love it”. There are no words that can truly express my gratitude.

To Minjai, who sat beside me on the floor and read through my dissertation using a cardboard box as w desk, thank-you for putting up with all the ups and downs and allowing me to indulge in my passion. Most importantly, thank-you for your love and support.

TABLE OF CONTENTS

LIST OF FIGURES

LIST OF ABBREVIATIONS

AChRs	Acetylcholine Receptors
AIP	Autocamtide 2-related Inhibitory Peptide
AMPA	α-Amino-3-hydroxy-5-methyl-4-isoxazolepropionic acid
AMPAR	α-Amino-3-hydroxy-5-methyl-4-isoxazolepropionic acid Receptor
AP	Action Potential
APC	Adenomatous Polyposis Coli
BDNF	Brain-Derived Neurotrophic Factor
BIS	Bisindolylmaleimide
Ca^{2+}	Calcium
CAM	Cell-Adhesion Molecule
CaMKII	Calcium/Calmodulin-Dependent Protein Kinase II
cAMP	3'-5'-Cyclic Adenosine Monophosphate
CM	Conditioned Media
CNS	Central Nervous System
DBS	Deep Brain Stimulation
DM	Defined Media
DMSO	Dimethyl Sulfoxide
E1	Electrode 1
E2	Electrode 2
E3	Electrode 3
E4	Electrode 4
EPSP	Excitatory Postsynaptic Potentials

GABA	gamma-Aminobutyric Acid
GAD65	Glutamate Decarboxylase 65
GAT-1	GABA Transporter 1
GTP	Guanosine-5'-triphosphate
IPSP	Inhibitory Postsynaptic Potential
ISI	Interspike Interval
L-EGF	*Lymnaea* Epidermal Growth Factor
L-MEN1	*Lymnaea* Multiple Endocrine Neoplasia I
LPeD1	Left Pedal Dorsal 1
LPeE	Left Pedal E
Lrp4	Low-density Lipoprotein Receptor-Related Protein 4
LTP	Long-Term Potentiation
MAPK	Mitogen-Activate Protein Kinases
MEA	Microelectrode Array
MuSK	Muscle Specific Kinase
NGF	Nerve Growth Factor
NMDA	N-methyl-D-aspartate
NMDAR	N-methyl-D-aspartate Receptor
NMJ	Neuromuscular Junction
NRCC	National Research Council of Canada
NT-3	Neurotrophin-3
NT-4	Neurotrophin-4
PDMS	Polydimethylsiloxane

pEPSP	Post-tetanic Excitatory Postsynaptic Potentials
PI	Polyimide
PKC	Protein Kinase C
PMA	Phorbol-12-Myristate 13-Acetate
PSP	Postsynaptic Potential
PTP	Post-Tetanic Potentiation
PVAc-B-8	Polyvinyl Acetate Benzophenone-8
RPeD1	Right Pedal Doral 1
RTK	Receptor Tyrosine Kinase
SiN	Silicon Nitride
siRNA	Short Interfering Ribonucleic Acid
STP	Short-term Potentiation
SynCAM	Synaptic Cell-Adhesion Molecule
Ti	Titanium
TiN	Titanium Nitride
TTX	Tetrodotoxin
VD4	Visceral Dorsal 4
VGCC	Voltage Gated Calcium Channel
VH/K	Visceral H/K
VI/G	Visceral I/G
VJ	Visceral J

Chapter 1: Introduction

1.1 General Introduction

The human brain is estimated to be composed of more than 86 billion neurons. Like the bricks of a skyscraper, these 86 billion neurons form the fundamental building blocks of the central nervous system, a neuroscience principal known as the neuron doctrine. However, to assume that the incredible cognitive capacity of a human brain to control behaviors from simple reflexes to complex motor patterns, cognition, and learning and memory is solely due to the number of neurons in a brain would be difficult to rationalize. For instance, a generic rodent brain is estimated to have 12 billion neurons, whereas a generic primate brain is estimated to contain approximately 93 billion neurons (Herculano-Houzel 2009). By this assumption, a generic primate should have the same if not greater functional and cognitive capacity than a human, which is clearly not the case. Instead, the complexity and high level of function seen in different species is not only attributed to the number of neurons, but also to the precise connections that are formed by these billions of neurons at a structure known as a synapse.

A synapse is a specialized communication structure found between two neurons. At a chemical synapse, an electrical signal generated by a neuron (presynaptic) is transduced into a chemical signal (neurotransmitter). This chemical signal travels across the synaptic cleft, where it elicits a response in the receiving neuron (postsynaptic neuron) when the chemical signal binds to specific receptors. In particular, a synapse is composed of a presynaptic specialization domain called the ‘active zone’, an electron-dense meshwork of proteins, which harbor neurotransmitters that are packaged in discrete synaptic vesicles. When an electrical signal triggers the presynaptic domain, the interplay of a complex of molecules initiates the fusion of vesicles to the active zone membrane, releasing their contents into the synaptic cleft, which diffuses towards the

postsynaptic membrane. On the postsynaptic side, directly opposite the presynaptic 'active zone', is a specialized domain also consisting of an electron-dense meshwork of proteins. These proteins are known to have domains that extend into the postsynaptic cytoplasm as well as externally towards the presynaptic active zone. This region is known as the postsynaptic density, where neurotransmitter receptors, voltage-gated ion channels, and signaling molecules are anchored (Waites et al. 2005). Together these components form the basic synapse.

In reality, it is the sum of these estimated 10^{14} synapses that enables the incredible capacity of the human brain (Drachman 2005). Therefore, to understand how the brain controls various functions and also to design strategies to repair damage to the nervous system, it is imperative to define the cellular and molecular mechanisms that determine this precise synaptic connectivity between neurons. This chapter will provide a literary review on the role of growth cones, cell-cell interaction, extrinsic trophic factors and activity on synapse formation. Further, a brief literary overview will be on provided on synaptic plasticity and our current views on short and long-term synaptic plasticity. A review of additional areas of nervous system development, including cell differentiation, proliferation, migration, and axonal pathfinding is beyond the scope of this thesis chapter, but excellent review articles can be found at: (Raper and Mason 2010; Myers et al. 2011; Greig et al. 2013; Florio and Huttner 2014; Guo and Anton 2014; Kumamoto and Hanashima 2014; Paridaen and Huttner 2014; Robichaux and Cowan 2014).

1.2 Growth Cones

Growth cones are found at the leading edge of proliferating neurites, providing both sensory and motility function. They were first described by Santiago Ramon y Cajal as being a "club or battering ram" with "exquisite chemical sensitivity" that could move with "impulsive

force" and "overcome obstacles…until it arrives at its destination" (Ramón y Cajal 1909). The "cone" description of these growth organelles derives from the account of their three dimensional conical structure as they grow through the three-dimensional extracellular milieu during development. However, when grown in cell culture on a two-dimensional surface, the growth cone is flattened into an almost fan shaped pattern with three distinct regions termed the peripheral zone (contains branched and long parallel bundles of actin filament), central region (contains mitochondria and exocytotic vesicles), and an intermediate zone, or the transitional zone (Rodriguez et al. 2003), which is thought to contain the myosin contractile structures that regulate actin and microtubule trafficking between the two regions **(Fig. 1.1)** (Medeiros et al. 2006; Burnette et al. 2008). While there is still some debate as to how growth cones mediate guidance of proliferating neurites, it is generally believed that selective actin polymerization/depolymerization forms the basis of this guidance. Specifically, receptor activation of the actin molecular "clutch" allows for directional actin polymerization, which in turn guides these proliferating neurites (Suter and Forscher 1998; Lowery and Van Vactor 2009).

A growth cone moves through its extracellular milieu by interaction with cell adhesion molecules found on the surface of other cells and via the attractive and repulsive effects of diffusible molecules found in the extracellular milieu. These chemical signals act as "traffic signs" which are interpreted by the growth cone as either "stop" or "go" signals. Hence, with the abundance of these molecular cues spaced closely together, the daunting task of a single axon proliferating across large distances can be divided into multiple simple steps. The chemoattractant and repulsive cues during axonal path finding have been a topic of rather comprehensive study in the past several decades. For instance, factors identified in previous axon guidance studies (Dickson 2002; Chilton 2006) including morphogens (Zou and Lyuksyutova

2007), secreted transcription factors (Brunet et al. 2005; Butler and Tear 2007), neurotrophic factors (Gundersen and Barrett 1979; Sanford et al. 2008), cell adhesion molecules (Schwabe et al. 2013) and neurotransmitters (Mattson et al. 1988; Spencer et al. 2000) have all been shown to be key guidance molecules in guiding growth cones to allow for axonal proliferation and target finding.

However, despite the detailed research into the guidance of growth cone during development, the potential for growth cones to form synapses is not well understood. Prior to target cell contact, it has been demonstrated that growth cones possess the capacity to spontaneously release neurotransmitters in both vertebrate (Gao and van den Pol 2000) and invertebrate (Spencer et al. 1998; Yao et al. 2000) models. Further, growth cones appear to have functional transmitter receptors that can detect and respond to exogenous neurotransmitter stimuli prior to synapse formation **(Fig 1.1)** (Haydon et al. 1985; Lankford et al. 1988; McCobb and Kater 1988; Zheng et al. 1994; Spencer et al. 2000). As these studies demonstrate the early expression of synaptic machinery even prior to target cell contact, it has been typically accepted that pre-assembled components of synaptic machinery exist in a neuron to allow for an expedited synaptogenic program upon initial contact of pre- and postsynaptic partners. This concept has been termed the “ready-set-go” model of synapse formation (Haydon and Drapeau 1995). However, notwithstanding the demonstration that these pre-assembled synaptic components exist prior to synapse formation, the precise capacity of the growth cone to initiate synapse formation and the temporal pattern required to form functional synapses following initial contact has not been evaluated. Further, the capacity for a growth cone to maintain a synapse—in the absence of cell body transcription or *de novo* protein synthesis machinery—is not known. This particular lack of information is due, in part, to difficulties in electrophysiologically evaluating synapses

formed at growth cones and their contact sites, when the cell bodies are themselves located at quite some distance away.

Thus far, elegant imaging studies have demonstrated that pre-synthesized “packets” of presynaptic machinery can be visualized prior to synaptic contact. For instance, these “packets” contained GFP tagged synaptobrevin, a component of the presynaptic release machinery and were seen to be circulating in the neuritic processes prior to synapse formation. Upon contact of potential targets, these packets were then shown to rapidly traffic towards new contact sites (Ahmari et al. 2000). Similar rapid recruitment of PSD-95 (Okabe et al. 1999) and NMDAR/AMPAR (Washbourne et al. 2002) have also been observed within minutes to hours following target cell contact. The presence of these pre-assembled packets of machinery found both pre- and postsynaptically align precisely with the theory that synaptic machinery is “ready, set and go” (Haydon and Drapeau 1995). However, similar evidence for the temporal pattern of functional synapse formation has not yet been achieved, nor has the capacity for growth cones and various cellular compartments to form synapses been evaluated. This question will be addressed in chapter 3 of my thesis.

1.3 Synapse formation at the neuromuscular junction

The neuromuscular junction (NMJ) is a synapse that is formed between a motor neuron and a muscle fibre. Synapses at the NMJ are easily accessible due to their large size, which makes them amenable to experimental manipulation. Specifically, they can be isolated and defined at the level of a single presynaptic motor neuron and its postsynaptic muscle fibre target (Kandel et al. 2000; Witzemann 2006; Wu et al. 2010). Further, such a model has been relatively easy to culture in laboratory environments and with the advent of transgenic manipulation

technology, we have been able to dissect the molecular players involved in synapse formation. Hence, a large proportion of our knowledge base in synapse formation has been derived from studies conducted at the NMJ.

The functional neurotransmitter seen at the NMJ in vertebrates is acetylcholine (ACh). During activation of a motoneuron, ACh is released from the axonal terminal and binds to a high concentration of acetylcholine receptors (AChRs) in a region known as the postsynaptic density found on individual muscle fibres. This binding action results in the activation of ligand-gated sodium channels, resulting in muscle depolarization and a subsequent action potential. This depolarization in turn activates VGCCs and the ryanodine receptors of the sarcoplasmic reticulum, resulting in an intracellular calcium rise and muscle fibre contraction. While conceptually similar to synapses found in the central nervous system, where synapses are formed between two neurons, there are fundamental differences in both the molecular composition and the mechanisms behind the NMJ synapse formation.

For instance, prior to synapse formation, pre-patterned clusters of AChRs exist in a clustered pattern within the central region of muscle fibres (Lin et al. 2001; Yang et al. 2001; Flanagan-Steet et al. 2005; Panzer et al. 2006). These clusters exist independent of nerve fibre innervation, as diaphragmatic muscle in mutant mice that lack motor fibre innervation continued to express pre-patterned AChR clusters in the central part of muscle fibres (Yang et al. 2001). Therefore, it has generally been thought that these pre-patterned regions on muscle fibres are a potential preset area for synapse formation. As such, these regions restrict the proliferation of motor neuron fibres and restrict specific synapse formation to the central region of a muscle fibre (Kim and Burden 2008). However, in contradiction to this, *in vitro* cultures of rodent embryonic diaphragmatic muscle reveal that synapses also form in muscle regions regardless of prior pre-

patterned AChRs (Lin et al. 2008). Therefore, the precise role that these pre-patterned clusters play in determining synapse formation has yet to be elucidated. Conversely, similar pre-patterned clusters have not been demonstrated in central neurons. Whether this is evidence for the absence of a similar phenomenon or simply a lack of sufficient investigation into this area has yet to be determined.

During synapse formation, as the presynaptic motor neuron axon process approaches the muscle fibre, agrin—an approximately 200 kDa protein with EGF-like signaling domains—is released from the terminal and deposited on the synaptic basal lamina. This agrin, in turn, induces the clustering of AChRs on muscle fibre via activation of a receptor tyrosine kinase known as muscle specific kinase (MuSK). In mice that are lacking agrin, synapses may initially form between the motoneuron fibre and the pre-patterned clusters of AChRs. However, the clusters dissipate several days following initial contact and the synapse is lost (Lin et al. 2005; Misgeld et al. 2005). Further, studies revealed that the knockdown or knockout of MuSK in mice result in a synaptic developmental pattern similar to that seen in agrin deficient mice. In the absence of MuSK, mice lack postsynaptic differentiation, whereby the AChRs and other synaptic molecules such as acetylcholinesterase are found to be uniformly distributed on muscle fibres rather than in differentiated clusters (Witzemann 2006; Wu et al. 2010).

Significant work has gone into understanding this interaction of agrin and MuSK. Early on, it was revealed that no direct interaction occurs between these two molecules. Rather, binding occurs via a co-receptor which forms a receptor complex with MuSK (Glass et al. 1996). More recently, this co-receptor was identified as the low-density lipoprotein receptor-related protein 4 (Lrp4), an agrin co-receptor (Kim and Burden 2008; Zhang et al. 2008). The Lrp4

protein has a high affinity for direct interaction with agrin, and its extracellular domain has been shown to interact with the extracellular domain of MuSK (Zong and Jin 2013).

Downstream of Lrp4-MuSK activation, several proteins have been identified. Particularly, Dok-7, Crk and Crk-L adaptor proteins are activated and can reciprocally activate MuSK in the signal transduction pathway via a mechanism, which is not yet fully understood (Burden et al. 2013). The mechanism was thought to at least involve an increase in the recycling of AChRs to the muscle fibre surface, which would normally have been destined for degradation (Brenner and Akaaboune 2014). Regardless, the end result of this molecular interaction is the recruitment and stabilization of AChR clusters. Additional proteins such as Rac/Rho and GTP-binding proteins, which regulate actin organization, are also activated downstream of agrin activity, and are important in the early and late formation of pre-patterned clusters, respectively (Weston et al. 2000; Weston et al. 2003).

Further, genetic studies have demonstrated that ACh, which is also released by the presynaptic terminal, is the key modulator for dispersing these pre-clustered AChRs. Agrin counters this effect of ACh by stabilizing AChRs and any new synapses that are formed (Kummer et al. 2006).

In summary, agrin binding Lrp4/MuSK signaling complex in muscle fibres is thought to trigger cytoskeletal reorganization for AChR redistribution and anchoring and stabilize AChR to the muscle fibre surface. However, despite similarities between the NMJ and CNS synapses, evidence suggests that there are clear differences between the mechanism of synaptogenesis.

1.4 Neuromuscular Junction Versus Central Synapse Formation

In comparison to the relatively well understood synapse formation at the NMJ, the precise mechanisms involved in central synapse formation are less well elucidated. This lack of fundamental knowledge is in part due to the numerous neuronal types and heterogeneous neurotransmitters released at central synapses compared to the solitary neurotransmitter and homogenous pre- and postsynaptic cells found at the NMJ. As discussed above, NMJ development relies on the presence of agrin, in addition to other molecules such as calcitonin gene-related peptides, neuregulin and Wnt ligands. All these molecules are released from the presynaptic terminal and are important players in the maturation of NMJ synapses (Lu et al. 1999; Lin et al. 2001; Kummer et al. 2006; Shi et al. 2012). Similar studies in the CNS, however, suggest a central versus peripheral dichotomy in synapse formation. Specifically, the importance of agrin in NMJ synapse formation has not been as clearly demonstrated in central synapses (Cohen-Cory 2002). For example, in earlier studies, when agrin-null hippocampal and cortical neurons from mice embryos were cultured *in vitro*, they appeared to develop normally (Li et al. 1999; Serpinskaya et al. 1999; Kroger and Schroder 2002). However, in more recent studies using cell culture preparation and agrin antisense oligonucleotides (Bose et al. 2000) or lentivirus expression of agrin siRNA (McCroskery et al. 2009), a reduced number of synapses was observed with inhibition of agrin expression. Yet, in the study by McCroskery et al. (2009), it was oddly a reduction in postsynaptic rather than presynaptic agrin release that had the greatest effect on number of synapses formed. Hence, there are clear differences between the role of agrin in NMJ and central synapses.

Further, while the precise role of transmitter-receptor interaction and cell-cell signaling have been unequivocal at the NMJ, a similar understanding for the importance of these mechanism in central synapses is less clear (Cohen-Cory 2002; Kummer et al. 2006). For

instance, AChR clustering at the NMJ, which is the first sign of synaptic development, proceeds normally even when neuronal activity is blocked pharmacologically by tetrodotoxin (TTX) (Cohen-Cory 2002; Wu et al. 2010). Additionally, blocking transmitter-receptor interaction with cholinergic antagonists, curare or α-bungarotoxin, does not perturb normal patterns of synaptic connectivity at the NMJ (Harris 1981; Yang et al. 2001; Cohen-Cory 2002). In contrast, similar conclusions cannot be drawn from studies in the brain where there have been controversial studies on the role of activity in CNS development. For instance, while some studies have shown that blocking electrical activity (Hubel and Wiesel 1963; Takada et al. 2005; Uesaka et al. 2005) or transmitter-receptor interactions in the brain (Rajan and Cline 1998; Rajan et al. 1999; Luthi et al. 2001) result in dramatic developmental abnormalities, opposing studies have also shown that synapses still form normally when neurotransmitter release is perturbed using pharmacological or genetic techniques to block neurotransmitter-receptor interaction in the brain (Verhage et al. 2000; Craig et al. 2006). For example, the deletion of the munc18-1 gene in mice, a neuron-specific protein implicated in the release of neurotransmitter from the presynaptic terminal, causes complete inhibition of transmitter release. Despite this, histological data demonstrates that normal brain assembly and proper morphologically defined synapses still formed (Verhage et al. 2000). The idea that perhaps transmitter release and the activation of its receptor is not necessary for synaptogenesis is further supported by studies that showed postsynaptic clustering of $GABA_A$ and NMDA/AMPA-type glutamate receptors, even with constant antagonist blocking of the receptor (Craig et al. 1994; Verderio et al. 1994; Mammen et al. 1997; Cottrell et al. 2000; Craig and Boudin 2001). However, in these studies, the evidence for synapses or the lack thereof was sought primarily through morphological evidence. Revelation of true function in these morphologically defined synapses is important as pre-assembled packets of synaptic machinery,

reminiscent of synapses, have been shown to occur independent of their contact with synaptic partners (Haydon and Drapeau 1995; Munno and Syed 2003; Sabo et al. 2006). Taken together, despite significant advances in our understanding of synapse formation at the NMJ, the fundamental mechanisms that govern synapse formation at the NMJ appear to be mechanistically different from those that regulate synapse formation in the brain. Therefore, it is imperative that although we use studies conducted at the NMJ to guide our investigation of central synapses, we should remain cautious as to their potential differences.

1.5 Central Synapse Formation: Cell-cell interaction

Unlike the homogenous pre- and postsynaptic synaptic partners found at the NMJ, the heterogenous population of cells found in central neurons adds an additional level of complexity to target cell recognition and synapse formation. In central synapses, the direct contacts between various types of cell-surface molecules of the pre- and postsynaptic neuron are important in target recognition, initiation of the synaptogenic program and stabilization of the synapse.

Cadherins are one of these families of homophilic cell-adhesion molecules (CAM) that are found on both pre- and postsynaptic neuronal membranes. Over 20 subtypes of classical cadherins have been identified and specific isoforms of cadherins have been found to be expressed in various parts of the brain. Hence, it has commonly been postulated that through homophilic interaction, the “matching” of cadherins in various cell types may allow for cell target specificity during synapse formation (Yagi and Takeichi 2000). In particular, one study showed that both CA3 and hippocampus dentate gyrus neurons express cadherin-9. When cadherin-9 was down-regulated in CA3 neuron, both the synaptic number and size of synapses

was perturbed between cultured hippocampal dentate gyrus neurons and target CA3 neurons. (Williams et al. 2011).

Another well studied CAM is integrins, a class of heterodimeric glycoproteins consisting of α and ß subunits that are part of the cell-surface molecules found on central neurons. Currently, eighteen α and eight ß isoforms have been characterized (Hynes 2002). Studies using mRNA mapping of the various brain regions of the adult rat brain demonstrate that there is a very different balance of integrin subunits expressed in the various brain fields (Pinkstaff et al. 1999). This was thought to allow for various brain regions to maintain a molecular identity that could potentially be used in target recognition during synapse formation. Similar to studies on cadherins, conditional knockout mice with selective loss of integrin α3 in excitatory forebrain cells resulted in normal synapses at P21, but showed a dramatic decrease in dendritic arbor stability and maintenance of synapses by P42 (Kerrisk et al. 2013). A similar perturbation of synaptic maturation, but not synaptic formation was demonstrated in cultured hippocampal neurons with antibody knockdown of ß3 integrin subunits (Chavis and Westbrook 2001).

Another group of CAMs that have been implicated in synapse formation are the neuroligin and ß-neurexin cell-surface molecules. Specifically, neuroligins are found on the postsynaptic membrane and bind to their counterpart, ß-neurexins, found on the presynaptic membrane surface (Bury and Sabo 2014). This interaction of neuroligin-1 and -2 have been shown to trigger the *de novo* formation of presynaptic structures. When non-neuronal cells expressing neuroligin were cultured with pontine axons, synaptic vesicles were seen to cluster at the axon terminals at the points of contact with these non-neuronal cells. Further, the presence of soluble ß-neurexin in culture solution prevents neuroligin activity, as demonstrated by the inhibition of vesicle clustering in axons (Scheiffele et al. 2000). This is thought to be due to the

saturation of neuroligin with freely unbound ß-neurexin, preventing them from interacting with presynaptic ß-neurexin.

Synaptic cell-adhesion molecules, or SynCAMs, are immunoglobulin-domain-containing proteins found exclusively in the brain at synaptic sites. Similar to neuroligin-ß-neurexin interactions, SynCAM expression in non-neuronal cells have been shown to induce presynaptic differentiation in cultured hippocampal neurons (Biederer et al. 2002).

While it is generally believed that various combinations of these identified CAMs contributes to the target cell recognition and the exquisite accuracy with which the brain can form proper synapses, the number of identified molecules to date cannot account for the sheer number of synapses, suggesting the presence of addition mechanisms. These mechanisms include extrinsic mechanisms such as trophic factors.

1.6 Central Synapse Formation: Neurotrophins

Neurotrophins or extrinsic trophic factors have been shown to be a critical component of proper neural development and function. In mammals, four neurotrophins, brain-derived neurotrophic factor (BDNF), neurotrophin-3 (NT-3), neurotrophin-4 (NT-4/5) and nerve growth factor (NGF) have been identified. These trophic molecules elicit their activity by binding to either the p75 neurotrophin receptor or the Trk family of receptor tyrosine kinases (TrkA, TrkB or TrkC) (Lu et al. 2005; Park and Poo 2013). While studies have shown neurotrophins to influence neuronal survival, differentiation, dendritic arborization and synaptic plasticity, less is known about how they influence synaptogenesis. Further, the precise cellular and molecular mechanisms by which trophic molecules regulate synapse formation remains unknown.

Studies depriving expression of neurotrophin receptors have demonstrated their importance in proper synapse formation. For instance, knock down of neurotrophin receptors trkB and trkC reduces axonal arborization and synaptic density in mouse hippocampal afferents (Martinez et al. 1998). Further, mice harboring a conditional trkB receptor mutation driven by a Cre/LoxP recombination system revealed that TrkB receptor signaling is required for the establishment of GABAergic synapses in the cerebellum. In particular, the knockout of TrkB expression resulted in the reduction of GAD65 and GAT-1, an enzyme and transporter involved in GABA expression, and resulted in an overall reduction in inhibitory GABAergic synapse formation (Rico et al. 2002).

Alternatively, manipulating the levels of neurotrophin expression has also shown similar effects on synapse formation. For instance, when neurotrophin levels were reduced in mice through genetic ablation of neurotrophin-3 expression, there was a loss of axonal bundles projecting from the thalamus to the cortex (Ma et al. 2002). In line with this study, when neurotrophin-3 was added to E16 rat hippocampal cultures, a sevenfold increase in the number of excitatory synaptic connections was observed (Vicario-Abejon et al. 1998). Similar changes were also seen in other neurotrophins. For example, increasing levels of BDNF enriched GluR2 and GluR3 expression in AMPA receptors of postsynaptic mice spiral ganglion neurons, while increasing levels of NT-3 increased the presence of two presynaptically localized proteins, synaptophysin and the t-SNARE, SNAP-25 (Flores-Otero et al. 2007). BDNF also increased synaptic contacts in the CA1 stratum radiatum in mice as determined through electron microscopy (Marler et al. 2008) and increased the number of excitatory inputs seen in cultured rat hippocampal neurons (Jacobi et al. 2009). Similarly, this was extended to NGF, which was shown to be both necessary and sufficient for the induction of postsynaptic density (PSD)

clustering on synapses between ganglionic sympathetic neurons of rat and mouse (Sharma et al. 2010). A recent study has also shown that NT-3 released by local epithelial cells regulated hair cell ribbon synaptic density in mice cochlea. NT-3 was also important in the regeneration of these ribbon synapses following acoustic damage (Wan et al. 2014). Conversely, the role of neurotrophins was shown to also be equally important in inhibitory synapses, where the rate of inhibitory glycinergic and GABAergic synapse formation was increased through the addition of BDNF to cultures (Carrasco et al. 2007).

Notwithstanding the research demonstrating the importance of trophic factors in synaptogenesis, it is still not entirely clear as to the precise site of trophic factor activity. Studies thus far have suggested that trophic factors can affect either the presynaptic, postsynaptic or both sites during synapse formation. In some instances, the site of neurotrophic factor activity has been shown to be predominately presynaptic. Studies have demonstrated that BDNF can enhance glutamatergic synaptic release in rat hippocampal cultures (Lessmann et al. 1994; Lessmann and Heumann 1998), adult rat hippocampal slices (Kang and Schuman 1995; Scharfman 1997) and rat visual cortex synapses (Akaneya et al. 1997; Carmignoto et al. 1997). This enhancement of glutamatergic synaptic transmission is also implicated in other neurotrophic factors such as NT-4/5 and NT-3 (Lessmann 1998). Conversely, neurotrophins can also act on the postsynaptic neuron, where they modulate synaptic efficacy (Lessmann 1998). In one study, it was reported that BDNF determines DA-D3 receptor expression and maintenance in the developing brain, a receptor whose density is lowered in Parkinson's disease (Guillin et al. 2003). BDNF has also been implicated in the modulation of NMDA receptors where BDNF application enhances NMDA receptor glutamate currents (Kim et al. 2006; Crozier et al. 2008). However, despite these studies on trophic factor and synapse formation in glutamatergic, GABAergic and

dopaminergic synapses, fewer studies have shown similar links between trophic factor and cholinergic synapse formation at the CNS level.

Studies from our lab have further shown that trophic factors derived from brain conditioned medium are important for excitatory cholinergic synapse formation (Munno et al. 2000). Specifically, excitatory but not inhibitory cholinergic synapse formation requires extrinsic trophic factors derived from *Lymnaea* brain conditioned medium (CM-made by incubating isolated *Lymnaea* brains in defined medium) (Hamakawa et al. 1999; Woodin et al. 1999; Woodin et al. 2002; Meems et al. 2003). When cholinergic synaptic pair Visceral Dorsal 4 (VD4) and Left Pedal Dorsal 1 (LPeD1-cellular partners that forms an excitatory cholinergic synapse *in vivo*) were isolated and placed together in cell culture, an improper inhibitory synapse (not seen *in vivo*) developed. It was subsequently discovered that only when they were cultured in the presence of CM did they reform their proper excitatory synapse, which was electrophysiologically similar to those seen *in vivo* (Woodin et al. 1999; Woodin et al. 2002). On the other hand, trophic factors were not important in the reformation of inhibitory synapses between VD4 and Right Pedal Dorsal 1 (RPeD1) (Feng et al. 1997) or Left Pedal A/E cluster neurons (Data not published).

Although the precise trophic molecule(s) contained in CM responsible for proper excitatory synapse formation are not fully identified, the CM-induced effects were partially mimicked by *Lymnaea* epidermal growth factor (L-EGF) isolated from the animal's albumin gland. Similar to the excitatory synapse promoting effects of CM, the effects of L-EGF were also mediated through RTKs (Hamakawa et al. 1999; Woodin et al. 2002; van Kesteren et al. 2008). Further, while L-EGF addition rescued excitatory synapse formation in VD4/LPeD1 synaptic pairs cultured in trophic factor lacking defined media (DM), knockdown of the cloned L-EGF

receptor abolished the effects of L-EGF (van Kesteren et al. 2008). Taken together, these studies show a novel role of trophic factors in the specific formation of cholinergic excitatory but not inhibitory synapses.

More recently, our lab has demonstrated that trophic factors triggered activity-dependent Ca^{2+} oscillations specifically in the postsynaptic (LPeD1) but not presynaptic (VD4) neuron. These Ca^{2+} oscillations, triggered through RTK signaling, were required for the functional expression of excitatory AChRs and required a protein synthesis-dependent cascade of events in the expression of these receptors (Xu et al. 2009). This signaling cascade may lead to the activation of the tumor suppressor gene L-MEN1 that encodes for menin, a transcription factor that has been linked to synapse formation between central neurons (van Kesteren et al. 2001) and the specific expression of postsynaptic excitatory nAChRs (Flynn et al. 2014). However, the specific mechanisms that link trophic factor activation to the final expression of nAChRs have not yet been defined, nor has the precise role of activity in synapse formation at a cellular level been well characterized. These cellular mechanisms will be discussed in C*hapter 4*.

1.7 Activity and synapse formation

In the more classical role of activity on neurodevelopment, significant research has been conducted. This role relates more directly to activity being a modifying factor for previously established synapses in determining which synapses are maintained and which ones are eliminated. Since the seminal work conducted by Hubel and Wiesel that showed deprivation of visual input in a cat prevented the proper formation of ocular dominance columns in the visual cortex, several pioneering research studies have unequivocally demonstrated that neuronal activity is an important component of synapse formation (Wiesel and Hubel 1963). For instance,

the silencing of neuronal activity through ion channel manipulation has also been attempted to determine the role of activity in synapse formation. Particularly, the expression of an inward rectifying potassium channel Kir2.1 that caused the hyperpolarization of neurons and subsequent silencing of network activity demonstrated a reduced incidence of synapse formation onto neurons that were silenced (Burrone et al. 2002). However, to distinguish between whether the reduction in synapse number was due to an absolute reduction in synapse formation or an increase in elimination due to activity manipulation has been difficult to fully distinguish. One particular study was able to distinguish the reverse rationale whereby increasing cellular activity resulted in a corresponding increase in synapse formation (Soto et al. 2012). Specifically, in Crx-/- mutant mice where spontaneous activity in retinal ganglion cells was increased, it was shown with live imaging that indeed there was an increase in the numbers of bipolar-to-RGC synapses with no change in the rates of elimination.

In this classical model of neurodevelopment, the formation of synaptic connectivity during embryonic development was thought to be independent of electrical activity. However, more recent research demonstrates that activity may also play a role in synaptic formation—prior to any formed synaptic connectivity. These roles include (1) the development of a proper complement of ion channels required for neuron functionality, (2) the specification of the proper neurotransmitter phenotype and (3) the proper development of neurotransmitter receptors.

For instance, blocking Ca^{2+}-dependent action potentials results in the developmental suppression of the rapidly activated potassium currents in ascidian muscle (Dallman et al. 1998). Further, Ca^{2+} transients generated by voltage-gated channels early in development have been implicated in the formation of subsequent Na^{+}-dependent spikes and K^{+} currents (Desarmenien and Spitzer 1991; Gu and Spitzer 1995). Additionally, activity has been implicated in

neurotransmitter specification. For example, changes in activity frequency have been shown to regulate the number of neurons expressing excitatory and inhibitory neurotransmitters (Borodinsky et al. 2004). In *Xenopus* spinal neurons, suppressing activity causes an increase in the number of neurons expressing excitatory neurotransmitters, while a subsequent increase in spiking activity increases the number of neurons expressing inhibitory neurotransmitters while reducing the number expressing excitatory neurotransmitters (Borodinsky et al. 2004). Similar phenomena are also observed in both embryonic chick and rat neurons. In these studies, Ca^{2+}-dependent action potentials are important in the regulation of neurotransmitter expression (Ahmed et al. 1983; Nerbonne and Gurney 1989; McCobb et al. 1990). This was shown to mechanistically involve activity induced tyrosine hydroxylase expression, allowing for the synthesis of an inhibitory neurotransmitter (Brosenitsch and Katz 2001).

Subsequent studies also demonstrate that neurons will change their neurotransmitter receptor phenotype to match the change in transmitter expression. This includes studies in embryonic Xenopus muscle cells that show an initially glutamate, GABA, glycine and ACh receptor expressing muscle will switch to a purely AChR expressing muscle cell with an increased presynaptic activity and subsequent cholinergic output. However, when activity of the motor neuron is inhibited, the muscle cell continues to express all the original types of receptors without the switch over (Borodinsky and Spitzer 2007). However, the underlying cellular and molecular mechanisms by which activity regulate neurotransmitter receptor expression has not been previously well established—in part due to the lack of studies on understanding activity at the level of a single cell.

The significance of activity and patterned activity in developmental programs are well established in the literature. As discussed above, studies have identified the role of activity in

controlling neurotransmitter and receptor specification (Marek et al. 2010; Spitzer 2012), synapse formation (Kay et al. 2011), and receptor expression (Kalashnikova et al. 2010). Particularly, patterned activity has been shown to be critical in the formation of functional spinal and optical circuits (Zhang and Poo 2001; Borodinsky et al. 2012), as well as the regulation of neurite outgrowth (Fields et al. 1990), ion channel expression, and gene expression (Sheng et al. 1993; Fields et al. 1997; Buonanno and Fields 1999; Brosenitsch and Katz 2001; Klein et al. 2003). Moreover, it has been demonstrated that neurotrophic factors can act not only to regulate the excitability of neurons but also influence their firing patterns (Davis-Lopez de Carrizosa et al. 2010).

Similar to the differential effects of activity on various cell types in synapse formation, it was noted that an increase in action potential firing specific to a particular cell type of *Lymnaea stagnalis* neurons was noted in neurons that expressed excitatory nAChRs, but not in neurons that expressed inhibitory nAChRs. The respiratory neuron VD4 which expresses inhibitory nAChRs did not show an increase in electrical activity following trophic factor addition. However, LPeD1, which expresses excitatory nAChRs in the presence of trophic factor, showed a profound increase in the action potential frequency. When activity was blocked in the presence of trophic factors, excitatory nAChR expression was blocked (Xu et al. 2009). Previous observations in mammalian studies have also reported that neurotrophic factors require concurrent electrical activity in the neurons to elicit some of their effects (Meyer-Franke et al. 1995; McAllister et al. 1996; Boulanger and Poo 1999; Du et al. 2000) and that the addition of trophic factors leads to an increase in electrical activity and excitability (Shen et al. 1994; Zhang et al. 2008; Murray and Holmes 2011). However, systematic characterization of the activity induced by trophic factor addition have not been performed, especially in a longitudinal manner.

Studies to date have only looked at short time points and quantitative characterization have not been performed. In *Chapter 4*, I utilize microelectrode array (MEA) technology to perform long-term, non-invasive recordings of individual neurons during synaptic development.

1.8 Synaptic Plasticity

Synapses are not a static entity. Rather, a synapse is malleable, with the ability for the strength of a synapse to be heightened (potentiated) or dampened (depressed). Additionally, neurons are also constantly regulated to exist in a stable state over long periods of time. This is due to homeostatic synaptic plasticity. In particular, this form of plasticity promotes network stability through the modulation of global synaptic strength (Vitureira et al. 2012). This ability for modulation of synaptic strength at the level of the synapse or the network is a fundamental component of a functioning nervous system known as synaptic plasticity. Together, these mechanism of plasticity allows for the nervous system to adapt to sensory input, in response to our ever-changing environments and is a key component for the survival of an organism.

Furthermore, synaptic plasticity is thought to be an important part of early neurodevelopment, with increasing studies demonstrating that perturbation of synaptic plasticity mechanisms underlies the pathophysiology of neuropsychiatric disorders (Crabtree and Gogos 2014). Therefore, to understand normal nervous system function and to develop a means to repair these pathologies, it is important to understand the precise cellular and molecular mechanisms that underlie the various forms of synaptic plasticity.

Our current classification of synaptic plasticity is dependent on their time duration of activity. For instance, changes in synaptic strength can be transient, lasting from milliseconds to seconds, and are categorized as being short-term synaptic plasticity (Regehr 2012). These forms

of synaptic plasticity are thought to underlie short-term memory (Barak and Tsodyks 2014). Conversely, changes in synaptic strength can persist up to hours, to days and perhaps even longer and are collectively known as long-term synaptic plasticity (Yang and Calakos 2013). Accordingly, these longer lasting forms of synaptic enhancement or depression are thought to underlie the basis of long-term memory (Takeuchi et al. 2014).

1.8.1 Short-Term Synaptic Plasticity

Short-term presynaptic plasticity can be categorized into three different categories. These include (1) depression, (2) facilitation, and (3) augmentation/post-tetanic potentiation (PTP). In short-term synaptic depression, with two closely triggered stimuli, the second stimuli always evoked a reduced postsynaptic response compared to the first. This form of depression lasted from milliseconds to seconds. When additional stimuli were triggered, the depression would persist for a longer period of time from seconds to minutes. This was thought to be due to the depletion of the readily releasable pool with inadequate time for pool replacement to occur (Betz 1970; Zucker and Regehr 2002).

Conversely, facilitation demonstrated that the second stimuli following two triggered action potentials would always evoke an increased response compared to the initial stimuli, lasting on the order of milliseconds to seconds. Mechanisms underlying this form of short-term plasticity have been thought to be related to the residual calcium hypothesis, which suggests that elevated calcium remaining at a presynaptic bouton following stimulation would be additive to calcium entry from a subsequent action potential stimulation. The resultant higher concentration of intracellular calcium would result in the release of a larger number of vesicle (Katz and Miledi 1968). Additionally, the role of a presynaptic calcium sensor distinct from the release machinery,

synaptotagmin, may also play a role in allowing for facilitation to persist beyond the temporal pattern of residual calcium (Atluri and Regehr 1996; Bertram et al. 1996).

When additional stimuli were triggered at high frequency, augmentation and PTP were observed, which demonstrated a synaptic enhancement that lasted for seconds to several minutes. PTP refers to the increase in synaptic efficacy that occurs following a high-frequency tetanic stimulation, whereas augmentation lasts for a shorter duration and can be triggered by a lower-frequency, shorter-duration stimulation (Zucker and Regehr 2002). Mechanisms include an increase in action potential evoked calcium influx following tetanic stimulation (Habets and Borst 2006; Korogod et al. 2007). Similar to that observed in facilitation, residual calcium may also activate additional calcium sensors other than synaptotagmin. Studies have identified multiple molecules including protein kinase C (PKC) (Beierlein et al. 2007; Korogod et al. 2007), calmodulin and calcium/calmodulin-dependent kinase II (CaMKII) (Fiumara et al. 2007) in this form of short-term synaptic plasticity.

1.8.2 Long Term Synaptic Plasticity

More than one hundred years ago, Santiago Ramon y Cajal postulated that memories were stored in newly formed synaptic circuits and connections. Donald Hebb subsequently proposed that memories were formed through the modification of the strength of pre-existing synaptic connections via pre- and postsynaptic correlation of activity (Hebb 1949), colloquially known as “cells that fire together, wire together”. However, it was not until the 1970s when this phenomenon was demonstrated in the hippocampus. Bliss et al. (1973) demonstrated that when they stimulated the excitatory synapses in the hippocampus, they could demonstrate a potentiation of synaptic efficacy which remained for hours to days. This phenomenon eventually

came to be known as long-term potentiation (LTP) (Bliss and Gardner-Medwin 1973; Bliss and Lomo 1973).

Mechanisms underlying LTP/Long Term Depression (LTD) have been the topic of extensive study over the years. In particular, synapses in the CA1 region of the hippocampus have contributed significantly to understanding the mechanisms behind LTP (Bayazitov et al. 2007) and LTD (Stanton et al. 2003). While it is likely that multiple mechanism on both the pre- (Padamsey and Emptage 2014)and postsynaptic (Granger and Nicoll 2014) side are involved in these long-term synaptic plasticity phenomenon, the use of complex mammalian models to dissect out the mechanism behind synaptic plasticity may also contribute to the confusion. Therefore, to study a novel form of short-term synaptic plasticity, I have opted to utilize the *Lymnaea* soma-soma model.

1.9 *Lymnaea* as a model system

While significant advances have been made in the field of understanding synaptogenesis, there continues to be fundamental knowledge gaps in our understanding of central synapse formation. In particular, questions still remain as to the precise temporal pattern of early synapse formation and the importance of transcription and *de novo* protein synthesis in the formation and maintenance of these synapses. Further, while the importance of extrinsic trophic factors in synapse formation has been demonstrated, the precise cellular mechanism underlying their actions remains elusive. This lack of fundamental knowledge is due primarily to the complexity of mammalian models where large numbers of brain cells assembled into complex neural networks make it rather difficult to study synapse formation at the level of a single synapse. Therefore, in our lab we have opted to use the simple molluscan model, *Lymnaea stagnalis* (**Fig.**

2.1Ai,Aii), whose entire CNS comprises of approximately 20000 neurons with *in vivo* synaptic circuits that have been extensively defined and mapped. Under a dissection microscope, these neurons can be readily identified based on size, location and color (**Fig. 2.1B+insert**). More importantly, we have the capacity to extract individual neurons and subsequently promote the reformation of their proper synaptic connections *in vitro.* These synapses can be in the form of neurite-neurite configuration or in our further simplified soma-soma synaptogenic model (**Fig. 2D**), where identified pre- and postsynaptic neurons are juxtaposed in culture, allowing the reformation of proper synaptic connections independent of neuronal outgrowth. This model thus grants us the unique opportunity to specifically study synapse formation without the confounding role of neuronal growth (Feng et al. 1997).

As discussed above, our lab has previously demonstrated the importance of intrinsic cell-cell signaling (ie. transmitter-receptor interaction) in proper synapse formation (Meems et al. 2003). In addition, we have also demonstrated that extrinsic trophic molecules play an integral role in synapse formation. Specifically, trophic factors have been shown to be necessary for excitatory but not inhibitory synapse formation (Hamakawa et al. 1999; Woodin et al. 1999; Woodin et al. 2002; Meems et al. 2003; Xu et al. 2009; Flynn et al. 2014). Our lab has gone on to demonstrate that downstream of trophic factor signaling, the activation of a receptor tyrosine kinase (RTK) triggers Ca^{2+} oscillations in the postsynaptic neuron but not the presynaptic neuron. These Ca^{2+} oscillations are necessary for the expression of proper excitatory receptors (Xu et al. 2009). Despite these studies, the precise mechanisms that enable the expression of specific, excitatory AChRs involved in excitatory synapse formation still remain poorly understood.

1.10 Specific Aims

The main objective of my research is to utilize a well characterized *in vitro* cell culture model system to elucidate the mechanisms that mediate the formation and plasticity of specific synapses. Specifically, utilizing the well characterized *Lymnaea stagnalis* model to (1) study the role of growth cones and trophic factors in synapse formation and to (2) characterize a novel form of synaptic plasticity. The specific aims of my research include:

Specific Aim #1: (1) Using a novel model system, to determine the capacity for growth cones to form/maintain synapses, and to investigate the temporal patterns of synaptogenesis. (2) To develop a novel amperometric technology to permit long-term non-invasive recording of neurotransmitter release dynamics in a developing synapse/network—Chapter 3.

Specific Aim #2: (1) Using novel microelectrode array (MEA) recording technology to determine the role of trophic factors and trophic factor induced activity on the regulation and expression of functional excitatory AChRs. (2) To develop novel biotechnology with the capacity to perform long-term recordings of both ion channel activity and intracellular Ca^{2+} levels—Chapter 4.

Specific Aim #3: To investigate and characterize the cellular and molecular mechanisms behind a form of short-term potentiation observed between VD4 and LPeD1—Chapter 5.

Figure 1.1 Growth Cone

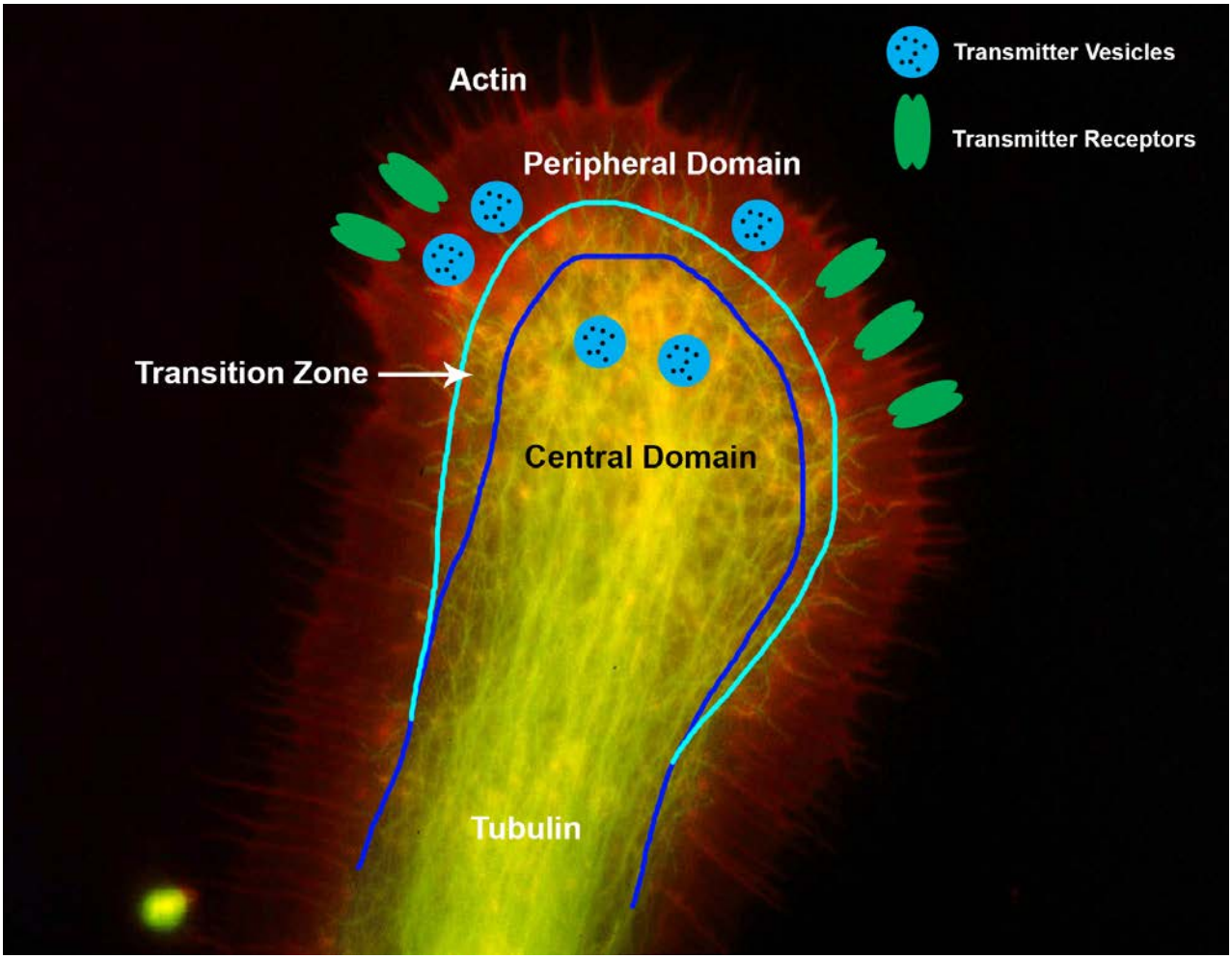

Figure 1.1 Schematic diagram of growth cone, their compartments and function

A growth cone has three distinct regions termed the peripheral zone that predominantly contains actin, a central domain that (contains mitochondria and exocytotic vesicles), and a transitional zone, which harbours the myosin contractile structures that regulate actin and microtubule trafficking between the two regions. Previous studies have revealed that that growth cones have transmitter vesicles and the proper release machinery prior to contact with their synaptic partners. In addition, growth cones also express transmitter receptors that are functional in advance of synapse formation.

Chapter 2: Materials and Methods

2.1 Animal Care

Lymnaea stagnalis (Gastropoda, Pulmonata, Basommatophora, Lymnaeidae) **(Fig. 2.1Ai, Aii)**, the common fresh water pond snail, were reared at room temperature (21-23^{o}C) in well-aerated, filtered and de-chlorinated tap water. The animals were exposed to a 12 hour light and 12 hour dark cycle and fed twice a week with fresh romaine lettuce and once a week with Purina Trout Chow® (Purina Mills, MO, USA). The snails were originally derived from an inbred population obtained from the Free University of Amsterdam (the Netherlands) and maintained at the Snail Animal Care Facility at the University of Calgary.

2.2 Dissections

A comprehensive description of the cell culture procedure has been published elsewhere (Syed et al. 1999) and also in a video journal (Py et al. 2012). *Lymnaea stagnalis* were removed from the tank and their shells were removed with a pair of blunt forceps. The animals were then anesthetized for ten minutes in a solution of *Lymnaea* saline (in mM: 51.3 NaCl, 1.7 KCl, 4.0 $CaCl_2$, and 1.5 $MgCl_2$) mixed with Listerine™ (ethanol, 21.9%; methanol, 0.042%) to create a 10% solution (volume/volume). Subsequently, the animals were removed from the solution and pinned into a saline filled, Sylgard dish with insect pins. Using forceps and fine dissection scissors (Fine Science Tools, #5, BC, Canada), a dorsal midline incision was made on the animal's anterior body and the skin spread open using insect pins to expose the brain. The brain was then extracted by severing the tissue connecting the brain to the body and then stored in a normal saline solution containing gentamicin (50 μg/mL, Antibiotic Saline).

2.3 Conditioned Media

Conditioned media (CM) was prepared by incubating isolated *Lymnaea* brains in defined medium (DM-serum-free 50% L-15 medium with 20 µg/mL of gentamicin and inorganic salts at mM: 40 NaCl, 1.7 KCl, 4.1 $CaCl_2$, 1.5 $MgCl_2$ and 10 HEPES at pH 7.9). Specifically, brains were isolated from animals 3-5 months old (shell length 20-30 mm) and then transferred through a sequence of 7-8 petri dishes containing antibiotic saline ("wash"). Brains were left in each petri dish for approximately 10 minutes with occasional gentle agitation. Following the final "wash", the brains were transferred into an autoclaved, Sigmacote® (Sigma) treated glass petri dish containing 6 mL of DM (serum-free 50% L-15 medium with 20 µg/mL of gentamicin and inorganic salts at mM: 40 NaCl, 1.7 KCl, 4.1 $CaCl_2$, 1.5 $MgCl_2$ and 10 HEPES at pH 7.9) (2 brains/1mL of DM). Dish was then placed into a humidified incubation chamber at room temperature for 3 days. At the end of the incubation, the CM was used fresh or collected and kept frozen at -20^{o}C until used.

2.4 Cell Culture

2.4.1 Brain Preparation and Cell Extraction

In cell culture, brains were isolated from animals 1-2 months old (shell length 15-20 mm). Following extraction, the brains were washed three times (10 minutes each wash) in antibiotic saline. Next, the central ring ganglia were treated in DM containing trypsin enzyme (2 mg/mL; Sigma, St. Louis, MO) for 21 minutes. This was then followed by a treatment in trypsin inhibitor (2 mg/mL; Sigma) for 15 minutes. In both treatment conditions, the dishes were gently agitated approximately every 5 minutes. Following this treatment, the brains were pinned dorsal side up onto a Sylgard dish containing high osmolarity DM (750 µL of 1 M glucose added to 20

mL DM to increase solution osmolarity from 130-145 to 180-195 mOsm; **Fig. 2.1B**). Using a pair of fine forceps, both the outer and the inner sheaths of the brain were manually removed, exposing the individual neurons VD4 and LPeD1 **(Fig. 2.1B insert)**. The neurons were then extracted using gentle suction applied through a Hamilton 500 µL syringe paired with a fire-polished, Sigmacote® (Sigma) treated glass pipette (60-70 µM tip diameter) and a Narashige micromanipulator (MM-202, MM204).

2.4.2 Culture Surface Preparation

Extracted neurons were suspended in high osmolarity DM in fire-polished, Sigmacote® (Sigma) treated pipettes and transferred to various culture conditions before being gently expelled and placed into a specific configuration. Specifically, culture surfaces included glass-coverslip attached dishes (made by drilling 15 mm diameter holes in the bottom of plastic culture dishes and attaching glass coverslips (22x22mm, Baxter) across the hole with silicone glue (Dow Corning)), micro-electrode array chips **(Fig. 2.2A)**, planar patch clamp chips (Silicon Nitride variant and Poly-imide variant; **Fig. 7.1A, 7.2A**), planar amperometry chips **(Fig. 7.3C)** and contact imaging chips **(Fig. 7.4B)**. Each of these culture surfaces were treated with poly-L-lysine for 2 hours to form an adsorbed substrate layer before being rinsed three times with autoclaved deionized water.

2.5 Sharp Electrode Electrophysiology

2.5.1 Sharp Electrode Intracellular Recordings: Isolated Cells

Cellular membrane potentials, neuronal activity, and synaptic potentials were recorded using conventional intracellular recording techniques. Glass microelectrodes (1.5 mm internal

diameter; World Precision Instruments, Sarasota, FL, USA) were pulled using a vertical pipette puller (David Kopf Instruments, 700C) calibrated to produce electrodes with resistances in the range of 20-60 MΩ. Neurons were visualized using either an inverted microscope (Axiovert 100TV; Zeiss, Thornwood, NY, USA) or an upright microscope (Olympus BX61WI; Olympus Canada, Richmond Hill, Ontario, Canada). The electrodes were filled with a saturated solution of K_2SO_4 and then connected to the amplifier headstages. Subsequently, they were fixed onto two metal arms controlled by Narashige (Tokyo, Japan) micromanipulators (MM202 and MM204) on the inverted microscope or MPC-200 (Paired with ROE-200 and MP285 motorized drivers; Sutter Instrument, CA, USA) on the upright microscope. A ground electrode formed by a chloridized silver wire was place into the bath solution. The electrodes were then manipulated close to the cell and then impaled into the cell of interest. To record and stimulate neurons, current was injected into the somata using an amplifier (Dual Channel Intracellular Recording Amplifer IR-283; Cygnus Technology, Delaware Water Gap, PA, USA). The amplified electrical signals were then relayed through a digitizer (Digidata 1322A or Digidata 1440A; MDS Inc, Toronto, Canada) and recorded on Axoscope 9.0 or 10.0 (MDS Inc, Toronto, Canada).

2.5.2 Functional Acetylcholine Receptor Assay

The functional responses of AChRs was tested via application of ACh while simultaneously performing sharp electrode intracellular recording on the neuron of interest. Specifically, ACh was dissolved in DM to form a 1 µM solution (A-112; Research Biochemicals; Natick, NA, USA). The ACh solution was loaded into glass microelectrodes with an opening diameter of 5 µm. The electrode was then mounted on a pressure injection system

(PV800; World Precision Instruments; Sarasota, FL, USA) and puffed onto individual neurons by applying 12 psi pressure for 500 ms pulses.

2.6 Microelectrode Array Recording

2.6.1 Hardware and Software

Neurons cultured on MEAs (**Fig. 2.2A,C**, TiN electrodes, SiN isolator and Ti contact pads; electrodes at 200 µM spacing, 30 µm diameter with internal reference; Multichannel Systems, Reutlingen, Germany) were recorded using Multichannel System's MEA amplifier and PCI acquisition card (**Fig. 2.2B**; MEA1060; Multichannel Systems). The recordings were displayed and saved using MC_Rack 4.5.3 **(Fig. 2.2D)**.

2.6.2 Recording Protocol

Activity recordings were made from the neurons for 2 hours in DM, with a brief pause in recording to perform functional AChR assay (see above) followed by a switch into CM and 10 further hours of recording before another AChR assay was performed. During the 2 hour DM recordings, a DM to DM switch was performed to control for any possible mechanical disturbance-induced activity.

2.6.3 MEA Recording Analysis

The recordings were processed using MC_Rack software. Using the spike counting function, every individual action potential and its associated timestamp was extracted. The output from MC_Rack was then processed by Excel (Microsoft; Redmond, WA, USA) to yield the number of action potentials per hour as well as the interspike intervals (ISI; time elapsed

between two adjacent action potentials). The inverse of the ISI (1/ISI) was calculated and used to calculate frequency and to generate frequency plots as a way to visualization activity variability over time.

2.7 Ca^{2+} imaging

Fura-2 AM (Molecular Probes, Carlsbad, CA, USA), a cell-permeable ratiometric Ca^{2+} sensor, was used to determine changes in the intracellular Ca^{2+} levels. A detailed Ca^{2+} measurement procedure has been described elsewhere (Doran and Goldberg 2006; Xu et al. 2009). In brief, presynaptic VD4 neurons injected with 2 mM of Fura-2 were exposed alternately to excitation wavelengths of 340 and 380 nm using a high-speed wavelength switcher lamp, Lambda DG4 (Sutter Instrument, Novato, CA, USA), while cellular activity was electrophysiologically manipulated. The emitted fluorescence signal was collected at 510 nm by a Retiga Ex digital CCD camera. Images were acquired with Northern Eclipse software running the IonWaveN subprogram (Empix Imaging, Canada). The free intracellular Ca^{2+}concentration ($[Ca^{2+}]_i$) was estimated based on values obtained with a Fura-2 Ca^{2+} imaging calibration kit (*F*-6774, Molecular Probes) according to Kao (1994).

2.8 Immunostaining

Cultured cells and growth balls were fixed with 4% paraformaldehyde for 30 min in phosphate-buffered saline (PBS) containing 3 mM EDTA and 0.02% glutaraldehyde, which were then permeabilized in 0.5% NP-40. F-actin was labeled with RITC phalloidins (Molecular Probes, Carlsbad, CA, USA). Tubulin was labeled with a mouse monoclonal antibody targeting β-tubulin (Boehringer-Mannheim). Secondary antibodies were obtained from Vector Labs

(Burlingame, CA, USA). The preparations were rinsed with PBS and incubated with 25 units of RITC phalloidin diluted for 1 h at room temperature. The cells were rinsed with PBS and then incubated with 1:100 β-tubulin antibody for 1 hour. The cultures were subsequently rinsed and incubated with 1:20 FITC-conjugated anti-mouse IgM for 1 hour. Coverslips were mounted in PBS/glycerol (15–85%) containing 1%-n-propylgalate. Soma and growth cones were viewed under Zeiss (Axiovert 135) fluorescent microscope and photographed by a Retiga Ex digital CCD camera. Images were acquired with Northern Eclipse software (Empix Imaging, Canada).

2.9 Pharmacological agents

Staurosporine, bisindolylmaleimide I hydrochloride (BIS), phorbol 12-myristate-13-acetate (PMA), KN-93, KN-92, autocamtide 2-related inhibitory peptide (AIP) and W-7 were all purchased from Calbiochem (Gibbstown, NJ, USA). Tubocurarine chloride hydrate was purchased from Sigma-Aldrich. All drugs were dissolved in DMSO (DMSO < 0.01%) with the exceptions of tubocurarine chloride hydrate, AIP and W-7, which were dissolved in *Lymnaea* saline. All chemicals listed below were dissolved in DM at a concentration such that the added volume into CM was less than 1% of total CM volume. In the experiments with the protein synthesis blocker anisomycin (12.5 µg/mL; A9789; Sigma-Aldrich), the cells were pre-incubated with anisomycin in DM prior to CM addition. Cadmium was used at a final concentration of 100 µM and nifedipine at 10 µM.

2.10 Drug injections

To selectively expose neurons to compounds and to minimize the variable time required for the drugs to cross the membrane, various drugs were specifically pressure injected into

presynaptic cells. Specifically, low resistant electrodes (5-10 MΩ resistance) were loaded with 1 μL of the drug to be injected. Using a similar setup as described above, the somata were impaled as per the electrophysiological recording protocol and the desired solution injected by brief pressure pulses (0.5-1s, 15-20 psi). Visual verification of an intracellular fluid bubble was an indication that the solution had been properly injected into the cell.

2.11 Sniffer cell and single somata measurements

DA release from RPeD1 somas was detected on a single gold electrode and compared to DA sensitive VD4 neurons. To accomplish this, first, VD4 neurons were isolated from *Lymnaea* central ring ganglia and placed into a hemolymph coated glass coverslip dish in DM to allow their axons to resorb. Next, RPeD1 neurons were isolated and placed adjacent (approximately 10 to 20 μm) to the recording electrode on the planar MEA. Prior to amperometric measurements, the previously isolated VD4 neurons were taken from the dish and placed adjacent (approximately 10 to 20 μm) to an RPeD1 neuron **(Fig. 2.3)**. Both VD4 and RPeD1 neurons were impaled with sharp electrodes and electrophysiological recordings were obtained. While tetanic stimulations of RPeD1 neurons (10+ action potentials) were triggered to evoke DA release, VD4 neurons were held at sub-threshold potentials (approximately −56 mV) to detect ("sniff") DA release as indicated by a hyperpolarizing response (Lovell et al. 2002). For amperometric measurements, the electrode adjacent to the RPeD1 cell was held at +450 mV vs. Ag|AgCl reference electrode for recording DA release. Recordings were conducted at a sampling rate of 500 Hz. An electrode located away from the isolated neurons was also utilized to record noise and to act as a control.

2.12 Data and statistical analysis

Paired-sample Student's *t*-tests were used to determine statistical significance between pre-tetanus and post-tetanus excitatory postsynaptic potentials (EPSPs) in experiments for triple soma pairs, receptor sensitization, time dependency of STP and kinase inhibition experiments. A univariate ANOVA was used to analyze all other studies. All statistical analysis was conducted on raw EPSPs and Ca^{2+} concentrations except when noted in the results where the analysis was conducted on percentage enhancement values. Student's *t*-test and univariate ANOVAs were performed using SPSS 13.0 for Windows and Prism GraphPad 5 (GraphPad Software Inc., La Jolla, CA, USA). Significance was assumed if p-values were < 0.05 ($p < 0.05$). In all the graphs, post-tetanic EPSP (pEPSP) amplitudes were expressed as a percentage of pre-tetanic EPSPs.

Figure 2.1

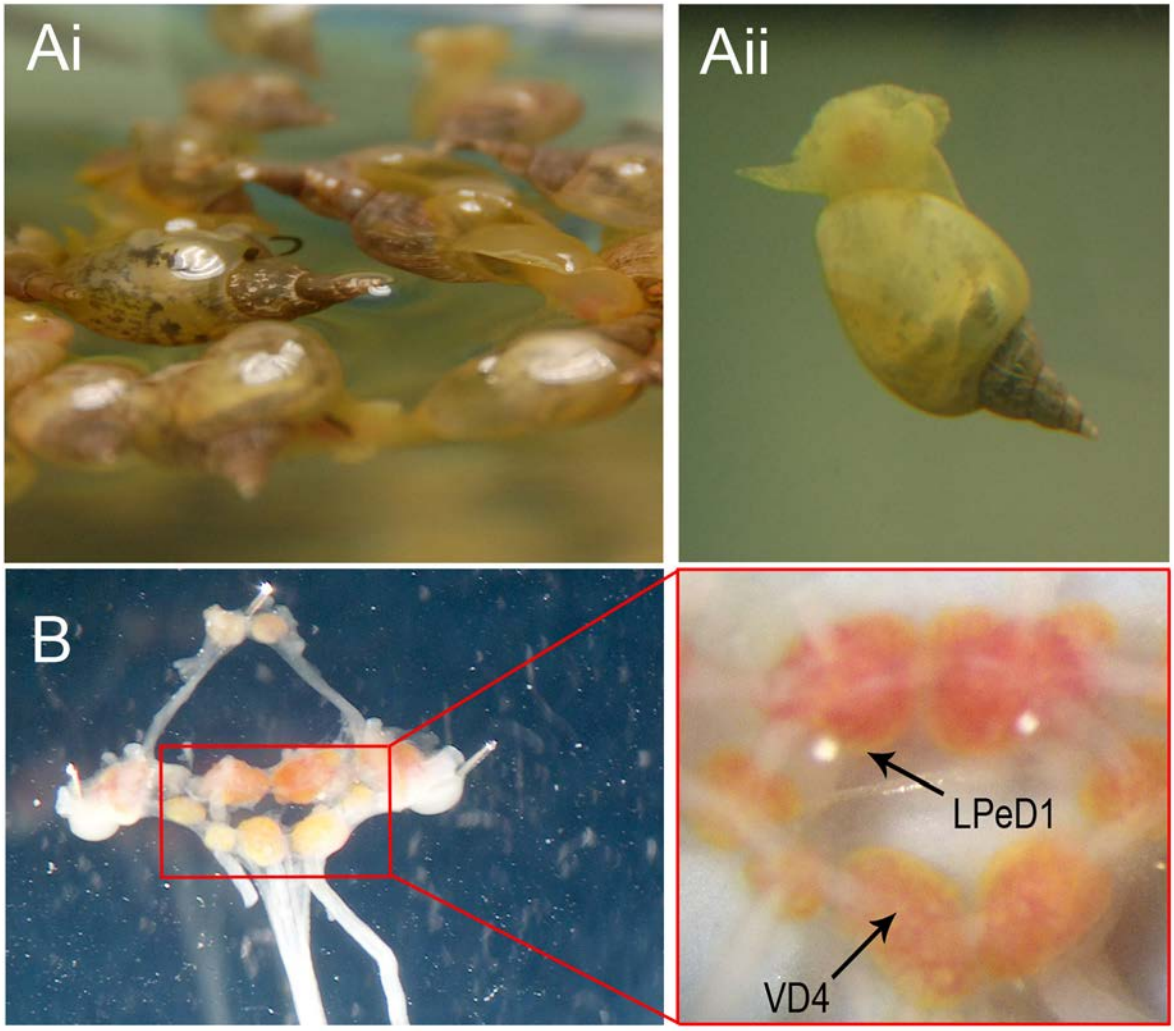

Figure 2.1: The freshwater mollusc, *Lymnaea stagnalis*, as a model for studying neuronal activity and synapse formation

(Ai) *Lymnaea stagnalis.* **(Aii)** Dorsal surface of *Lymnaea stagnalis.* **(B)** The central ring ganglia were isolated from the animals. The commissure joining the left and right cerebral ganglia was cut and the brain was spread apart and pinned onto a Sylgard dish with the dorsal side of the brain exposed. Individual cells could be distinguished under a dissection microscope as seen in the expanded view of the central ring ganglia. The locations of two cells of interest, visceral dorsal 4 (VD4) and left pedal dorsal 1 (LPeD1), are shown by the thin arrows.

Figure 2.2

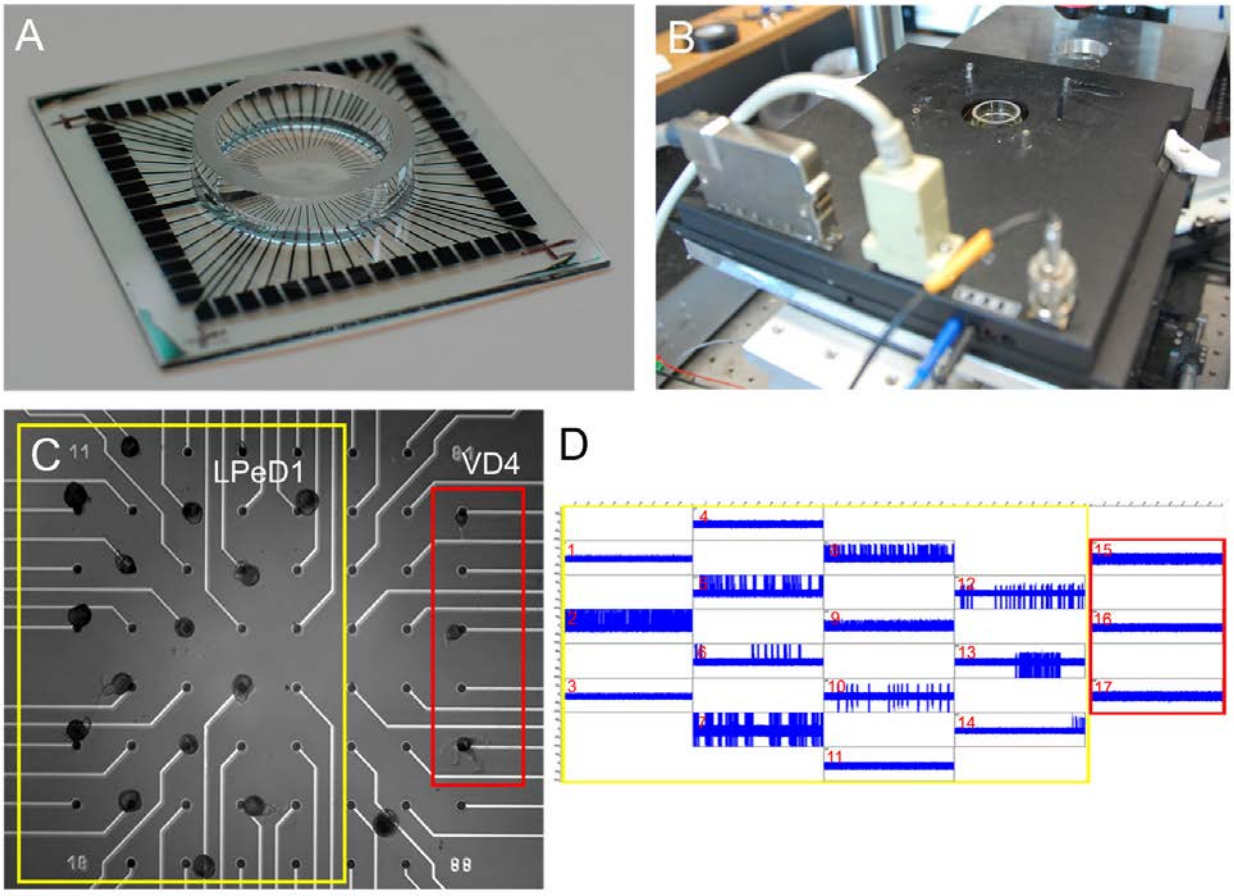

Figure 2.2: Microelectrode array recording

(A) Microelectrode array, TiN electrodes, SiN isolator and Ti contact pads. **(B)** A MEA1060 preamplifier was used to record from the microelectrode arrays. **(C)** In this microscope image, individual electrodes correspond to individual recording channels. Individual LPeD1 and VD4 neurons were placed on the electrodes allowing us to simultaneously record from multiple neurons. The electrodes are 30 µm in diameter and the distance between electrodes is 200 µm. **(D)** A ten minute simultaneous recording of all 60 channels. Neuronal activity is recorded on the MEA chip as a voltage change which can be seen on the tracing.

Figure 2.3

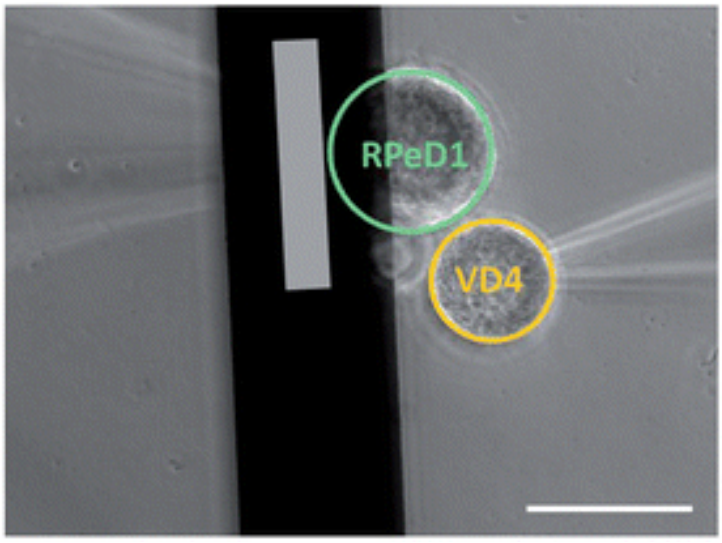

Figure 2.3: Sniffer cell experiment

An image showing the relative positions of the “sniffer” cell (VD4) and the detecting electrode (Gray bar) in relation to RPeD1. The RPeD1 neuron was placed at equal distances from the electrode and the sniffer cell (VD4). Scale bar is 100 µm.

Chapter 3: The temporal patterns of synaptogenesis between the isolated growth cones of *Lymnaea* neurons and the neurotransmitter release properties of various neuronal compartments

Sections of this chapter have been published in the following manuscripts:
Luk C.C., Schmold N.M., Lee T.K. and Syed N.I. (2010) A novel approach reveals temporal patterns of synaptogenesis between the isolated growth cones of *Lymnaea* neurons." European Journal of Neuroscience **32**(9): 1442-1451. – *Reproduced with permission from John Wiley & Sons.*

Patel B.A., **Luk C.C.**, Leow P.L., Zaidi W., Lee A.J., Syed N.I. (2013) A planar microelectrode array for simultaneous detection of electrically evoked dopamine release from distinct locations of a single isolated neuron. Analyst. **138**(10):2833-2839. – *Reproduced with permission from The Royal Society of Chemistry.* http://pubs.rsc.org/en/content/articlelanding/2013/an/c3an36770c#!divAbstract

3.1 Introduction

Growth cones located at the tips of growing neurites are critical mediators of synapse formation during development, neuroplasticity and regeneration (Munno and Syed 2003; Wiersma-Meems et al. 2005; Bradke et al. 2012; Hur et al. 2012). Previous studies have demonstrated that individual growth cones have the ability to autonomously perform multiple neuronal functions. For instance, vertebrate and invertebrate growth cones are able to secrete and detect neurotransmitters (Haydon et al. 1984; Davis et al. 1992; Ivgy-May et al. 1994; Sabo and McAllister 2003), and harbour preassembled 'packets' (Haydon and Drapeau 1995) of the synaptic machinery (synaptic vesicles etc.) prior to contact with their synaptic partners. These 'pre-assembled' elements of the synaptic machinery may empower growth cones to be primed for synapse formation immediately upon contact with their respective targets. Whereas a number of important contributions have been made in defining the timing of molecular events underlying synapse assembly in vertebrate synapses (Ahmari et al. 2000; Friedman et al. 2000; Ziv and Garner 2004), direct electrophysiological evidence for synaptogenesis between pre- and postsynaptic neurons at the growth cones levels is still lacking. This lack of functional evidence

for synapse formation between growth cones is due to the fact that synaptic sites are often located at a distance from recording sites (i.e., the somata) and are, therefore, inaccessible to direct electrophysiological analysis. Several investigators have, however, isolated growth cones from their somata in order to study the extent to which growth cone functions as an autonomous cellular compartment (Davis et al. 1992; Ivgy-May et al. 1994). For instance, in 1983, Young and Poo demonstrated that the growth cones of isolated *Xenopus* neurons are capable of spontaneous ACh release in culture. Furthermore, *Xenopus* embryonic myocytes, or myoballs, have also been used successfully to 'sniff' neurotransmitter release from developing *Drosophila* giant neurons (i.e., prior to synaptic contact) (Chow and Poo 1985). Other elegant studies have visually demonstrated that synaptic vesicles are bidirectionally transported to and from the growth cone and have the ability to fuse with the growth cone membrane prior to synapse formation (Sabo and McAllister 2003; Alberts et al. 2006). Similarly, Haydon and colleagues (1984) showed that the growth cones of individually identifiable *Helisoma* neurons could detect and respond appropriately to exogenously applied 5-HT. Studies using *Helisoma* have further demonstrated that the isolated growth cones could: (1) generate action potentials that are unique to neuron type and similar to those elicited at the soma (Guthrie et al. 1989), (2) independently regulate intracellular calcium levels (Rehder et al. 1991), and (3) synthesize proteins *de novo* for at least two days following their isolation from the somata (Davis et al. 1992; Crispino et al. 2014). Thus, there exists ample plausible evidence that both intact (with somata) and severed growth cones are capable of invoking either preassembled or *de novo* synthesized secretory machinery to initiate early steps of synaptogenic program. Whether this initial assembly of 'ready made' (Young and Poo 1983) synaptic structures could also result in consolidated synapses in the absence of somata-based signaling has not, however, been established.

Furthermore, the precise timing of the growth cone mediated steps underlying synaptogenesis has not been functionally revealed between central neurons.

A number of key questions regarding synapse formation between growth cones remain to be answered. For example, how long after initial physical contact does synaptic transmission begin between the growth cones of pre- and postsynaptic neurons? What are the temporal patterns of synaptic connectivity? Are single growth cones able to establish multiple synapses with different targets? Do synapses consolidate in the absence of somata based signaling? Does a growth cone retain its previous "contact memory" and "history" of transient synaptic contact? This study was designed to address these important questions in the field of neurodevelopment, regeneration and synaptic plasticity. Specifically, I isolated growth cones from individually identified *Lymnaea* pre- and postsynaptic neurons and tested for their ability to form specific synapses in the absence of the somata. Like the study conducted on *Helix aspersa* neurons by Marom and Dagan (1987), I found that the isolated growth cones from *Lymnaea* neurons rolled up into "growth balls". I demonstrate that the growth balls from presynaptic neuron, RPeD1 and its postsynaptic partners visceral (V) H/K, VJ, and VI/G develop specific excitatory, inhibitory, or biphasic synapses respectively. These synapses were target cell contact specific and similar to those seen *in vivo* (Winlow et al. 1981; Syed and Spencer 1994). While Chow and Poo (1985) were able to successfully use the "myoballs" as sensitive probes for neurotransmitter detection, I was able to take the growth balls a step further as they could also both 'sniff' transmitter release and act as synaptic partners. Finally, to further characterize the capacity of individual neuronal compartments to release neurotransmitter as autonomous structures—including the somata, proximal axon, distal axon and the axon terminal—I developed a novel microelectrode array planar amperometry technology in collaboration with the University of Brighton (UK). These

microelectrode arrays allowed us to detect DA release concurrently at multiple sites—at a resolution, never attained before, and allowed for us to begin understanding the capacity for the various neuronal compartments to autonomously initiate neurotransmitter release.

In summary, I provide the first electrophysiological account of the temporal patterns of synaptogenesis at the resolution of individual growth cones and achieved a technical milestone to further concurrently decipher the transmitter secretory dynamics of various neuronal compartments over an extended time period in a non-invasive manner.

3.2 Results

3.2.1 Severed growth cones transform into neuronal 'growth balls'.

Individually identified presynaptic neurons RPeD1 (dopaminergic) and its postsynaptic partners VH/K, VI/G, and VJ were isolated in cell culture in the presence of brain-conditioned medium (CM) and allowed to extend processes overnight. All cells plated on poly-L-lysine substrate exhibited robust growth within 24 hours of cell culture **(Fig. 3.1A)**. A sharp micropipette was used to sever the growth cones from their intact axon **(Fig. 3.1A-C)**. Immediately after truncation, the cut ends of the axons sealed off and the severed growth cones continued to extend for a few minutes (**Fig. 3.1D-I**), whereas new growth cones emerged from the intact neurites and continued to extend as before. Within a couple of hours of their isolation, the severed growth cones transformed into 'growth balls' (**Fig. 3.1J-L**). Despite physical contact between the proximal axon and its truncated growth cone (**Fig. 3.1H-J**), the two compartments failed to rejoin. To reveal the cytoskeletal rearrangement of the truncated growth cones and their corresponding growth balls, I performed immunocytochemistry to label actin and β-tubulin.

Actin and β-tubulin labelling of an intact RPeD1 growth cone is shown in **Fig. 3.1M** series. The truncated growth cone maintained its cytoskeletal structure similar to that of intact growth cones, whereby the lamellipodium consisted primarily of actin and the microtubules comprised the bulk of the central core of the growth cone and the extending neurite (**Fig. 3.1Mi-Mii**). However, once a growth cone transformed into a growth ball, both the actin and the tubulin collapsed into a mesh occupying the central and the peripheral domain respectively (**Fig. 3.1Miii)**.

3.2.2 Growth balls are electrophysiologically viable, release transmitter, express transmitter receptors and develop specific synapses in culture.

Intact growth cones have previously been shown to contain neurotransmitter vesicles and receptors (Haydon et al. 1984; Ivgy-May et al. 1994) and are known to release a variety of neurotransmitters in culture (Young and Poo 1983). To test whether the growth balls from the presynaptic neuron RPeD1 could release neurotransmitter following electrical stimulation, the RPeD1 growth ball was impaled with an intracellular electrode. The growth balls of RPeD1's postsynaptic partners VJ and VH/K were also impaled with a sharp electrode and manipulated in close proximity (10-15 μm) to the RPeD1 growth ball (but not contacting) to act as a neurotransmitter 'sniffer' cell. Action potentials induced in RPeD1 growth balls produced an inhibitory, non-synaptic response in VJ growth balls (**Fig. 3.2Ai**; n=5) and an excitatory response in VH/K growth balls (**Fig. 3.2Bi**; n=11). Specifically, to stimulate the release of transmitter from RPeD1 growth balls, I triggered a tetanic pulse consisting of a train of 10+ action potentials. This resulted in a hyperpolarization of VJ growth balls (**Fig. 3.2Ai**) with a mean potential response of -4.8 ± 0.11 mV and a depolarization in VH/K growth balls (**Fig.**

3.2Bi) with an average amplitude of 8.4 ± 0.25 mV. These non-synaptic responses were blocked with the DA antagonist sulpuride (10^{-4}M – not shown) and were mimicked by exogenous DA application (10^{-6}M; **Fig. 3.2Aii, Bii**). Exogenously applied DA generated a hyperpolarizing response of -6.9 ± 0.49 mV in VJ growth balls (**Fig. 3.2Aii**; n=5), while a depolarizing response of 7.31 ± 0.31 mV was detected in VH/K growth balls (**Fig. 3.2Bii**; n=12). All growth cones investigated in this study remained electrophysiologically viable for several days (3-4 days). In summary, these studies demonstrate that growth balls are electrophysiologically viable and have the capacity to release neurotransmitter and retain the excitatory and inhibitory receptor properties of their respective somata even when isolated.

Next, I tested the ability of both presynaptic and postsynaptic growth balls to establish specific synapses in culture. To this end, both the pre- and the postsynaptic growth balls were impaled with sharp intracellular electrodes and brought into direct contact with each other for 20-30 minutes to allow for a chemical synapse to form. Intracellular current was then injected into the presynaptic RPeD1 growth ball to elicit action potentials and corresponding excitatory or inhibitory postsynaptic potentials (PSPs) were detected in the postsynaptic growth balls derived from VH/K, VI/G, and VJ growth cones. I found that within several minutes of pairing, growth balls began to reform their respective synapses such that a single action potential elicited in the presynaptic RPeD1 growth ball generated a 1:1 PSP in the postsynaptic growth ball. These synapses were similar to those observed *in vivo*. Specifically, after 20-30 minutes of pairing, single presynaptic action potentials induced a 1:1 excitatory postsynaptic potential (EPSP) in the VH/K growth ball (6.9 ± 0.57 mV, **Fig. 3.3A;** n=7), a 1:1 inhibitory postsynaptic potential (IPSP) in the VJ growth ball (8.47 ± 0.59 mV, **Fig. 3.3C;** n=12) and a 1:1 biphasic response in the VI/G cell growth ball (**Fig. 3.3D;** n=10) where a fast excitatory PSP was followed by a

longer inhibitory PSP response (excitatory component 3.8 ± 0.26 mV; inhibitory component 9.1 ± 0.72 mV). As opposed to the non-synaptic compound depolarization and hyperpolarization observed in the previous "sniffer" growth ball experiments, 1:1 EPSPs were indicative of a true synaptic connection rather than a non-synaptic response. It is also important to note that in order to detect non-synaptic release, a burst of action potentials was always required, while this was not a prerequisite for detecting synaptic responses. Further, to demonstrate the specificity of this response and to rule out electrical coupling, postsynaptic growth balls were induced to fire a burst of action potentials and a corresponding response in presynaptic RPeD1 growth balls was monitored for (**Fig. 3.3B;** n=17). Whereas I failed to detect any response in RPeD1 growth balls following postsynaptic stimulation, subsequent stimulation of RPeD1 growth balls generated corresponding EPSPs in VH/K growth balls. Taken together, these data demonstrate that RPeD1 growth balls reform proper excitatory, inhibitory and biphasic synapses in culture and that these synapses are similar to those *in vivo* (Winlow et al. 1981).

3.2.3 Temporal patterns of synaptic connectivity and efficacy of synaptic transmission between the growth balls.

To define the precise timing of synapse formation as well as synaptic strength between the growth balls, I monitored synaptic responses from the point of contact to 40 minutes post-contact (n=6). Specifically, growth balls were impaled with sharp electrodes and juxtaposed as described above (**Fig. 3.4A**). A univariate ANOVA revealed a significant effect of time post-contact on the synaptic strength [$F_{(5,36)} = 77.76$; $p < 0.001$]. I discovered that within 2-10 minutes of contact, 1:1 EPSPs were clearly discernable with an average amplitude of 1.5 ± 0.64 mV (**Fig. 3.4Ai**). Tukey's post-hoc test revealed that the efficacy of this synaptic strength increased

significantly to 6.9 ± 0.62 mV ($p < 0.001$) after 15-25 minutes of contact (**Fig. 3.4Aii,C**). However, within 30-40 minutes the synaptic strength decreased significantly to 2.1 ± 0.41 mV ($p < 0.001$) (**Fig. 3.4Aiii,C**) with a complete loss of synaptic response by 60 minutes (data not shown). Exogenous application of DA (10^{-5} M) did, however, continue to produce a depolarizing response with an amplitude of 7.20 ± 0.86 mV in the postsynaptic VH/K growth balls (**Fig. 3.4Aiii inset**; n=5). A t-test revealed that this response did not differ significantly from that observed when DA was exogenously applied to the VH/K growth balls prior to contact with an RPeD1 growth ball (7.31 ± 0.37 mV, $p = 0.14$). These data demonstrate that the loss of functional connectivity beyond 40 minutes post-contact does not involve a reduction in the postsynaptic receptor function (compare **inset A** to **inset Aiii**, **Fig. 3.4**). These data also show that synapses can be established between pre- and postsynaptic growth balls within minutes of contact and that the efficacy of this transmission reaches its peak value 15-25 minutes post-contact and declines to initial contact levels between 30-40 minutes.

The above data clearly demonstrate that the synaptic strength established between individually identified growth balls diminishes over time. To further rule out the possibility that the presynaptic growth balls simply ran out of transmitter contents, fresh postsynaptic growth balls were juxtaposed next to the "original" presynaptic RPeD1 growth balls (**Fig. 3.4B**). I discovered that the second VH/K growth ball also established a synapse with a previously paired RPeD1 growth ball (that could not consolidate its synapse with the first VH/K growth ball). A univariate ANOVA revealed a significant effect of time post-contact on synaptic strength [$F_{(5,51)} = 39.75$; $p < 0.001$]. Interestingly, however, a Tukey's post-hoc comparison showed that the second VH/K growth ball juxtaposed with the original RPeD1 growth ball exhibited larger synaptic responses during the initial 2-10 minute period (7.9 ± 0.66 mV) as compared with the

first VH/K growth ball (1.5 ± 0.64 mV; $p < 0.001$) (**Fig. 3.4Bi,C**). Incidentally, the efficacy of synaptic transmission between RPeD1 growth balls and their second VH/K partner reached a peak value within 15-25 minutes (6.5 ± 0.70 mV) (**Fig. 3.4Bii,C**), and also diminished significantly within 30-40 minutes of contact (2.00 ± 0.37 mV; $p < 0.001$) (**Fig. 3.4Biii,C**).

Taken together, the above data demonstrate that specific synapses can develop within minutes of contact between isolated growth balls and reach maximum efficacy within 15-25 minutes. The efficacy of this synaptic transmission, however, decreases significantly within 30-40 minutes. Our data also demonstrate that prior pairing with a postsynaptic target may prime the presynaptic growth ball for synapse formation, significantly enhancing synaptic strength upon immediate contact with a second target. This synapse, however, is also transient and the synaptic strength is reduced significantly over time (30-40 min) **(Fig. 3.4C)**. In summary, while growth balls are capable of immediate synapse formation, these synapses are not maintained in the absence of intact somata/neurites.

3.2.4 Both pre- and postsynaptic somata are required for "synapse sustainability".

To demonstrate that both the pre- and postsynaptic somata are required for the formation of a consolidated synapse, I paired postsynaptic growth balls with intact, presynaptic growth cones (i.e. soma intact). Specifically, RPeD1 neurons (presynaptic) and VH/K neurons (postsynaptic) were isolated and allowed to extend their processes in cell culture. A growth ball derived from an isolated VH/K growth cone was paired with the growth cone of an intact presynaptic RPeD1 neuron (**Fig. 3.5A inset**; n=5). A univariate ANOVA revealed a significant effect of time post-contact on synaptic strength [$F_{(4,25)} = 35.48$; $p < 0.001$]. Like the synapses formed between two growth balls, intracellular recordings indicated that within 5 minutes post-

contact, stimulation of the intact RPeD1 growth cones produced EPSPs in VH/K growth balls with an amplitude of 0.39 ± 0.11 mV (**Fig. 3.5A**). Tukey's post-hoc test showed that the synaptic efficacy continued to increase significantly 10 minutes post-contact as stimulation of RPeD1 growth cones generated 1:1 EPSPs in VH/K growth balls at a mean amplitude of 2.7 ± 0.46 mV; $p < 0.005$) (**Fig. 3.5B**) with a further increase and plateau at 20 minutes post-contact (5.6 ± 0.53 mV; $p < 0.001$). Although there was no further significant increase in EPSP amplitude at 30 minutes post-contact (6.1 ± 0.57 mV; $p=0.903$), spikes were often triggered in the VH/K growth balls (**Fig. 3.5C**). However, similar to the previous experiments, the synapse only lasted transiently before decreasing in strength within 35 minutes post-contact (EPSP amplitudes were reduced to 2.3 ± 0.38 mV; $p < 0.001$) (**Fig. 3.5D**) and losing synaptic response completely at 60 minutes.

To show that the somal compartment of presynaptic RPeD1 still retained the capacity to form synaptic connections, the VH/K growth balls were gently removed using sharp micropipettes and without disruption to the RPeD1 cell body, an isolated VH/K soma from another brain (cultured in the same dish) was placed adjacent to RPeD1 in soma-soma configuration. After 12-18 hours of culture, this soma-soma pair developed an excitatory synapse, demonstrating that the RPeD1 somal compartment is indeed competent to form a stable synapse (data not shown). I could not, however, test the same paradigm when an RPeD1 (presynaptic) growth ball was brought into contact with an intact VH/K (postsynaptic) growth cone as the responses were electrophysiologically undetectable due to the fact that the postsynaptic recording site at the VH/K soma was too far from the site of the synapse.

3.2.5 Multiple synapses can form concurrently with three different targets.

To test, whether single presynaptic growth balls could develop multiple synapses with three different postsynaptic growth balls, I simultaneously paired three growth balls (derived from VH/K and VI/G growth cones) with a single RPeD1 growth ball (**Fig. 3.6A**; n=3). Synapses were then tested over time. I found that within minutes, action potentials induced in RPeD1 triggered 1:1 EPSPs in VH/K growth balls and a biphasic PSP in VI/G growth balls. Specifically, simultaneous recording from all four growth balls showed that within 25 minutes post-pairing, all three postsynaptic growth balls reformed their specific connections (**Fig. 3.6B**). VH/K(a) and VH/K(b) growth balls reformed their excitatory synaptic connection with an average amplitude of 8.2 ± 1.9 mV while VI/G reformed its biphasic synapse (Excitatory component 3.9 ± 0.68 mV; Inhibitory component 7.3 ± 0.84 mV) with the RPeD1 growth ball. Importantly, a t-test revealed no significant effect on synaptic strength when comparing triple paired VH/K growth balls to single paired VH/K growth balls at peak synaptic strength ($p = 0.174$). Interestingly, the temporal pattern of connectivity in this triple configuration was identical to that of single pairs (data not shown). These results thus demonstrate the capacity of a single growth ball to form multiple synaptic connections simultaneously with different partners and with equal synaptic strength. These synapses were also not, however, maintained over an extended period in the absence of the soma/neurite.

In attempting to decipher the mechanism behind the initiation of synapse formation, there remained questions regarding the initial steps involved in early synapse formation. Specifically, it remained unclear to us whether early neurotransmitter release was indeed important in the initiation of synapse formation, given the capacity for growth balls to harbor synaptic release machinery and also actively release neurotransmitter even prior to contact with their postsynaptic targets (Young and Poo 1983; Sabo and McAllister 2003; Alberts et al. 2006). However, given

the limited capacity of the “sniffer cell” to detect a large spatial area of release, no current assay or tool existed to answer this question. Therefore, to characterize the release dynamics of individual neurons and their various compartments over a large spatial area, I needed to develop a technology that would allow for the precise quantification of neurotransmitter release at the level of a single soma, axon and growth cone.

3.2.6 Development of a novel chip to detect neurotransmitter release from growth cones and growth balls.

Although the “sniffer cell” could reliably detect neurotransmitter release, the gold standard for the quantification of individual vesicular release is the use of carbon fiber microelectrode probes in a technique known as amperometry. This technique involves the use of an electrode held at a potential (ie. ~700 mV) which is high enough to cause the oxidation of oxidizable neurotransmitters (ie. DA, norepinephrine, epinephrine and 5-HT) (Westerink 2004). Therefore, when the surface of the carbon fiber electrode is placed in contact with neurotransmitter molecules, fixed quantities of electrons are “removed” per neurotransmitter via the oxidative process. The size of the detected current is therefore proportional to the released quantity of oxidizable neurotransmitter.

However, despite the excellent temporal resolution achieved with a single carbon fiber microelectrode, its ability to interrogate multiple sites or a motile process remains poor. Having this capacity remains important given that neuronal processes can span multiple centimeters and a single neuron can have multiple release sites concurrently. Further, being able to interrogate the release dynamics of an entire network of cultured cells during synaptogenesis is not feasible with a single carbon fibre electrode. Therefore, to overcome these technical challenges, we designed a

microelectrode array, which contains multiple electrodes patterned onto a planar surface with each acting as an amperometric electrode (Patel et al. 2013). We demonstrate here that with this device, we were able to simultaneously record from multiple sites of a single neuron, ranging from the cell body to the entire length of its axon. Further, we demonstrate that this microchip is as effective as a "sniffer cell", which is currently the gold standard for detecting neurotransmitter release in the *Lymnaea* model. A brief description of the amperometry microchip fabrication process is provided in the appendix (Chapter 7), and additional details can be found in our published manuscript (Patel et al. 2013).

3.2.6.1 Comparison of the planar amperometry chip to the "sniffer" cell assay in detecting dopamine release from RPeD1

To compare the planar amperometry chip with the "sniffer cell", a single RPeD1 neuron was axotomized and placed adjacent to a gold sensing electrode held at a potential of +450 mV *vs*. Ag|AgCl. Next, to allow simultaneous measurement and comparison, a freshly isolated "sniffer" VD4 somata was then placed at equidistance from RPeD1 on the opposing side (**Fig. 3.7A**). Both RPeD1 and VD4 were impaled with an intracellular sharp electrode and recorded electrophysiologically. As expected, we found that evoked tetanic stimulation of RPeD1 led to non-synaptic inhibitory responses in the sniffer soma VD4. A maximum inhibitory response of 5 ± 2.4 mV was achieved after 4.3 ± 0.7 s of stimulation (n = 8; **Fig. 3.7B,** C). The large variance in membrane potential change is suspected to be due to uneven expression of receptors on the sniffing soma—a variable that cannot be controlled between individual "sniffer" cells. Therefore, the use of VD4 as a neurotransmitter detection cell may provide qualitative data, but cannot provide quantitative information. On the other hand, simultaneous measurement of

neurotransmitter release using the electrode revealed a maximum oxidation current of 478 ± 76 pA, which was observed 3.6 ± 0.3 s post stimulation (**Fig. 3.7D, E, F**). Using the quantitative nature of amperometry, this oxidative current was calculated to be equivalent to the release of 308 ± 49 nM of DA from RPeD1. In summary, this study demonstrates that the microchip gold electrode has better temporal response to released DA and shows more reliability in their ability to detect DA as evident with their low variation in their detection of released DA compared to the "sniffer" cell ($p < 0.01$).

3.2.6.2 Planar amperometry chip can also detect serotonin from LPeD1 but cannot detect acetylcholine release from VD4

We next tested the ability of our chip to detect neurotransmitter release from VD4 neuron, which releases ACh (an electrically inactive molecule), a molecule that cannot be oxidized by the gold electrode (**Fig. 3.8A**). As expected, tetanic stimulation of VD4 cultured adjacent to a +450 mV *vs*. Ag|AgCl electrode did not result in the detection of ACh release as indicated by the lack of current changes (n=6; **Fig. 3.8B**). The repeated measurement of six VD4 neurons consistently showed that no current was detectable (**Fig. 3.8C**). Next, to test our chip's ability to also detect 5-HT release from LPeD1, we adopted the same configuration and experimental paradigm (**Fig. 3.8D**). As expected, tetanic stimulation of LPeD1 resulted in an electrical response from the amperometry electrode (n=6; **Fig. 3.8E**). Our data quantification revealed that the chip was able to detect a fairly consistent level of release with a low standard deviation (**Fig. 3.8F**). Oxidation currents of 314 ± 27 pA (n=6) was detected by the individual electrode closest to LPeD1 following stimulation. This current corresponds to 176 ± 15 nM of 5-HT. In summary, this experiment demonstrates that the planar amperometry chip can reliably

and specifically detect the release of oxidizable neurotransmitters and current changes in the electrode. The detection is limited to molecules that are easily oxidized such as DA and in this case 5-HT, while molecules that are not easily oxidized such as ACh cannot be detected using the current configuration. It is important to note that this study unequivocally shows that the electrical current measured is indeed due to the detection of neurotransmitters and not due to electrical activity of the stimulated neuron.

3.2.6.3 Concurrent multiple site measurements over the length of a single isolated neuron

To test for the ability of our planar amperometry chip to record from multiple sites in a single neuron, including its somata and axonal process, an RPeD1 neuron was extracted with its axon and placed across several electrodes (**Fig. 3.9A**). Specifically, in our configuration, the soma was placed on electrode 1 (E1) with the axon crossing over electrode 2 (E2), electrode 3 (E3) and the terminal placed over electrode 4 (E4). These four electrodes plus a fifth (control) electrode located at a distant site, electrode 12 (E12), were held at a potential of +450 mV *vs.* Ag|AgCl. A tetanic pulse was elicited in RPeD1 via sharp-electrode and measurements were conducted at various time points over a 4 hour time period (**Fig. 3.9B**). We found that immediately after the neuronal isolation, neurotransmitter release was greatest at E3. However, by four hours, the greatest release was seen at the soma on E1 site. The lowest level of neurotransmitter release was consistently seen on E4, the axon terminal. When comparing changes recorded at individual electrodes, DA release at the soma immediately following isolation was 89 ± 2 nM, but increased to 132 ± 3 nM after 4 hours ($n=5$, $p < 0.001$). A similar increase was observed at the axon terminal, with an increase from 67 ± 8 nM to 96 ± 6 nM. In

contrast, release from the axon at E2 and E3 significantly decreased after 4 hours (**Fig. 3.9C**; $n=5$, $p < 0.01$).

Taken together, this novel technology not only provided us with a better tool to monitor transmitter release as compared with “sniffer cells” and “growth balls”, but shows that neurotransmitter release is highly dynamic. In particular, we demonstrated that the amount of vesicular release at various sites along an isolated neuron can rapidly change within 30 minutes and continue to show change up to 4 hours post isolation. Further, we demonstrate that multiple release sites including the soma, proximal axon, distal axon and axon terminal have the capacity to release neurotransmitter even prior to synapse formation.

3.3 Discussion

In this chapter, I achieved two of my specific objectives. Firstly, using a novel "growth ball" model system, the capacity for growth cones to form/maintain synapses, and the temporal patterns of synaptogenesis were investigated. Secondly, a novel planar amperometry technology was developed in collaboration with Dr. Patel to further explore the secretory capabilities of neurons and their axons.

During development, neurons extend elaborate processes with great precision towards their potential targets located at some distance from the soma. Such a task is assigned by neurons to their growth cones that are located at the tip of an elongating axon or dendrite. While studies have demonstrated the involvement of growth cones in axonal guidance and target cell recognition (Farrar and Spencer 2008; Lowery and Van Vactor 2009; Sutherland et al. 2014), less is known about their role in synapse formation—despite it being the initial structure that contacts the postsynaptic cell.

Studies have shown that growth cones are endowed with multiple elements of synaptic machinery prior to synapse formation. For instance, presynaptic release machinery (Ivgy-May et al. 1994; Ahmari et al. 2000; Sabo and McAllister 2003; Alberts et al. 2006) and postsynaptic receptors (Haydon et al. 1984; Zhong et al. 2013) are present in growth cones before synaptic contact. A growth cone's ability to release transmitter either spontaneously or when evoked has also been documented in a variety of models (Hume et al. 1983; Young and Poo 1983; Delaney et al. 1989; Haydon and Zoran 1989; Diefenbach et al. 1999; Liou et al. 1999; Sabo and McAllister 2003; Alberts et al. 2006). Yet, despite various studies suggesting that growth cones possess all of the necessary machinery for synapse formation, direct electrophysiological evidence is still lacking.

In this study, I used isolated growth cones that were transformed into growth balls as a novel means to study synapse formation. This preparation allowed us to manipulate individual growth balls from pre- and postsynaptic cells to define the temporal patterns of specific synapse formation at a high resolution. Several studies conducted in vertebrates have demonstrated that upon postsynaptic contact, vesicle recycling machinery appears to be concentrated at the site of contact and that within hours to days, active zones and vesicle pools assemble (Friedman et al. 2000; Ziv and Garner 2004; Okabe 2013). For instance, early studies using GFP tagged PSD-95 revealed that these postsynaptic protein dense specializations found in synapses could rapidly localize to excitatory postsynaptic sites within hours of observing cultured hippocampal pyramidal neurons (Okabe et al. 1999). Additionally, NMDAR and AMPAR subunits were found to be rapidly recruited to sites of where presynaptic axon contacted postsynaptic dendrite, as rapidly as 2-28 minutes following contact in dissociated rat cortical neurons (Washbourne et al. 2002). Furthermore, spontaneous synaptic events have also been observed in hippocampal cell culture as early as 2 days in culture (Basarsky et al. 1994), whereas functional active zones may form as early as 25-30 minutes after the initial cell-cell contact (Friedman et al. 2000). However, despite the powerful tool that imaging provides in understanding early formation and trafficking of synaptic proteins (Okabe 2013), it is unclear how many of these early synapses and clusters of synaptic proteins go on to become functional synapses (Sabo et al. 2006). This study contributes further to the field of synaptogenesis by providing direct evidence vis-à-vis the precise temporal patterns of functional synaptic connectivity at the level of single pre- and postsynaptic growth cones. Furthermore, I provided the first direct evidence that molluscan growth balls (and thus growth cones) contain all of the necessary machinery to establish functional, dopaminergic synapses. Specifically, using isolated growth balls from well-defined

pre- and postsynaptic neurons, I have demonstrated that specific excitatory, inhibitory and bi-phasic (excitation followed by inhibition) synapses similar to those that exist *in vivo* (Winlow et al. 1981; Syed and Spencer 1994), can develop within minutes of contact between the growth balls. These newly formed synapses strengthen with time reaching their *in vivo* strength within 15-25 minutes. This synaptic strength decreases significantly, however, over time (30-40 minutes) and eventually the synaptic connectivity is lost completely within an hour (not shown). This loss of connectivity could not be attributed to the run-down of the transmitter contents, or receptor inactivation as the postsynaptic growth balls were responsive to exogenously applied DA. Moreover, the presynaptic growth balls that appeared to have exhausted their transmitter contents developed stronger synapses immediately after contact with a fresher postsynaptic growth ball. These data add to our previous study where synaptic transmission between intact growth cones from RPeD1 and its target cells could not be detected until an hour after contact (Spencer et al. 2000). In the present study, however, it was possible for me to detect transmission between the cells within minutes (2-10 minutes) of growth ball contact.

While the growth cone may be capable of establishing synapses with any given target, its ability to concurrently innervate multiple partners has never been demonstrated. This study is therefore the first to show that when paired with three different postsynaptic target growth cones at the same time, RPeD1 growth balls could establish appropriate excitatory and bi-phasic synapses with all three postsynaptic targets simultaneously. These data further reveal a previously unappreciated ability of the growth cone to establish multiple synapses with different types of targets, underscoring the fact that in the absence of their soma, growth cones can execute their synaptogenic program with exquisite accuracy.

Unlike previous studies showing that severed *Helisoma* growth cones 'rejoin' their intact neurites (Davis et al. 1992; Guthrie et al. 1994), the isolated growth cones in our study did not re-connect with their neurites. Rather, within an hour following their isolation, growth cones collapsed into a growth ball similar to that of *Helix aspera* growth cones (Marom and Dagan 1987). This discrepancy between the studies may have to do with the fact that in the present study, growth cones were isolated with only a small portion of their neurite intact, whereas in *Helisoma*, the growth cones were severed with an extended portion of their neurite intact. As such, the microtubule and the actin mesh in our study may have collapsed more rapidly (**Fig. 3.1M**) as compared to *Helisoma* neurites that were cut at some distance from the base of the growth cone. In fact, I observed that the isolated growth cones may take up to several (2-5) hours to collapse if a lengthier neurite were left intact (data not shown). It is important to note that once the growth cone transformed into growth balls, the cytoskeleton rearranged in such a way that the F-actin primarily occupied the center of the growth ball, surrounded by the microtubules.

Actin has been implicated in maintaining and organizing synapse structure both pre- and postsynaptically and this disruption of normal F-actin arrangement may also explain the inability of growth balls to maintain their specific synapses (Allison et al. 1998; Allison et al. 2000; Zhang and Benson 2001; Charrier et al. 2006; Hanley 2014). For instance, Zhang and Benson (2001) found that disrupting actin filaments with latrunculin A results in a loss of immature synapses formed in rat hippocampal neurons (5-6 days *in vitro*) but that it does not disrupt mature synapses (18-20 days *in vitro*) suggesting the importance of actin in the early maintenance of synaptic receptors. Moreover, Charrier et al. (2006) showed that pharmacological disruption of F-actin and microtubules at glycinergic synapses results in an increase in glycine receptor lateral diffusion between synaptic and extrasynaptic sites with a decrease in receptor

stay time at the synapse. A further recent review discusses the importance of actin in AMPAR trafficking during development and synaptic plasticity (Hanley 2014). Thus, while growth balls are capable of releasing and sensing neurotransmitters, they may not have the proper cytoskeletal structure to establish appropriate presynaptic active zone and postsynaptic density required for synapse consolidation.

The lack of the soma or neurite may be another reason why synapses could not be consolidated. In addition to a potential role in maintaining normal cytoskeletal structure, intact somata and neurites seem to be important for the transcription and translational machinery required for synapse formation (Ji and Jaffrey 2014). In *Lymnaea,* for example, the molluscan homologue of multiple endocrine neoplasia type 1 (MEN1) was shown to encode the transcription factor *menin*, which is up-regulated during synapse formation and is required in the postsynaptic soma for both excitatory and inhibitory synapse formation (van Kesteren et al. 2001; Flynn et al. 2014). Furthermore, previous work from our lab also shows that axons isolated from pre- and postsynaptic *Lymnaea* neurons will form synapses as long as the presynaptic cell body is present, while the presence of the postsynaptic cell body is not as important (Meems et al. 2003; Xu et al. 2014). Our current study, however, suggests that the presence of both the pre- and postsynaptic somata are required for synapse consolidation. The difference between our study and studies performed on axons may lie in the fact that differences exist between isolated axons and growth cones. In the experiments conducted with isolated axons it is plausible that all required synaptogenic molecules such as relevant mRNA and proteins may have already been allocated to the long axonal process left intact (Wang et al. 2014). In other words, had a longer neurite been truncated with the growth cone, a consolidated synapse may have formed. However, this was not possible, since it was necessary to leave a short neurite stump behind in order for the

growth cones to roll up into spheres that could be manipulated. Taken together, with all previously published studies, the data present here demonstrate that while the extrasomal compartment of both pre- and postsynaptic neurons are endowed with synaptogenic capabilities, the consolidation of these synapses might, however, be contingent upon the somata-based molecular machinery. It is likely that either MEN1 or other transcriptional factors, which were shown previously to be essential for synapse formation between *Lymnaea* neurons (van Kesteren et al. 2001; Flynn et al. 2014), could serve as the synapse "consolidation" molecules. While this possibility needs to be demonstrated experimentally, the innate propensity of growth cones to recognize potential synaptic targets and establish "initial" synaptic contacts—in the absence of either the axonal segment or the somata—cannot, however, be undermined.

In this study, I also demonstrated that the efficacy of the synaptic formation to a fresher postsynaptic growth ball was significantly enhanced as compared with the first growth ball in the same time interval post-contact. I propose that an initial synaptic contact may have 'primed' the presynaptic growth ball for a stronger synapse. Consistent with this interpretation are previous studies showing that contacts between synaptic partners induce changes in the presynaptic neuron (Zoran et al. 1991; Dai and Peng 1993; Zoran et al. 1993; Ghirardi et al. 2004; Turner et al. 2011). For example, in the snail *Helisoma*, contact between buccal motor neurons and their target muscle not only elevated intracellular Ca^{2+} immediately upon contact, but also resulted in the coupling of the presynaptic action potential with transmitter release machinery (Zoran et al. 1991). Further studies by Zoran *et al.* (1993) revealed that contact between neuron B19 and its muscle target triggered elevated Ca^{2+} levels in the soma and neurites that persisted even after the removal of the muscle target. This similar phenomenon has been also demonstrated in chick ciliary ganglion neurons where growth cone contact with target muscle cells triggered

intracellular elevations in cytosolic free calcium that are initiated at the point of growth cone contact and spread throughout the axon and somata within minutes. This phenomenon was target cell contact specific (Graf et al. 1999). Similarly, Dai and Peng (1993) also observed that contact leads to enhanced transmitter release. This was again seen in *Helisoma* B110 motoneurons, whereby contact of the neuritic proccesses with synaptic muscle targets resulted in a more efficacious release of ACh as demonstrated by increased amplitude of evoked PSPs (Turner et al. 2011). Conversely, target cell contact of a *Helix* growth cone with a non-synaptic target resulted in the inhibition of neurotransmitter release, a process which was shown to require *de novo* protein synthesis and is mediated by the inhibition of cAMP-dependent PKA and MAPK-Erk, the same protein kinases that mediate the increase in neurotransmitter release following target cell contact (Ghirardi et al. 2004). In this study, I provide the first functional evidence for target cell contact-induced priming of a presynaptic growth cone and demonstrate its ability to expedite subsequent synapse formation. However, given the nature of the "sniffer cell" or "sniffer" growth ball assay, I was not able to quantitatively demonstrate a change in efficacy of neurotransmitter release following initial contact.

Specifically, although the growth ball model coupled with sharp electrode intracellular recording could provide information regarding the formation of electrophysiological synapses, there still remained several questions regarding the change in the efficacy of vesicular release from individual growth balls. For instance, what is the temporal time period of this efficacy change and to what degree does the efficacy of neurotransmitter release change? Is extrasynaptic and synaptic release influenced equally? Also, is the priming of the growth cone for release a local or global phenomenon? Such questions could only be answered if I could simultaneously determine the precise spatial and temporal secretory capabilities of all neuronal compartments,

including the soma, proximal and distal axon and other various neuritic processes. In this study, I demonstrate that the development of the novel planar MEA allowed for the interrogation of neurotransmitter release over a large spatial area. In particular, the array of electrodes functioned as individual neurotransmitter sensors, which could simultaneously detect neurotransmitter release over multiple areas of a single neuron and its axonal process. The use of gold electrodes coupled with our novel fabrication technique (described in Chapter 7 - Appendix) resulted in a planar MEA with excellent sensitivity and response time for detecting DA. During repeated measurements of DA, the gold electrodes were not prone to loss of sensitivity over 4 hours.

Various types of MEAs have been developed for neurochemical monitoring. These include multi-barrel carbon fibre electrodes (Zhang et al. 2008; Zhang et al. 2011) and carbon-ring electrodes (Lin et al. 2012) that allow for up to 15 individual electrodes to exist within one single device. However, these electrodes are not feasible for use on isolated neurons in culture given the inability for neurons to be cultured directly on these surfaces. Current MEAs have been also developed for recording DA release *in vivo* (Zachek et al. 2009; Carabelli et al. 2010; Trouillon et al. 2010; Zachek et al. 2010; Talauliker et al. 2011). However, given that the current goal in these studies have been to place the electrodes as close together as possible and minimize the size of the devices, with the intent of eventually implanting these electrodes *in viv*o, these devices are not suited for the recording of large neuronal networks nor are they practical for recording single neurons. With our current device, multiple recording electrodes over a large area have the potential to record neurotransmitter release dynamics at multiple sites either within a single neuron or within a network of developing neurons. Hence, with this technology the fundamental principles behind how neurotransmitter release dynamics change during various stages of synaptogenesis can be adequately investigated.

In summary, I have developed a novel, albeit technically challenging system to study the early events in synapse formation between isolated growth cones in the absence of somata signaling. I have also demonstrated for the first time the precise temporal pattern underlying early synapse formation in *Lymnaea* growth balls. While this study endorses growth cone's innate propensity for synapse formation and rapid maturation, the growth cones were unable to sustain and consolidate new synapses when isolated from their soma. Further, with the development of a novel technology to interrogate and quantify neurotransmitter release, our next focus will be on understanding how neurotransmitter release changes during the synaptogenic program and to understand their release dynamics at the various neuronal compartments including growth cone, axon and the somata.

Finally, when neurotransmitter release is altered, as is the case in neurodegenerative diseases such as Parkinson's, the nervous system function is rendered dysfunctional. Current pharmaceuticals given to Parkinson's patients, for symptom management, elevate DA levels in the brain, albeit in a highly uncontrolled manner and are thought to potentially result in drug-induced toxicity and exacerbate neurodegeneration (Lipski et al. 2011). Further, the efficacy of oral DA enhancing drugs remains variable with different patients. Therefore, deep brain stimulation (DBS) electrodes with more controlled release are deemed suitable for certain patients. However, even DBS often does not provide optimized therapy given the lack of biofeedback between intraparenchymal levels of DA and the need for further stimulation. The development of this microchip provides one potential means of creating a biofeedback loop, which couples a neurotransmitter sensor with a DBS electrode. I propose that the DA detection chip offers a tremendous opportunity as a future potential for therapeutic devices.

Figure 3.1

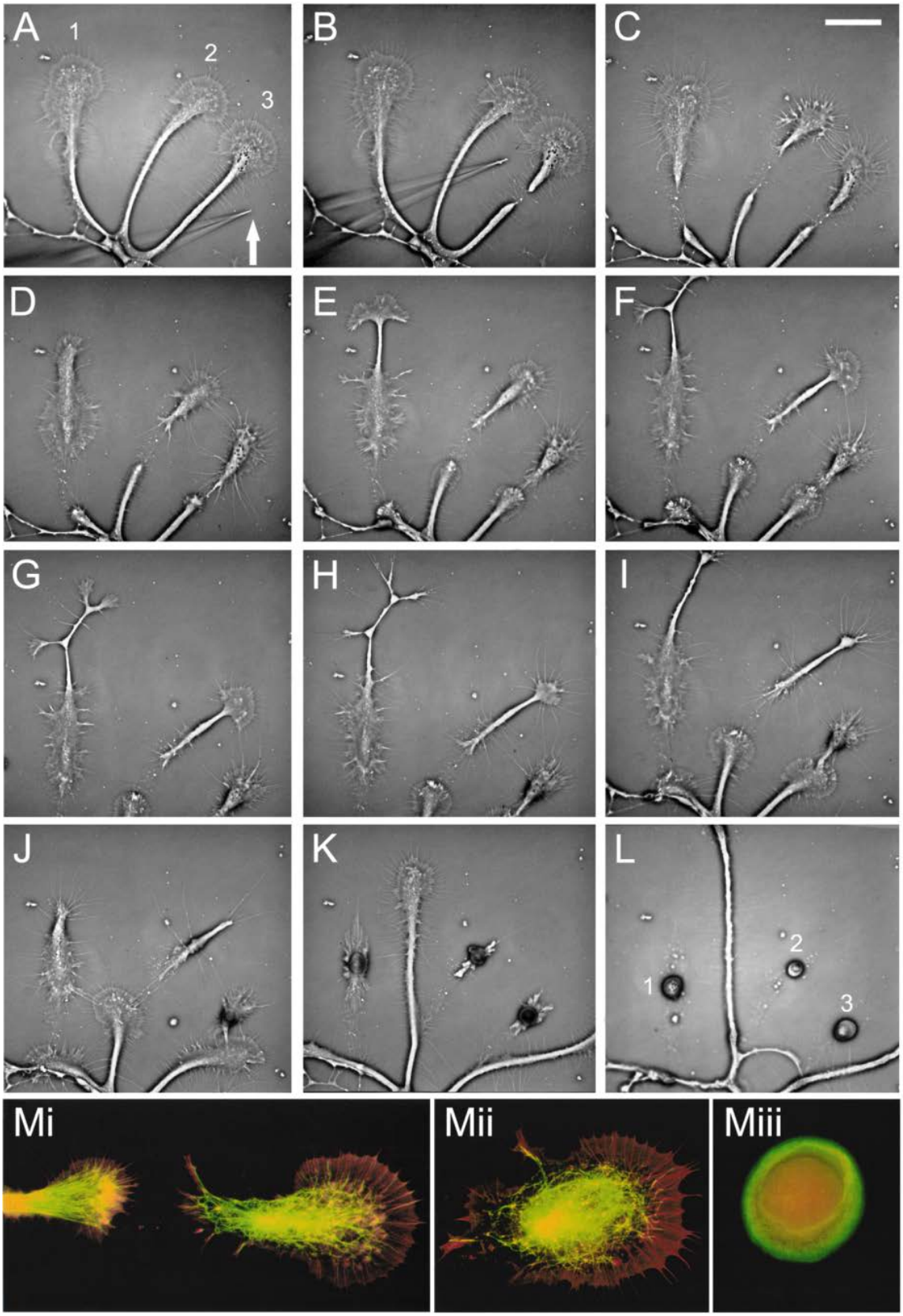

Figure 3.1: Isolated growth cones transform into "growth balls" with rearranged actin and β-tubulin.

(A) Presynaptic neuron right pedal dorsal 1 (RPeD1) was isolated and grown in brain-conditioned medium. RPeD1 neurons exhibited extensive neurite outgrowth with robust growth cones present at the leading tips of each neurite. **(B-C)** Using a sharp electrode (**A**-White Arrow), growth cones were truncated from their intact neuritis. Transected proximal neurites **(C)** and isolated growth cones sealed off and continued to grow with the development of new growth cones **(D-H)**. Despite contact between isolated growth cones and the proximal end of the cut neurite, the two compartments failed to rejoin **(I)**. Eventually isolated growth cones collapsed into growth balls **(K-L)**. To reveal changes in cytoskeletal structure of isolated growth cones, actin (red) and β-tubulin (green) immunocytochemistry was conducted. While isolated growth cones maintained the same cytoskeletal composition to that of intact growth cones **(Mi-Mii)**, the GB exhibited an inversion of these two components where actin was localized in the center of the growth balls with surrounding mesh of β-tubulin at the periphery **(Miii)**.

Figure 3.2

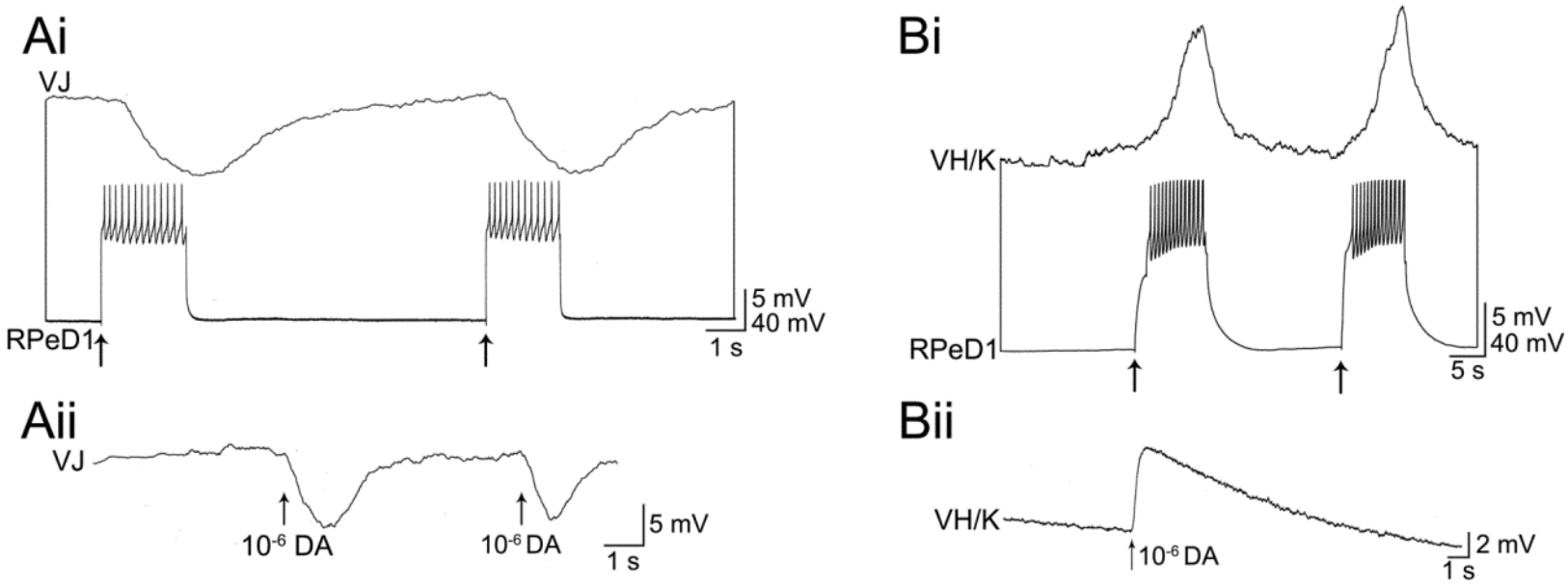
Ai
VJ
RPeD1
5 mV
40 mV
1 s
Aii
VJ
10-6 DA
10-6 DA
5 mV
1 s
Bi
VH/K
RPeD1
5 mV
40 mV
5 s
Bii
VH/K
10-6 DA
2 mV
1 s

Figure 3.2: Growth balls are electrophysiologically viable and retain the ability to release and detect neurotransmitter.

Isolated growth balls were tested for their ability to release and detect neurotransmitter. Presynaptic RPeD1 and postsynaptic visceral (V) J and VH/K growth balls were impaled with intracellular electrodes and maneuvered within close proximity to one another (10-15 μm). Induced action potential trains in RPeD1 triggered non-synaptic hyperpolarizing responses in VJ growth balls **(Ai)** (n=5) and depolarizing responses in VH/K growth balls **(Bi)** (n=11) demonstrating their ability to release and detect transmitter. These responses were mimicked with exogenous DA (10^{-6} M) application where a corresponding hyperpolarizing and depolarizing responses was observed in VJ **(Aii)** (n=5) and VH/K **(Bii)** growth balls (n=7) respectively.

Figure 3.3

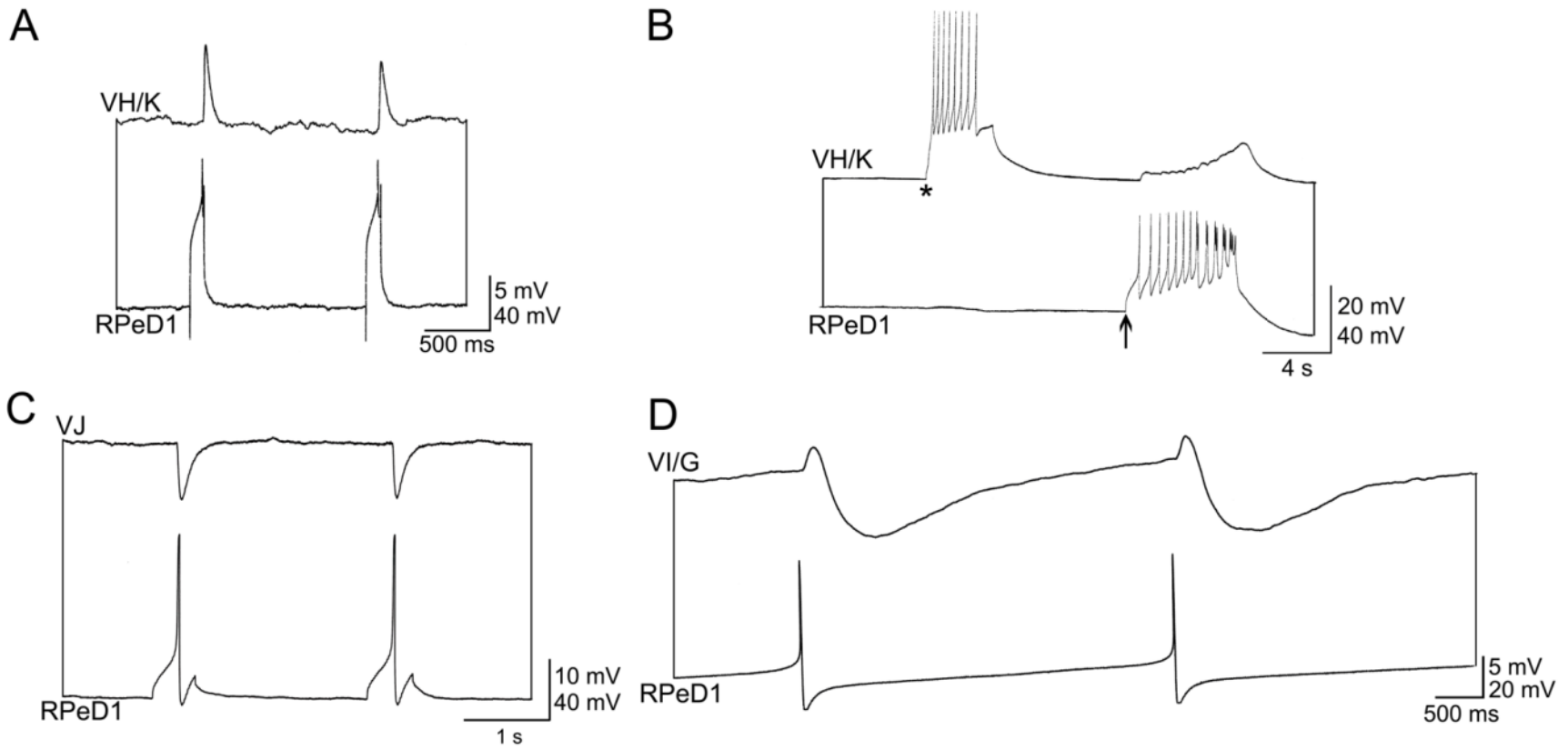
A
VH/K
RPeD1
5 mV
40 mV
500 ms
B
VH/K
*
RPeD1
20 mV
40 mV
4 s
C
VJ
RPeD1
10 mV
40 mV
1 s
D
VI/G
RPeD1
5 mV
20 mV
500 ms

Figure 3.3: Pre- and postsynaptic growth balls reform their specific synapses in culture. Presynaptic RPeD1 growth balls juxtaposed with postsynaptic VH/K, VI/G, VJ growth balls were able to recapitulate their specific synapses as seen in vivo within 20-30 minutes post-contact. RPeD1 growth ball reformed its excitatory synapse with VH/K growth ball **(A)** where single RPeD1 action potentials triggered 1:1 excitatory postsynaptic potentials (EPSP) in VH/K growth ball (n=7). To rule out electrical coupling and to demonstrate the specificity of synapse formation, the postsynaptic VH/K growth balls were induced to fire a burst of action potentials (asterisk), which did not result in a corresponding response in the presynaptic neuron **(B)** (n=17). Similarly, RPeD1 growth ball reformed synapses with its inhibitory partner, VJ **(C)** (n=12) and a biphasic synapse with VI/G **(D)** (n=10).

Figure 3.4

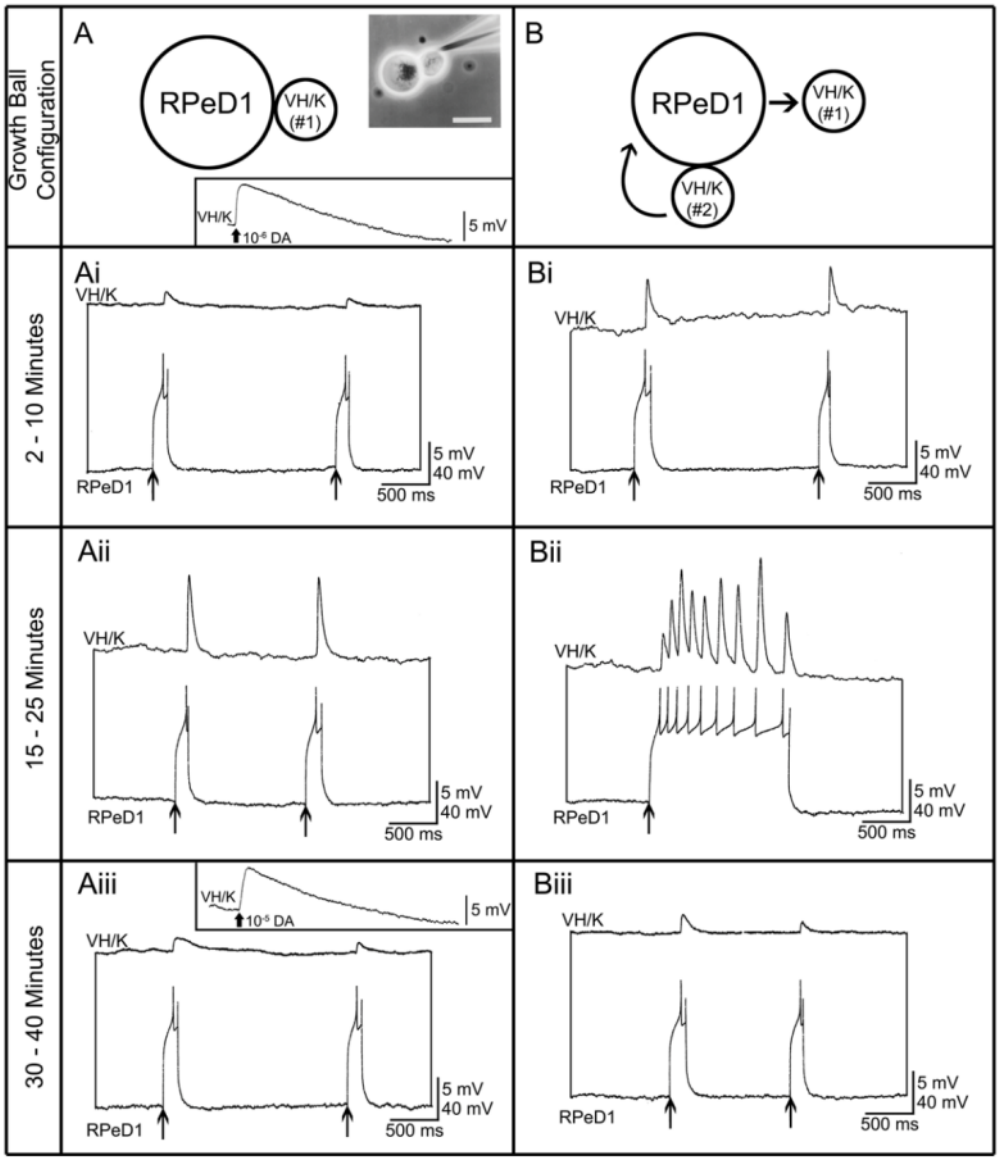
Growth Ball Configuration
A
RPeD1
VH/K (#1)
VH/K
10-6 DA
5 mV
B
RPeD1
VH/K (#1)
VH/K (#2)
2 - 10 Minutes
Ai
VH/K
5 mV
40 mV
RPeD1
500 ms
Bi
VH/K
5 mV
40 mV
RPeD1
500 ms
15 - 25 Minutes
Aii
VH/K
5 mV
40 mV
RPeD1
500 ms
Bii
VH/K
5 mV
40 mV
RPeD1
500 ms
30 - 40 Minutes
Aiii
VH/K
10-5 DA
5 mV
VH/K
5 mV
40 mV
RPeD1
500 ms
Biii
VH/K
5 mV
40 mV
RPeD1
500 ms

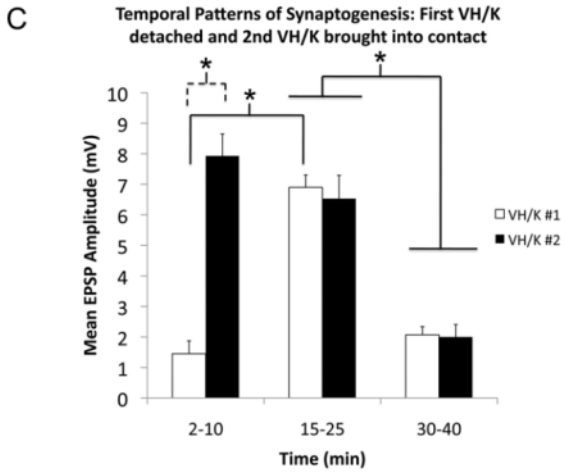
C
Temporal Patterns of Synaptogenesis: First VH/K detached and 2nd VH/K brought into contact
Mean EPSP Amplitude (mV)
0
1
2
3
4
5
6
7
8
9
10
2-10
15-25
30-40
Time (min)
VH/K #1
VH/K #2
*
*
*

Figure 3.4: Temporal pattern of connectivity between RPeD1 and VH/K growth balls.

The temporal patterns of synaptic connectivity between RPeD1 growth balls and their excitatory postsynaptic VH/K target growth balls were tested **(A)** (n=6). Prior to pairing postsynaptic VH/K growth balls, exogenous DA (10^{-6} M) was applied to show properly functioning DA receptors **(A-inset)**. These growth balls were then paired with RPeD1 growth balls and within 2-10 minutes following contact, synaptic transmission was detected. Action potentials induced in RPeD1 (arrow) triggered 1:1 excitatory postsynaptic potentials (EPSPs) in VH/K growth balls **(Ai)**. The synaptic strength significantly increased and reached maximum EPSP amplitude within 15-25 minutes post-contact **(Aii)**. However, 30-40 minutes post-contact, synaptic efficacy was reduced with an eventual disappearance of the synaptic communications between the growth balls **(Aiii)**. This loss of synaptic response did not involve postsynaptic receptor desensitization as the application of exogenous DA (10^{-5} M) to VH/K #1 induced a depolarizing response **(Aiii inset)** (n=5). To rule out the possibility that the loss of synapse was due to depletion of neurotransmitter content, the first VH/K growth ball (VH/K #1) was removed and a second VH/K growth ball (VH/K #2) was added to the original RPeD1 growth ball **(B)**. Similar to VH/K #1, synaptic transmission was detected within 2-10 minutes post-contact **(Bi)**. However, the amplitude of the observed EPSP was significantly larger than that detected in VK#1 at the same time post-contact. The synapse was maintained 15-25 minutes post-contact **(Bii)** before diminishing in strength 30-40 minutes post contact **(Biii)**. The mean EPSP amplitudes of VH/K #1 and VH/K #2 are summarized in **(C)** with significance determined with $p < 0.005$. Within group comparison was statistically tested using a univariate ANOVA with a Tukey's post-hoc test.

Figure 3.5

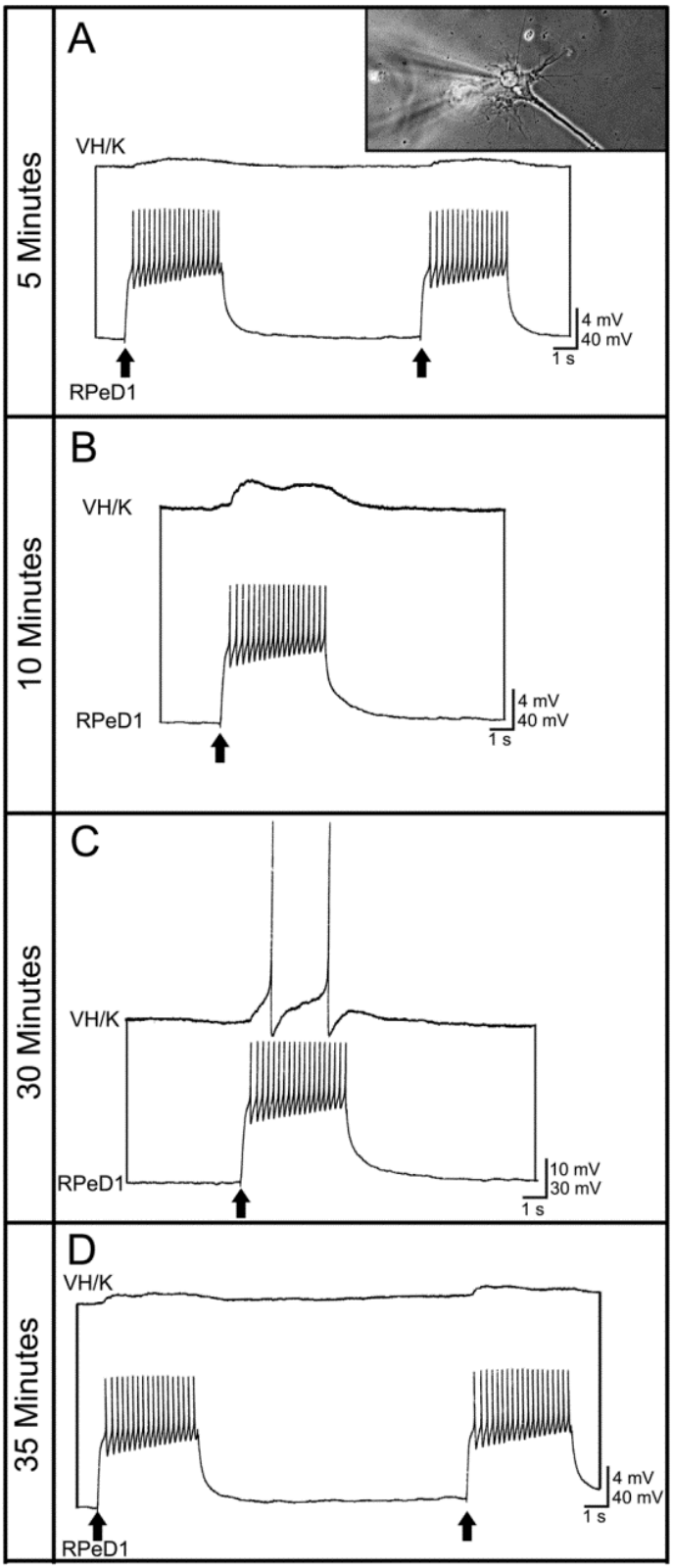
A
5 Minutes
VH/K
4 mV
40 mV
1 s
RPeD1
B
10 Minutes
VH/K
RPeD1
4 mV
40 mV
1 s
C
30 Minutes
VH/K
RPeD1
10 mV
30 mV
1 s
D
35 Minutes
VH/K
4 mV
40 mV
1 s
RPeD1

Figure 3.5: Both pre- and postsynaptic somata are required for "synapse sustainability". An intact presynaptic RPeD1 growth cone (soma attached) was paired with a postsynaptic VH/K growth ball (A inset) (n=5). I observed that within 5 minutes post contact, synaptic transmission could be detected in VH/K growth balls **(A)**. The amplitude of synaptic transmission increased by 10 minutes post contact **(B)** reaching a maximum synaptic strength by 30 minutes where an induced train of action potentials in RpeD1 triggered action potentials in VH/K growth balls **(C)**. This synapse was not maintained as a reduction in synaptic strength was observed by 35 minutes post contact **(D)** with an eventual loss of synaptic response by 1 hour.

Figure 3.6

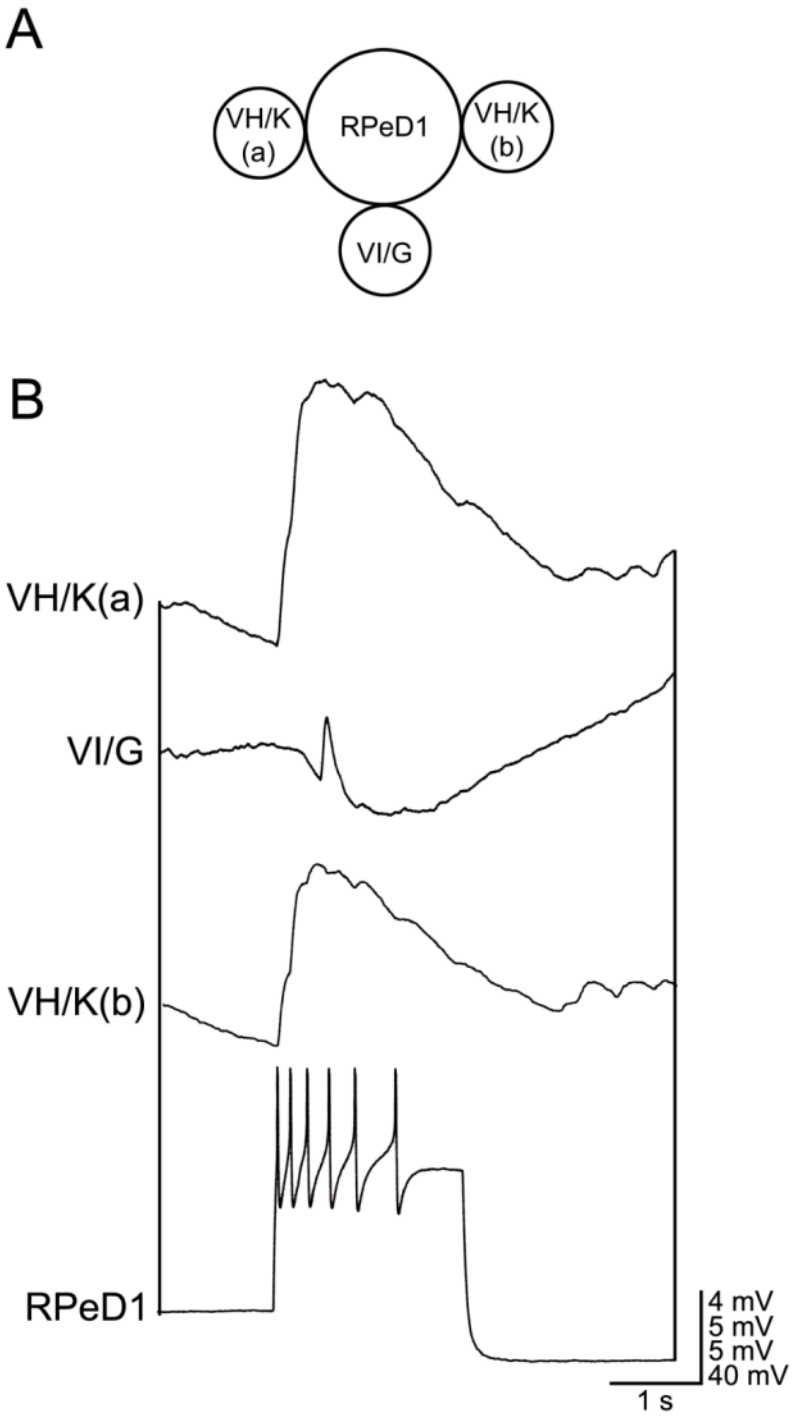

Figure 3.6: A single growth ball can simultaneously form multiple synapses with three different targets.

A single RPeD1 growth ball was paired with two VH/K growth balls and a VI/G growth ball simultaneously **(A)** (n=3). Within 25 minutes post-pairing, all three postsynaptic growth balls reformed their specific connections with the presynaptic RPeD1 growth ball. Action potentials induced in the RPeD1 growth ball triggered EPSPs in both VH/K(a) and VH/K(b) growth balls and a biphasic response in VI/G growth balls **(B)**. When the synaptic strength of triple-paired VH/K(a) and VH/K(b) growth balls were compared to single-paired VH/K growth balls using a univariate ANOVA, there was no statistical difference in the size of their respective EPSPs.

Figure 3.7

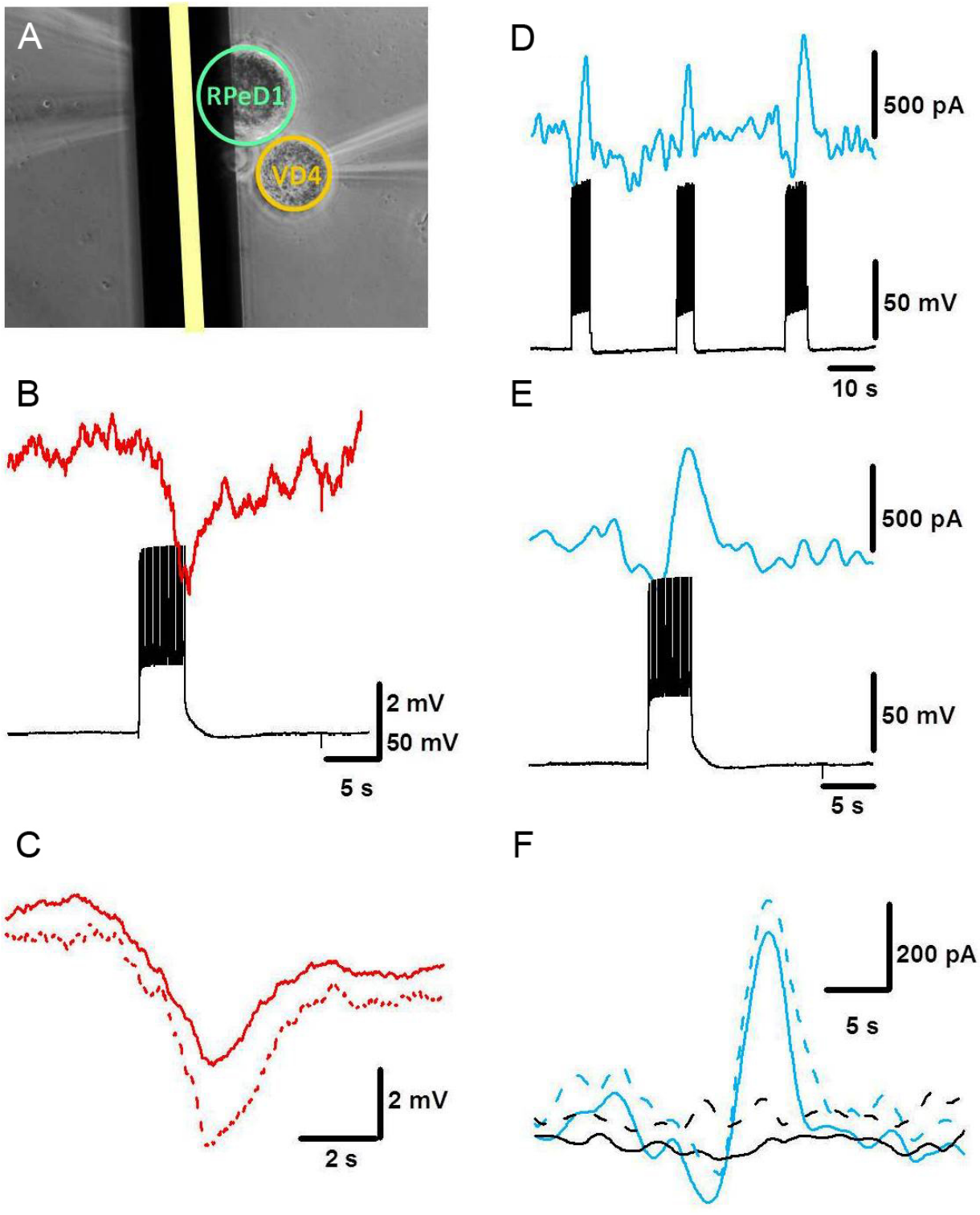
A
RPeD1
VD4
B
2 mV
50 mV
5 s
C
2 mV
2 s
D
500 pA
50 mV
10 s
E
500 pA
50 mV
5 s
F
200 pA
5 s

Figure 3.7: Comparing "sniffer" cell to planar amperometry electrode

To compare the amperometry chip with an establish technique for neurotransmitter detection in *Lymnaea*, **(A)** a VD4 somata expressing DA receptors was used to detect or 'sniff' DA release from the RPeD1 neuron. The RPeD1 neuron was placed at equidistance from the electrode and the VD4 somata, as shown. The thick yellow bar shows the active region of the microelectrode. When a tetanic pulse was triggered in RPeD1 **(B)**, hyperpolarization was observed in the VD4 membrane potential, precisely the same response observed when exogenous DA is applied on VD4. **(C)** The mean response from the sniffer cell (solid red line) and standard deviation (dashed line) is shown (n = 8). **(D)** When the microelectrode was used as the sensor, multiple tetanic stimulations evoked in RPeD1 resulted in corresponding current changes in the microelectrode. **(E)** An individual response from the electrode is shown. The mean response from the microelectrode is shown in the solid blue line and standard deviation in the blue dashed line. As a control, an adjacent electrode with no cell (center of electrode to adjacent center of electrode is 300 µm apart) was also measured and shown in black. All electrochemical measurements were carried out at +650 mV vs. Ag|AgCl.

Figure 3.8

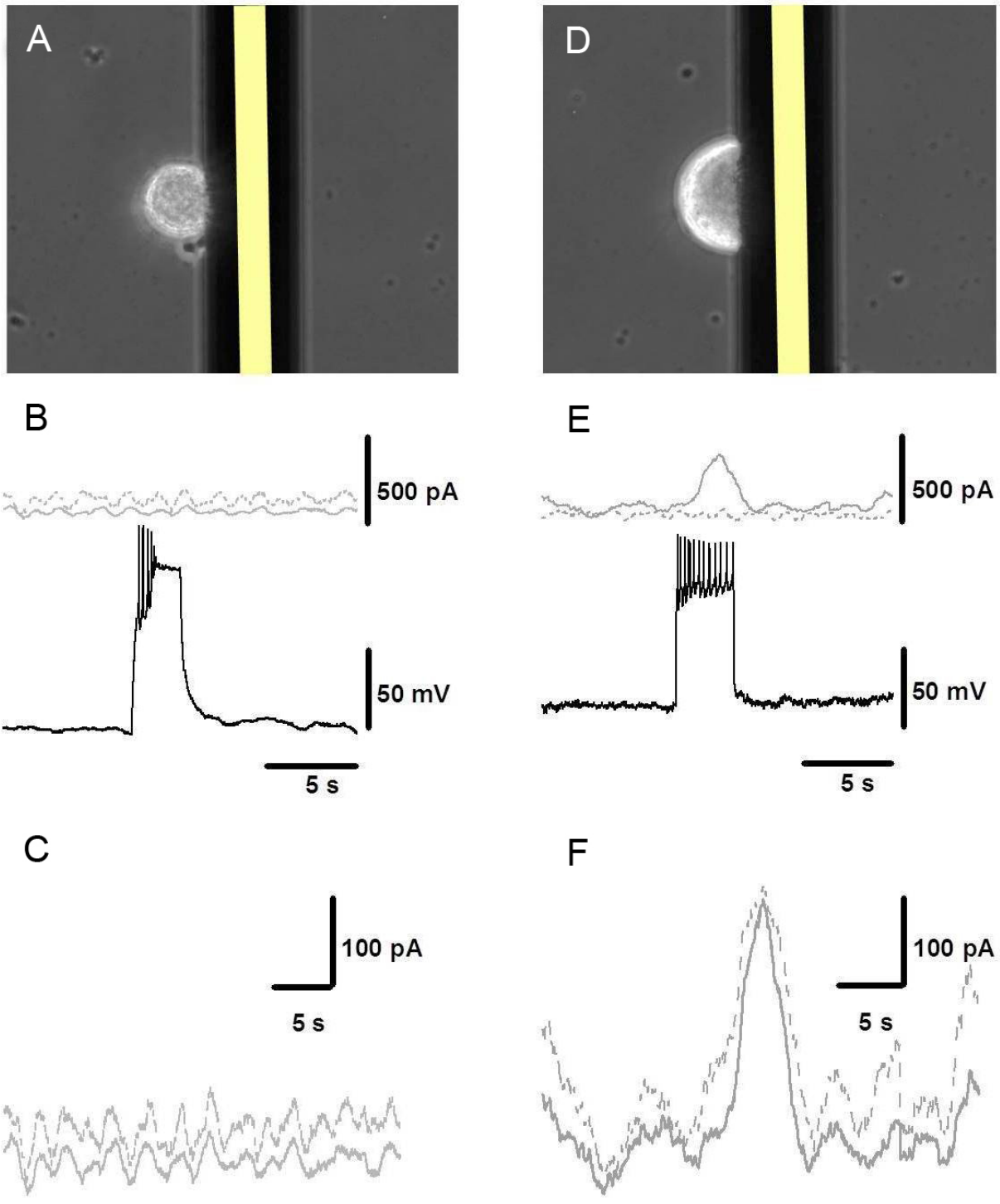

Figure 3.8: Measuring neurotransmitter release from VD4 (ACh; non-electrically active) and LPeD1 (serotonin; electrically active)

A single VD4 neuron was isolated and placed adjacent to a gold sensing electrode **(A)**. VD4 was impaled with an intracellular electrode and depolarized to trigger a tetanic stimulation. **(B)** As expected, we found that the electrode was not able to detect ACh release from VD4 neurons due to the inability for ACh to be oxidized like DA or 5-HT. The solid line depicts the current response for the detecting electrode and the dotted line a control response from an adjacent electrode with no neuron. Over an average of 6 cells, the **(C)** mean of the measured electrochemical response (solid line) and the standard deviation (dashed line) is shown. Next, to test the ability for the planar amperometry chip to detect another neurotransmitter, serotonergic LPeD1 was isolated and cultured adjacent to a gold electrode similar to the above described protocol. **(E)** Tetanic stimulation of LPeD1 triggered a response in the microelectrode (solid line) compared to an adjacent control electrode with no neuron (dashed line). **(F)** Over an average of 6 cells, the means electrochemical response (solid line) and standard deviation (dashed line) is seen.

Figure 3.9

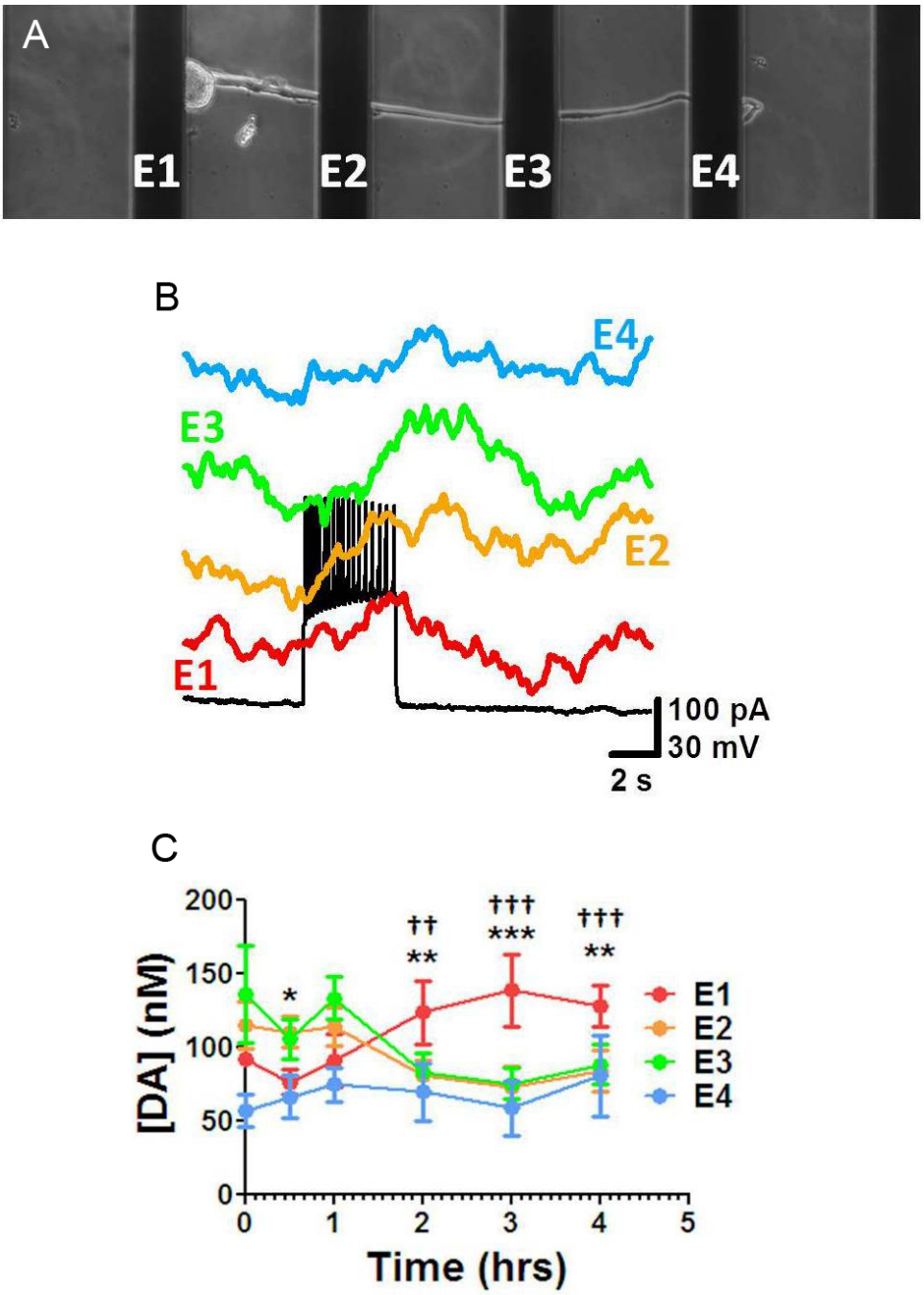
A
E1
E2
E3
E4
B
E4
E3
E2
E1
100 pA
30 mV
2 s
C
[DA] (nM)
200
150
100
50
0
0
1
2
3
4
5
Time (hrs)
*
††
**
†††
***
†††
**
E1
E2
E3
E4

Figure 3.9: Measurement of the spatial release of dopamine from various parts of an isolated neuron

(A) A single RPeD1 neuron and its axon was isolated and cultured over multiple microelectrodes. The cell body is located on E1 and the terminal on E4 with the axon spanning E2 and E3. **(B)** The RPeD1 soma was impaled with a sharp-electrode and a tetanic stimulation pulse was elicited while simultaneous multi-site electrically-evoked DA release was detected by the four electrodes. This sample trace shows the electrochemical response to RPeD1 stimulation immediately following isolation. Subsequently, the electrochemical response was measured 30 minutes and then at one, two, three and four hours following isolation. The electrochemical measurements and calculated nanomolar concentrations of DA is shown in figure **(C)**. We observed a change in DA release capabilities at different regions of the neuron. Data shown as mean ± standard deviation, (n=4) $*p<0.05$, $**p<0.01$, $***p<0.001$ for E1 vs. E2 and E3; $\dagger\dagger p<0.01$, $\dagger\dagger\dagger p<0.001$ for E1 vs. E4.

Chapter 4: Trophic Factor-Induced Activity 'Signature' Regulates the Functional Expression of Postsynaptic Excitatory Acetylcholine Receptors Required for Synaptogenesis and the Development of Novel Biotechnology for the Long-term Interrogation of Neuronal Changes during Development

Sections of this chapter have been published in the following manuscripts:
Martina, M., **Luk C.,** Py C., Martinez D., Comas T., Monette T., Denhoff M., Syed N. and Mealing G.A. (2011). "Recordings of cultured neurons and synaptic activity using patch-clamp chips." Journal of Neural Engineering 8(3): 034002. *–Reproduced with permission from IOP Publishing Limited.*

Mudraboyina A.K., Blockstein L., **Luk C.C.**, Syed N.I., Yadid-Pecht O. (2014) A novel lensless miniature contact imaging system for monitoring calcium changes in live neurons. IEEE Photonics Journal. **6**(1):1-15. *– Reproduced with permission from IEEE.*

4.1 Introduction

Activity-dependent mechanisms have previously been shown to be important in the formation of both excitatory and inhibitory synaptic connectivity in the developing brain (Feller 1999; Hanson and Landmesser 2003; Gonzalez-Islas and Wenner 2006; Kerschensteiner 2013) as well as synaptic plasticity (Atwood and Karunanithi 2002; Burrone et al. 2002; Hubener and Bonhoeffer 2014). However, unequivocal evidence for direct involvement of electrical activity in coordinating precise patterns of neuronal connectivity is still lacking. For instance, while both spontaneous and experience-driven neuronal activity patterns are considered necessary for the refinement of synaptic connectivity in the visual system (Constantine-Paton et al. 1990; Katz and Shatz 1996; Zhang and Poo 2001; Debski and Cline 2002; Tao and Poo 2005; Kerschensteiner 2013; Ackman and Crair 2014; Assali et al. 2014), as well as transmitter release and receptor expression (Lissin et al. 1998; O'Brien et al. 1998; Kilman et al. 2002; Borodinsky et al. 2004; Wang et al. 2005; Dulcis and Spitzer 2012; Guemez-Gamboa et al. 2014), our understanding of the underlying cellular and molecular mechanisms are unclear. This lack of knowledge in the field of neurodevelopment owes its existence to the fact that direct, controlled, non-invasive and

simultaneous measurements of electrical activity patterns of both pre- and postsynaptic neurons cannot be achieved, nor can they be manipulated experimentally over an extended period through conventional electrophysiological techniques. Further, because direct, long-term intracellular recordings from both pre- and postsynaptic neurons are not feasible in most model systems, only extracellular field recordings or short-term ion channel recordings have been used to deduce the involvement of electrical activity during neurodevelopment (Gaze et al. 1974; Holt and Harris 1983; Kirkby et al. 2013; Ackman and Crair 2014; Assali et al. 2014).

Trophic factors and their receptors have recently been shown to affect neuronal excitability by modulating ion channel function, transmitter release or synaptic plasticity, contributing to synapse assembly and efficacy(Park and Poo 2013). Specifically, studies in mammals have reported that neurotrophins trigger increases in electrical activity and excitability (Shen et al. 1994; Zhang et al. 2008; Murray and Holmes 2011) and that the neurotrophic factors influence activity-dependent processes for synapse formation and synaptic plasticity (Meyer-Franke et al. 1995; McAllister et al. 1996; Boulanger and Poo 1999; Du et al. 2000). However, precise target sites for trophic factor actions—whether pre- or postsynaptic—and the underlying steps remain poorly defined. Previous studies in *Lymnaea* have demonstrated that extrinsic trophic factors derived from brain conditioned medium (CM-a trophic factor laden culture media) are necessary for excitatory but not inhibitory synapse formation (Feng et al. 1997; Hamakawa et al. 1999; Woodin et al. 1999; Xu et al. 2009; Schmold and Syed 2012) and that this synapse formation likely involves trophic factor mediated changes in neuronal excitability. Specifically, Xu et al. (2009) noted that CM triggers an increase in postsynaptic activity in LPeD1 neurons, whereas a similar increase in electrical activity was not seen in the presynaptic neuron, visceral dorsal 4 (VD4). When the activity in LPeD1 was selectively blocked via

intracellular electrode hyperpolarization of LPeD1 neurons exposed to trophic factors, excitatory synapse formation between VD4 and LPeD1 failed to proceed (Xu et al. 2009). These observations demonstrated that postsynaptic activity is important for proper excitatory synapse formation. However, the mechanisms underlying trophic factor induced activity-dependent mechanism of synapse formation remained undefined.

Here, I utilized neuron-chip interfacing technology to obtain non-invasive, long-term activity recordings from individual neurons. I demonstrate that following CM addition, the activity pattern of postsynaptic neuron, LPeD1, undergoes a shift from inconsistent, high variance activity to a more consistent, low frequency variance over a period of 10 hours. The neurons that exhibited this activity pattern were more likely to express functional excitatory nicotinic acetylcholine receptors (nAChRs) than those that did not. Further, calcium channel blockers and *de novo* protein synthesis inhibitors impeded trophic factor induced activity patterns and subsequent expression of functional excitatory nAChRs.

From these data, it is postulated that trophic factor induced, activity-dependent mechanisms underlying synapse formation invoke (1) a rise in intracellular Ca^{2+} and (2) the modulation of neuronal membrane ion channel functions. However, to further validate the role of these two mechanisms in synapse formation, it is necessary to acquire tools that permit long-term, non-invasive monitoring of both intracellular calcium levels and ion channel activity, a feat that is technically not feasible with current technologies such as conventional calcium imaging and patch clamping.

Here I also report on two novel biotechnologies that allowed us to perform (1) long-term and stable interrogation of ion channel function in cultured LPeD1 neurons and (2) measurements of intracellular Ca^{2+} levels in LPeD1 cultured neurons. Specifically, these

technologies are the planar patch-clamp microchip (Martinez et al. 2010; Py et al. 2010; Martina et al. 2011) and the lensless micro imaging platform (Blockstein et al. 2012; Mudraboyina et al. 2014). These two technologies I consider important for further dissecting the roles of trophic factors and to define precise mechanisms underlying synapse formation.

In summary, in this study, I report on a novel mechanism whereby a specific activity "signature" was deemed necessary to prime the postsynaptic neuron for excitatory synapse formation and synaptic plasticity, through the functional expression of excitatory nAChRs. We further developed two novel biotechnologies that are crucial for our understanding of the precise mechanism underlying this activity "signature" and the expression of nAChRs.

4.2 Results

4.2.1 Trophic factors trigger activity in the post- but not the presynaptic cell.

Trophic factors present in *Lymnaea* CM are required for excitatory but not inhibitory synapse formation (Woodin et al. 1999). The CM-induced effects are also mimicked by *Lymnaea* epidermal growth factor purified from *Lymnaea* albumin glands, human EGF and TGF alpha. More recently, the *Lymnaea* EGF receptor was cloned and its knock down prevented both CM and EGF-induced excitatory synapse formation (van Kesteren et al. 2008). Here, to ensure that a full complement of all naturally occurring trophic molecules secreted intrinsically by the brain tissue are present, I opted to use *Lymna*ea CM. It is important to note that all CM-induced effects reported here are also mimicked by LEGF, albeit less consistently.

To test for the effects of CM on isolated presynaptic VD4 and postsynaptic LPeD1 neurons, cells were placed on individual microelectrode array (MEA) electrodes overnight in DM **(Fig. 4.1B)**. Twelve to eighteen hours post-isolation, all cells were simultaneously recorded for two hours. This initial two-hour period served as control recordings for VD4 and LPeD1 neurons prior to CM exposure. In all cases, neither LPeD1 nor VD4 exhibited any persistent activity during these control recording periods (**Fig. 4.1A**). Next, CM was exchanged with DM and an additional 10 hours of recordings were conducted. Whereas CM addition did not have any significant effect on VD4, the activity in LPeD1 increased significantly **(Fig. 4.1A)**. Specifically, within the first hour, small bursts of action potentials (~2-3 AP/burst) were recorded in LPeD1. In the second hour, the size of the bursts (~4-5 AP/ burst) as well as the frequency of the bursting events increased. The third and fourth hour revealed a further increase in the duration of bursting activity (~7-10 AP/burst) with the fifth hour showing larger bursts of activity that were comprised of 15-30 action potentials per event. From the sixth to the tenth hour, LPeD1 neurons

exhibited an almost persistent level of action potential firing, marked by brief periods of inactivity. Conversely, no activity change was observed in VD4 over the 10 hour period. Hence, trophic factors triggered activity in postsynaptic LPeD1 neurons, but not presynaptic VD4. As a control experiment, DM was exchanged with fresh DM to rule out mechanical artifacts that may have caused neuronal excitability. I saw no change in activity (data not shown). I next performed quantitative measurements of LPeD1 activity.

4.2.2 Trophic factors selectively trigger a progressive increase in LPeD1 activity over a 10 hour period.

To quantify CM-induced activity increases, I analyzed the total number of action potentials in LPeD1 neurons in 20 minutes bins, using VD4 neurons as a control. Prior to the addition of CM, VD4 and LPeD1 neurons were relatively quiescent (**Fig. 4.2A,B**). Upon CM addition, control VD4 neurons did not show any change in activity, whereas LPeD1 neurons exhibited a rapid increase in spiking, which ramped up over the next ten hours recording period (**Fig. 4.2A,B**). To determine statistical trends in activity changes, the data were binned into two-hour blocks. I found that following CM addition, the immediate activity increase in the first 0-2 hours was significantly greater compared to control. This trend continued until hours 6-8, at which point activity peaked and maintained a steady level until the termination of recording at ten hours (**Fig. 4.2C**; n=33). All levels of activity following CM addition were significantly greater than when cells were maintained in DM ($p<0.05$). Activity during the 4-6, 6-8 and 8-10 hours increased significantly from the initial 0-2 hours ($p<0.05$). Furthermore, activity at hours 6-8 and 8-10 was also significantly greater than hours 2-4 ($p<0.05$). These data thus suggest that CM induced activity in LPeD1 increases until a plateau is reached during hours 6-8 and 8-10

post addition of the CM. The peak level of activity occurred at hours 6-8 following the CM addition (5011±660) and did not change significantly at hours 8-10 ($p>0.05$). In all instances observed, a large increase in LPeD1 activity was observed immediately following CM addition (n=33), while VD4 remained unresponsive (**Fig. 4.2C**; n=9).

4.2.3 nAChR phenotype in LPeD1 is correlated with different trophic factor induced activity patterns.

To test for the presence of functional excitatory nAChRs, intracellular recording were coupled with exogenous ACh applications. Similar to our previous studies (Xu et al. 2009), LPeD1 neurons cultured in DM were inhibitory. However, following CM exposure, a portion of the LPeD1 cells switched from inhibitory to excitatory (15/33) **(Fig. 4.3Bi)**. In particular, ACh application resulted in an excitatory response, which triggered action potentials in LPeD1. In a smaller population of cells, either no or an incomplete changeover was observed, with some LPeD1 neurons remaining either inhibitory (9/33) **(Fig. 4.3Bii)** or changing into an intermediary phase known as the "biphasic" response (9/33; elements of excitation and inhibition) **(Fig. 4.3Biii)**. All three different end-point phenotypes were stratified and correlated with their activity pattern **(Fig. 4.3A)**. In cells exhibiting an inhibitory response to ACh, an immediate increase in activity was noted following the CM exposure, which remained unchanged over time. In contrast, in excitatory LPeD1 neurons, there was a pattern of increasing activity over time which eventually transitioned into more consistent firing that persisted throughout the experiment. Conversely, in biphasic neurons, a similar trend towards increased activity seen in excitatory LPeD1 neurons was observed. This response to CM, however, appeared to be delayed in some neurons whereby the activity onset occurred approximately three hours after the addition

of CM. Additionally, the total activity over a 10 hour time window was also less than that seen in neurons exhibiting an excitatory response. These data suggested to me that neurons exhibiting a biphasic phenotype exhibit characteristics intermediate of an inhibitory and excitatory response, which could potentially switch over to complete excitation given the additional time.

To further quantify this difference in activity patterns in the above three phenotypes, I examined the total number of action potentials over a 10 hour period following the trophic factor addition and correlated them to the phenotype observed at the end of 10 hours (**Fig. 4.3C**). I found that LPeD1 neurons that expressed functional excitatory nAChRs were significantly more active than those cells that expressed functional inhibitory nAChRs (both inhibitory LPeD1, VD4). However, there was no significant difference in activity between inhibitory LPeD1 and control VD4 ($p>0.05$) or between biphasic LPeD1 and excitatory LPeD1 ($p>0.05$). I did, however, observe a trend towards increased activity from inhibitory to biphasic to excitatory cells. These data suggest that the level of activity, specifically the total number of action potentials, is strongly correlated with an ultimate phenotype that a LPeD1 neuron exhibits following CM exposure.

Next, to further characterize differences in activity between the three phenotypes, I examined activity trends over the 10 hour period. A unique trend for each phenotype was observed (**Fig. 4.4A**). For instance, in LPeD1 neurons expressing only functional excitatory receptors, an immediate increase in activity following CM addition was noted at hours 0-2 after the CM addition, which continued to increase significantly before peaking and plateauing at hours 4-6. In LPeD1 neurons expressing a biphasic phenotype, an initial trend, similar to that of excitatory LPeD1 was noted (hours 0-4). However, the peak levels of activity were less than those observed in excitatory LPeD1 neurons. In contrast, in LPeD1 cells exhibiting an inhibitory

response, there was a similar immediate increase in activity after the CM addition at hours 0-2. However, the subsequent activity remained flat with no further increases following hours 0-2. These data thus suggest that the nAChR receptor phenotype in LPeD1 appears to be correlated with progressive increases in activity following the trophic factor addition. LPeD1 cells with excitatory nAChRs not only fired more action potentials but also exhibited a specific trend as compared to their counterparts expressing inhibitory nAChRs. These data also suggest that a specific pattern of activity is likely required for trophic factor induced functional excitatory receptor expression.

4.2.4 Patterned activity was correlated with excitatory nAChR expression.

To provide better characterization of the activity patterns over time, I captured an individual action potential and examined a "time stamp" for its occurrence. With these time logs, I calculated the interspike interval (ISI; time between two adjacent action potentials). I then measured the inverse of each ISI to provide a measure of frequency that corresponded directly with two adjacent action potentials. These ISIs were visualized on a scatterplot allowing us to determine variability, frequency and change in activity (**Fig. 4.4Bi,Bii**).

Using the above approach, cells were deemed to have a "patterned" activity after 10 hours of trophic factor exposure if, *(1)* there was a progression from high to low variability in frequency, and *(2)* the final frequency of activity ranged from ~1-1.5 Hz (**Fig. 4.4Bi**). In cells that were deemed to be "non-patterned", the action potential frequency continued to show *(1)* variability in their inverse ISI values as compared to the neurons with patterned activity (**Fig. 4.4Bii**; $p<0.05$) and *(2)* did not achieve a consistent ~1-1.5 Hz activity during the latter half of the recording.

With these criteria, I examined whether this "patterned" activity could be generalized to all LPeD1 neurons. I performed blind scoring of each cell's activity using the inverse ISI analysis and predicted the final cell phenotype (excitatory, inhibitory) using the above two criteria (**Fig. 4.4C**). I found that the expression of "patterned" activity was tightly correlated with excitatory receptor expression, with 73% of excitatory LPeD1 cells showing "patterned" activity based on the above criteria. In contrast, only 46% of biphasic LPeD1 and 10% of inhibitory LPeD1 fulfilled the criteria. These data demonstrate that "patterned" activity, as defined by our two above parameters may be required for the functional expression of excitatory nAChRs.

4.2.5 Activity was necessary for the expression and maintenance of excitatory nAChR expression.

To determine whether activity triggered by CM was indeed necessary for the expression of excitatory nAChRs, I used intracellular sharp electrodes to selectively hyperpolarize LPeD1 neurons that were exposed to CM. Neurons were impaled with sharp electrodes and a hyperpolarizing current was injected to prevent action potentials from firing. Following the eight hours hyperpolarization period and neuronal quiescence, I first found that cells remained physiologically viable and as robust as their control counterparts **(Fig. 4.5A)**. Using exogenous ACh application, I found that while 95% (n=20) of control neurons showed an excitatory response to exogenous ACh puffs, only 29% (n=7) of hyperpolarized neurons exhibited an excitatory response with the remaining 71% exhibiting an inhibitory response **(Fig. 4.5A)**. These data thus demonstrates that the activity triggered by CM is necessary for the expression of functional excitatory nAChRs.

Next, to determine whether the triggered activity was important for the maintenance of functional excitatory AChR expression, I washed out the CM following 10 hours of exposure and observed changes in activity patterns. I found that CM withdrawal and its replacement with DM significantly decreased activity immediately after the removal of the trophic support. Specifically, number of action potentials recorded in the two hour window following the removal of CM was 2248±501, which was significantly reduced ($p<0.05$) compared to the time periods 2-4 hours (3355±773), 4-6 hours (4521±900), 6-8 hours (4575±764) and 8-10 hours (4595±625) (n=10; **Fig. 4.5B)**. When tested with exogenous ACh following DM washout, all cells exhibited an inhibitory response. These experiments demonstrate that the activity induced by CM is not only necessary for triggering the functional expression of nAChR, but also required for the maintenance of these excitatory nAChRs.

4.2.6 Trophic factor effects on LPeD1 required the presence of the cell body.

Extrasomal compartments such as axons and dendrites are thought to exhibit trophic factor sensitivities, independent of their respective somata. Here, to determine the responsiveness of LPeD1 soma versus extrasomal (axonal) compartment to CM, I physically isolated the axon from the cell body, and tested its responsiveness to CM. To do this, neurons were extracted from the central ring ganglia with an extensive portion of their axons attached (~500 μm). The cell bodies were placed onto individual microelectrodes and their respective axons were gently laid across multiple adjacent electrodes. A fine sharp glass electrode was used to sever the cell body from its axon, resulting in an isolated somata and axon **(Fig. 4.6A)**. I found that when in DM, compared to the LPeD1 soma (which had little to no activity), the isolated LPeD1 axons exhibited a low level of tonic activity (n=4). When CM was subsequently introduced, the level of

tonic activity in the isolated axons increased **(Fig. 4.6Bi)**. However, unlike LPeD1 cell body, no change in patterned activity was observed in the axon **(Fig. 4.6Bii)**. A scatterplot reveals the temporal pattern of initial activity increases, which rapidly reached a steady state level **(Fig. 4.6C)**. When a one-way ANOVA was performed on the activity observed in the 2 hour bins, the increase was found not to be significantly different from that observed prior to CM exchange **(Fig. 4.6D)**. These data thus suggest that the CM- induced, long-term activity-dependent changes specifically impact somata and may thus require *de novo* protein synthesis and gene induction for the functional expression of nAChR.

4.2.7 *De novo* protein synthesis is required for activity changes following trophic factor addition.

Next, I examined potential mechanisms underlying the CM-dependent modulation of activity. New protein translation has previously been shown to be a requirement for the expression of excitatory nAChRs (Xu et al. 2009). However, whether long-term changes in activity patterns are also contingent upon *de novo* protein synthesis is yet to be studied. To determine this, I cultured LPeD1 neurons on MEAs in DM (1 hour) containing a protein synthesis blocker, anisomycin (15 µg/mL), prior to CM addition. I found that while treatment with anisomycin did not significantly affect the initial activity increases normally associated with CM at 0-2 and 2-4 hour time points, it did, however, block the activity increases normally seen at hours 4-6, 6-8 and 8-10 in CM (**Fig. 4.7Ai**). This suggests that *de novo* protein synthesis is required for the expression of stereotypical activity pattern seen in control LPeD1 neurons exposed to CM, but not for the induction of an immediate activity response. In addition,

exogenous ACh revealed that all anisomycin treated neurons exhibited an inhibitory response (**Fig. 4.7Aii**).

4.2.8 Calcium channel function is required for the upregulation and expression of patterned activity following trophic factor addition.

To determine whether longer-term changes in CM-induced activity patterns involved Ca^{2+} influx via the activation of voltage gated Ca^{2+} channel (VGCC), the channel activity was perturbed by a non-specific calcium channel blocker, cadmium, and a specific L-type calcium channel blocker, nifedipine (Spafford et al. 2006). I observed that treatment with either cadmium or nifedipine significantly reduced the total level of activity. Specifically, in excitatory LPeD1 neurons, 26349±13461 action potentials were elicited during the 10 hour period following CM exposure. In contrast, LPeD1 neurons treated with cadmium and nifedipine had on an average, 12864±6385 action potentials and 14063±6160 action potentials, respectively. When this activity was binned into two-hour blocks, no significant difference between excitatory LPeD1 neurons and cadmium or nifedipine treated neurons was observed at hours 0-2 and 2-4. However, by hours 4-6, 6-8 and 8-10, there was a significant reduction in the average number of action potentials ($p<0.05$; **Fig. 4.7B**). When the 1/ISI was plotted, I found that blocking VGCCs prevented the stereotypical activity pattern observed in excitatory LPeD1 neurons **(Fig. 4.7D)**. These data suggest that the Ca^{2+} influx through VGCCs is a requirement for subsequent, long-term increases in activity and pattern formation at later time periods following the CM exposure. Additionally, similar to what was observed in our previous studies, inhibiting Ca^{2+} influx through VGCCs perturbed the functional expression of excitatory nAChRs in CM exposed LPeD1 neurons **(Fig. 4.7Ci,Cii)**.

4.2.9 LPeD1 contact with presynaptic partner VD4 reduces trophic factor induced activity.

Next, to test whether pairing with a synaptic partner would alter trophic factor-induced activity patterns in LPeD1 neurons, presynaptic VD4 was juxtaposed with LPeD1 neurons in a soma-soma configuration in DM. The synaptic pairs were cultured on a high density microelectrode array (MCS-60HDMEA30/10iR-ITO-gr), permitting independent channel recordings of both pre- and postsynaptic neurons. Prior to CM addition, activity was recorded for a 30 minute time period to determine its basal levels. Similar to the activity seen in single isolated VD4 and LPeD1 neurons, a very low level of activity was observed in both synaptic partners. A 30 minute control recording of LPeD1 and VD4 neurons revealed an activity level of 1±4 AP and 1±3 AP (n=12), respectively. Both neurons were then impaled with intracellular sharp-electrodes and evidence for synaptic connectivity sought electrophysiologically. Neither a single action potential nor the tetanic burst elicited in VD4 generated a corresponding postsynaptic response in LPeD1, indicating the absence of a functional synaptic connection between the cells (**Fig. 4.8Bi**). Next, DM was exchanged with CM and activity was further measured for 10 hours. Similar to the responses seen in single neurons, I found that CM triggered an initial increase in activity. In contrast, however, this activity pattern tended to follow a trend similar to that observed in inhibitory and biphasic neurons rather than excitatory LPeD1 cells. For instance, within the first two hours following trophic factor addition, the paired LPeD1 neurons exhibited 1772 ± 732 AP, a value statistically similar to single excitatory LPeD1 neurons (2263 ± 1594)($p<0.05$). At hours 4-6, where a significant increase in activity was observed in single excitatory LPeD1 neurons (6027 ± 3361), synaptically paired LPeD1 neurons continued to express a level of activity that was statistically similar to inhibitory and biphasic neurons with 2436 ± 921 AP ($p>0.05$), but significantly reduced ($p<0.05$) compared to single

excitatory LPeD1 neurons. Activity at the remaining 6-8 hours and 8-10 hours revealed similar trends (**Fig. 4.8A**). Both single and paired VD4 neurons did not exhibit any significant response to trophic factors (data not shown). At the end of a 10 hours period, in all VD4/LPeD1 pairs, an excitatory synapse had formed whereby presynaptic activity triggered 1:1 postsynaptic potentials and a tetanic pulse elicited compound postsynaptic potentials (**Fig. 4.8Bii**).

Taken together, the above data demonstrates that in a paired configuration: (1) VD4 and LPeD1 neurons in DM behave similar to single, unpaired cells, (2) CM induced specific activity in the post- but not the presynaptic neuron, and (3) target cell contact prevented the "runaway" activity in LPeD1 cells seen in single cells after the CM exposure.

Notwithstanding the above studies, several questions vis-à-vis the involvement of trophic factors leading to the expression of nAChRs remain unanswered. For instance, our lab has demonstrated that trophic factors acting via receptor tyrosine kinases trigger action potentials in postsynaptic (LPeD1) but not presynaptic cell VD4, and that this activity invokes an immediate Ca^{2+} influx via voltage-gated calcium channels (Xu et al, 2009). In this chapter, I showed that the trophic factors not only trigger immediate action potentials but that these spikes gradually transform into a unique bursting pattern in progression with time. This transformation of single spikes into a bursting pattern requires *de novo* protein synthesis, suggesting a longer-term transformation and modulation of calcium channel expression and function may be a prerequisite for trophic factor mediated excitatory synapse formation. I thus posed the question whether trophic factor-induced change from single spikes to bursting is indeed a prerequisite to synapse formation, which in turn, is contingent upon the expression of voltage-gated Ca^{2+} channels and their activity. Because conventional patch-clamp and intracellular calcium measurement techniques only allow short-term interrogation of neuronal ion channel activities, I opted to

resolve this issue by developing two novel technologies. The first of these, developed in partnership with the National Research Council of Canada (NRCC), is a novel planar patch clamp chip that allows long-term (9-12 hours) analysis of ion channels. The second chip that I developed in collaboration with Dr. Yadid-Pecht (Schulich School of Engineering, University of Calgary) is based on a lensless miniature contact imaging system for monitoring calcium change in live neurons.

4.2.10 One-hole Silicon Nitride Planar Patch Clamp Chip

All excitable cellular functions rely upon ion channels, which are integrated into the plasma membrane of cells. Currently, the gold-standard technique for investigating ion channels is glass electrode patch clamping (Neher et al. 1978), a technology that has remained relatively unchanged since its inception. This approach requires the use of an expensive and rather complicated rig setup that includes a microscope, high precision micromanipulators, and an accompanying air table etc. However, due to the inherent unstable nature of a suspended glass electrode that is used to form a seal with a microscopic portion of a cell's membrane, it is technically challenging to perform long-term recordings (10 hours plus) on brain cells. This limitation creates a barrier for research that requires long-term recordings—as was the case in my research. In particular, for us to understand how the membrane ion channel complements and activity change following trophic factor exposure, I consider it imperative that I acquire stable means to interrogate ion channel activity over an extended period of time. To develop such a tool, we designed a system whereby cultured neurons could be patch-clamped with a stable seal in the absence of micromanipulators, microscopes or other equipment required for conventional patch clamp technology.

The solution to this problem was the development of a planar patch clamp chip (**Fig. 7.1A**). In this technology, the conventional patch pipette opening is mimicked by an aperture fabricated into a planar silicon surface. Therefore, the neuron can be brought to the aperture rather than manipulating a large pipette to the neuron itself—the most unstable part of a conventional patch-clamp system. However, several criteria needed to be fulfilled to obtain high-fidelity recordings first. These included (1) low shunt capacitance, (2) low access resistance, (3) high cell membrane-to-aperture seal resistance, (4) high dielectric rigidity of the material and (5) a thin membrane due to the small size of the aperture required, but mechanically strong enough to be suspended. To fulfill these criteria a silicon nitride layer with a single aperture was suspended over a layer of silicon. Brief descriptions of the silicon nitride planar patch clamp chip and the poly-imide planar patch clamp chip fabrication process are provided in appendix (Chapter 7 - Appendix) with further details found in our published manuscripts (Py et al. 2010; Martina et al. 2011).

4.2.10.1 Patch clamp recordings from the one-hole silicon nitride chip

To perform recordings on the one-hole silicon patch clamp chips (**Fig. 7.1A**), individual *Lymnaea* neurons (LPeD1, VD4) were extracted and selectively placed over top of the aperture (**Fig. 4.9A,B**). Following two hours of culture, whereby the neurons could properly adhere to the poly-lysine coated surface, the chips were tested with an Axopatch 200B (Axon Instruments, Foster City, CA) amplifier. The recording electrode from the headstage was connected with the tubing from the patch chip and a reference electrode was placed into the culture well. A total of 11 chips with cultured neurons were tested, with five of these chips showing a large capacitive transient in response to a series of test voltage steps. These large capacitive transients suggested

that the five samples were likely already spontaneously in a whole cell configuration. Of the remaining six chips, four had a resistance of 14.2 ± 6.2 MΩ, but no corresponding large capacitive transients. These four chips likely did not form high cell membrane-to-aperture seals to allow for proper recording from the cells. The remaining two displayed an infinite resistance or "overload" of the patch amplifier, suggesting that an air bubble may have developed over the aperture, disrupting the electrical continuity of the chip. Of the five chips that displayed a large capacitive transient, we conducted both current-clamp and voltage clamp recordings on each of the chips. We found that as we provided negative step current pulses to the neuron, a hyperpolarization of the membrane potential was observed. Conversely, as we elicited positive step current pulses, we observed depolarization of the membrane potential until the neuron reached a threshold potential, resulting in the elicitation of action potentials. These action potentials increased in frequency as we further depolarized the neuron (**Fig. 4.9C**). This is the first such recording of cultured neurons on a planar patch-clamp chip, revealing the robustness and high fidelity of the neurochip. To determine the fidelity and resolution of our recordings in comparison to conventional forms of patch-clamp recordings, we calculated the rise times of currents recorded during the rising phase of the action potential in voltage clamp mode. From 10% to 90% of the maximum signal, we recorded a rise time of 0.69 ± 0.27 ms (n=5) which is in line with previous recordings of Na^+ conductance channels in *Lymnaea* neurons from 0.99 to 2.72 ms. This suggests that we are able to record in the upper echelon of conductance signals observed in *Lymnaea* neurons, with no signal loss (Gilly et al. 1997).

4.2.10.2 Patch clamp recordings on synaptically connected neurons on the one-hole silicon nitride chip

With the capacity to record established, and verification that the chip was indeed able to capture the highest frequencies of activity from our cultured neurons, we were interested in determining whether the chip could also detect synaptic activity, specifically postsynaptic currents. Using our soma-soma model, we cultured a single postsynaptic LPeD1 neuron overtop of the aperture and then placed the presynaptic VD4 neuron either on top of (stacked) or beside the LPeD1 neuron (**Fig. 4.10A,B**). We paired pre- and postsynaptic neurons overnight in a soma-soma configuration and allowed them to develop synapses. By the time, neurons switch from tonic spiking to a bursting pattern and are expected to have develop synapses (8-12 hours), we performed sharp-electrode intracellular electrophysiology on the presynaptic neuron while recording the synaptic currents in the postsynaptic LPeD1 neuron from the chip. Using the sharp-electrode, we depolarized the VD4 neuron to a sub-threshold potential while monitoring the postsynaptic LPeD1 neuron. No change in the postsynaptic neuron was detected, suggesting that there was no electrical coupling between the neurons (**Fig. 4.10D**). Next, when we depolarized the neuron to trigger action potentials in VD4, we observed that the chip was able to detect synaptic potentials in LPeD1 as seen by the membrane depolarization concurrent with each presynaptic action potential (**Fig. 4.10D**). These data not only validate the biocompatibility of our planar patch clamp chip (healthy neurons, robust ionic currents and no electrical coupling), but also demonstrate their ability to monitor membrane voltage and synaptic currents over an extended time period.

Next, to further demonstrate the high fidelity recordings of the 1-hole SiN chip, we induced short-term potentiation in the neuron and attempted to use the chip to detect a form of synaptic short-term potentiation observed in this synaptic pair *(Details of this form of synaptic plasticity discussed in Chapter 5)* (Luk et al. 2011). Specifically, we showed that following a

tetanic stimulation (a high frequency train of action potentials), the postsynaptic potential (PSP) triggered subsequent to this induction protocol were potentiated. While in current-clamp mode the postsynaptic neuron was held at -83 mV membrane potential. We show that single action potentials (thin arrow) results in a 1:1 PSPs that were detected by the chip. A subsequent train of action potentials with a tetanic stimulation results in a compound PSP, which was also detected by the chip (asterisk). Following this tetanic stimulation induction protocol, a subsequent action potential results in a PSP with a potentiated amplitude (thick arrow), which is detected by the chip recording (**Fig. 4.11A**). When we switched into voltage-clamp mode and held the neuron at -65 mV, we were again able to detect synaptic currents resulting from the tetanic stimulation—in addition to the potentiated synaptic current following the tetanic induction protocol (**Fig. 4.11B**).

Next, to verify that the recorded electrical activity in the postsynaptic neuron was indeed a chemical synapse, we attempted to block synaptic transmission between VD4/LPeD1 with the nAChR antagonist, tubocurarine chloride. A solution of tubocurarine chloride dissolved in DM was added to the chip to produce a final concentration of 100 μM. Following this protocol, we depolarized VD4 neuron and allowed for it to tonically fire action potentials while continuing to monitor PSP activity in LPeD1. Within 10 to 15 seconds of tubocurarine chloride addition, EPSP amplitudes in LPeD1 were noted to decrease until a complete block was achieved (**Fig. 4.12**). This provided further evidence that the 1-hole SiN chip was indeed detecting synaptic activity.

Finally to demonstrate the continuity between the subterranean circuit and the whole-cell, we exchanged the microfluidics channel pipette solution with a solution containing the fluorescent dye Lucifer yellow (2 mM) and allowed for the chip to sit undisturbed for 15 minutes. We then imaged the chip using confocal microscopy, which showed that the postsynaptic LPeD1 neuron attached to the chip had been filled with the dye, while the

presynaptic neuron remained unfilled (**Fig. 4.10B, C**). This is the first published case where synaptic currents have been recorded from cells cultured on a planar patch clamp chip.

However, despite the broad functional abilities of the SiN chip, to monitor synaptic currents, it was necessary to be able to record currents from more than one neuron. Specifically, it was necessary to have more than one independent recording aperture on the culture surface. With the SiN chip, due to the innate properties of the silicon crystal structure and the resulting etching patterns of the silicon wafer, the smallest distance achievable between two apertures would be ~600 µm (Py et al. 2010). This distance would not be practical for recording from both a presynaptic and postsynaptic neuron in our soma-soma model, where the approximate distance between the centers of two synaptically paired neurons (VD4 radius~25 µm; LPeD1 radius~35 µm) would be approximately 60 µm. Therefore, it was necessary for us to design a second chip with two apertures to simultaneously record two separate sites in a single culture system. To do this, we chose a different design and fabrication material that consisted of a hybrid polyimide (PI) surface with a polydimethylsiloxane (PDMS) subterranean structure (**Fig. 4.13**).

4.2.11 Two-Hole Polyimide Planar Patch Clamp Chip

4.2.11.1 Patch clamp recordings from a two-hole polyimide/polydimethylsiloxane chip

To test the two-hole PI chip (**Fig. 7.2A**), individual neurons were cultured on each of the apertures (**Fig. 4.13A,B**). A total of eight microchips were tested where four had only one neuron over the aperture and the remaining four had neurons over both of the apertures. In the 12 neurons tested, two had a high seal resistance of 5.5 and 8.3 GΩ, suggesting cell-attached configuration; four neurons had large capacitive transients, suggesting a whole-cell patch-clamp configuration; six neurons showed a lower resistance of 4.03 ± 0.6 MΩ with no large capacitive

transient, suggesting that the membrane-to-aperture seal did not form properly and we could not record activity in these six cells. With the two cells in cell-attached configuration, we could not record single channel activity. However, by applying suction in the subterranean channel, a typical procedure used for rupturing the cell membrane in conventional patch clamping, the cell began displaying large capacitive transients, suggesting a rupturing of the membrane and entry into whole-cell configuration. Similar to the one-hole SiN chip, we tested these six neurons in both current-clamp and voltage clamp mode. We provided step currents in current-clamp mode and observed action potentials when the membrane potential had reached threshold. Conversely, when we switched to voltage-clamp mode, we were able to record currents from the action potentials (**Fig. 4.13C**). We found that these currents had a rise time (10-90%) of 0.84 ± 0.02 ms, meaning that the PI chip also had the temporal resolution to detect signals in the upper echelon as described above. Further, to test the stability of the neuron following initial recordings, we continued to incubate the neurons and showed that even up to twelve hours following initial recordings, the neuron retained its whole-cell patch clamp configuration despite repeated movement to and from incubators and could continue to be recorded from. This study is the first to demonstrate a planar patch-clamp device detecting whole-cell patch clamp currents on cultured neurons from two separate sites and is a critical step to detecting currents from synaptically connected neurons. More importantly, the stability of the recordings over a long time period provides us the ability to monitor ion channel activity over an extended period of time. Particularly, to be able to record single and synaptically connected LPeD1 and VD4 neurons and their changes in ion channel activity and complement over the 10 hour period following CM exposure. This technology can now be used to answer the questions of whether

Ca^{2+} channel expression and functional changes are concomitant with trophic factor-induced modulation of single spikes to a bursting pattern.

Next, in previous studies by Xu et al. (2009), trophic factor mediated excitatory synapse formation was found to involve activity induced intracellular Ca^{2+} oscillations in the postsynaptic LPeD1 neuron but not the presynaptic VD4 neuron. In our current study, we find that blocking VGCCs resulted in the lack of activity "signature" and a subsequent lack of functional excitatory nAChR expression. However, until now, the precise patterns and levels of intracellular calcium have only been monitored for short time periods, owing to the fact that extended recordings have been difficult to achieve with photo-bleaching of the dye and evaporation of the culture media, all problems that prevent long term recordings. Faced with this technical challenge, I set out to overcome this hurdle by developing another tool that could offer a cheaper and rather non-invasive alternative to existing conventional calcium imaging technology. We thus developed a novel imaging platform that would allow for low excitation light imaging and also have the portability to be kept in an incubator during imaging.

4.2.12 Contact Imaging

Non-invasive imaging of neuronal activity in a large network is pivotal to understanding brain function and development. Currently, this is achieved through the use of calcium sensitive dyes such as Fura-2 and conventional microscopy, which requires cumbersome optical components including lenses, prisms, filters and a high precision microscope body. Due to these components, such systems are generally large, expensive and immobile. Further, to achieve emission signals from fluorescent markers that can be detected by these systems, high levels of

excitation light are required. This results in a more rapid degradation of the fluorescent markers in a process known as photo bleaching, preventing long-term recordings from being achieved.

Hence, our goal was to simplify the imaging process to produce a "contact imaging platform" whereby the specimens/cells could be cultured directly onto an image sensor and the fluorescent image acquired by projecting light through the sample onto the sensor. This approach eliminates several intermediate optical components that are required in conventional microscopy. The advantage to this design change is decreased cost, significant reduction in size and weight of a fluorescent imaging system, increased sensitivity of the image detector while retaining adequate signal to noise ratio, a larger imaging field encompassing greater areas of a neuronal network and most importantly for my purposes, the ability to conduct long term Ca^{2+} imaging on developing neurons.

We demonstrate a contact imaging system (**Fig. 7.4**) utilizing a custom designed Polyvinyl acetate Benzophenone-8 (PVAc-B-8) filter manufactured on top of a CMOS image sensor. Unlike previous attempts, this system is designed for fluorescent imaging via two excitation wavelengths, 340nm and 380nm. This is important because it allows for the monitoring of intracellular [Ca^{2+}] changes of Fura-2 loaded neurons. The ratiometric dye not only can be used to detect Ca^{2+} change, but can be converted into an intracellular molar concentration. The development of a contact imaging platform for a ratiometric dye is something that has not been achieved previously and is a critical step to studying long term network activity patterns during nervous system development.

Specifically in my research, I deemed it necessary to perform long term Ca^{2+} imaging of individual LPeD1 neurons on the time scale of up to 10 hours. However, as pointed out above, the current technique of using inverted light microscopy and fura-2 imaging does not permit long

term recordings due to photo-bleaching of the dye and extensive sample exposure to the ambient environment. Contact imaging offers the benefits of having higher light detection efficiency (detection of emission light at lower levels than is permissible by a standard light microscope) as well as the portability of being maintained in an incubator while imaging. Brief descriptions of the lensless miniature contact imaging system and its filter's fabrication process is provided in the appendix (Chapter 7 - Appendix) with further details found in our published manuscripts (Blockstein et al. 2012; Mudraboyina et al. 2014).

4.2.12.1 Detecting Fura-2 loaded *Lymnaea* neurons

To test the ability of the contact imaging device to detect fluorescence from Fura-2AM loaded *Lymnaea* neurons at 340nm and 380nm excitation, LPeD1 neurons were extracted and cultured onto a sensor coated with the PVAcB-8/SiO_2 filter overnight (**Fig. 4.14C**). The next day, the neurons were loaded in a 10 µM solution of Fura-2AM for 60 minutes and then washed with DM. We found that when we illuminated the sample with excitation wavelengths 340 nm and 380 nm with a DG-4 lamp, a fluorescence signal was observed in both wavelengths (**Fig. 4.14A,B**). A total of nine neurons (n=9) were tested and a mean signal for each neuron was calculated by summing the fluorescent signal from each pixel and normalizing by the area (of the neuron). We found that the mean signal detected at 340 nm excitation was 91 ± 20, while the mean signal detected with 380 nm excitation was 21 ± 5. For measurements between experiments and the two excitation wavelengths, we kept the light intensity constant, the integration time at 500ms and the sensor gain and offset at zero. Auto-fluorescence was controlled for by imaging the neurons prior to the loading of Fura-2AM. We found that without

fura-2AM loading, the neurons did not express fluorescence when illuminated with 340 nm and 380 nm.

4.2.12.2 Contact imaging chip is capable of detecting live changes in calcium levels

As discussed earlier in the chapter, trophic factors induce an activity increase in LPeD1 neurons which trigger Ca^{2+} oscillations (Xu et al. 2009), an important mechanism behind the functional expression of nAChRs. Therefore, our aim was to test whether the contact imaging chip had the temporal resolution and range to image live changes in intracellular Ca^{2+} levels. To trigger activity in these neurons, we exposed the neurons to a high potassium solution (1M KCl). The KCl caused the neurons to depolarize, trigger action potentials and then subsequently trigger a rise in intracellular Ca^{2+}. We were able to continually record the change in neuronal fluorescence over a period of 205 seconds with both the 340nm and 380nm excitation wavelengths (**Fig. 4.15A,B**). With the ability to detect Ca^{2+}changes at a temporal resolution that matches the activity patterns in *Lymnaea* neurons, the contact imaging device allows us to perform Ca^{2+} imaging experiments. In addition, the contact imaging platform provided a more efficient light collection capability, which meant that the threshold for light detection was lower than that provided by conventional light microscopy. This property can, however, be altered depending on the image sensor utilized, given the large range of sensitivities that can be achieved with various commercially available image sensors. In future experiments, it will be important to demonstrate that a lower excitation light can also be utilized, preventing the fura-2 dye from bleaching as quickly, thus allowing us to achieve longer term recordings of Ca^{2+} activity.

4.2.12.3 The contact imaging platform has a significantly larger field of view compared to conventional microscopy

In conventional fluorescent microscopy, there is an inverse relation between the magnification used and the size of the imaged area. For effective light collection, high magnification oil immersion objectives are usually used, resulting in a small visible area of several hundred by several hundred micrometers. For instance, in previously reported work from our lab, we used a fluorescence microscope limited by a 300μm (height) * 400μm (length) field of view with a 40x oil immersion object lens (Blockstein et al. 2012). In contact imaging, however, the field of view is limited only by the size of the sensor array. The use of our Aptina MT9V032 sensor with dimensions of 4.51mm * 2.88mm results in an area that is over 100 times larger than the sensor view capable on our light microscope, allowing us to image a significantly larger part of any neural network. A sample image with six cultured neurons obtained from our contact imaging chip demonstrates the large field of view compared to the view that a microscope would be capable of capturing at 40x magnification (**Fig. 4.16**). While it could be argued that a lower magnification objective could provide an equally large field of view, the result of using a lower power objective is a loss of light collection efficiency. On the other hand, increasing the field of view in contact imaging only requires the use of a larger imaging sensor with no corresponding loss of light collection efficiency.

Taken together, this novel technology provides us with an imaging platform that can monitor intracellular Ca^{2+} changes with the fluorescent indicator, Fura-2, over an extended period of time. The current limitations of using Fura-2 for long term imaging of developing neurons include photo-bleaching of the indicator and exposure of the culture to the ambient environment for extended periods of time. This imaging platform provides a solution to both of

these limitations. Due to time constraints, I did not, however, come around to testing its utility in my experiments aimed at determining how trophic factor-induced calcium dynamics may change over an extended time period, and whether base-line Ca^{2+} kinetics and bursting-induced fluxes play significant role in excitatory synapse formation and nAChR expression in LPeD1 neurons.

4.3 Discussion

This study further underscores the importance of neurotrophic factors in eliciting unique patterns of activity, which are not only neuron, but also pairing status specific. I also showed that the trophic factor-induced activity patterns are prerequisite for the functional expression of nAChRs and synaptogenesis. I demonstrated, for the first time, that neurotrophic factors evoke a unique "signature" of electrical activity postsynaptically, which begin within minutes of neuronal exposure, last for hours and corresponds well with the functional expression of excitatory nAChRs. This study is also the first to relate various patterns of activity to the functional expression and maintenance of excitatory nAChRs. In addition, in an attempt to understand the mechanisms behind these trophic factor induced activity patterns in synapse formation, we developed two types of novel biotechnology that allows for us to perform long-term recordings of both ion channel activity and intracellular Ca^{2+} levels.

I am cognizant of the fact that the addition of the technology development section in this chapter may have disrupted my thought process in deciphering the fundamental mechanisms underlying trophic factor and activity-induced excitatory synapse formation. I do, however, feel strongly that one of the rate limiting factors for our advancement in the field of neuroscience is the absence of appropriate tools and technology breakthroughs—without these, unraveling the interworkings of developing and developed brain will remain challenging. Therefore, I feel that the discussion of these technologies that were developed in the context of a biological question that could not be answered with current technology is an important justification for future biotechnology development.

The hypothesis that patterned, spontaneous activity is important for brain circuit formation stems from the Hebbian model which postulates that repeated stimulation of

postsynaptic neurons by their presynaptic partners may result in the strengthening of the synapse (Hebb 1949). Extensive work in retinal (Huberman et al. 2008) and cochlear projections (Kandler et al. 2009) have demonstrated the importance of spontaneous activity and also specific patterns of activity in facilitating circuit development. However, almost all studies to date have focused on presynaptic activity patterns, which over an extended period of time during various developmental time frames have not been fully defined. In this study, I provided the first direct evidence that trophic factors acting exclusively on the postsynaptic cell trigger an activity pattern that primes the neuron for excitatory synapse formation—independent of presynaptic activity. It is also important to note that CM induced two unique activity patterns; one being an immediate triggering of action potentials, followed by a transition to more sustained bursting over an extended time period. Immediate changes were observed in both the somata and its isolated axon, whereas the bursting patterns required somata, *de novo* protein synthesis and VGCC activity. These data thus demonstrate that although trophic factors may induce immediate global changes in activity, it is the pulsatile Ca^{2+} entry through voltage gated channels that may underlie gene induction required for the expression of excitatory nAChRs. It therefore stands to reason that perhaps during cholinergic circuit development and plasticity, the brain may follow synaptogenic rules that are analogous to those of the neuromuscular junction, whereby the muscle can define synaptic sites independent of the presynaptic neuron. Further development and refinement of these synaptic sites would, however, rely upon presynaptic signaling and the trophic factors present in the extracellular milieu (Wu et al. 2010).

In this study, I showed that the cell body and *de novo* protein synthesis are crucial for an immediate enhancement of activity and its transition from low levels to a more persistent bursting pattern. While the precise nature of synthesized proteins remains elusive, there is strong

indication that it may involve *de novo* synthesis of Ca^{2+} channels, which in turn may contribute towards sustained bursting pattern that I observed in this section. Alternatively, Ca^{2+} entering through these channels, or its activated signaling cascade, may act as an inductive signal underlying the synthesis of new nAChRs (West and Greenberg 2011). Accordingly, when I blocked Ca^{2+} channels with cadmium or nifedipine, both the bursting activity and the functional nAChR expression were perturbed.

The idea that the Ca^{2+} influx through VGCC into the cytoplasm activates gene expression is well established. Pulsatile Ca^{2+} entry has been established as an important trigger for controlling the levels of postsynaptic receptor expression and even regulating cell cycle events such as mitosis and apoptosis (Borodinsky et al. 2012). Any increase in activity may thus lead to an enhancement of intracellular calcium which is then detected by calcium-binding proteins such as calmodulin or even directly by transcription factors to alter gene expression(Faas et al. 2011; West and Greenberg 2011). With a progression from low activity to persistent bursting seen in LPeD1 neurons, the amount of Ca^{2+} entering the cytoplasm may thus be sufficient to trigger downstream mechanisms mediating molecular transcription and translation. In support, I found that neurons with high variance activity did not express excitatory receptors, suggesting that the observed stereotypical activity pattern seen in excitatory LPeD1 neurons may be the optimal frequency required to maintain intracellular Ca^{2+} levels sufficient for downstream signaling cascades. The above notion supports the idea that a minimal Ca^{2+} "threshold" achieved by a unique pattern of activity "signature" is required for the expression (single) and consolidation (paired cells) of nAChR.

A *Lymnaea* homologue of the multiple endocrine neoplasia type 1 (MEN1) tumor suppressor gene that encodes for the expression of transcription factor menin was previously

shown to be required in the postsynaptic neuron for proper synapse formation (van Kesteren et al. 2001). More recently, it was demonstrated that LPeD1 neurons treated with nifedipine and shown to express functionally inhibitory nAChRs could be rescued to become functionally excitatory nAChRs following the injection of synthetic *Lymnaea* MEN1 (Flynn et al. 2014). These studies suggest that the molecules activated downstream of the Ca^{2+} signaling cascade may involve the activation of *Lymnaea* MEN1. Further studies are, however, required to reveal a direct correlation of activity patterns to the specific mRNA expression levels of MEN1.

Interestingly, in single cells, trophic factors set the patterns of activity in a "runaway" mode while LPeD1 pairing with its synaptic partner resulted in "scaling down" of this activity to a level similar to that seen in DM. It appears that in single cells, a high level of patterned activity might serve to sustain the expression of excitatory nAChR, priming the neurons for immediate synaptogenesis upon contact with its partner cells. In contrast, in paired cells, synaptic partnership and receptor localization at the contact sites may eliminate the need for a "runaway" activity-mediated expression of nAChRs, thus scaling down both the activity and the receptor expression. This notion is consistent with observations at the neuromuscular junction (NMJ), whereby contacts between motor neurons and their synaptic muscle partners results in synaptic site specific localization of nAChRs and a down regulation of extra-synaptic receptor expression (Merlie et al. 1984; Tsay and Schmidt 1989). In summary, my data provides further unique insights into trophic factor mediated actions on neuronal activity and its specific regulation of nAChR expression. Based on the data presented here, I propose that trophic factors are essential not only for the developmental expression but also the maintenance of nAChR during synaptic plasticity underlying learning and memory. In the absence of trophic factors and the ensuing perturbed activity, the cholinergic networks will be rendered dysfunctional as we see during

neurodegenerative diseases such as Alzheimer disease (Allen and Dawbarn 2006; Schindowski et al. 2008; Nagahara et al. 2009). Whereas several studies have demonstrated a predominant presynaptic locus of neurotrophin action on cholinergic neurons, a similar postsynaptic role may also be plausible.

Although trophic factor induced activity and specific patterns of activity or its "signature" was shown to be important in functional excitatory nAChR expression and synapse formation, several questions still remained in regards to the underlying mechanism by which this occurred. While the use of MEAs in this study afforded us the ability to perform long term non-invasive recordings of neuronal electrical activity during synapse reformation, analogous technologies do not exist for the long-term monitoring of ion channel activity or intracellular calcium levels. In this study, the development of our novel planar patch clamp chip allowed for the long-term, stable interrogation of ion channel activity in individually cultured cells; these techniques enable a tool chest that can be exploited further. While all current prototypes of planar patch clamp chips only allow for freely suspended cells to be patched and require suction to draw the neuron to the aperture for the formation of a giga-seal (Fertig et al. 2002; Sigworth and Klemic 2005; Baaken et al. 2008), none of these current technologies allow for cultured neurons to be investigated. In particular, this poses problems with studying synaptically connected neurons. In summary, these studies are the first to show two different planar patch clamp chips that have the ability to *1) record action potentials in both current and voltage clamp mode, 2) record synaptic currents and potentials, 3) record short term potentiation between a single synapse and 4) maintain and record a stable patch for over 12 hours as demonstrated by stable recordings from the same chip performed 12 hours apart*. On the medical science front, the ability to interrogate ion channel activity over an extended period of time has great implications for studying synaptic

development and changes in neuronal membrane properties during long term development, a keystone of neuroscience that is relatively untouched. Particularly, future studies to dissect how the ion channel complement and membrane excitability of neurons changes during synaptic development will be a crucial next step to our current study. Further implications to this technology can also be felt on the pharmaceutical development front, whereby this technique will now allow for medium throughput drug screening for ion channel diseases, a process which had previously been very slow.

Additionally, we also developed a complete bio-compatible fluorescence contact imaging system. We show that our system is indeed capable of detecting intracellular calcium changes in Fura-2 loaded neurons. This platform is not only a reduction in size and cost from traditional imaging setups, but also allows for longer term imaging of low fluorescent signals due to the close proximity of the sensor to the specimen. This sensor also enables multiple neurons over a large surface area to be imaged simultaneously, an option that is not readily available in conventional light microscopy. The ability to interrogate calcium activity over extended periods is critical for our efforts to decipher trophic factor induced calcium oscillations during the development of the cholinergic synapse between VD4 and LPeD1. This can now be explored further in our lab. However, on a larger scale, this technology has even wider implications. For instance, future utility of the current technology include situations where conventional fluorescence microscopes fail to provide a solution such as fluorescent imaging of the brain in freely moving animals *in vivo* (Kerr and Nimmerjahn 2012).

Figure 4.1

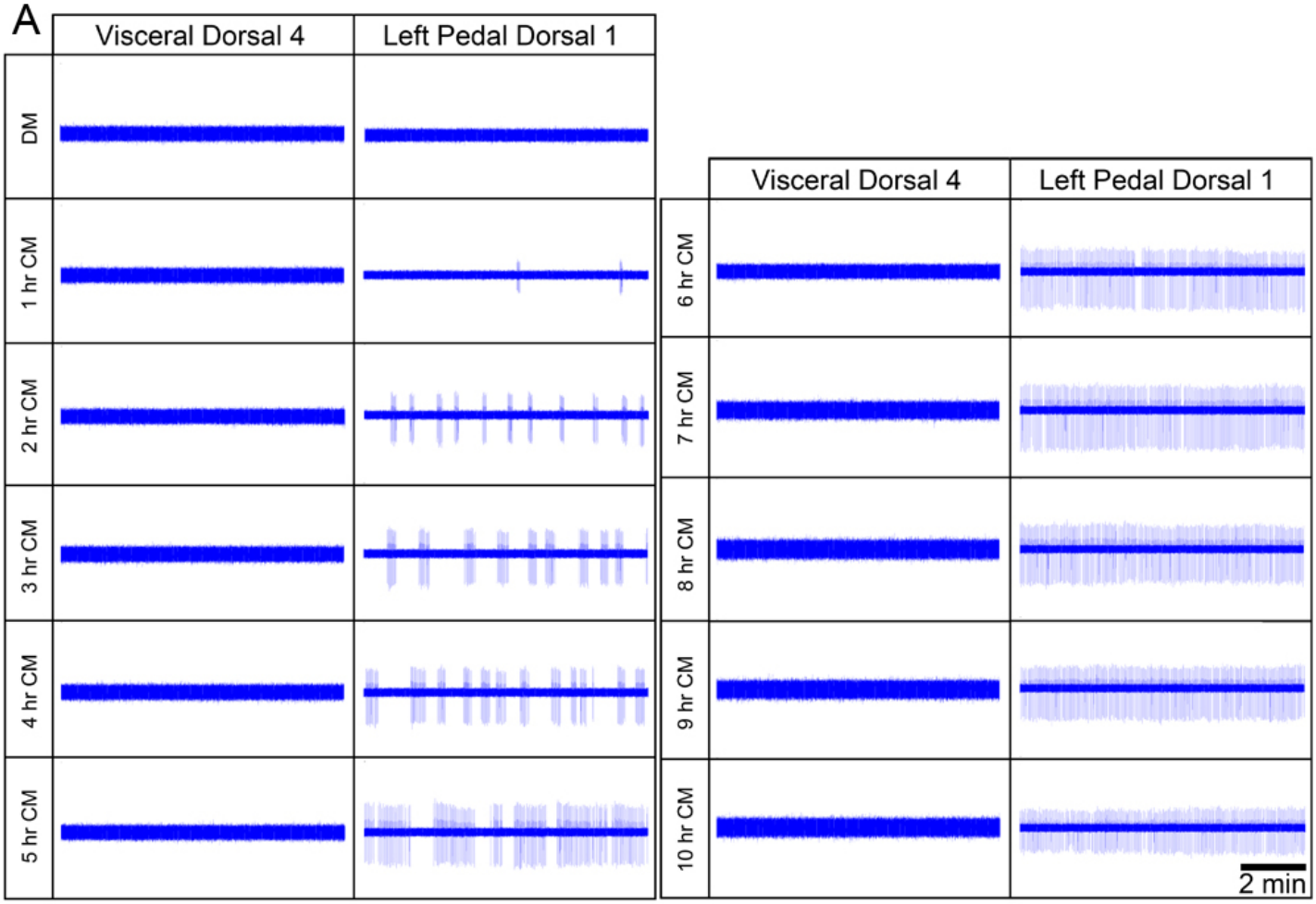
A
Visceral Dorsal 4
Left Pedal Dorsal 1
DM
1 hr CM
2 hr CM
3 hr CM
4 hr CM
5 hr CM
6 hr CM
7 hr CM
8 hr CM
9 hr CM
10 hr CM
2 min

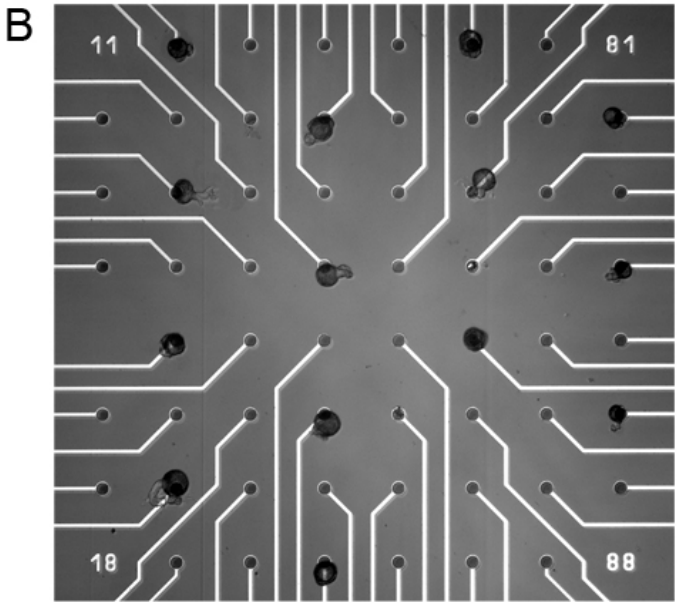
B
11
81
18
88

Figure 4.1: Activity of VD4 and LPeD1 neurons following exposure to CM.

Neuronal electrical activity was observed over a 12 hours period using microelectrode arrays. VD4 and LPeD1 neurons were cultured on microelectrode arrays in DM (without trophic factors) overnight and CM (with trophic factors) was added the next day following 2 hours of control DM recordings. **(A)** A sample 5 minutes trace obtained during DM control and every hour following CM introduction is shown. **(B)** A representative figure of neuronal placement on the chip. The first three columns on the left are LPeD1 neurons, and the last column on the right shows VD4 neurons.

Figure 4.2

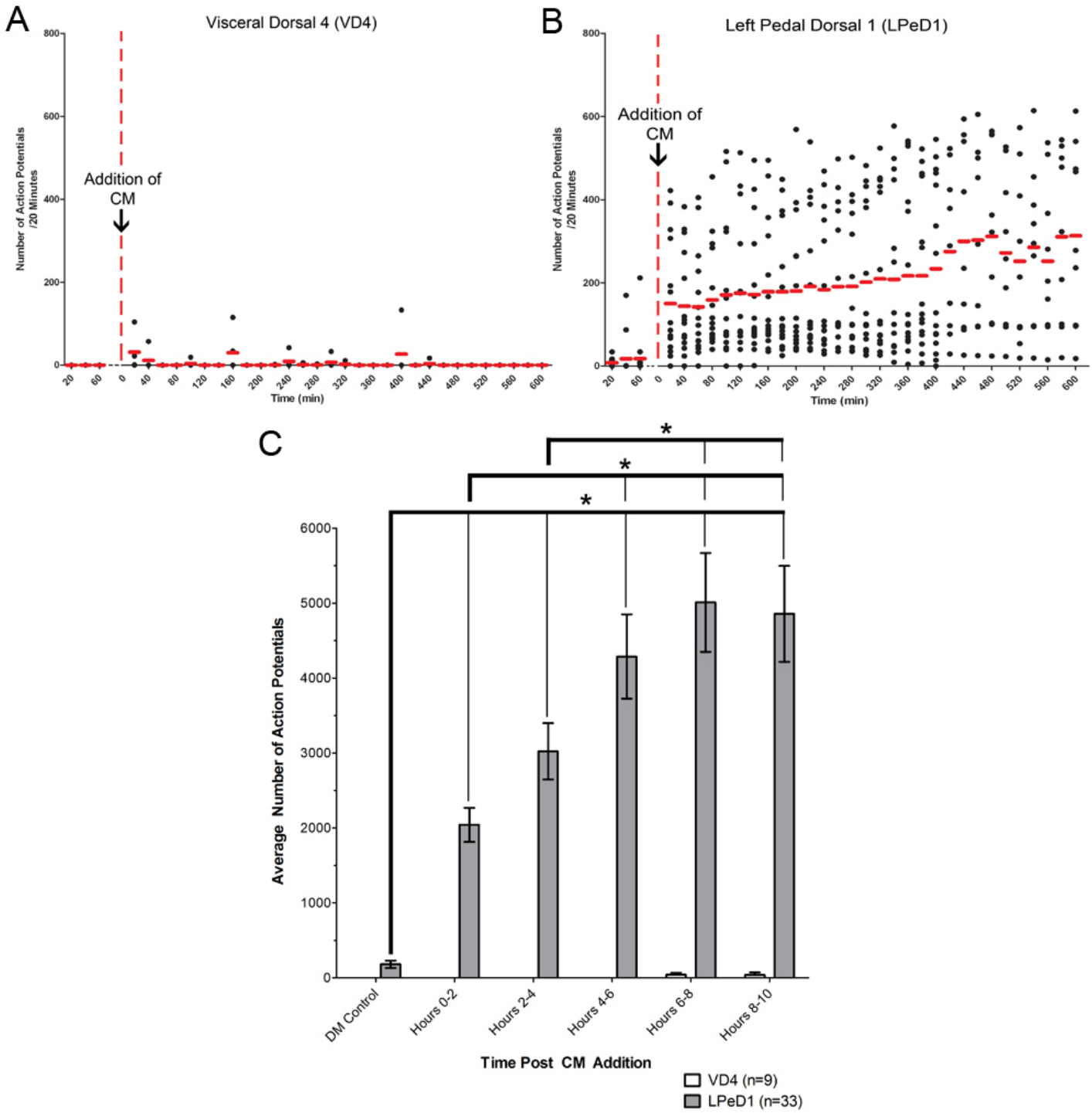
A
Visceral Dorsal 4 (VD4)
Number of Action Potentials /20 Minutes
Addition of CM
Time (min)
B
Left Pedal Dorsal 1 (LPeD1)
Number of Action Potentials /20 Minutes
Addition of CM
Time (min)
C
Average Number of Action Potentials
DM Control
Hours 0-2
Hours 2-4
Hours 4-6
Hours 6-8
Hours 8-10
Time Post CM Addition
VD4 (n=9)
LPeD1 (n=33)

Figure 4.2: LPeD1 and VD4 activity in 20 minute and 2 hour bins following exposure to CM.

Neuronal activity is shown as observed over a 10 hour period using microelectrode arrays. VD4 and LPeD1 neurons were cultured on the microelectrode arrays in DM (without trophic factors) overnight, and CM (with trophic factors) was added the next day following 2 hours of control DM recordings. Activity from **(A)** VD4 and **(B)** LPeD1 isolated neurons is shown in the scatterplot with the red line designating the mean number of action potentials for 20 minute bins. The activity was then **(C)** further binned into two hours periods for both VD4 and LPeD1 neurons and a one-way ANOVA showed significant differences at different time periods, with a maximal activity plateau reaching between 5-10 hours. Note a rapid rise in activity in LPeD1 following CM addition as compared to that observed in VD4, which did not exhibit a similar response. Significant differences are denoted with an asterisk (*) and significance was assumed if $p<0.05$.

Figure 4.3

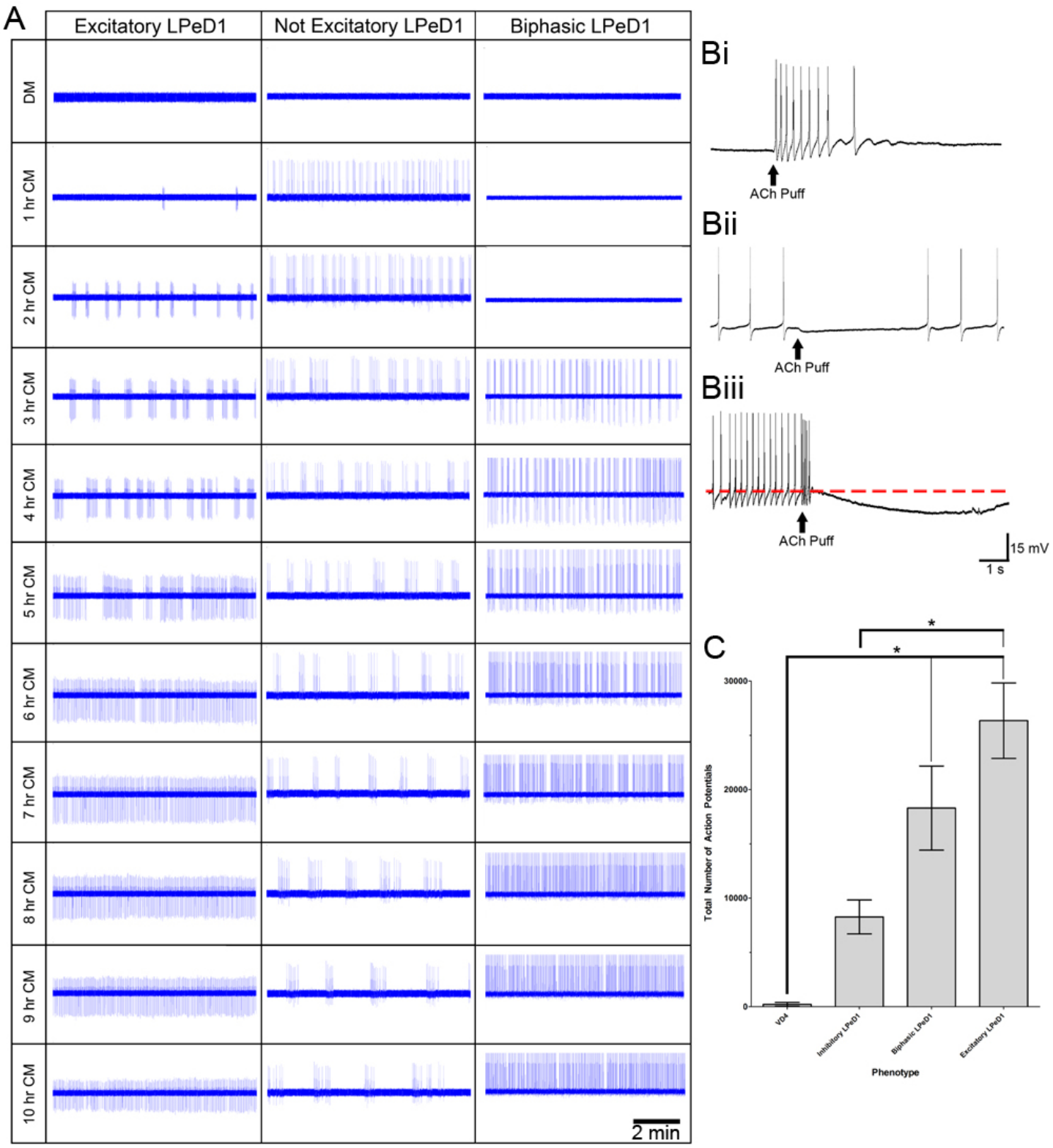
A
Excitatory LPeD1
Not Excitatory LPeD1
Biphasic LPeD1
DM
1 hr CM
2 hr CM
3 hr CM
4 hr CM
5 hr CM
6 hr CM
7 hr CM
8 hr CM
9 hr CM
10 hr CM
2 min
Bi
ACh Puff
Bii
ACh Puff
Biii
ACh Puff
15 mV
1 s
C
Total Number of Action Potentials
30000
20000
10000
0
*
*
VD4
Inhibitory LPeD1
Biphasic LPeD1
Excitatory LPeD1
Phenotype

Figure 4.3: Total number of action potentials versus final functional AChR phenotype. **(A)** The activity triggered in response to conditioned media was different for all three phenotypes of isolated LPeD1 neurons. The figure shows 10 minutes samples of activity observed at various time points following the CM exposure. Three different LPeD1 phenotypes were deciphered by neuronal responses to exogenously applied ACh, which elicited 3 different effects, excitatory **(Bi)**, inhibitory **(Bii)**, and biphasic (**Biii**; elements of both excitation and inhibition). In **(Bi)**, application of ACh excited the cell, eliciting action potentials and increasing the frequency of activity. In **(Bii)**, ACh inhibited the cell, stopping the firing of action potentials and inducing a decrease in neuronal membrane potential. In **(Biii)**, ACh elicited an action potential that was followed by a subsequent decrease in membrane potential (a pre-application potential line is shown as a red dotted line to aid in visualization). ACh applications are indicated by a solid arrow. The total LPeD1activity is stratified according to neuronal response to ACh application **(C)**. It can be seen that cells with excitatory response had higher levels of activity than those that exhibited an inhibitory response. Significance is denoted with an asterisk (*) and is assumed if $p<0.05$.

Figure 4.4

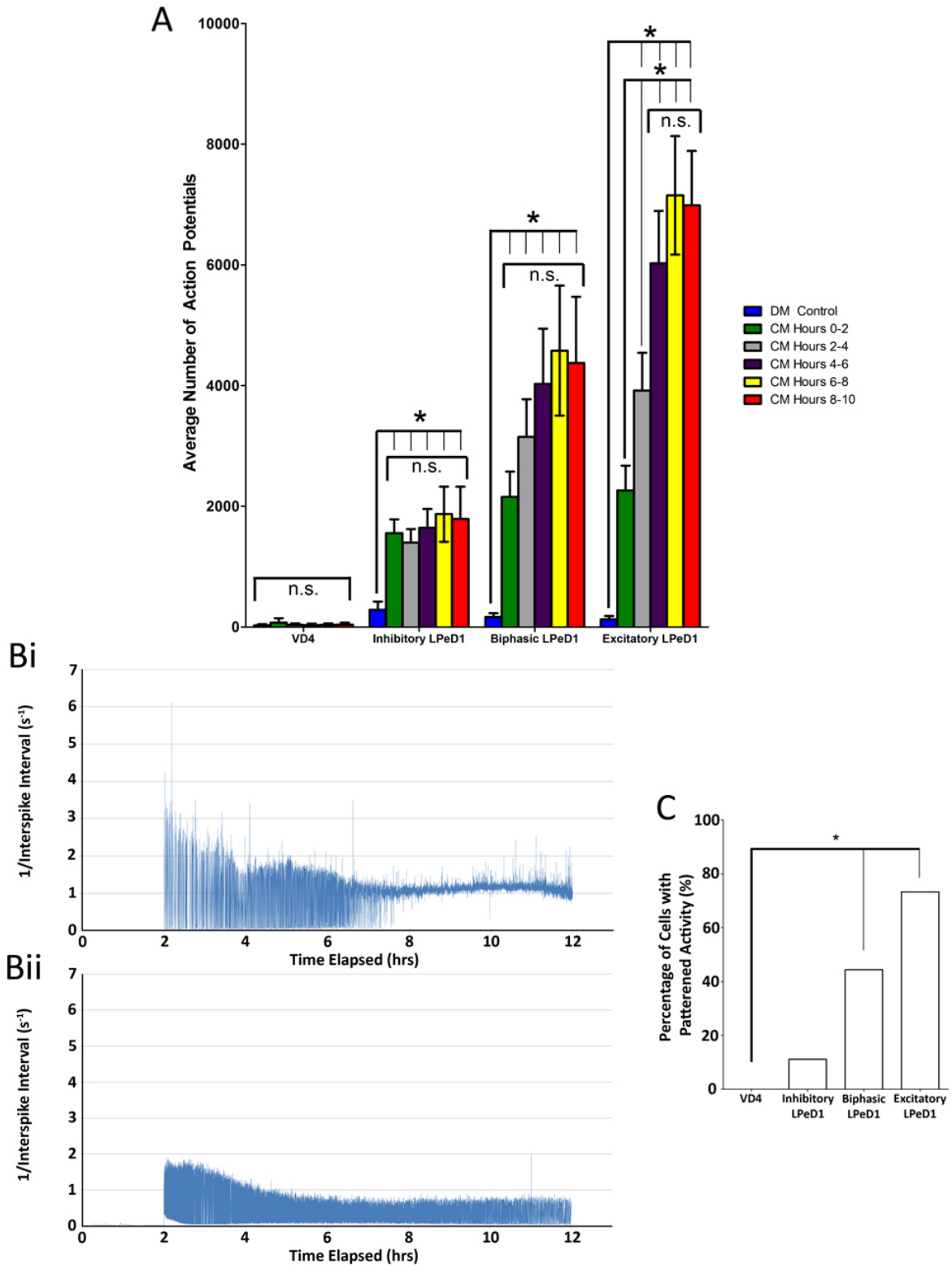
A
Average Number of Action Potentials
10000
8000
6000
4000
2000
0
n.s.
*
n.s.
*
n.s.
*
VD4
Inhibitory LPeD1
Biphasic LPeD1
Excitatory LPeD1
DM Control
CM Hours 0-2
CM Hours 2-4
CM Hours 4-6
CM Hours 6-8
CM Hours 8-10
Bi
1/Interspike Interval (s-1)
Time Elapsed (hrs)
Bii
1/Interspike Interval (s-1)
Time Elapsed (hrs)
C
Percentage of Cells with Patterened Activity (%)
*
VD4
Inhibitory LPeD1
Biphasic LPeD1
Excitatory LPeD1

Figure 4.4: Neuronal activity in inhibitory, biphasic and excitatory LPeD1 cells and the corresponding activity pattern expressed as 1/interspike interval.

(A) Neuronal electrical activity observed over a 12 hour period of VD4 and LPeD1 cells that responded to ACh with inhibitory, biphasic, and excitatory responses. VD4 and LPeD1 neurons were cultured overnight on MEAs in DM and control recordings were obtained in DM followed by CM exposure. The responses of LPeD1 cells to ACh were tested 10 hours following CM addition. Each measure of activity represents the average number of action potentials recorded per a 2 hour period. Note the different responses of LPeD1 cells exposed to CM among the various different LPeD1 phenotypes. Next, to examine activity over an extended period of time, the interspike interval (ISI; time elapsed between two action potentials) was calculated and the inverse of the ISI was taken to give a measure of frequency. Using this protocol, I examined the firing pattern and found that a characteristic of **(Bi)** excitatory LPeD1 neurons was a progression of activity towards a tightly regulated firing rate of approximately 1 Hz, while the firing frequency of **(Bii)** inhibitory cells did not undergo this change in pattern and neurons continued to fire at a highly variable rate. After fingerprinting this pattern, I correlated the patterned activity with receptor expression using blinded scoring. It can be seen that **(C)** excitatory receptor expressions is significantly correlated with patterned activity. Significant differences are denoted with an asterisk (*) and significance is assumed if $p<0.05$. Non-significantly different groups were designated with “n.s.”.

Figure 4.5

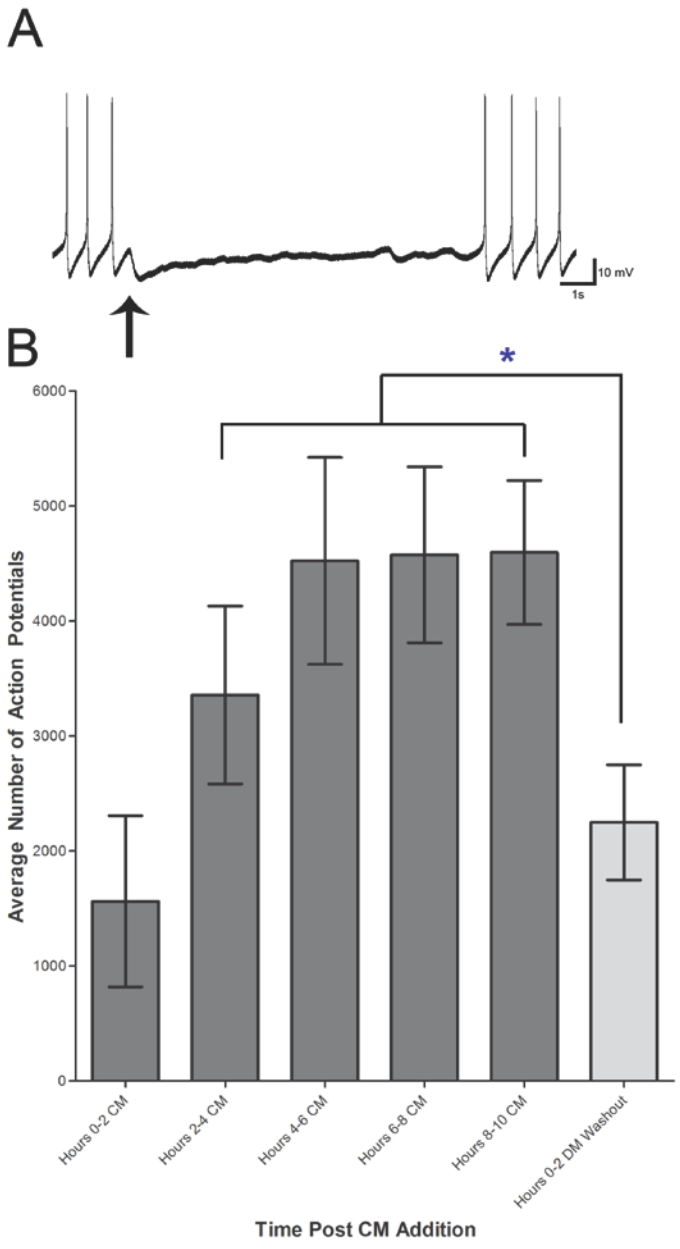
A
10 mV
1s
B
*
6000
5000
4000
3000
2000
1000
0
Average Number of Action Potentials
Hours 0-2 CM
Hours 2-4 CM
Hours 4-6 CM
Hours 6-8 CM
Hours 8-10 CM
Hours 0-2 DM Washout
Time Post CM Addition

Figure 4.5: LPeD1 hyperpolarization inhibits excitatory nAChR expression and that the presence of trophic factors is necessary to maintain activity in LPeD1.

To determine whether activity is important for the expression of excitatory nAChRs, an intracellular sharp-electrode was used to inject hyperpolarizing current into LPeD1 neurons maintained in CM. **(A)** I found that the neurons hyperpolarized for 8 hours remained robust as demonstrated by their ability to elicit action potentials. However after blocking trophic factor induced activity, the LPeD1 neurons failed to express excitatory nAChRs despite being exposed to CM. Exogenous application of ACh (thin arrow) confirmed this by showing a reduction in spontaneous activity with each application. **(B)** Next, to determine whether the maintenance of activity in LPeD1 is CM dependent, the solution was washed out with DM after 10 hours of CM exposure. I found that following the CM withdrawal, LPeD1 activity significantly decreased to a level similar to that observed in the initial two hours following CM exposure. Significant differences are denoted with an asterisk (*) and is assumed if $p<0.05$.

Figure 4.6

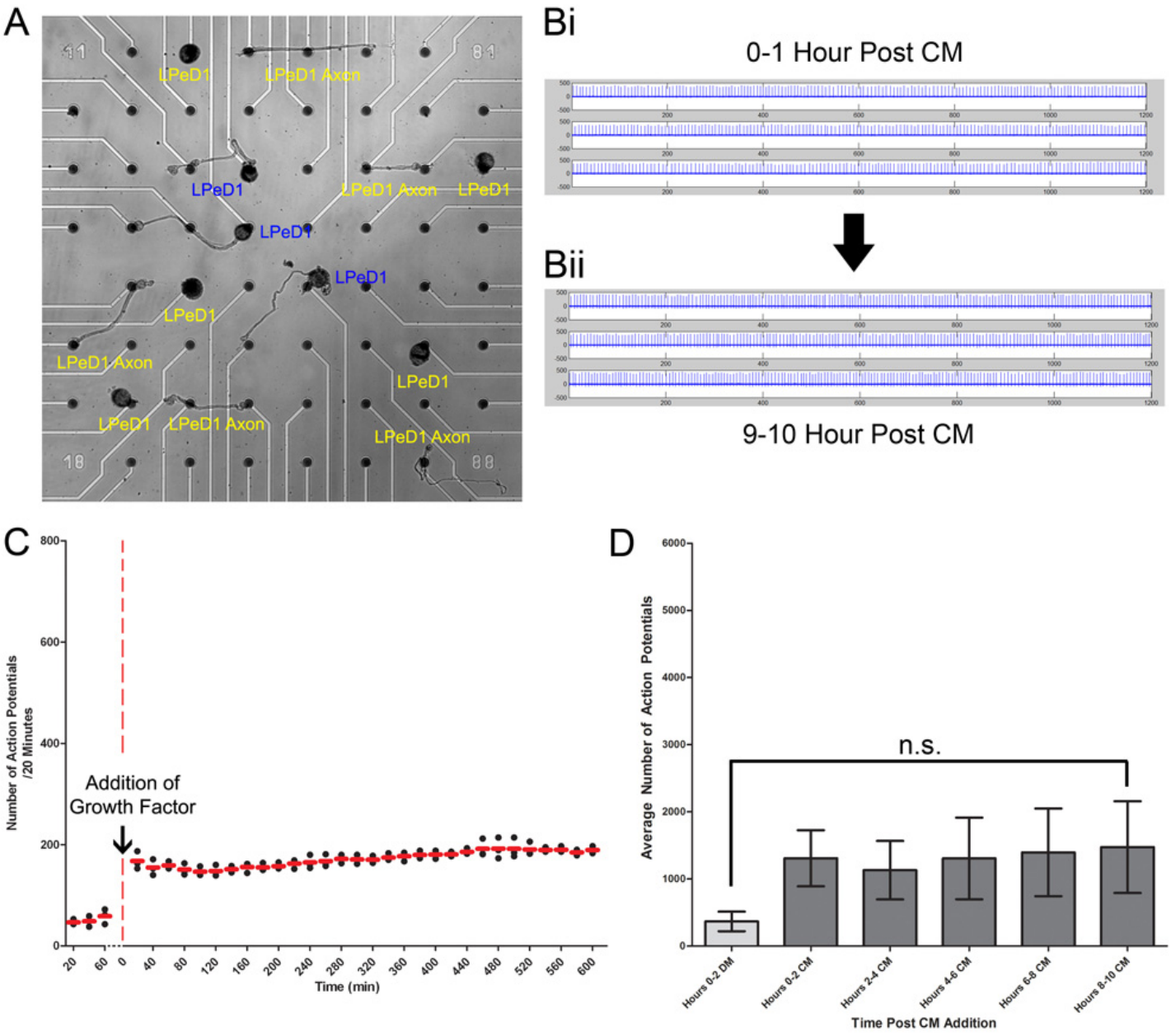
A
LPeD1
LPeD1 Axon
LPeD1
LPeD1 Axon
LPeD1
LPeD1
LPeD1
LPeD1
LPeD1 Axon
LPeD1
LPeD1
LPeD1 Axon
LPeD1 Axon
Bi
0-1 Hour Post CM
Bii
9-10 Hour Post CM
C
Number of Action Potentials /20 Minutes
Addition of Growth Factor
Time (min)
D
Average Number of Action Potentials
n.s.
Hours 0-2 DM
Hours 0-2 CM
Hours 2-4 CM
Hours 4-6 CM
Hours 6-8 CM
Hours 8-10 CM
Time Post CM Addition

Figure 4.6: Trophic factor induced activity increase requires the somata.

To test for trophic factor-induced activity in different cellular compartments (somal versus axonal) of LPeD1 neurons, I **(A)** cultured LPeD1 and its axons across multiple microelectrodes in DM, and severed the cell body from the axon. The resulting isolated axon was then monitored for electrical activity as CM was introduced (n=4). I found that immediately following CM introduction, an **(Bi)** activity increase in the isolated axon was observed. However, unlike the activity pattern observed in the cell body, axonal activity **(Bii)** did not increase over time into the characteristic pattern seen in the cell body. Rather, the isolated axon maintained a **(C)** constant level of activity. **(D)** This increase was found to not be significantly different as determined by a one-way ANOVA, $p>0.05$. Non-significantly different groups were designated with "n.s."

Figure 4.7

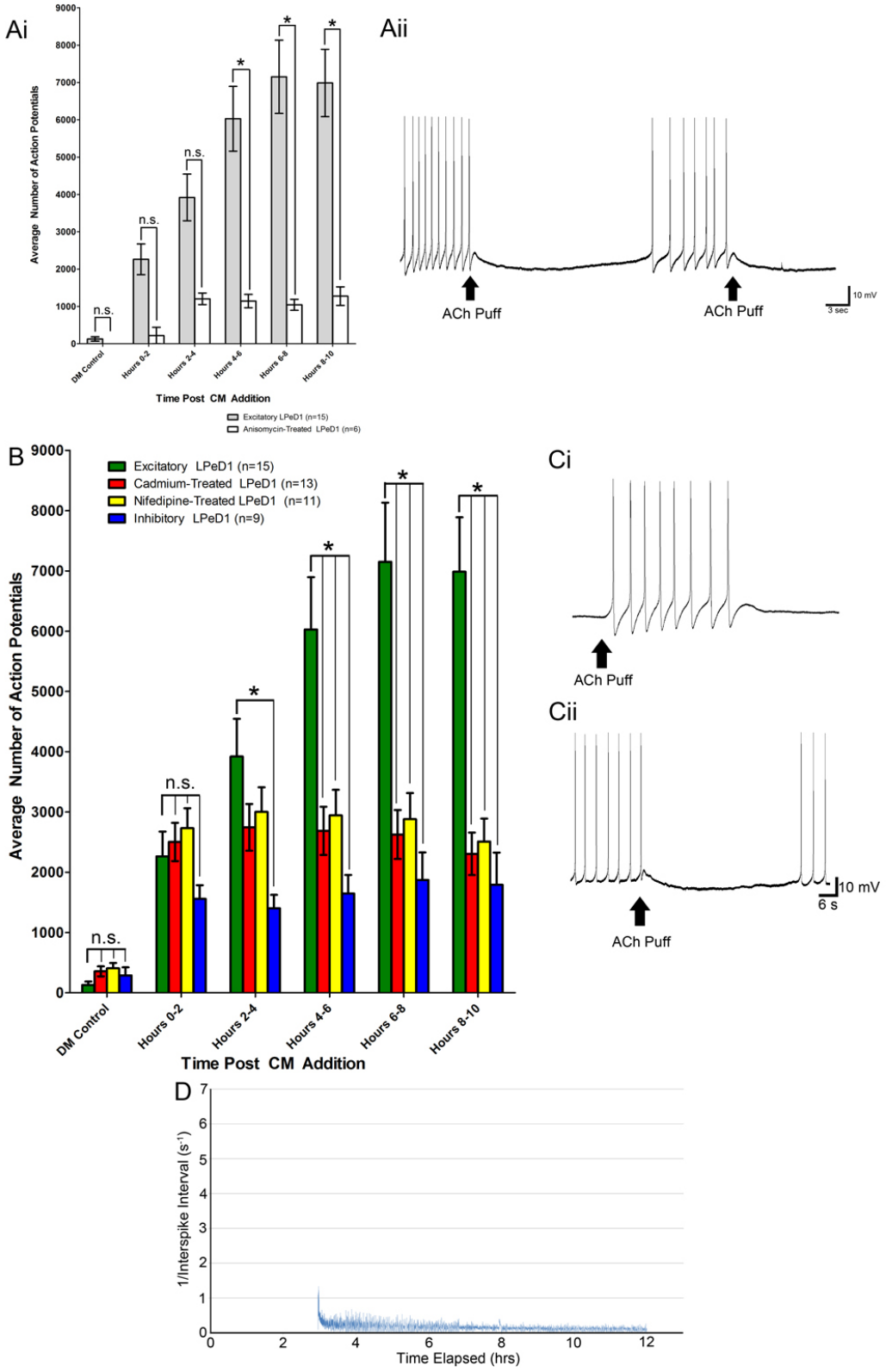
Ai
Average Number of Action Potentials
n.s.
n.s.
n.s.
*
*
*
DM Control
Hours 0-2
Hours 2-4
Hours 4-6
Hours 6-8
Hours 8-10
Time Post CM Addition
Excitatory LPeD1 (n=15)
Anisomycin-Treated LPeD1 (n=6)
Aii
ACh Puff
ACh Puff
10 mV
3 sec
B
Excitatory LPeD1 (n=15)
Cadmium-Treated LPeD1 (n=13)
Nifedipine-Treated LPeD1 (n=11)
Inhibitory LPeD1 (n=9)
Average Number of Action Potentials
Time Post CM Addition
Ci
ACh Puff
Cii
ACh Puff
10 mV
6 s
D
1/Interspike Interval (s-1)
Time Elapsed (hrs)

Figure 4.7: Perturbation of *de novo* protein synthesis and voltage gated calcium channel activity inhibits CM induced activity in LPeD1 neurons.

The role of protein synthesis in long-term changes in activity/patterns induced by CM was investigated using the protein synthesis blocker anisomycin. **(Ai)** The activity of anisomycin treated LPeD1 cells was compared to controls over a period of 10 hours. In the presence of anisomycin, neurons failed to exhibit changes to their activity in response to CM. Specifically, activity was significantly reduced in hours 4-6, 6-8 and 8-10 in LPeD1 neurons exposed to anisomycin plus CM. **(Aii)** When exogenous ACh was pressure applied onto these neurons, all anisomycin treated LPeD1 neurons expressed inhibitory AChRs. Next, **(B) c**alcium channels on LPeD1 exposed to CM were blocked either with cadmium or nifedipine. While no significant difference in activity was seen in the 4 hours following CM addition, a significant reduction in activity levels was noted in the 5-10 hour range. This reduction in activity resembled that seen in inhibitory LPeD1 neurons. **(Ci)** Exogenous ACh application to control LPeD1 neurons showed an excitatory response, demonstrating the presence of excitatory nAChRs. However, in **(Cii)** nifedipine treated LPeD1 neurons, exogenously applied ACh exhibited an inhibitory response, suggesting the lack of an excitatory nAChR expression. **(D)** The graphical representation for 1/ISI showed that nifedipine prevented the development of patterned activity. Significance is denoted with an asterisk (*) and is assumed if $p<0.05$. Non-significantly different groups were designated with “n.s.”

Figure 4.8

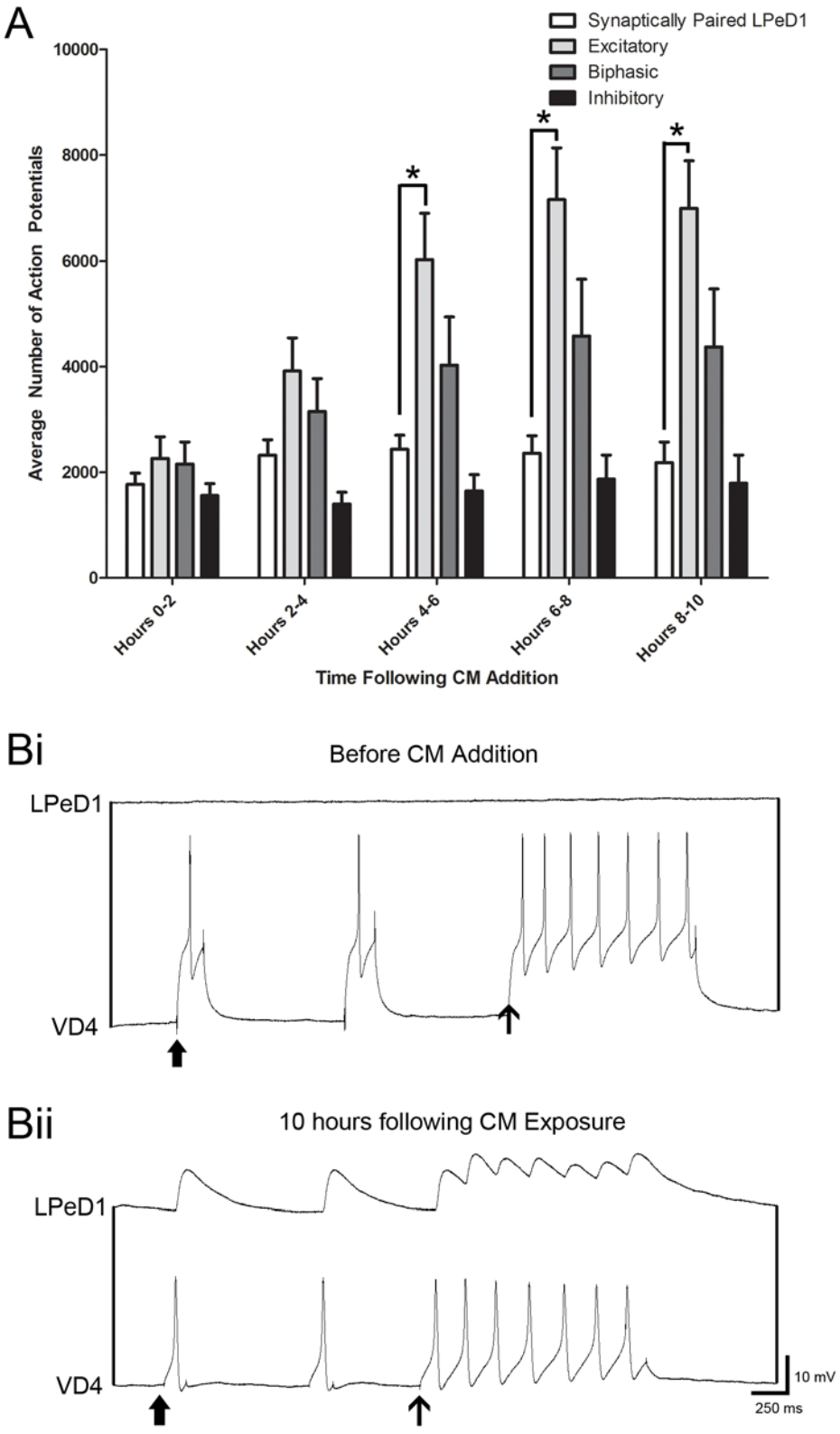
A
Synaptically Paired LPeD1
Excitatory
Biphasic
Inhibitory
Average Number of Action Potentials
10000
8000
6000
4000
2000
0
*
*
*
Hours 0-2
Hours 2-4
Hours 4-6
Hours 6-8
Hours 8-10
Time Following CM Addition
Bi
Before CM Addition
LPeD1
VD4
Bii
10 hours following CM Exposure
LPeD1
VD4
10 mV
250 ms

Figure 4.8: LPeD1 contact with presynaptic partner VD4 reduces trophic factor induced activity.

To determine the effects of target cell contact on trophic factor induced activity, VD4 was paired overnight with LPeD1 in soma-soma configuration in DM (without trophic factors). **(A)** LPeD1 activity was then recorded in CM (with trophic factors) for a period of 10 hour. While the level of activity seen in the first 0-2 and 2-4 hours was not different from that seen in the single LPeD1 neurons exhibiting an excitatory response, it was, however, significantly reduced in hours 4-6, 6-8 and 8-10. The activity observed in hours 4-10 was not significantly different from that seen in inhibitory and biphasic single LPeD1 neurons, demonstrating that target cell contact reduced trophic factor induced activity in LPeD1. **(Bi)** Neurons were electrophysiologically tested for the presence of functional synapses. I found that neither single action potentials (thick arrow) nor a burst of tetanic spikes (thin arrow) elicited any response in postsynaptic LPeD1, suggesting that no functional synapse had formed in the DM. **(Bii)** Following CM exposure for 10 hours, a single action potential (thick arrow) elicited a 1:1 EPSP while a tetanic pulse (thin arrow) resulted in compound EPSPs, demonstrating the presence of a functional excitatory synapse. Significant differences are denoted with an asterisk (*) and significance is assumed if $p<0.05$.

Figure 4.9

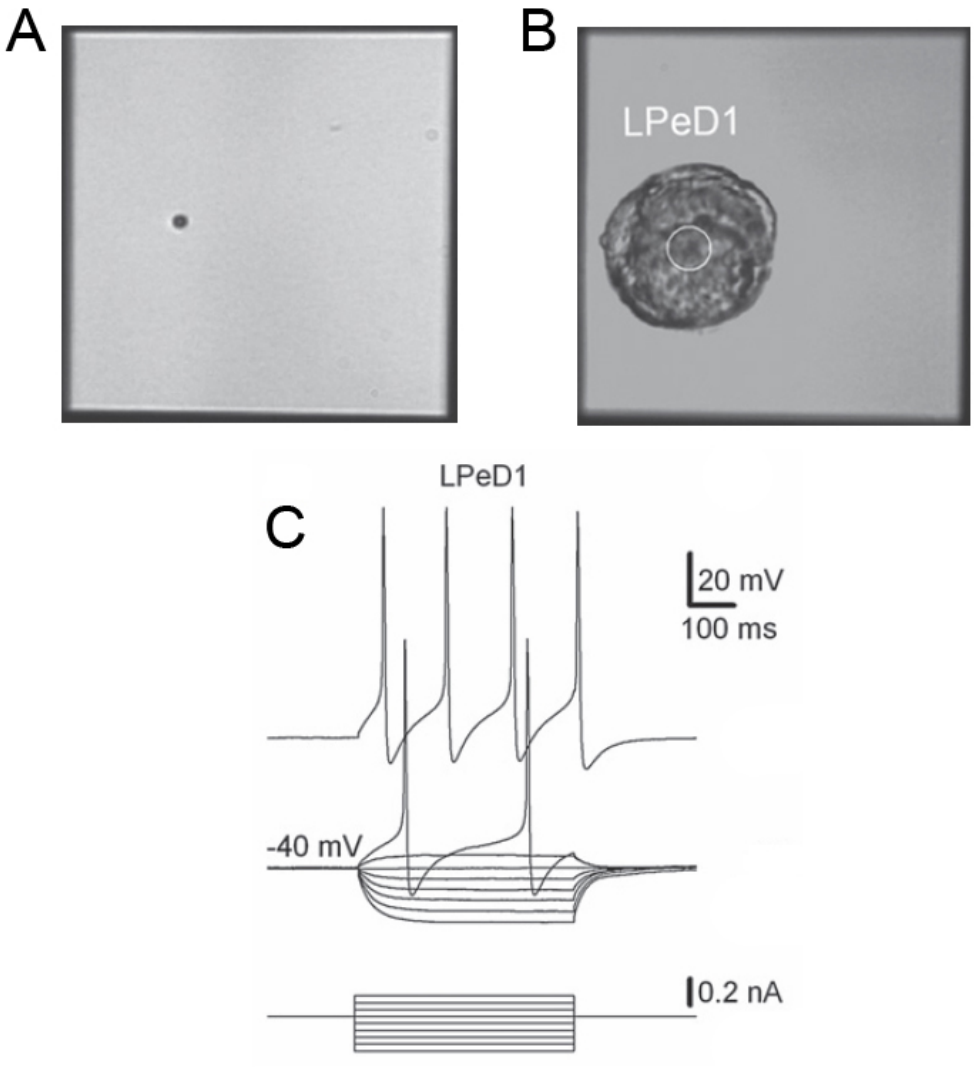

Figure 4.9: The silicon nitride planar patch clamp chip is able to record neuronal voltage changes in response to step currents.

Silicon nitride planar patch clamp chip shows the 100 µm square chip, the top of the truncate pyramid formed by the silicon wafer and the 2 µm aperture which is joined with the subterranean channels containing the pipette solution and providing a continuous electrical pathway to the patch clamp head stages. The image in **(A)** shows the square chip and aperture prior to culturing and **(B)** following culturing of and LPeD1 neuron. The white circle highlights the approximate location of the aperture. A physiological voltage responses of LPeD1 to a series of intracellular current pulses **(C)** through the silicon nitride chip are shown.

Figure 4.10

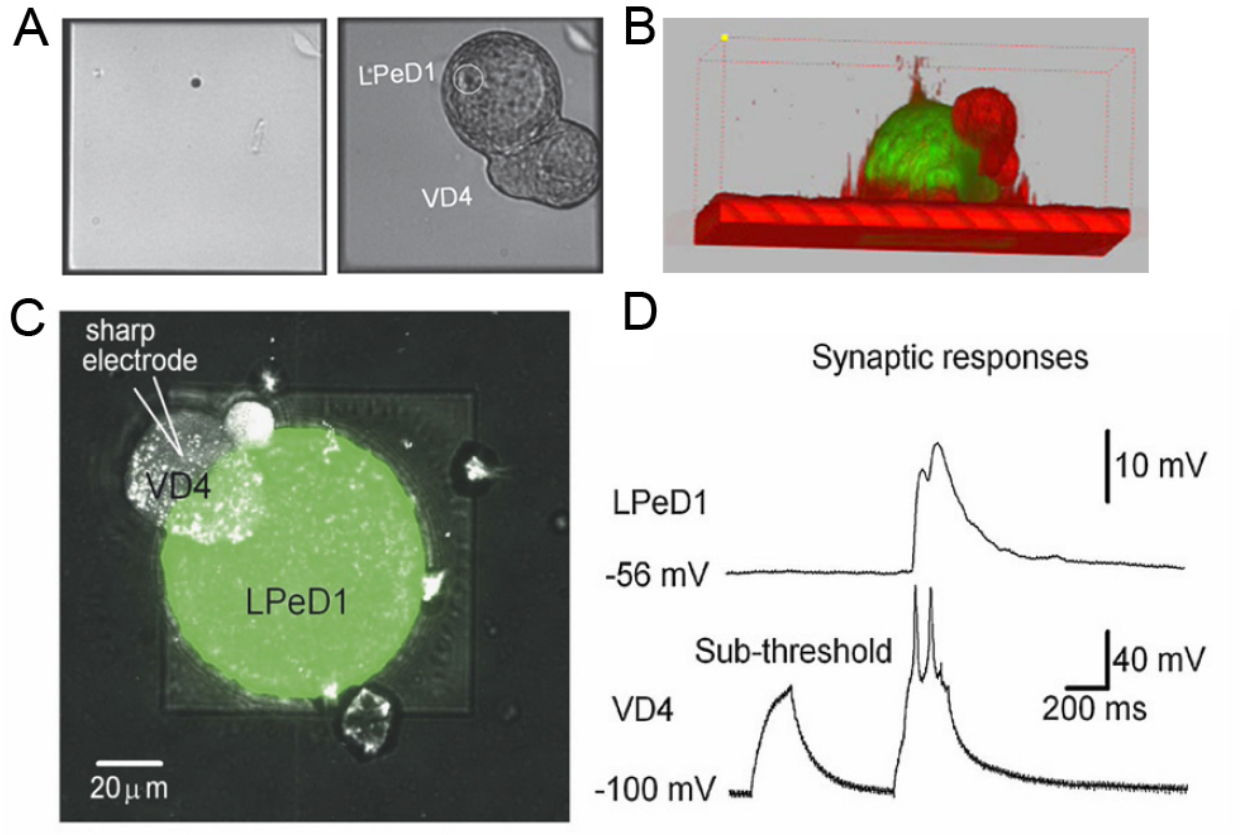
A
LPeD1
VD4
B
C
sharp
electrode
VD4
LPeD1
20μm
D
Synaptic responses
10 mV
LPeD1
-56 mV
Sub-threshold
40 mV
VD4
200 ms
-100 mV

Figure 4.10: Detecting synaptic potentials on the silicon nitride planar patch clamp chip. Using the soma-soma model for synapse formation, postsynaptic LPeD1 was cultured overtop of the aperture. Next, the presynaptic VD4 was placed either adjacent **(A)** or on top **(B)** of the LPeD1 neuron and the synapse was allowed to form overnight. The next day, VD4 was impaled with a sharp-electrode intracellular electrode **(C)**. We found that triggering action potentials in VD4 resulted in 1:1 excitatory postsynaptic potentials in LPeD1 which were reliably detected by the silicon nitride planar patch clamp chip. To ensure the patch clamp chip was indeed detecting postsynaptic potentials elicited in LPeD1 and to ensure the presence of a chemical synapse and to rule out electrical coupling between the VD4 and LPeD1 neuron, a sub-threshold depolarization of VD4 neuron did not result in any detected membrane potential change in LPeD1 as detected by the chip. In addition, to test whether the subterranean channel solution was continuous with the intracellular compartment, the solution was replaced with a Lucifer yellow dye. It was shown that within minutes of replacing the solution, the dye was able to pass through the aperture and diffuse into the neuron as seen with the Lucifer yellow filling seen in **(B)** and **(C)**.

Figure 4.11

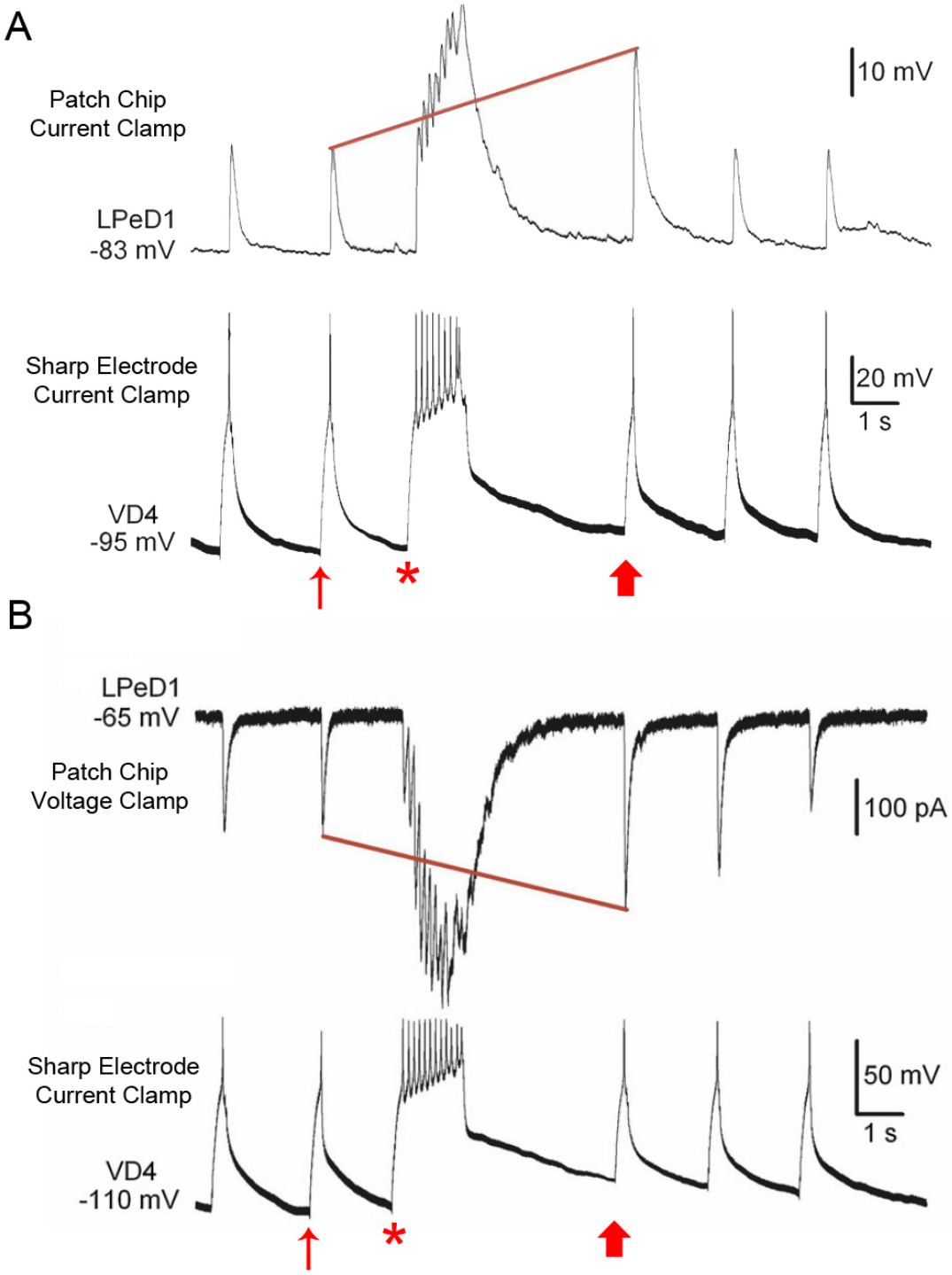
A
Patch Chip
Current Clamp
LPeD1
-83 mV
10 mV
Sharp Electrode
Current Clamp
VD4
-95 mV
20 mV
1 s
*
B
LPeD1
-65 mV
Patch Chip
Voltage Clamp
100 pA
Sharp Electrode
Current Clamp
VD4
-110 mV
50 mV
1 s
*

Figure 4.11: The silicon nitride planar patch clamp chip has the resolution to detect synaptic plasticity changes in postsynaptic potentials.

To demonstrate the high fidelity of the silicon nitride planar patch clamp chip, we induced short term synaptic potentiation *(Details of this form of synaptic plasticity discussed in Chapter 5)* in the LPeD1 neuron and attempted to use the chip to detect the resultant change. Specifically, while LPeD1 was recorded with the silicon nitride patch clamp chip while the VD4 was under current clamp via sharp electrode intracellular recording. LPeD1 was current clamped at -83mV **(A)** and we showed that following tetanic stimulation of the presynaptic VD4 neuron (asterisk), the amplitude of the excitatory postsynaptic potential was larger or potentiated (thick arrow) compared to an excitatory postsynaptic potential elicited prior to the tetanic stimulation (thin arrow). The chip was able to reliably detect these amplitude changes at a resolution that was similar to that observed during conventional patch clamping. Next, we switch the LPeD1 to voltage clamp mode and held the neuron at a potential of -65 mV (B). Similar to that observed in current clamp mode, single presynaptic action potential prior to tetanic stimulation (thin arrow) resulted in an excitatory postsynaptic current detected reliably by the silicon nitride planar patch clamp chip. Following tetanic stimulation (asterisk), a subsequent action potential triggered in presynaptic VD4 resulted in an excitatory postsynaptic current which was potentiated and larger in amplitude which again was reliably detected by the planar patch clamp chip.

Figure 4.12

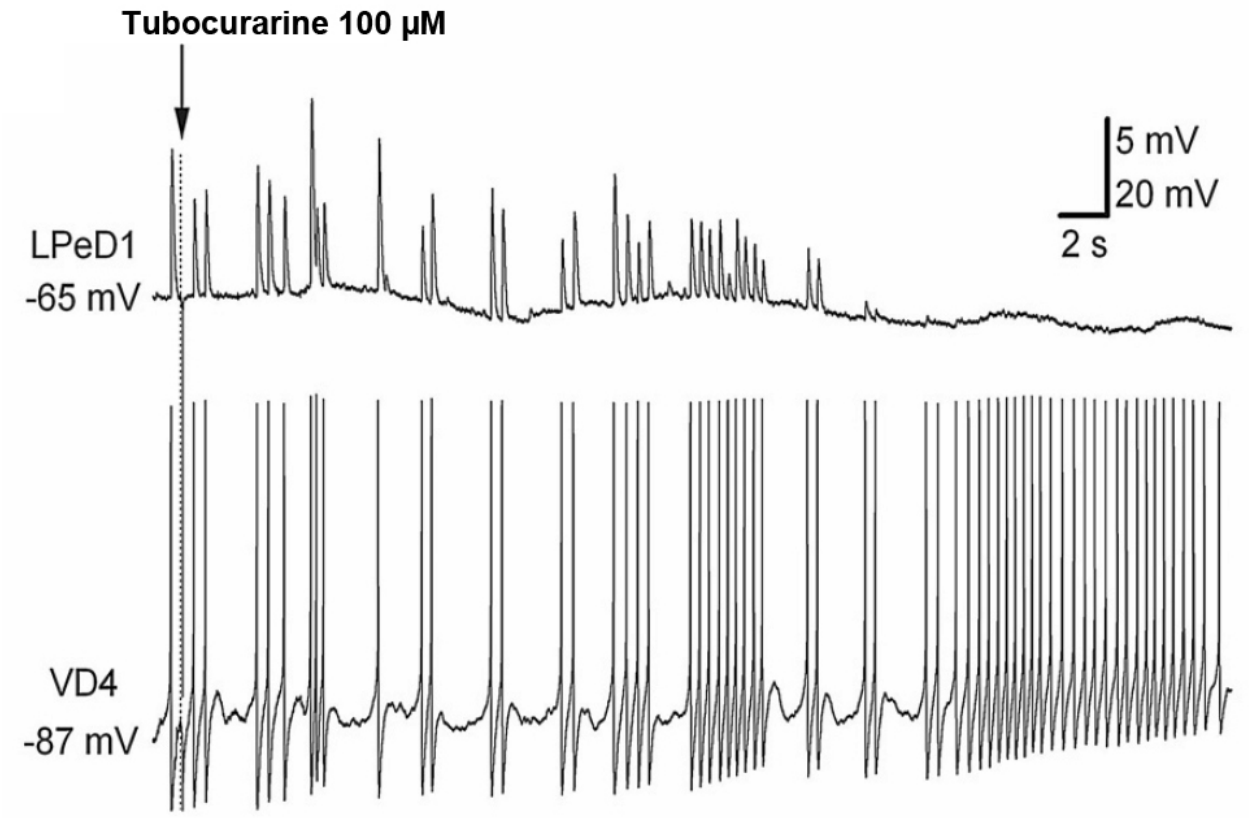

Figure 4.12: The LPeD1 responses to VD4 stimulation can be blocked by acetylcholine receptor antagonist tubocurarine.

To demonstrate that the response between VD4 and LPeD1 was a chemical synapse, a cholinergic antagonist, tubocurarine, was perfused into the bath solution of a spontaneously firing VD4 with an LPeD1 being recorded by the chip. Within 14 seconds of perfusion, a gradual reduction in the amplitude of LPeD1 postsynaptic potentials was noted until no response was observed despite increasing the frequency of VD4 action potential firing. This experiments demonstrates that the silicon nitride planar patch clamp chip is indeed recording postsynaptic potentials.

Figure 4.13

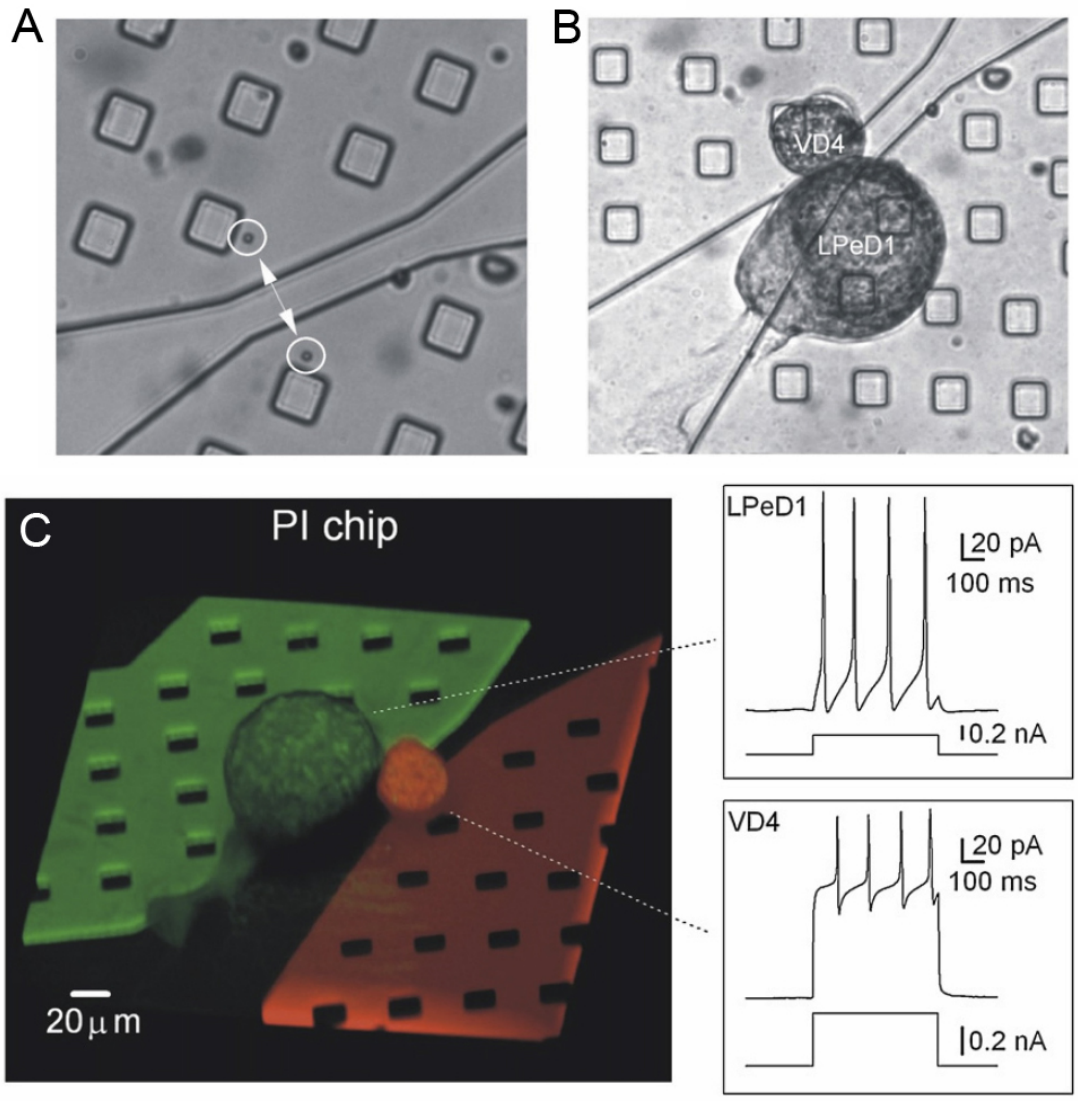
A
B
VD4
LPeD1
C
PI chip
20 µm
LPeD1
20 pA
100 ms
0.2 nA
VD4
20 pA
100 ms
0.2 nA

Figure 4.13: The polyimide planar patch clamp chip is able to record neuronal voltage changes in response to step currents.

The polyimide planar patch clamp chip shows the two independent channels containing the subterranean pipette solution and their respective support posts. The recording apertures 4 µm in diameter can be seen in each of the channel (circled in white) and are spaced 60µm apart. The image in **(A)** shows the apertures prior to culturing and **(B)** the placement of the neurons following culture of presynaptic VD4 and LPeD1 neuron. To demonstrate the ability to perfuse solution from the subterranean channel into specific neurons, LPeD1 channel was filled with Lucifer yellow dye (2 mM; green) and the VD4 channel was filled with Texas-red Sufonyl Chloride (0.5 mM; red). Thirty-three optical sections were collected with a z-step increase of 3 µm per scan and a 3D image was compiled **(C)**. The image depicts two channels with differing fluorescent dyes which have diffused through the aperture intracellularly. A simultaneous physiological voltage recording of LPeD1 (**C-top**) and VD4 (**C-bottom**) to a series of intracellular current pulses through the polyimide chip are shown.

Figure 4.14

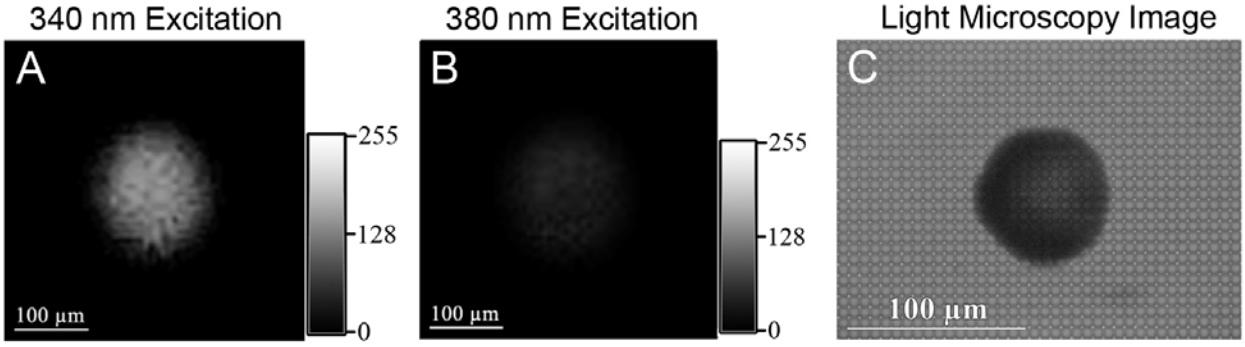

Figure 4.14: Fluorescent images detected by the contact imager.

Fluorescent images of fura-2 loaded LPeD1 neurons were captured at the two fura-2 excitation wavelengths **(A)** 340 nm and **(B)** 380 nm by the contact imaging device. The 340 nm excitation wavelength correspond to the fura-2 indicator when bound to calcium and the 380 nm excitation wavelength to the unbound fura-2 molecule. A greyscale gradient map is seen to the right of figure A and B. **(C)** A light microscopy image shows the relative size of an LPeD1 neuron in comparison to a single sensing pixel.

Figure 4.15

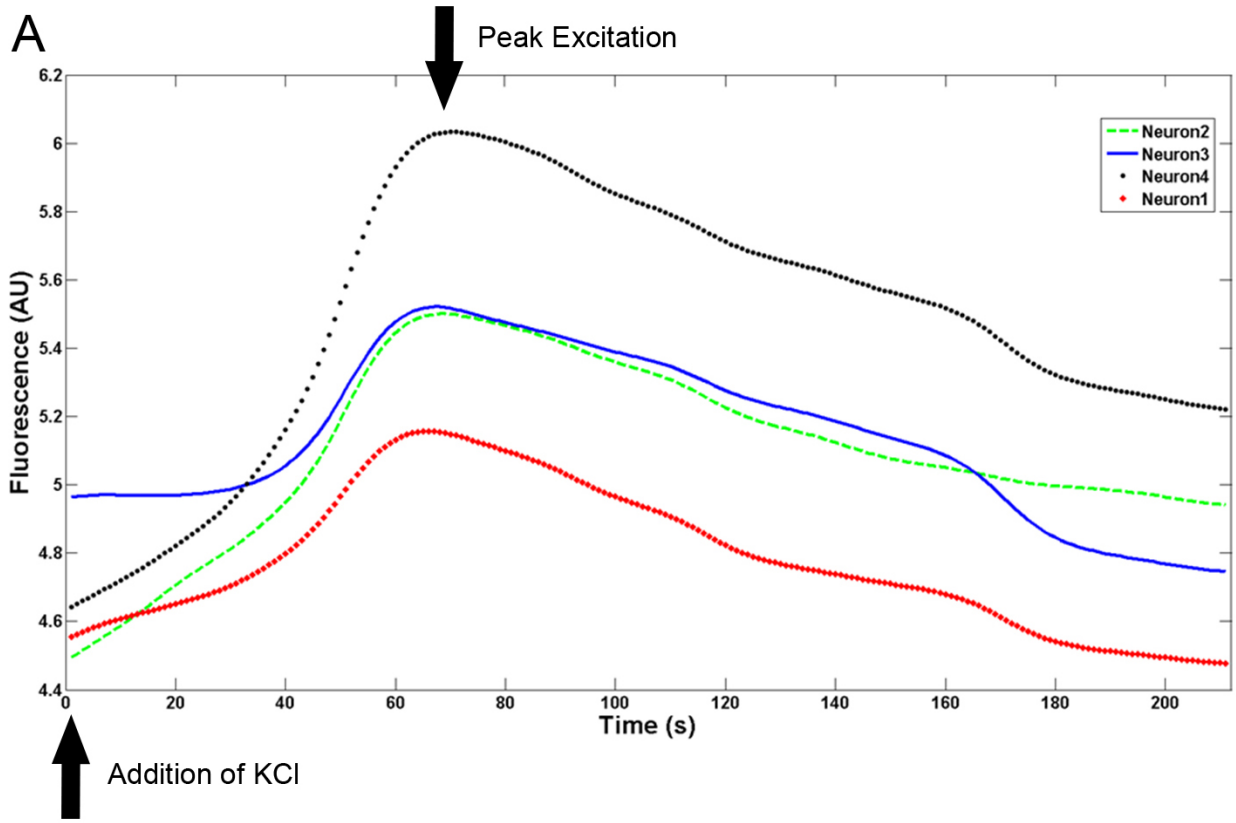

Figure 4.15: The contact imager is able to detect changes in calcium levels in real time. To test the ability of the system to monitor changes in intracellular calcium over time, 50uL of 1M KCl was added locally to the 2mL petri dish **(A)**. KCl caused the neurons to depolarize and trigger action potentials, therefore causing a rise in the intracellular calcium levels of the neurons. This change is depicted graphically where four different LPeD1 neurons were simultaneously monitored (at 340 nm excitation light). Within 70 seconds following the addition of KCl, the maximum level of fluorescence is detected as indicated by the peak excitation. **(B)** Sample images of the emission fluorescence for excitation at both 340 nm and 380 nm wavelengths at various time points (0 s, 110 s and 205 following KCl addition) can be seen. Both a grayscale and pseudocolor representation of the fluorescence is shown.

Figure 4.16

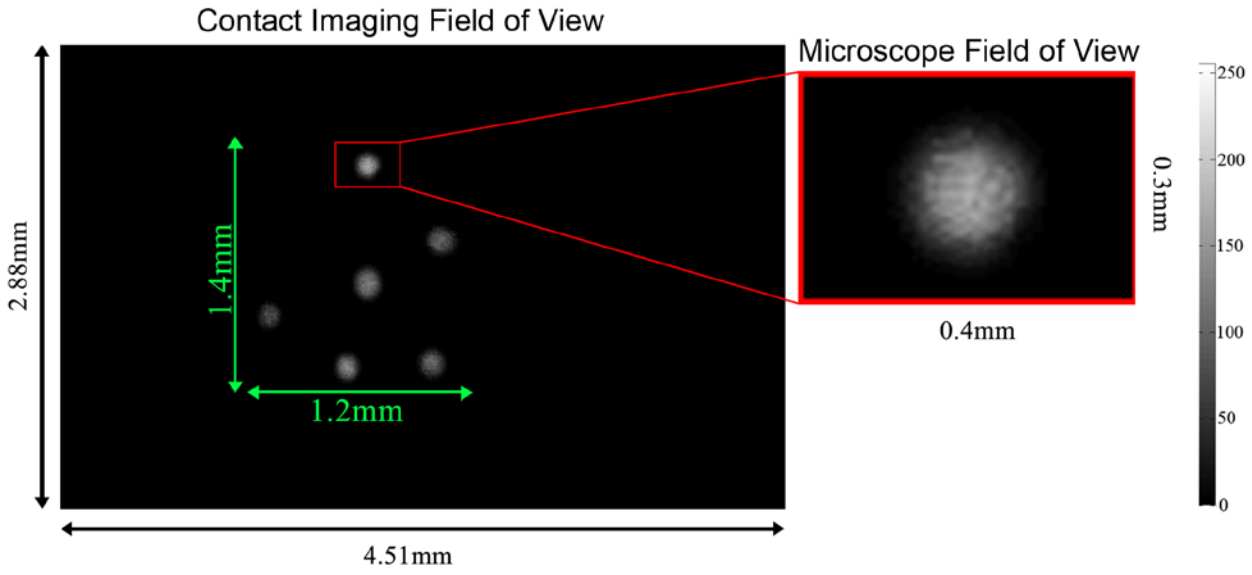

Figure 4.16: The contact imager has a larger field of view than is permissible with conventional microscopy.

The contact imaging field of view provides a detection area of 2.88mm x 4.51mm. As shown, all six LPeD1 neuron can be simultaneously visualized and detected with a large amount of additional area surrounding the neurons for further interrogation. In comparison to conventional microscopy with a 40x oil immersion objective, the field of view would only be able to interrogate one neuron at a time (red box indicates field of view) with dimension of 0.3mm x 0.4 mm.

Chapter 5: A Novel Form of Presynaptic Calcium/Calmodulin Dependent Kinase II short-term potentiation between *Lymnaea* neurons

Sections of this chapter have been published as:
Luk C.C., Naruo H., Prince D., Hassan A., Doran S.A., Goldberg J.I. and Syed N.I. (2011). "A novel form of presynaptic CaMKII-dependent short-term potentiation between Lymnaea neurons." European Journal of Neuroscience. 34(4):569-577. – *Reproduced with permission from John Wiley and Sons.*

5.1 Introduction

Neuronal communications between synaptically paired cells exhibit a high degree of synaptic plasticity, enabling a network to generate behaviorally relevant and functionally meaningful outputs. All chemical synapses undergo activity-induced changes in synaptic efficacy either by potentiating or depressing their synaptic strength (Feldman 2009), and thus enable an animal to adapt to its ever changing environment. These changes in synaptic strength could either be short or long term, and may form the basis for both short and long-term memory, respectively (Kandel et al. 2014).

Short-term potentiation (STP) is a form of synaptic plasticity that is thought to underlie short-term or working memory in many model systems (Baddeley 1992; Fisher et al. 1997; Wang et al. 2006). Two of the major contributing forms of STP include facilitation (lasts hundreds of milliseconds) and post-tetanic potentiation (PTP; lasts from seconds to several minutes) (Zucker and Regehr 2002; Fioravante and Regehr 2011; Regehr 2012). In PTP, a brief pulse of presynaptic activity generally results in a short-term increase in the efficacy of synaptic transmission between paired cells in a variety of invertebrates [Crayfish NMJ (Delaney et al. 1989), *Helix* central synapses (Pivovarov and Drozdova 2002), *Aplysia* NMJ (Fox and Lloyd 2001)] and vertebrate [NMJ , hippocampus (Brager et al. 2003), rat calyx of Held (Korogod et al. 2005)] synapses. Presynaptic residual Ca^{2+} hypothesis is generally thought to account for PTP at a variety of synapses. This hypothesis suggests that residual calcium from a previous burst of

activity is thought to enhance transmitter release in subsequent action potentials (Zucker and Lando 1986). Whereas the postsynaptic changes include receptor sensitization and Ca^{2+}-induced release of retrograde signals that act back on the presynaptic cell to enhance subsequent transmitter release (Zucker and Regehr 2002; Regehr 2012). However, the precise mechanisms underlying PTP remain to be fully defined.

In this study, I have identified and characterized a novel form of STP, which shares features with PTP while exhibiting several unique characteristics not described previously. Using well-defined excitatory synapses between *Lymnaea* pre- and postsynaptic neurons, I provide evidence for a form of STP that is use- but not time-dependent and requires pre- but not postsynaptic CaMKII activity.

5.2 Results

5.2.1 Synapses between VD4 and its postsynaptic partners exhibit short-term synaptic plasticity

In both the *in vivo* and *in vitro* soma-soma configurations, the cholinergic neuron visceral dorsal 4 (VD4) makes well-defined excitatory and inhibitory synapses with its postsynaptic partner cells (Feng et al. 1997; Hamakawa et al. 1999; Woodin et al. 1999; Woodin et al. 2002; Xu et al. 2009). These *in vitro* reconstructed synapses are highly reliable and exhibit STP (Naruo et al. 2005), but the underlying mechanisms remain unknown. Hence, to define the cellular and synaptic mechanisms underlying this short-term synaptic plasticity, cells were paired in a soma-soma configuration overnight and synapses tested after 12-18 hours in culture. I discovered that induced action potentials in VD4 generated 1:1 excitatory postsynaptic potentials (EPSPs - **Fig. 5.1A**) in its partner left pedal dorsal 1 (LPeD1) neuron (current clamped at -100 mV in all

experiments, unless specified otherwise). However, following a presynaptic tetanic stimulation (comprising of 8-14 action potentials at ~10 Hz), a subsequently triggered action potential generated an EPSP that was significantly larger compared to the pre-tetanic spikes (**Fig. 5.1A**). Specifically, when I compared EPSP amplitudes triggered by 10 presynaptic action potentials before and after the tetanic stimulation, a one-way ANOVA revealed a significant effect of tetanic stimulation on the EPSP amplitude ($F_{19,180} = 3.837$, $p < 0.001$, n=10). Specifically, a Tukey's post-hoc test revealed that the EPSP following tetanic stimulation was significantly ($p < 0.001$) greater than all 10 EPSPs prior to tetanic stimulation and the 9 EPSPs following the potentiated EPSP.

Further characterization of synaptic potentiation revealed that the amplitudes of the first two pEPSPs (post-tetanus EPSP) were significantly larger than the EPSP prior to the tetanic stimulation (**Fig. 5.1Bi**). Specifically, while the average amplitude of the EPSP prior to tetanic stimulation was 9.7 ± 0.53 mV (n=30), an action potential generated in VD4 3-5 seconds following the tetanus, resulted in an EPSP whose amplitude was approximately 2.5 times greater (248%, 24.1 ± 0.88 mV, $p < 0.001$, n=30) (**Fig. 5.1Bi and Bii**) than its pre-tetanus counterpart. I observed that the synaptic strength returned to its baseline after one or two induced action potentials in the presynaptic VD4 neuron.

Next, to determine the stimulation paradigm required for potentiation, I tested the minimum number of action potentials in a tetanic pulse that would be required for potentiation. I injected a square depolarizing current pulse (eliciting a ~10 Hz tetanic burst) and systematically controlled the duration of stimulation that elicited desired number of action potentials (2 to 14 action potentials) during a tetanic stimulation. I found that a minimum of 7 action potentials per tetanic stimulation were required for reliable induction of a pEPSP that was significantly greater

than control EPSPs ($F_{12,119} = 10.999$, $p < 0.001$, n = 7-15) (**Fig. 5.1Ciii**). Tetanic pulses with total action potentials below this "threshold" (**Fig. 5.1Ci**) failed to elicit potentiation, whereas tetanic pulses comprising of greater than 7 action potentials always resulted in a potentiated EPSP post-tetanus (**Fig. 5.1Cii**). I did not, however, observe a significant difference between the amplitude of potentiated EPSPs generated with a tetanic pulse consisting of between 7-14 APs. Hence, for all subsequent tests, a 10 Hz stimulation comprising of 7-14 action potentials was used to induce potentiation.

To demonstrate that this observed STP is functionally relevant and can indeed generate action potentials in LPeD1 following presynaptic tetanic stimulation, the postsynaptic cell was held closer to its resting potential (-60 mV). Whereas single presynaptic action potentials rarely generated 1:1 spikes in the postsynaptic cell, post-tetanus action potentials produced single spikes in LPeD1—provided that it was held closer to its resting membrane potential (**Fig. 5.2A**). Next, to test the specificity of this STP, I concurrently paired a single VD4 cell overnight with its excitatory (LPeD1) and inhibitory (left pedal E - LPeE) partner respectively, and synapses were tested electrophysiologically. Specifically, VD4 was soma-soma-soma paired with LPeD1 and LPeE neurons (**Fig. 5.2Bi**) and simultaneous intracellular recordings were made after 10-24 hours of cell pairing. Induced action potentials in VD4 generated 1:1 EPSPs (LPeD1) and inhibitory postsynaptic potentials (IPSPs – LPeE, held closer to its resting membrane potential -60mV) in its synaptic partners. The amplitude of both EPSPs (10.1 ± 0.45 mV) and IPSPs (-5.1 ± 0.31 mV) were significantly enhanced following the presynaptic tetanus with amplitudes of 26.0 ± 2.2 mV ($p < 0.001$) and -30.5 ± 2.2 mV ($p < 0.001$) respectively (n=7, **Fig. 5.2Bii and Biii**). Taken together, these data demonstrate that the specificity of synaptogenesis between VD4 and its excitatory and inhibitory partners is not only maintained in a soma-soma-soma configuration,

but that both synapses also exhibit short-term potentiation. These aspects of short-term potentiation between VD4 and its synaptic partners are analogous to those observed at a variety of other vertebrate and invertebrate (Zucker and Regehr 2002; Xu et al. 2007) synapses.

5.2.2 STP at the VD4-LPeD1 synapse is use- but not time-dependent and does not involve postsynaptic receptor sensitization

In all previously reported instances of STP, synaptic potentiation was shown to be time-dependent (Fioravante and Regehr 2011). However, in contrast to these previously published accounts, I found that STP at the VD4-LPeD1 synapse is use- but not time-dependent. Specifically, VD4 and LPeD1 cells were paired overnight and STP demonstrated as above. Using the same tetanic induction protocol, I measured the post-tetanus EPSP amplitudes 3, 5, 10, 60 seconds, 30 minutes and 5 hours following tetanic stimulation. I found that the synapse remained potentiated from seconds (**Fig. 5.3A**) to as long as 5 hours following tetanic stimulation – provided that the presynaptic cell was prevented from firing an action potential after the tetanus. Triggering the post-tetanus action potential in VD4 at 3 seconds (303.1 ± 54 %; n = 11; $p < 0.001$), 5 seconds (300 ± 23.8%; n = 8; $p < 0.001$), 10 seconds (256.5 ± 13.6 %; n = 11; $p < 0.001$), 60 seconds (262.7 ± 30 %; n = 11, $p < 0.001$), 30 minutes (356.9 ± 38.8%; n = 10, $p < 0.001$), and even up to 5 hours (347.5 ± 38.8%; n = 5, $p < 0.001$) following tetanus resulted in significant synaptic enhancement. This enhancement was depotentiated following one or two action potentials in all cases. When I compared the amplitude of the pEPSPs ($F_{5,50}$ = 0.317; $p = 0.901$) or the percent synaptic enhancement ($F_{5,50} = 1.224$; $p = 0.312$), I found that there was no significant difference between the potentiated response measured at any time point. These data thus demonstrate that STP at the VD4 and LPeD1 synapse is indeed use- and not

time-dependent (**Fig. 5.3A**) whereby the potentiated strength is similar from 3 seconds to 5 hours following tetanic induction and were depotentiated following one or two action potentials triggered in the presynaptic neuron. Several aspects of this form of STP have since been computationally modeled elsewhere (Mehta et al. 2013).

I next asked whether STP at the VD4/LPeD1 synapse involves postsynaptic receptor sensitization as was observed in *Helix* (Pivovarov and Drozdova 2002)—a closely related species. To address this issue, cells were paired overnight and synapses tested electrophysiologically. Prior to a tetanic burst, ACh (VD4's neurotransmitter) was applied exogenously to the contact site using a fast perfusion system and the extra-synaptic responses monitored. I reasoned that if ACh release from VD4 during tetanus were to sensitize ACh receptors (AChR), then the same puff of exogenous ACh over the contact site would most likely generate a much greater response as compared to the pre-tetanus pulse. However, I discovered that the presynaptic tetanus failed to augment the extrasynaptic response to exogenously applied ACh (10^{-5}M; pre-tetanus puff of 10.0 ± 0.21 mV compared to post-tetanus puff of 10.4 ± 0.6 mV, $p = 0.29$), while the synaptic response still exhibited STP (EPSP of 9.1 ± 0.64 mV compared to pEPSP of 28.6 ± 6.1 mV; n=6, $p < 0.01$ **Fig. 5.3B and C**). Taken together, these data demonstrate that STP at the VD4/LPeD1 synapse does not involve postsynaptic receptor sensitization.

5.2.3 STP at the VD4-LPeD1 synapse does not involve presynaptic residual calcium

I next sought to determine whether presynaptic residual Ca^{2+} could account for the STP observed at the VD4-LPeD1 synapse. To test this possibility, I imaged VD4 cell using the Ca^{2+} indicator dye Fura-2 both before and after the tetanic stimulation of VD4. Specifically, VD4

paired in a soma-soma configuration overnight with an LPeD1 cell was injected with Fura-2 (**Fig. 5.4Ai**) and images acquired both before and after the tetanus. As shown previously (Feng et al. 2002), the voltage-induced Ca^{2+} hotspots were clearly discernable in VD4 at its contact point with LPeD1 (**Fig 5.4Aii**). Ratiometric Ca^{2+} images were acquired at various time intervals – prior to pre-tetanus action potential, during the action potential, during the tetanus and during the post-tetanus action potential. I found that although both single action potentials (459.5 ± 11.4 nM pre-tetanus; 409.5 ± 34.2 nM post-tetanus) and the tetanus pulse (1235.3 ± 51.7 nM) raised Ca^{2+} from the baseline (307.3 ± 9.5 nM), the elevated Ca^{2+} did, however, return to its basal level within a matter of seconds (**Fig. 5.4Aiii,iv**). These data rule out the possibility of residual Ca^{2+} being the potential mechanism for the STP observed at the VD4-LPeD1 synapse.

5.2.4 STP at the VD4-LPeD1 synapse requires protein kinases but not protein kinase C

Previous studies in both vertebrate (Stevens and Sullivan 1998; Berglund et al. 2002) and invertebrates (Fossier et al. 1990) have implicated PKC in STP (Giese and Mizuno 2013). To test for the involvement of this kinase, I first used a non-specific inhibitor of protein kinases. Cells were soma-soma paired overnight and STP tested electrophysiologically. Staurosporine (50nM) – a non-selective inhibitor of all protein kinases was injected into the VD4 soma and STP was examined again. I found that within ten minutes of injection, both the synaptic transmission and the STP were significantly reduced (**Fig. 5.5A**). For instance, the normal EPSP amplitude of 9.7 ± 3.1 mV was reduced to 5.8 ± 1.0 mV ($p < 0.001$), whereas the pEPSP amplitude of 23.7 ± 4.9 mV recorded under normal conditions was also reduced to 7.3 ± 2.1 mV ($p < 0.001$, n=31) (**Fig. 5.5A** inset). Thus, staurosporine reduced the synaptic enhancement of the pEPSP amplitude from

244% in control conditions to 126%. These data thus demonstrate the involvement of protein kinases in both the baseline synaptic transmission as well as the STP.

To determine the precise identity of this protein kinase, I next asked the question whether protein kinase C activity might underlie the STP at the VD4-LPeD1 synapse. To test this possibility, PKC activity [which has been implicated in PTP at a number of synapses – (Fossier et al. 1990; Stevens and Sullivan 1998; Berglund et al. 2002; Syed 2006)] was manipulated either through its inhibitor bisindolylmaleimide (BIS) or its activator Phorbol-12-Myristate-Acetate (PMA). In particular, VD4/LPeD1 soma-soma synapses were reconstructed *in vitro* and the PKC antagonist, BIS (Rosenegger and Lukowiak 2010) at a final bath concentration of 1 μM or 250 nM, was added to the bath. Unlike the effects observed following staurosporine treatment, perturbation of PKC activity had no significant effect on synaptic transmission (control EPSP, 9.8 ± 2.9 mV; 250 nM BIS, 9.8 ± 1.4 mV [$p = 0.639$]; 1μM BIS, 10.0 ± 1.8 mV [$p = 0.581$]), nor was the STP affected (control pEPSP, 23.3 ± 3.9 mV; 250 nM BIS, 23.9 ± 4.1 mV [$p = 0.731$]; 1 μM BIS, 24.2 ± 5.0 mV [$p = 0.659$]) following 60 minutes of drug application (**Fig. 5.5Bi**). Similarly, activating PKC with its agonist PMA (250 nM) also failed to affect synaptic transmission (control EPSP, 10.4 ± 4.7 mV; 250 nM PMA, 10.1 ± 1.7 mV [$p = 0.730$]) or STP (control pEPSP, 24.9 ± 4.1 mV; 250 nM PMA, 24.1 ± 4.1 mV [$p = 0.681$]) (**Fig. 5.5Bii**; n=20). These results thus rule out the involvement of presynaptic PKC in the STP observed at the VD4/LPeD1 synapse.

5.2.5 STP involves Calcium/Calmodulin-dependent protein kinase II

In the absence of PKC involvement, I next sought to determine whether another protein kinase, Calcium/Calmodulin Kinase II (CaMKII), which has been implicated in various forms of

synaptic plasticity (Fink and Meyer 2002; Shonesy et al. 2014), was involved in this STP. To test this, VD4/LPeD1 cells were paired and a specific CaMKII inhibitor KN-93 (100nM) was injected intracellularly into the VD4 somata. I found that within 10 minutes of KN-93 injections, both the baseline synaptic transmission and the STP were significantly reduced (**Fig. 5.6A**). Specifically, injection of KN-93 reduced EPSP amplitudes from 10.4 ± 3.2 mV in control to 6.6 ± 2.5 mV, while pEPSP was significantly reduced from 26.5 ± 4.6 mV to 7.2 ± 2.1 mV (**Fig. 5.6A**; n=31 $p < 0.001$). This accounted for a reduction in synaptic enhancement from 255% in control to 109% in KN-93 injected synaptic pairs. As a negative control, I also injected either DMSO alone (carrier solution, data not shown) or an inactive analogue (KN-92) of KN-93, which was also dissolved in DMSO. I found that the inactive analogue neither affected synaptic transmission nor the STP (**Fig. 5.6B**, n=21). In particular, control EPSPs (11.1 ± 3.5 mV) and pEPSPs (28.7 ± 7.9 mV) did not differ significantly from those seen in KN-92 injected cells (control EPSPs: 11.5 ± 1.6 mV, $p = 0.693$; pEPSPs: 29.5 ± 6.2 mV, $p = 0.750$) (**Fig. 5.6B**).

To further demonstrate the specificity of KN-93's effects, I also injected the presynaptic cell with a specific CaMKII inhibiting peptide - autocamtide-2-related inhibitory peptide (1μM). I found that this peptide inhibitor also specifically suppressed both the synaptic transmission and the STP at the VD4/LPeD1 synapse. EPSP amplitudes were reduced from 22.56 ± 1.82 mV to 15.33 ± 0.4 mV and pEPSP amplitudes were reduced from 41.68 ± 1.18 mV to 15.59 ± 0.51 mV (n=8, $p < 0.05$) (**Fig. 5.6C**) (LPeD1 neurons were held at a resting membrane potential of -120 mV for this experiment). This demonstrated a reduction in synaptic potentiation from 185% in control to 102% in AIP injected pairs.

To further characterize the role of CaMKII in STP, I examined the role of Ca^{2+}-Calmodulin (CaM), a regulator of CaMKII (Xia and Storm 2005). A CaM inhibitor, W-7 (1 μM),

was bath applied prior to testing the STP at the VD4-LPeD1 synapses. Within 20 minutes of the drug application, both the base line synaptic transmission and STP were significantly reduced ($p < 0.001$) (**Fig. 5.6D**). In particular, EPSP amplitudes were reduced from 20.08 ± 0.59 mV to 10.07 ± 0.37 mV and pEPSP amplitudes were reduced from 40.53 ± 0.66 mV to 10.52 ± 0.41 mV (n=7 control, n=12 W-7) (to magnify the amplitude of VD4-induced EPSP in LPeD1 further, the postsynaptic cells in this series of experiments were also held at a resting membrane potential of -120 mV). Taken together, these data provide evidence for a direct involvement of presynaptic CaMKII in synaptic plasticity at the VD4-LPeD1 synapse.

5.3 Discussion

In this chapter, I have identified and characterized a novel form of synaptic plasticity between soma-soma paired *Lymnaea* neurons VD4 and LPeD1. Unlike previously described forms of short-term potentiation, the plasticity at the VD4 and LPeD1 synapse was time independent. Specifically, in the absence of activity, the STP persisted from several seconds to hours, provided that the presynaptic cell was kept silent after the single tetanic stimulation. This potentiation was, however, depotentiated upon triggering one or two action potentials. While this form of potentiation persists for a longer duration than other previously described forms of STP, its induction requires a short presynaptic burst and exhibits a rapid onset. Moreover, the synaptic potentiation between VD4 and LPeD1 undergoes rapid depotentiation suggesting that it has hallmarks of STP. In contrast, the STP at the VD4/LPeD1 synapse lasts beyond previously defined times of short-term potentiation provided that the presynaptic cell is kept silent. I propose here that this potentiation is mediated through CaMKII, which may provide the molecular switch that can remove temporal limitation on short-term plastic changes. In this form of STP, there does not appear to be a need for postsynaptic receptor sensitization, nor does it require presynaptic residual Ca^{2+}. Similarly, our data rule out the involvement of protein kinase C. This study thus identifies several novel mechanisms that may be involved in short-term potentiation at these well-defined synapses, in the absence of confounding involvement of either glia or other connected neurons. As mentioned previously, this form of STP has been computationally modeled in collaboration with Dr. Mehta (Mehta et al. 2013).

Although both short and long-term synaptic plasticity has been investigated in a wide variety of vertebrate and invertebrate preparations, and in some cases well characterized, the precise cellular and molecular mechanisms remain, however, unresolved. For example, it is

unclear as to what extent different forms of synaptic plasticity share common mechanisms. In some cases, STP is dependent on presynaptic residual Ca^{2+} at the crayfish (Tang and Zucker 1997) and mouse neuromuscular junction (David and Barrett 2003), whereas at an *Aplysia* central synapse, a postsynaptic increase in $[Ca^{2+}]_i$ is thought to regulate STP (Bao et al. 1997; Schaffhausen et al. 2001). Here, I have demonstrated that a single presynaptic cell can effectively regulate the efficacy of its STP at both excitatory and inhibitory synapses and that the potentiated response does not involve postsynaptic receptor sensitization. These data are therefore in contrast to previous studies in the snail *Helix* where postsynaptic AChR sensitization was considered sufficient to account for STP between the LPa3 and RPa3 neurons *in vivo* (Pivovarov and Drozdova 2002). Previous studies have often attributed STP to residual Ca^{2+}, whereby Ca^{2+} remaining in the nerve terminal following the stimulus augments subsequent activity (residual calcium hypothesis) (Zucker and Regehr 2002). For instance, the role of residual Ca^{2+} in producing STP is well documented at both the crayfish NMJ (Tang and Zucker 1997) and the *Aplysia* sensory-motor neuron synapses (Bao et al. 1997). In contrast to these previous findings, our Ca^{2+} imaging data show that the synapse between VD4-LPeD1 remains potentiated long after Ca^{2+} returns to its basal levels following the tetanic stimulation. Moreover, our data show that the Ca^{2+} signal between the pre- and the post-tetanus action potentials also does not change significantly. Consistent with these observations are studies conducted in mammals where STP at the Schaffer collateral synapses in the rat hippocampus has also been shown to persist twice as long as the elevated Ca^{2+} levels in the presynaptic terminal (Brager et al. 2003).

PKC has previously been implicated in synaptic potentiation. For instance, it is known to increase the refilling rate and the size of the readily releasable pool of vesicles at central

mammalian synapses (Stevens and Sullivan 1998; Berglund et al. 2002; Syed 2006; Chu et al. 2014). In particular, elegant studies have demonstrated that various isoforms—PKCγ and PKCβ—of PKC differentially regulate vesicular release probability as well as the size of the readily releasable pool (Chu et al. 2014). This has further been shown to relate to the innate ability for PKCβ to sense calcium signals through its C2 calcium binding domain (Fioravante et al. 2014). Related to our *Lymnaea* model, the facilitation of neurotransmitter release at cholinergic synapses between *Aplysia* buccal neurons have also been noted (Fossier et al. 1990). Whereas the data in the above studies demonstrated the involvement of Ca^{2+} activated PKC in synaptic potentiation, here I found that PKC does not regulate STP at the VD4/LPeD1 synapse. Rather, I discovered another protein kinase, CaMKII, to be the key mediator of this plasticity.

I found that the Ca^{2+}-binding protein, calmodulin (Activator of CaMKII) (Wayman et al. 2008; de Jong and Fioravante 2014), also serves as a key signaling protein in synaptic plasticity at the VD4-LPeD1 synapse. Previous studies have shown that, Ca^{2+} binding to calmodulin induces a conformation change, thereby increasing the affinity of calmodulin for CaMKII (Schulman 1993). In response to Ca^{2+}-calmodulin binding, the auto-inhibitory subunit is displaced leading to the activation of CaMKII. Subsequent autophosphorylation of threonine 287 on CaMKII allows for the activation of this enzyme removing its dependence on Ca^{2+}/calmodulin (Schulman 1993; Hodge et al. 2006; Shonesy et al. 2014). This property of CaMKII could explain the use-dependence rather than time-dependence of PTP observed at the VD4/LPeD1 synapse such that active CaMKII can maintain potentiation in the absence of continuous cellular activity. In addition, CaMKII has previously been shown to be involved in synaptic plasticity at multiple synapses where it integrates Ca^{2+} signals in synaptic plasticity (Fink and Meyer 2002). For instance, CaMKII has been implicated in LTP (Malenka et al. 1989;

Malinow et al. 1989; Tomita et al. 2005; Lee et al. 2009; Shonesy et al. 2014), LTD (Mulkey et al. 1993; Stevens and Wang 1994; Coultrap et al. 2014), PTP (Chapman et al. 1995), STP (Jin and Hawkins 2003) and also as a regulator of the frequency-response function of the synapse underlying LTD and LTP (Mayford et al. 1995). Further, studies have shown that mice with heterozygous null mutation for α-CaMKII exhibit severe working memory deficits - a form of memory that relies upon PTP (Yamasaki et al. 2008). Recent studies in cultured *Helix* neurons have also demonstrated an activity dependent form of plasticity whereby tetanic stimulation with a minimum frequency induces PTP (Fiumara et al. 2005). Like our current study, this form of PTP was also CaMKII dependent (Fiumara et al. 2007), but in contrast to the use-dependent nature of our STP, this form of PTP only persisted for 3 to 4 minutes.

Previously, a form of use-dependent synaptic potentiation has been described in the CA1 area of the rat hippocampus by Volianskis and Jensen (2003). Similar to our data, field EPSP recordings showed that tetanic stimulation (theta burst stimulation) could induce potentiation as early as two minutes and up to six hours following tetanisation. When the synapses were stimulated at different time points following a tetanus, the potentiated response was found to depotentiate following a specific number of stimulations. This study thus bears strong resemblance to the STP described in our study, which is also shown to persist from seconds up to hours. Unlike the hippocampal slice preparation, however, where multiple stimulations were required to depotentiate the synapses, in our model the synapses depotentiated following only one or two action potentials. Whereas the field recordings may have invoked multiple synaptic sites with myriad synaptic partners in the hippocampus, our study provides more direct and unequivocal evidence that often single action potentials may be sufficient to depotentiate synapses between bursting neurons such as VD4.

While the precise mechanism by which CaMKII elicits it potentiating effect following tetanic stimulation remains unknown, other studies suggest synapsin proteins as a critical mediator for short-term plasticity. For instance, inhibition of synapsin in *Helix* (Fiumara et al. 2007; Giachello et al. 2010) or *Aplysia* (Humeau et al. 2001) synapses perturbs PTP, while increasing synapsin activity has the opposite effect (Humeau et al. 2001). Further, studies in drosophila demonstrate that CaMKII-mediated synapsin phosphorylation is important for the potentiation of GABAergic synapses between multiglomerular local circuit interneurons and projection neurons in the antennal lobe (Sadanandappa et al. 2013). Hence, I suggest that CaMKII phosphorylation of synaptic vesicle proteins such as synapsin, may enhance vesicle release and hence regulate neurotransmitter release (Lonart and Simsek-Duran 2006) in an activity-dependent manner.

Figure 5.1

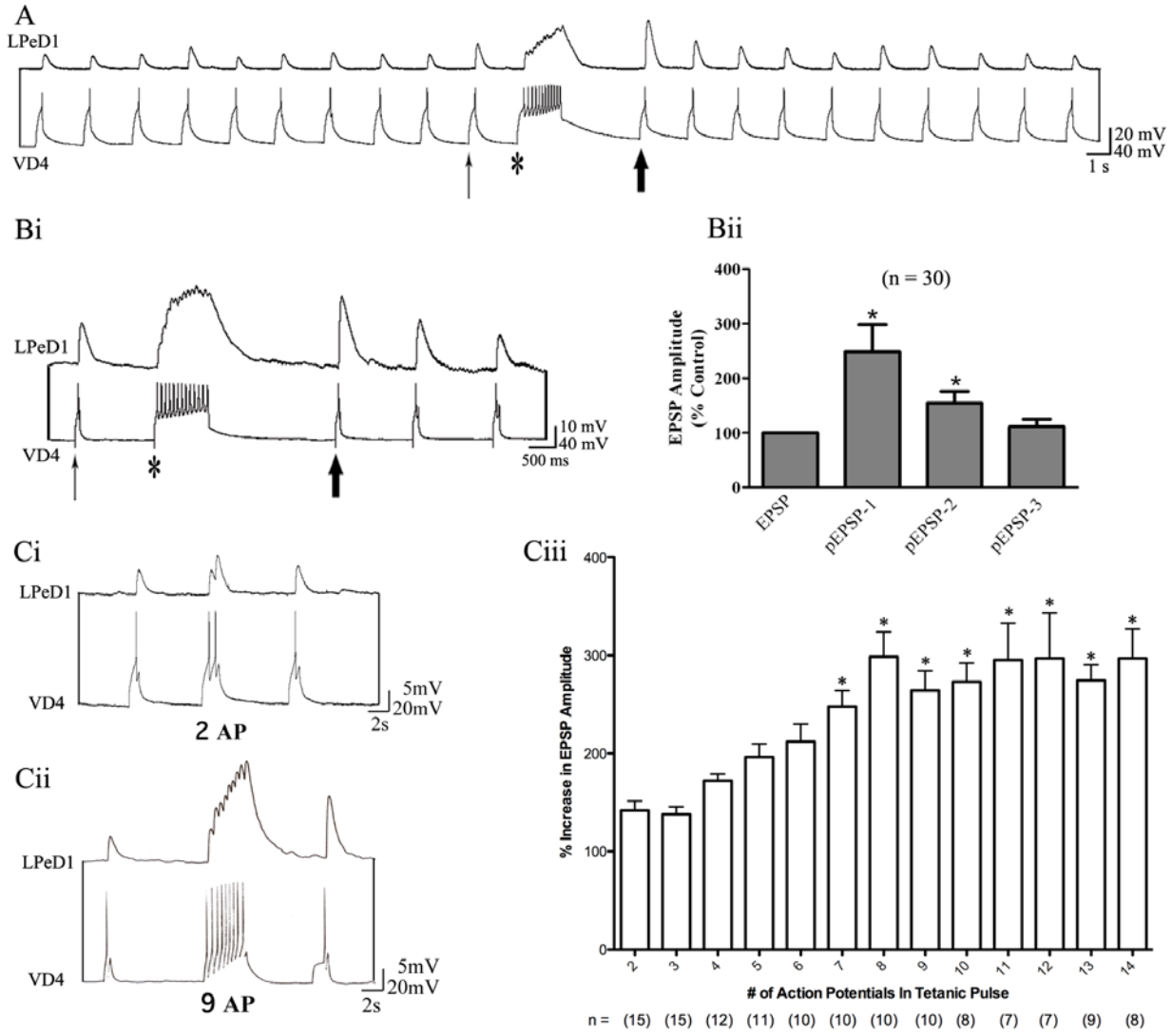
A
LPeD1
VD4
20 mV
40 mV
1 s
Bi
LPeD1
VD4
10 mV
40 mV
500 ms
Bii
(n = 30)
EPSP Amplitude (% Control)
400
300
200
100
0
EPSP
pEPSP-1
pEPSP-2
pEPSP-3
Ci
LPeD1
VD4
5mV
20mV
2s
2 AP
Cii
LPeD1
VD4
5mV
20mV
2s
9 AP
Ciii
% Increase in EPSP Amplitude
400
300
200
100
0
2 3 4 5 6 7 8 9 10 11 12 13 14
# of Action Potentials In Tetanic Pulse
n = (15) (15) (12) (11) (10) (10) (10) (10) (8) (7) (7) (9) (8)

Figure 5.1: Synapse between VD4 and its postsynaptic partners exhibit a form of short-term potentiation.

Neurons VD4 and LPeD1 were soma-soma paired overnight and their synapses tested electrophysiologically. **(A)** Induced action potentials in VD4 (at arrows) elicited 1:1 excitatory postsynaptic potentials (EPSPs) in LPeD1. A presynaptic burst, comprising 8-14 action potentials in VD4 (indicated by the asterisk) resulted in a compound postsynaptic potential (PSP). Subsequent single spikes in VD4 following the tetanic burst (indicated by the thick arrow) produced an EPSP with an amplitude several hundred percent larger than the EPSP elicited by the pre-tetanus action potential (indicated by the thin arrow). **(Bi)** Characterization of the EPSP amplitude prior to and following tetanus revealed that while tetanic stimulation potentiates the subsequent EPSP, this only last for one or two action potentials before returning to pre-tetanus EPSP amplitudes. **(Bii)** Summary data shows a 248% increase in the EPSP amplitude following the tetanus with a decline back to pre-tetanus EPSP amplitude levels following two action potentials (n=30). While **(Ci)** two action potentials failed to generate a potentiated response, **(Cii)** a tetanic burst comprising of nine action potentials (~10 Hz) elicited a potentiated response. A one-way ANOVA analysis on percentage enhancement as compared to control with a Tukey's Post Hoc test revealed that a minimum of 7 action potentials were necessary to reliably generate a post-tetanic EPSP. This is summarized in **(Ciii)**. Significance was determined using a univariate ANOVA with significance determined by $p < 0.05$. Significant synaptic enhancement is indicated by an asterisk.

Figure 5.2

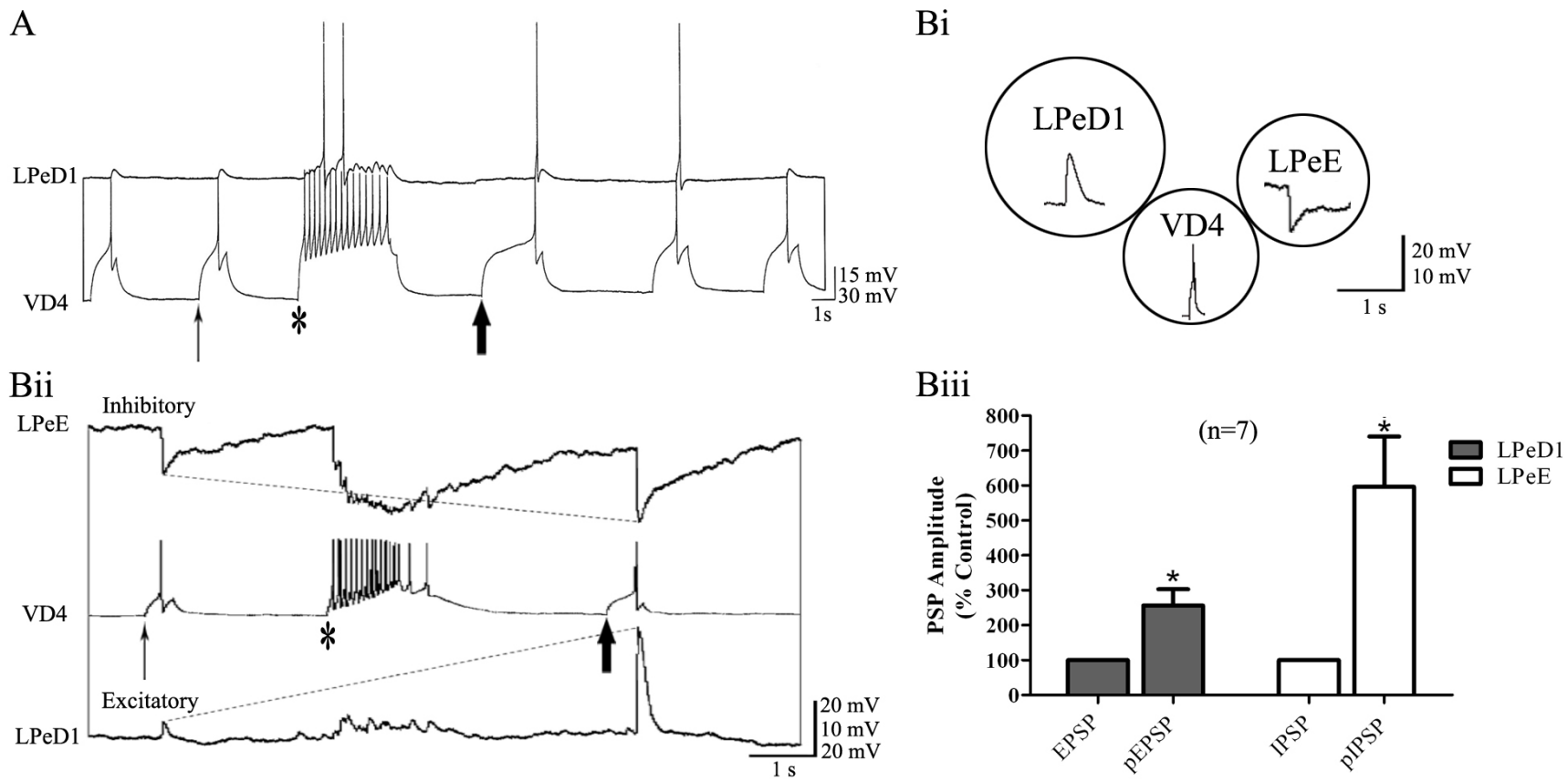
A
LPeD1
VD4
15 mV
30 mV
1s
Bi
LPeD1
LPeE
VD4
20 mV
10 mV
1 s
Bii
Inhibitory
LPeE
VD4
Excitatory
LPeD1
20 mV
10 mV
20 mV
1 s
Biii
(n=7)
PSP Amplitude (% Control)
800
700
600
500
400
300
200
100
0
LPeD1
LPeE
EPSP
pEPSP
IPSP
pIPSP

Figure 5.2: VD4 potentiates both excitatory and inhibitory synapses.

(A) While pre-tetanus EPSPs elicited by VD4 only produced sub-threshold EPSPs (thin arrow), increase in EPSP amplitude triggered action potentials after the tetanus (see thick arrow). **(Bi)** To further test the specificity of VD4-induced STP, I used a triple cell, soma-soma-soma configuration whereby a single VD4 was paired overnight with its excitatory (LPeD1) and inhibitory (LPeE) partner neurons. **(Bii)** Using simultaneous intracellular recordings from all three neurons, I show that following tetanic stimulation both excitatory and inhibitory synapses exhibit potentiation. **(Biii)** Summary data showing a 256% enhancement of excitatory (LPeD1) and 597% enhancement of inhibitory synapses (LPeE) (n=7) between VD4 and its synaptic partners. Significance was determined using a Students' t-test with significance determined by $p < 0.05$. Significant synaptic enhancement is indicated by an asterisk.

Figure 5.3

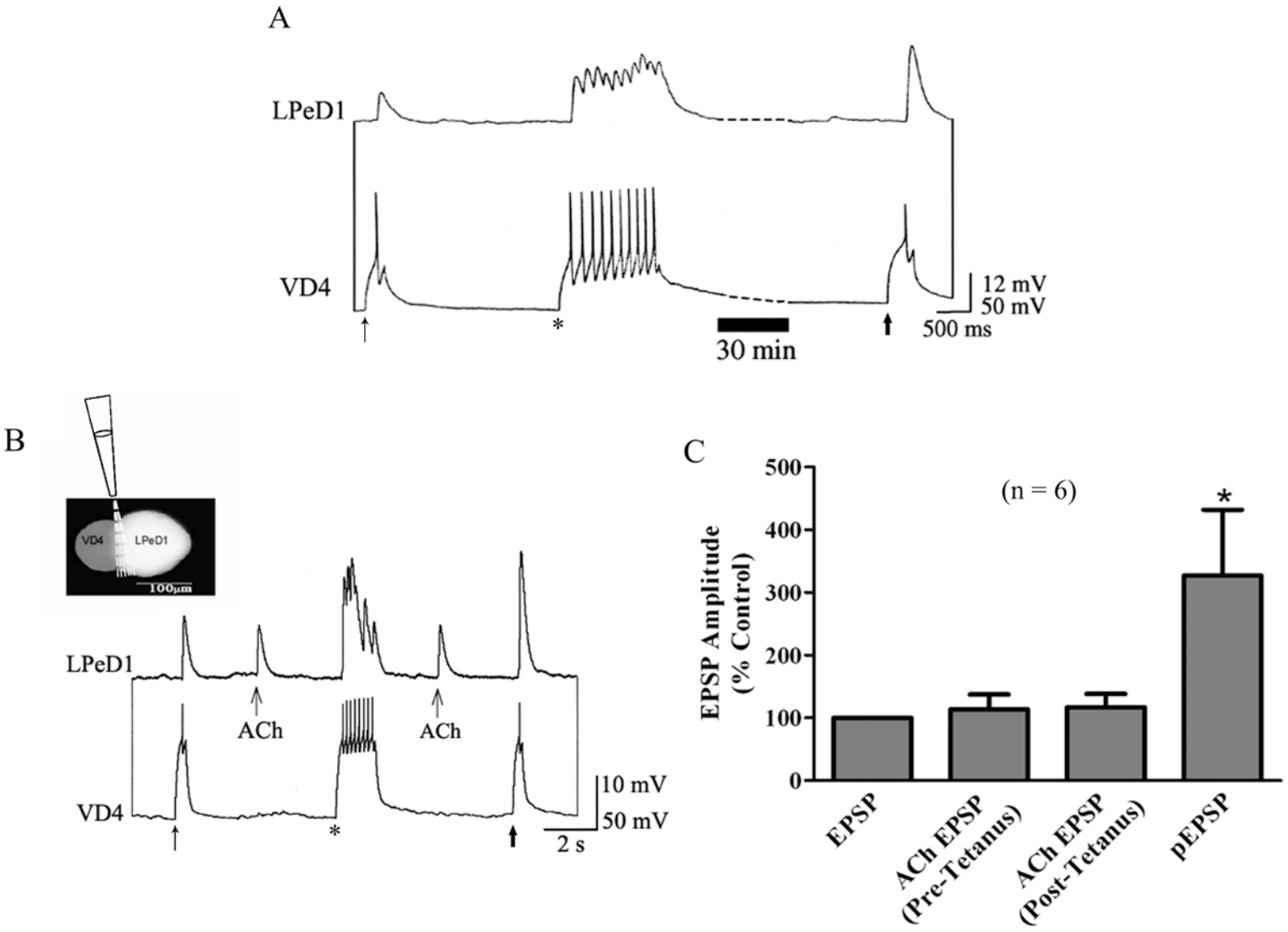
A
LPeD1
VD4
12 mV
50 mV
500 ms
30 min
B
VD4
LPeD1
100µm
LPeD1
ACh
ACh
VD4
10 mV
50 mV
2 s
C
(n = 6)
EPSP Amplitude (% Control)
500
400
300
200
100
0
EPSP
ACh EPSP (Pre-Tetanus)
ACh EPSP (Post-Tetanus)
pEPSP

Figure 5.3: Short-term potentiation at the VD4-LPeD1 synapse is use but not time-dependent, and does not involve postsynaptic receptor sensitization.

(A) *In vitro* reconstructed synapses between VD4/LPeD1 were tested electrophysiologically. Induced action potentials in VD4 (at thick arrow) following presynaptic tetanus spike (at asterisk) generated potentiated EPSPs in LPeD1 with amplitudes significantly greater than the pre-tetanus spike (at thin arrow) – notwithstanding the fact that the post-tetanus action potential was delivered after an interval of 30 minutes (see black bar and the dashed line, n=10). **(B)** To rule out the possibility that the STP at VD4/LPeD1 synapse involved ACh receptor sensitization, neurons were cultured overnight and ACh was pressure applied at the contact site between the cells (insert) both before and after the tetanic stimulation. Exogenous application of ACh (10^{-5}M) both prior to and following the tetanus elicited identical non-synaptic responses, which were comparable to that of the elicited EPSPs but smaller than the pEPSP amplitude. **(C)** Summary data comparing the amplitude of the cholinergic responses to induced EPSPs and the post-tetanic EPSP (pEPSP). Significance was determined using a paired Students' t-test between the ACh induced response before and after tetanus with $p < 0.05$. Significant synaptic enhancement is indicated by an asterisk.

Figure 5.4

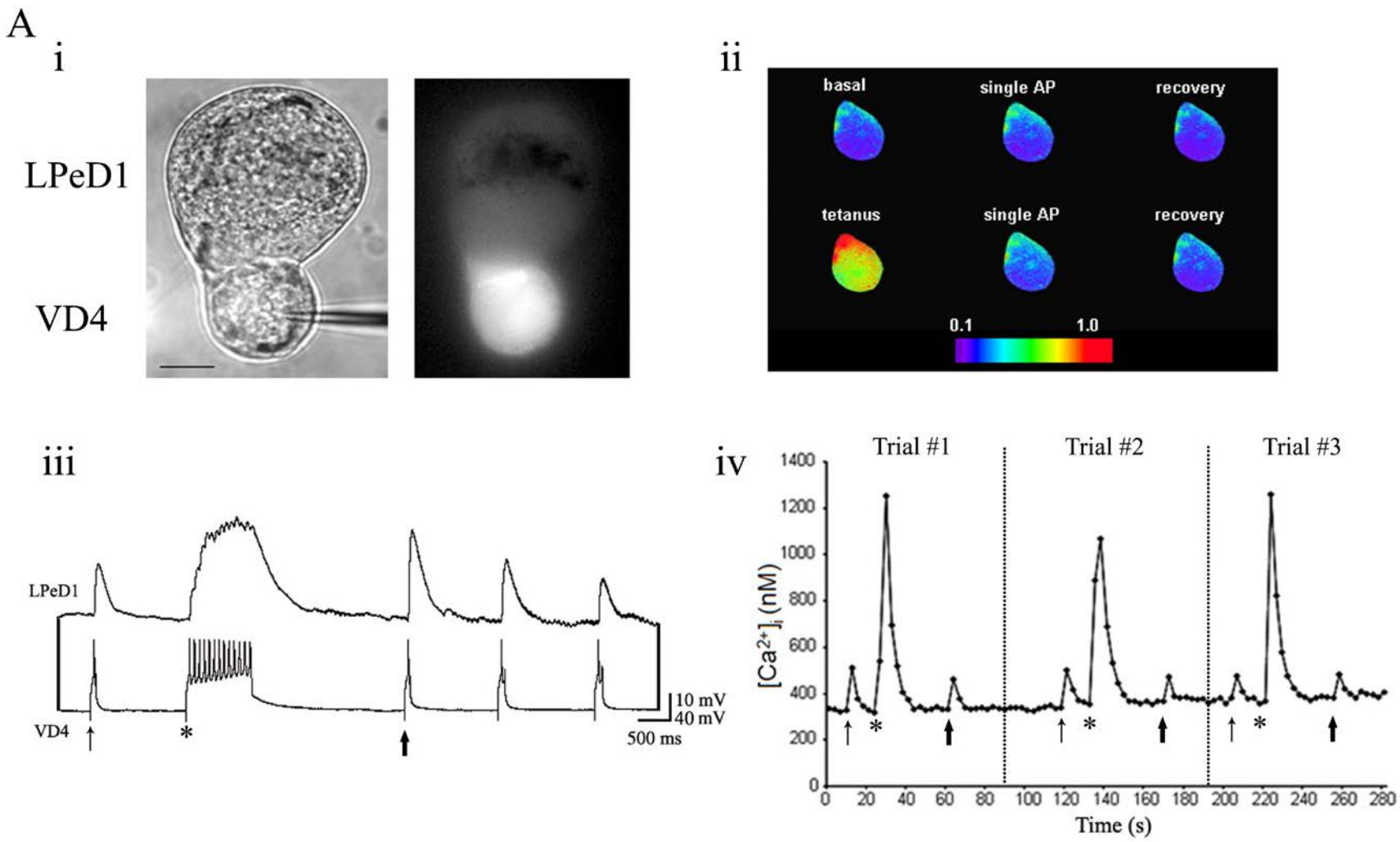
A
i
LPeD1
VD4
ii
basal
single AP
recovery
tetanus
single AP
recovery
0.1
1.0
iii
LPeD1
VD4
10 mV
40 mV
500 ms
iv
Trial #1
Trial #2
Trial #3
[Ca2+]i (nM)
Time (s)

Figure 5.4: Short-term potentiation at the VD4-LPeD1 synapse does not involve postsynaptic Ca^{2+} or residual presynaptic Ca^{2+}.

(Ai) To rule out the involvement of residual calcium in STP, Ca^{2+} indicator dye Fura-2 was injected intracellularly into VD4. **(Aii)** Ratiometric images were acquired prior to, during and after the tetanic stimulation. Activity-induced Ca^{2+} hotspots were clearly discernable at the contact site between the paired cells. **(Aiii)** The kinetics of the intracellular Ca^{2+} signal was analyzed prior to, during and after the presynaptic tetanus. I found that the intracellular Ca^{2+} levels both after a single action potential and the tetanic burst returned quickly to their resting levels. The data for multiple trials conducted on the same cell is presented in **(Aiv)** with the pre-tetanus action potential (thin arrow), tetanus (asterisk) and post-tetanus action potential (thick arrow) tested in three trials.

Figure 5.5

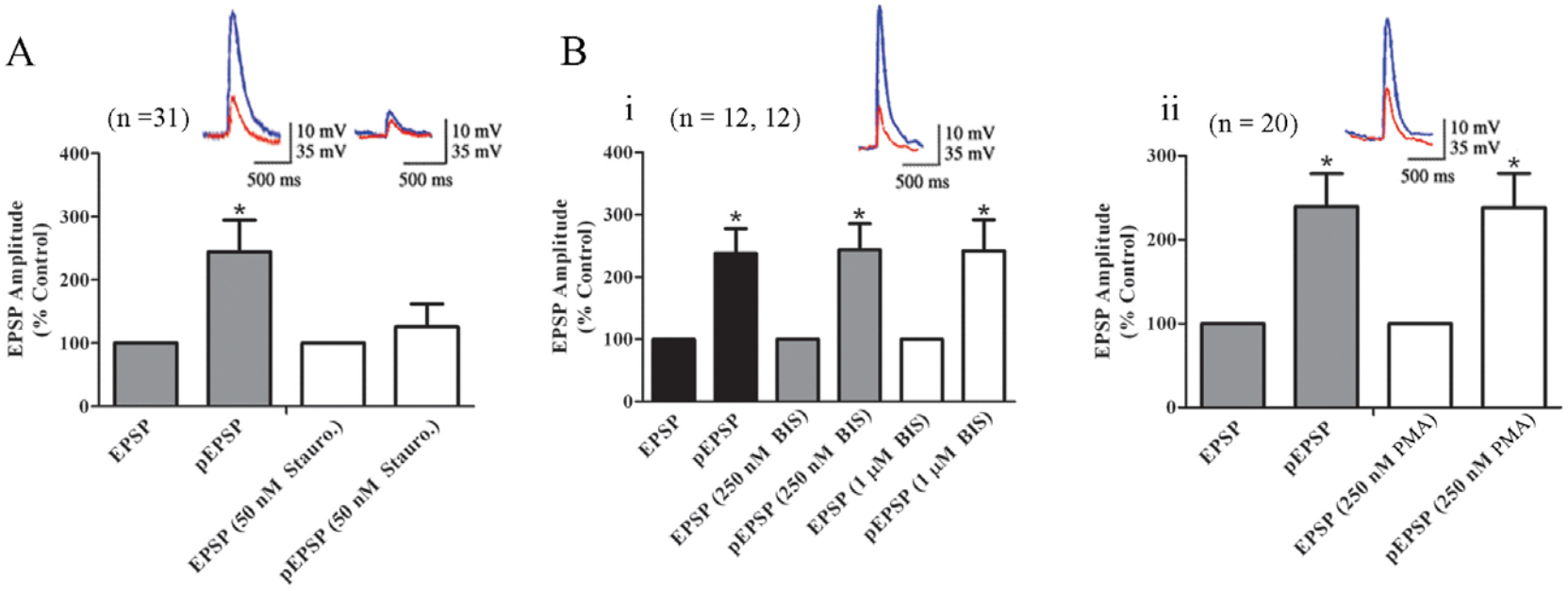
A
(n =31)
10 mV
35 mV
500 ms
10 mV
35 mV
500 ms
EPSP Amplitude
(% Control)
400
300
200
100
0
*
EPSP
pEPSP
EPSP (50 nM Stauro.)
pEPSP (50 nM Stauro.)
B
i
(n = 12, 12)
10 mV
35 mV
500 ms
EPSP Amplitude
(% Control)
400
300
200
100
0
*
*
*
EPSP
pEPSP
EPSP (250 nM BIS)
pEPSP (250 nM BIS)
EPSP (1 μM BIS)
pEPSP (1 μM BIS)
ii
(n = 20)
10 mV
35 mV
500 ms
EPSP Amplitude
(% Control)
300
200
100
0
*
*
EPSP
pEPSP
EPSP (250 nM PMA)
pEPSP (250 nM PMA)

Figure 5.5: Short-term potentiation at the VD4-LPeD1 synapse requires protein kinases but not protein kinase C.

(A) Staurosporine (50 nM) significantly reduced the amplitude of VD4-induced STP in LPeD1 from 244% in control conditions to 126% in the drug treated cells (n=31). The insert trace on the left provides a representative example of EPSP prior to tetanus (light line) and pEPSP following tetanus (dark line) in control conditions and the trace on the right provides a representation for cells treated with the non-specific inhibitor for protein kinases. **(Bi)** To test whether PKC may be the protein kinase involved in this STP, specific PKC inhibitor bisindolylmaleimide was applied to VD4/LPeD1 pairs at a concentration of 250 nM and 1 μM (n=12 in both cases). Blocking PKC activity did not affect STP between VD4 and LPeD1 pairs. Insert trace shows potentiation following PKC inhibition; EPSP (light line) and pEPSP (dark line). **(Bii)** Similarly, activating PKC with Phorbol-12-Myristate-Acetate at a concentration of 250 nM also failed to affect STP (n=20). Likewise, an insert trace shows potentiation following PKC inhibition; EPSP (light line) and pEPSP (dark line). Significance was determined using a paired Students' t-test with $p < 0.05$. Significant synaptic enhancement is indicated by an asterisk.

Figure 5.6

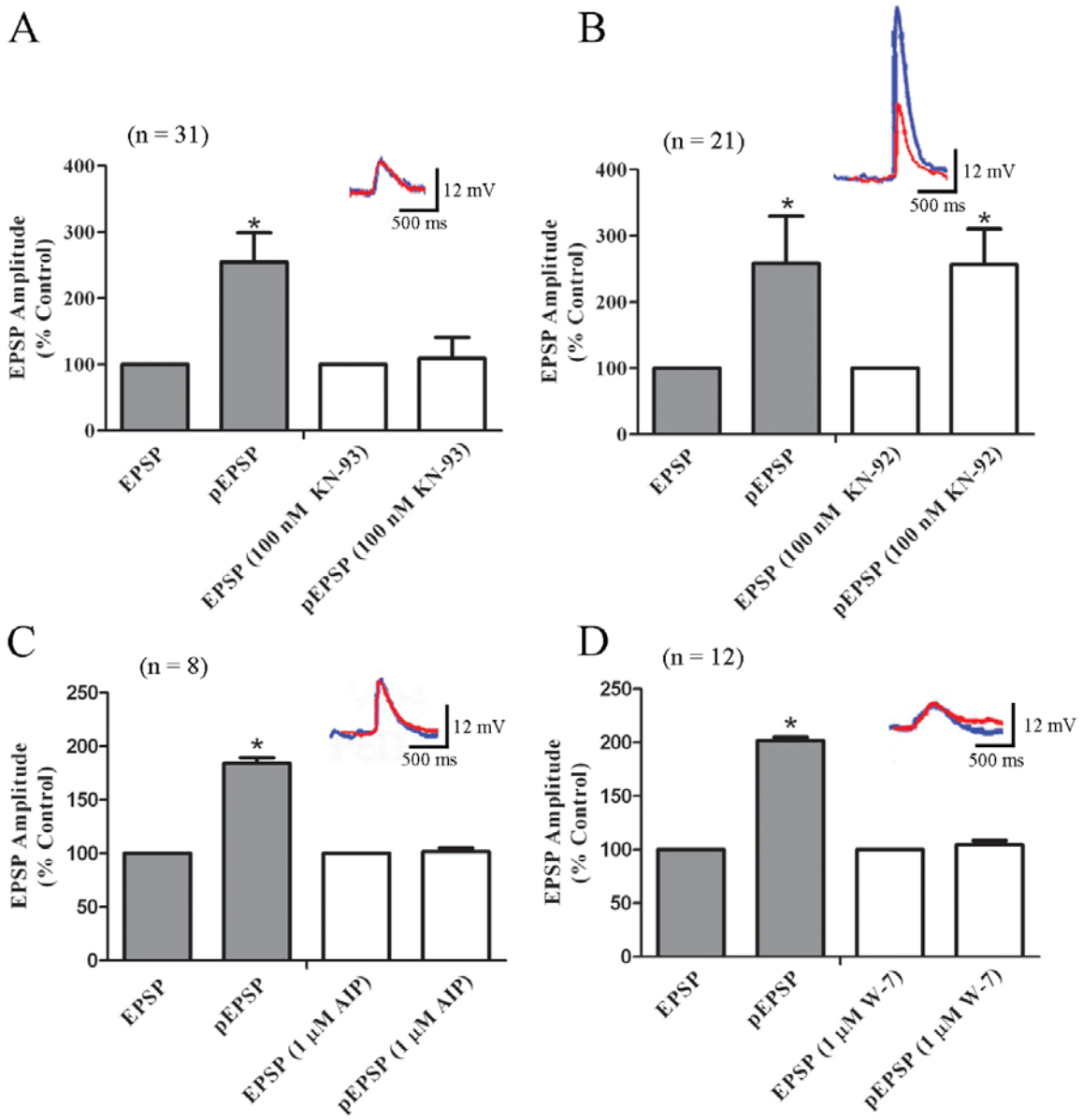
A
(n = 31)
EPSP Amplitude (% Control)
400
300
200
100
0
12 mV
500 ms
*
EPSP
pEPSP
EPSP (100 nM KN-93)
pEPSP (100 nM KN-93)
B
(n = 21)
EPSP Amplitude (% Control)
12 mV
500 ms
*
*
EPSP
pEPSP
EPSP (100 nM KN-92)
pEPSP (100 nM KN-92)
C
(n = 8)
EPSP Amplitude (% Control)
250
200
150
100
50
0
12 mV
500 ms
*
EPSP
pEPSP
EPSP (1 μM AIP)
pEPSP (1 μM AIP)
D
(n = 12)
EPSP Amplitude (% Control)
12 mV
500 ms
*
EPSP
pEPSP
EPSP (1 μM W-7)
pEPSP (1 μM W-7)

Figure 5.6: Short-term potentiation involves calmodulin and the Calcium/Calmodulin-dependent protein kinase II.

(A) To test whether Ca^{2+}-Calmodulin complex activated CaMKII activity in VD4, the presynaptic cell was treated either with the CaMKII antagonist KN-93 (100 nM) or its inactive analogue. KN-93 injected into VD4 blocked STP expression in LPeD1 with a pEPSP reduction from 255% to 109% (n=31). Insert trace shows EPSP (light line) and the pEPSP (dark line) for KN-93 treated cell pairs **(B)** To rule out non-specific effects of KN-93, its inactive analogue KN-92 was also tested using the same protocol. I discovered that KN-92 did not perturb STP at the VD4-LPeD1 synapse (n=21). The insert shows that the pEPSP (dark line) is enhanced from the EPSP (light line). **(C)** To further test the involvement of CaMKII in the activity induced STP, a specific peptide inhibitor of CaMKII (autocamtide-2-related inhibitory peptide; 1 μM) was injected in VD4 prior to simultaneous intracellular recordings between the cells. The cells injected with the peptide also failed to exhibit STP (n=8) as demonstrated by the lack of potentiation in the pEPSP (dark line) from the EPSP (light line). **(D)** To determine if STP at the VD4 and LPeD1 synapse involved CaMKII activator, calmodulin, VD4 was injected with W-7 at a concentration of 1 μM. W-7 completely blocked the STP in LPeD1 (n=12). Insert trace shows the EPSP (light line) and the pEPSP (dark line) for a W-7 treated cell pair. Significance was determined using a paired Students' t-test with $p < 0.05$. Significant synaptic enhancement is indicated by an asterisk.

Chapter 6: General Discussion and Future Direction

6.1 General Discussion and Future Direction

Synapse formation involves a multitude of spatially and temporally interdependent steps; these include cell fate specification, cell migration, axon pathfinding, dendritic outgrowth, synaptic target specification followed by the assembly of synaptic machinery—all culminated into synaptogenesis. Whereas, every brain cell must pass through each of the above steps to reach maturity and become a functional part of any given network, a neuron may, however, be engaged in multiple steps simultaneously, which results in an unfathomable complexity of synaptic assembly. Notwithstanding the significant contributions made by vertebrate model organisms in deciphering various steps underlying synapse formation (Herculano-Houzel 2009), the intricate nature of synaptic connectivity and the speed of the synaptogenic program, have limited our understanding of how networks of brain cells acquire their final patterns of connectivity. Hence, in this thesis, to study the mechanisms underlying synapse formation and function and to dissect the role of various cellular compartments in synapse formation, I utilized *Lymnaea stagnalis* as my model system. In particular, its large, individually identifiable and well-characterized neurons allowed for: (1) a highly reproducible and reliable procedure to isolate individual neurons and to reconstruct their synapses with high temporal and spatial fidelity and resolution in cell culture, (2) the ability to manipulate individual pre- and postsynaptic growth cones, isolated axons and the somata. Utilizing these unique attributes of this model, the main objective of my research was to take advantage of this well characterized *in vitro* cell culture model system to elucidate the mechanisms that mediate the formation and plasticity of specific synapses. Specifically, I attempted to decipher both intrinsic cellular properties (growth cones, axons, somata) mediating the initiation and maintenance of synapse

formation, and how this program was influenced by extrinsic molecular—such as trophic factors. Further, I attempted to understand the functional side of these synapses by looking at a form of short-term plasticity and elucidating its underlying mechanism.

It is generally believed that prior to synaptogenesis, the synaptic components of both pre- and postsynaptic sites are pre-synthesized and can then be rapidly assembled upon contact with specific synaptic targets. This has been observed at the pre-synaptic terminal, whereby their ability to release synaptic vesicles either spontaneously or when evoked (electrophysiologically or upon contact with synaptic partners) has been demonstrated. Functional neurotransmitter receptors and the responding synaptic machinery (ion channels etc.) exist prior to synapse formation. The pre-assembled components of synaptic machinery allow for an expedited synaptogenic process to occur once target cell contact is achieved—a narrative that is often referred to as "ready-set-go" (Haydon and Drapeau 1995). However, our understanding of where these synaptic components reside (axon or growth cones) and their ability to form functional synapses is limited.

In this study, I have demonstrated that growth cones, when isolated from their axons remain electrophysiologically viable. Further, these isolated growth cones retain the ability to release neurotransmitters and continue to express neurotransmitter receptors. Interestingly, I provided the first ever evidence that the isolated growth cones can form functional synapses with their corresponding synaptic partner growth cones. However, the synapses formed between the growth balls were transient and could only be maintained for 30-45 minutes in the absence of their corresponding somata. Another intriguing observation that I made was that after the formation of the first synapse, these growth cones appeared to have been "primed" for

subsequent synapse formation—meaning that the time course to achieve maximum synaptic amplitude occurred more rapidly.

While elegant imaging studies have previously shown that synaptic machinery can rapidly translocate to areas of synaptic contact (Friedman et al. 2000; Ziv and Garner 2004; Okabe 2013), they have not previously been able to demonstrate that the resulting synapses were indeed functional, nor has the time course to functional synapse been established. The present study is thus the first to demonstrate that the synaptic machinery required for functional synapse formation indeed resides within growth cone and that synapses can form as quickly as minutes following the contacts between specific synaptic partners. To the best of my knowledge, this study may be the only one to have provided an unequivocal evidence for the concept of the "ready-set-go" concept of synapse formation. Moreover, this study is also the first to show that in the absence of the pre- and postsynaptic soma/axon, the synapses formed between the "orphaned" extracellular compartments are incapable of retaining these newly formed synapses. These data thus demonstrate that while growth balls may harbor a natural propensity to secure synapse formation, its sustainability will, however, be compromised in the absence of somata-based signaling and support. Further, this study also offers insight into how "prior contact memory" of a growth cone with its synaptic target is retained to "prime" the growth cone to facilitate and expedite any future synaptogenic program. My thesis falls short in chasing the underlying mechanisms underlying this contact mediated "priming" of presynaptic growth cone for all future synapse formation. However, this will be an interesting avenue to pursue in the future studies. All I can speculate at this stage is that perhaps the initial contacts between synaptic partners may have enhanced the efficacy of presynaptic calcium channels as has been reported previously (Zoran et al. 1991; Dai and Peng 1993; Zoran et al. 1993). If indeed target

cell contact resulted in an intracellular calcium rise, which allowed for the growth ball to be primed for subsequent synapses, studies using caged calcium and flash photolysis to artificially raise calcium levels should result in a similar priming effect.

Whereas, I demonstrated that the presynaptic growth balls could release DA and that the DA receptors were present on the postsynaptic growth balls, one may argue that all the detected postsynaptic activity was due to non-synaptic transmitter release. Notwithstanding the strong evidence that the responses detected between the growth balls indeed exhibited all hallmarks of synaptic (ie. 1:1 PSPs, compound PSP with distinct phases) and not non-synaptic release (requiring bursts of action potentials to elicit any cellular response), it will be important to seek morphological evidence that the recorded responses were indeed synaptic. This will include the use of presynaptic release machinery antibody labeling (ie. Synaptophysin) and postsynaptic markers (ie. PSD-95), which are currently being tested. Further, using a previously defined method of cellular fixation and electron microscopy, we could also identify both pre- and postsynaptic localization of structural components (Feng et al. 1997). This will be the next step in using the growth ball model to characterize the temporal time course of early synaptogenesis.

The issue of resolving synaptic versus non-synaptic release intrigued me a great deal and evoked interest in developing a reliable tool to measure DA release from various cellular compartments at various developmental states. In collaboration with Dr. Patel, I thus developed a novel non-invasive planar amperometric platform (Chapter 3, Chapter 7) that allowed for me to specifically quantify the release of DA from various cellular compartments. This tool will not only serve us in the future to decipher the timing underlying the assembly of transmitter release machinery but could also be coupled with the deep brain stimulation (DBS) devices to serve as a detector and subsequent switch off function once adequate DA release is detected in the vicinity

of the electrodes. This will mitigate electro- and excito-toxic damage that results from uncontrolled electrical stimulation.

In addition to intrinsic cell-cell signaling, I also attempted to decipher the precise roles of extrinsic trophic factors in synapse formation and the underlying mechanisms. In particular, in *Lymnaea* central neurons, studies from our lab have demonstrated that trophic factors derived from CM are important for excitatory (Woodin et al. 1999; Munno et al. 2000; Woodin et al. 2002) but not inhibitory cholinergic synapse formation (Feng et al. 1997). Specifically, when VD4 and LPeD1 are cultured *in vitro*, the reformation of a proper excitatory cholinergic synapse that is normally seen *in vivo* requires the presence of extrinsic trophic factors derived from *Lymnaea* brain conditioned medium (Hamakawa et al. 1999; Woodin et al. 1999; Woodin et al. 2002; Meems et al. 2003; Flynn et al. 2014). Several previous studies have attempted to identify and characterize various trophic factors and their receptors in *Lymnaea*. Specifically, conditioned medium fractionation had previously identified a Cysteine Rich Neurotropic Factor (CRNF) (Fainzilber et al. 1996), which interacts with the vertebrate p75 receptor and promoted neurite outgrowth. Subsequently receptor tyrosine kinases were identified and characterized as being the target of trophic factor activity (van Kesteren et al. 2008). Similarly, a variety of mammalian trophic factors such as CNTF (Syed et al. 1996), NGF (Ridgway et al. 1991), EGF (Hamakawa et al. 1999; Munno et al. 2000; van Kesteren et al. 2008) were also shown to promote growth and synapse formation in a manner analogous to that of *Lymnaea* conditioned medium. We also demonstrated that the trophic factor/receptor signaling is indeed conserved across a variety of invertebrate species (Munno et al. 2000). Furthermore, *Lymnaea* EGF (L-EGF), isolated from the animals albumin gland, was shown by us to promote synapse formation between soma-soma paired *Lymnaea* neurons (Hamakawa et al. 1999; Munno et al. 2000; Woodin et al. 2002). More

recently, we cloned the *Lymnaea* EGF Receptor, which we found was not only activated by *Lymnaea* CM and L-EGF, but also human EGF and TGF alpha. Together, these studies have provided ample evidence vis-à-vis the nature of trophic factors present in CM and the receptors that they activate. Whereas all of the above trophic factors either obtained from CM fractionation or purified extracts mimicked, to some degree, the effects of *Lymnaea* brain conditioned medium, they did not, however, represent a full complement of naturally occurring *Lymnaea* trophic factors that mimic the physiological effects of CM (growth and synapse formation). For instance, while L-EGF was able to elicit similar activity patterns and trigger functional expression of excitatory nAChRs as seen in CM, the consistency seen was much lower (Chapter 4). As such, in this study, I opted to use CM to ensure that all potential factors that a neuron is likely to be subjected to *in vivo*—either during development or regeneration are included in our experiments.

More recently, it was demonstrated that trophic-factors induced activity-dependent Ca^{2+} oscillations specifically in the postsynaptic (LPeD1) but not presynaptic (VD4) neuron. This Ca^{2+} oscillation, triggered through receptor tyrosine kinase signaling, was required for the functional expression of excitatory AChRs and was contingent upon a protein synthesis-dependent cascade of events in the expression of these receptors (Xu et al. 2009). However, the specific mechanisms were not defined nor was the precise role of activity in synapse formation at a cellular level characterized. In this current study (Chapter 4), I have demonstrated that the trophic factors present in CM specifically act upon the postsynaptic neuron, LPeD1, to "prime" the cell to express functional excitatory nAChR. Trophic factors appear to induce an activity "signature" which consists of an increase in spontaneous LPeD1 activity. Over the 10 hours of development, this activity undergoes a change from inconsistent, high frequency variance

activity to a consistent, low frequency variance. It was clear that the neurons that demonstrated this trophic factor induced activity pattern were more likely to have an excitatory phenotype as determined by the exogenous application of ACh. I have demonstrated that both Ca^{2+} channel blockers and *de novo* protein synthesis blockers can perturb the trophic factor induced activity patterns and the subsequent expression of functional excitatory nAChRs. With these results, I hypothesize that trophic factors likely trigger the synthesis of *de novo* ion channels, with the most likely being voltage gated calcium channels. These channels in turn alter the intracellular level of calcium, which is hypothesized to be the signaling molecule for the downstream cascade of molecular events that ultimately leads to the expression and synthesis of excitatory nAChRs. One future studies would include taking these activity patterns or "signatures" and playing the activity back to naïve cells or even neurons of a different identity. I postulate that in the absence of trophic factors, the external induction of this activity pattern in LPeD1 via a microelectrode stimulator may mimic the development those exposed to CM.

Previously, van Nierop *et al.* (2005, 2006) have cloned and identified specific nAChR subunits that are involved in the formation of cation- and anion- selective nAChRs in *Lymnaea*. Homopentamers of these specific subunits were subsequently expressed in Xenopus laevis oocytes and the activity from these subunits were found to correspond to our observed excitatory and inhibitory nAChRs expressed on single LPeD1 neurons in the presence and absence of trophic factors respectively. Specifically, they have identified LnAChR subunit A as participating in cationic gating and LnAChR subunit B as a participant in anionic gating (van Nierop et al. 2005; van Nierop et al. 2006). To definitively demonstrate that activity is correlated the molecular expression of nAChRs, it will be important to utilize quantitative PCR studies and

correlated the expression of various nAChR subunits with activity. These studies will further allow for us to determine the precise subunit composition of these excitatory nAChRs.

Finally, from newly formed synapses to mature synapses, I sought out the mechanisms of synaptic plasticity in chapter 5. I discovered a novel form of synaptic potentiation that has both characteristics of short-term and long-term potentiation. Specifically, the induction of this particular form of plasticity is similar to that observed at other forms of short-term potentiation, whereby a brief period of high frequency activity in the form of a tetanic pulse is sufficient to induce the observed short-term potentiation. However, unlike other forms of short-term plasticity, whereby the potentiated response degrades within minutes of induction, this form of plasticity persisted for a much longer time period, lasting for up to hours and expanding into the time periods seen in long-term potentiation. I discovered that a unique attribute of this form of plasticity was that it was use- rather than time dependent. This meant that following a tetanic pulse induction protocol, as long as the pre-synaptic cell was kept silent—prevented from spiking—the synapse remained potentiated. However, once a single action potential was triggered, the synapse rapidly depotentiated. I demonstrated that this form of plasticity depends on the activation of the protein kinase CaMKII. I further hypothesize that the unique ability for CaMKII to be activated via Ca^{2+} and calmodulin may involve its autophosphoration; this would, however, need to be demonstrated via further experimentation. One particular experiment would involve utilizing a PP1 phosphatase inhibitor, the particular phosphatase that is involved in deactivating the autophosphorylation of CaMKII (Colbran 2004). We would hypothesize that a PP1 phosphatase inhibitor would decrease the activity threshold for activating CaMKII. Further, another experiment would include the use of flash photolysis to locally and specifically trigger a rise in intracellular calcium at the synaptic site by uncaging loaded Ca^{2+} compounds like DM-

nitrophen while utilizing pharmacological agents to manipulate CaMKII. This experiment would allow for us to delineate whether local calcium rise is a sufficient trigger for STP and the role of CaMKII in responding to Ca^{2+} changes. Further, the phosphorylation of vesicular release molecules such a synapsin downstream from activated CaMKII may also be a potential target for the observed potentiated response.

In this thesis, to further decipher the precise mechanism behind synapse formation, it was necessary for me to develop strategies to interrogate and assay neuron activity during the entire process of development as opposed to conducting "snap-shot" or short-term tests of neurons. Specifically, due to the limitations of conventional forms of technology such as sharp-electrode/patch-clamp electrophysiology, carbon-fibre amperometry or fluorescent calcium imaging, I was limited in both temporal and spatial recordings of neurons during development. In this thesis, three novel forms of biotechnology were thus developed, with the specific intent of answering future questions that I raised in chapter 3 and chapter 4.

Firstly, I helped develop a novel planar MEA with multiple planar electrodes that could detect neurotransmitter release. This MEA has the capacity to study both the neurotransmitter release dynamics during the development of synapses and neuronal networks. I further speculate that given the non-invasive nature of these electrodes and the recent developments in flexible materials that allow for MEAs and their respective electrodes to be contoured to any surface—such as the surface of a brain (Lacour et al. 2010)—there is the potential that these biosensors may possibly be integrated with DBS electrodes in Parkinsonian patients for a more tightly regulated feedback/stimulation treatment. For instance, the use of these sensors over a large area would allow for the detection of endogenous DA levels in the brain, which would in turn allow for a controlled level of stimulation to achieve therapeurtic levels.

With the planar patch clamp chips (both the SiN and the PI chips), this is the first study to show that a planar patch clamp chip interfaced with cultured neurons can record 1) action potentials, 2) synaptic currents and potentials and 3) monitor synaptic plasticity. The ability to interrogate ion channel activity on a planar patch chip opens up a whole new realm of biomedical research, which includes the ability to interrogate ion channel changes during development. New prototypes of these chips are now focusing on increasing the number of patch holes and the accompanying microfluidics. On the pharmaceutical development front, this technique will now allow for medium throughput drug screening for ion channel diseases such as in epilepsy, which had previously been a very slow process.

Finally, I have also helped develop a completely bio-compatible, fluorescence contact imaging system. We show that our system is capable of detecting intracellular Ca^{2+} changes in Fura-2 loaded neurons. This platform is not only a reduction in size and cost from traditional imaging setups, but also allows for longer term imaging of low fluorescent signals due to the close proximity of the sensor to the specimen. Further, this sensor also enables imaging of multiple neurons over a large surface area simultaneously, an option that is not readily available in conventional light microscopy. This unique ability to interrogate calcium activity over extended periods of time in a large network of neurons on a mobile device has implications for asking novel questions in regards to network development. We further suggest that the application of this contact imaging technology can be useful in other situations where conventional fluorescence microscopes fails to practically acquire images, such as fluorescence imaging of the brain in freely moving animals *in vivo*.

One of the final goals with the above discussed technologies is to ultimately combine them into a single platform that would allow for neurons to be cultured on a single microchip

that has the ability to simultaneously perform patch clamping, amperometric measurements of neurotransmitter release and Ca^{2+} imaging. Such a platform would be a true representation of a lab-on-a-chip.

In summary, utilizing the unique *Lymnaea stagnalis* model, I have demonstrated that isolated growth cones harbor all the necessary machinery for synapse formation and hence functional synapses can develop within minutes of contact. However, in the absence of the soma/axon, these growth cones cannot consolidate these newly formed synapses. Further, trophic factors can prime postsynaptic neurons to express functional excitatory nAChRs prior to synapse formation in an activity-dependent manner that requires specific patterns of activity. These studies further support the "ready-set-go" model of synapse formation, whereby preassembled synaptic machinery allows for an expedited synaptogenic program to proceed upon target cell contact. Finally, the synapses formed exhibit a unique form of use-dependent short-term potentiation that is reliant on CaMKII. Such a molecule appears to have the ability to bridge short-term with long-term potentiation (**Fig. 6.1**).

Figure 6.1

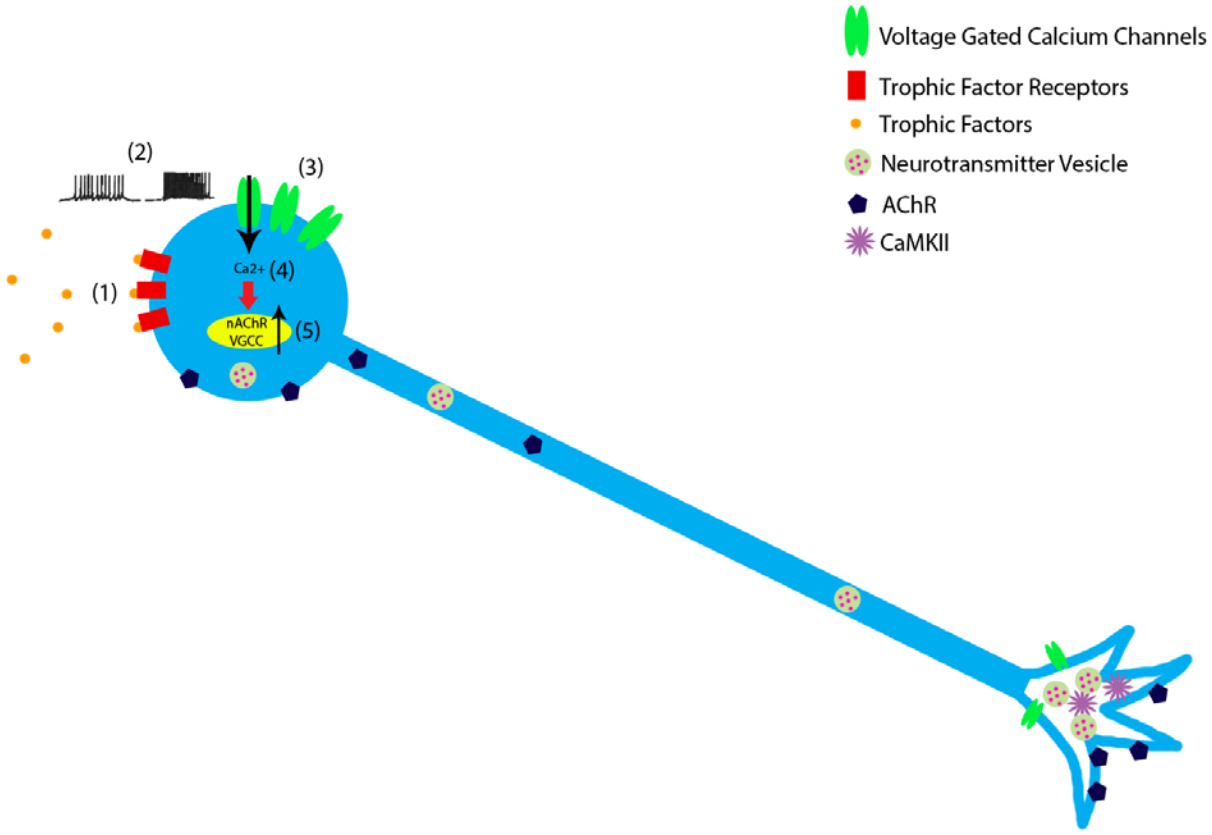
Voltage Gated Calcium Channels
Trophic Factor Receptors
Trophic Factors
Neurotransmitter Vesicle
AChR
CaMKII
(1)
(2)
(3)
Ca2+ (4)
nAChR
VGCC
(5)

Figure 6.1: Model for trophic factor mediated priming of postsynaptic neuron for synapse formation and the localization of pre-assembled synaptic machinery at the growth cone. In this thesis, I postulate that (1) Trophic factor binding to RTK triggers an (2) increase in patterned bursting activity. This activity subsequently (3) activates VGCC which causes an (4) intracellular Ca^{2+} increase. Ca^{2+} in turn triggers the (5) increase in VGCC and nAChRs expression and synthesis (*Chapter 4*). These nAChRs and synaptic vesicles are synthesized prior to synaptic contact and found to localize to multiple compartments of neuron. In particular, they can be found at the growth cones and are found to be fully functional. Hence, when a growth cone contacts its target, these readily assembled synaptic machinery can be rapidly engaged in synaptogenesis (*Chapter 3*). Further, in this study, I find that CaMKII is an important molecule that is involved in a novel form of use-dependent synaptic plasticity. It is unclear how CaMKII elicits its potentiating effects, but is thought that it may involve the phosphorylation of synaptic molecules such a synapsin *(Chapter 5).*

Chapter 7: Appendix I - Biotechnology Device Fabrication

Sections of this chapter have been published in the following manuscripts:
Patel B.A., **Luk C.C.**, Leow P.L., Zaidi W., Lee A.J., Syed N.I. (2013) A planar microelectrode array for simultaneous detection of electrically evoked dopamine release from distinct locations of a single isolated neuron. Analyst. **138**(10):2833-2839. – *Reproduced with permission from The Royal Society of Chemistry* http://pubs.rsc.org/en/content/articlelanding/2013/an/c3an36770c#!divAbstract

Py C., Denhoff M.W., Martina M., Monette R., Comas T., Ahuja T., Martinez D., Wingar S., Caballero J., Laframboise S., Mielke J., Bogdanov A., **Luk C.**, Syed N. and Mealing G. (2010). "A novel silicon patch-clamp chip permits high-fidelity recording of ion channel activity from functionally defined neurons." Biotechnology and Bioengineering **107**(4): 593-600. – *Reproduced with permission from John Wiley and Sons.*

Martinez D., Py C., Denhoff M.W., Martina M., Monette R., Comas T., **Luk C.**, Syed N. and Mealing G. (2010). "High-fidelity patch-clamp recordings from neurons cultured on a polymer microchip." Biomedical Microdevices **12**(6): 977-985. – *Reproduced with permission from Springer.*

Mudraboyina A.K., Blockstein L., **Luk C.C.**, Syed N.I., Yadid-Pecht O. (2014) A novel lensless miniature contact imaging system for monitoring calcium changes in live neurons. *IEEE Photonics Journal*. **6**(1):1-15. – *Reproduced with permission from IEEE.*

7.1 Planar Amperometry Chip

7.1.1 Fabrication of the Planar Amperometry Chip

The MEAs were fabricated on a glass substrate by using standard photolithography and wet etching processes. First, the soda-lime glass was cleaned in Piranha solution (H_2SO_4:H_2O_2, 4:1 ratio) and then dehydrated by baking the glass on a hot plate at a temperature of 200^{o}C. Next, both titanium and gold films were deposited on the glass using a sputtering technique (SRN610, Sorona Co., Korea). The patterns for the bar electrodes were created by photolithographic techniques and wet etching. Finally, an insulation layer of SiO_2 (1.5 µm) was deposited onto the surface of the electrodes. However, because of the uneven depth of the SiO_2 layer, planarization of the passivation layer was completed using a chemical mechanical planarization process. This included using a diamond conditioner (Ehwa Diamond, Korea) to polish the surface of the chip to produce a flat uniform surface. Finally, to expose the layer of gold, a final etch back process was performed with dry etching (**Fig. 7.1A**). The result of this process was a planar MEA consisting of twelve 25 × 150 µm gold electrodes (**Fig. 7.1B**). The specific electrode sizes were

chosen due to the large size of *Lymnaea* neurons (between 60 and 90 μm) that we were using in our experimentation. To finish packaging the planar amperometry chip, insulated copper wire was glued to the electrical gold pads by using conductive epoxy (CircuitWorks®) and then cured in the oven at 60°C for 30 minutes. Finally, a culture media well was created by gluing custom machined plastic dishes onto the chip with a medical silicone adhesive (MK3, Dr. Osypka GmbH, Germany). The final planar MEA can be seen in **Fig. 7.1C**. To prepare the surface for culture, a similar poly-L-lysine adsorption treatment was performed on these chips as described above.

7.2 One-hole Silicon Nitride Planar Patch Clamp Chip Fabrication

7.2.1 Surface Chip Fabrication

The silicon nitride chip surface was fabricated on a double-side polished (100) silicon wafer. The wafer was initially coated with a 1μm thick layer of silicon nitride film on both sides using a low-pressure chemical vapor deposition process. The process was calibrated to allow for low stress coating at 800-850^{o}C which builds the dense film that is resistant to KOH etch and free of pinholes and defect. The latter step was critical, given that neurons were to be cultured and grown across the surface of the chip. Next, using lithography techniques (reactive ion etch), a 3 or 4 μm hole or aperture was etched into the silicon nitride on one side of the silicon nitride coated silicon wafer **(Fig. 7.2Bi)**. On the opposing surface, in alignment with the 3 or 4 μm hole, a 600 μm x 600 μm square window was etched into the silicon nitride exposing the underlying silicon **(Fig. 7.2Bii)**. Next, the silicon bulk was then removed in a 30% KOH solution. Since the etching follows the crystallographic axis of silicon, when the silicon was fully etched from the 600 μm x 600 μm square window to the opposing 3 or 4 μm hole, the window was reduced to

the size of 100 µm x 100 µm. The result is a truncated pyramid forming the underside of the aperture **(Fig. 7.2Biii, Dii)**. Next, the bare walls of silicon exposed following the KOH etch and the underside of the exposed silicon nitride layer was passivated via deposition of a thick low stress plasma-enhanced chemical vapor deposition silicon dioxide film (PlasmaTherm 7000) **(Fig. 7.2Biv)**. In addition to passivating the bare silicon, the deposition of a silicon dioxide film also reduced the diameter of the aperture to approximately 2 µm while creating a smooth and rounded surface (**Fig. 7.2Di**).

7.2.2 Packaging the Silicon Wafer

The packaging for these silicon chips were machined out of Plexiglass G sheets. The packaging included a 16mm diameter and 6 mm deep well for the culture media with a square recess for the chip. A 1.5 mm diameter hole connects the chip aperture to the subterranean channel. Capillary glass with an outer diameter of 1.5 mm was glued (Stycast 1266 epoxy, Emerson & Cummings, Billerica, MA) to the two ends of the subterranean channel openings on the plexiglass package for attachment to the patch-clamp amplifiers. The chip was then glued onto the recess using a ring of Dow Corning RTV silicone 3140 glue in the recess. After the glue was dried, a second ring of silicone was applied around the chip to seal the top culture media chamber from the lower subterranean pipette media solution (**Fig. 7.2C**). A comprehensive description of the fabrication process has been published elsewhere (Py et al. 2010).

7.2.3 Preparation of one-hole silicon nitride chip for use

To prepare the one-hole silicon nitride patch clamp chips, poly-L-lysine was added to the culture well and allowed to adsorb to the chip surface for two hours. Following this, the poly-L-

lysine was aspirated and the surface was rinsed with filtered autoclaved deionized water. Next, we loaded the subterranean fluidics with our pipette solution (physiological saline in mM: 50 KCl, 5 MgCl2, 5 EGTA and 5 HEPES at pH 7.4 and osmolarity of 130 mOsm). To ensure electrical continuity and to maximize signal, it was crucial that the subterranean channels were loaded without any air bubbles in the well or near the aperture. Hence, we utilized a pressurized system **(Fig. 7.2E)** consisting of a pipette solution chamber pressurized at 1atm with nitrogen. This system allowed us to push fluid through the subterranean channels at a pressure that prevented the buildup of gas trapping. With the pressurized fluid in one end of the channel and the other end of the channel clamped, we applied constant pressure until a small fluid droplet could be seen coming out of the aperture on the top of the chip. The top of the chamber was then filled with either DM or CM (**Fig. 7.2A**). A comprehensive methods paper on the preparation of the one-hole silicon nitride chip has been published elsewhere (Py et al. 2012).

7.3 Fabrication of a Two-Hole Polyimide/polydimethylsiloxane Chip

7.3.1 Chip Structure fabrication

A schematic of the PI chip fabrication technique can be seen in **Fig. 7.3C**. Both the PDMS layer and the PI layer were fabricated on separate sheets of Si and Si/SiO_2 respectively and then aligned and bonded together. We have published a comprehensive fabrication protocol elsewhere (Martinez et al. 2010). To fabricate the polyimide layer, PI 2610 was spin coated at 2700 rpm on a Si/SiO2 wafer to achieve a final thickness of 3 μm. The wafer was then heated to cure the PI before a 50 nm aluminum mask layer was evaporated onto the PI film. Using standard photolithographic techniques, the apertures were patterned into the mask exposing the PI where the apertures were to be patterned onto **(Fig. 7.3E)**. Using a reactive ion etcher, the

exposed areas of the mask forming the apertures on the PI were removed and then the residual aluminum mask was removed with metal etchant leaving behind a layer of PI with two apertures patterned 100 µm apart on a Si/SiO_2 wafer **(Fig. 7.3B,D)**. Due to the irreproducible shrinking of PDMS upon curing, it was necessary to devise an alternative method to fabricating the subterranean channels with PDMS. Hence, a two-step method of combining two pieces of PDMS together was used to mitigate the shrinking of PDMS and allow for a reproducible production of the PDMS channels. First, the bottom supporting PDMS layer was made by pouring Sylgard 184 resin onto a Si wafer and allowed to cure for 3 hours at 120^{o}C. For the second and top layer, PDMS was spin coated on a Silicon wafer with a patterned SU8 layer forming the master mold for the subterranean channels and the supporting PDMS posts for the PI layer. The master mold with the PDMS was cured for 5 minutes at 95^{o}C before both the top and bottom layers were plasma treated and covalently bonded forming the subterranean channel layer of the patch clamp chip. Fluidic access holes were then punched through the PDMS layer at either end of the two channels using a machined syringe needle resulting a small 150 to 200µm access hole. With both the PI surface and the PDMS surface fabricated, the PDMS surface was air plasma treated and the PI surface was spin-coated (3000 rpm) with a VM-651 solution (0.1% in water, HD Microsystems). The two layers were aligned and bonded with a M9 flip-chip bonder at 2000 g force for 30 s. A final oven heating step at 65^{o}C for two hours was completed before peeling the PI/PDMS hybrid patch surface from the Si/SiO_2 chip. Similar to the one-hole SiN chip, a machined Plexiglas packaging with connectors was fabricated to align with the microfluidics on the PI/PDMS hybrid patch layer **(Fig. 7.3A)**.

7.3.2 Two-hole polyimide/polydimethylsiloxane chip preparation

Poly-L-lysine was added to the culture well and allowed to adsorb to PI surface for two hours before being aspirated and rinsed with filtered autoclaved deionized water. Next, we loaded the subterranean fluidics with our pipette solution (physiological saline in mM: 50 KCl, 5 MgCl2, 5 EGTA and 5 HEPES at pH 7.4 and osmolarity of 130 mOsm). Like the SiN chip, it was critical to attain electrical continuity with no air bubbles in the channel. However, unlike the high structural integrity of the SiN chip, pressure loading the pipette solution with 1atm pressurized fluid caused the PI to tear due to its lower tensile strength. Hence, the chip surfaces were made hydrophilic by doing a 5 minute sterilization in an air plasma cleaner (Harrick Plasma, Ithaca, NY), and the pipette solution was loaded by allowing the solution to flow through the chip via gravity. The top of the chamber was then also filled with either DM or CM. A comprehensive methods paper on the preparation of the two-hole PI/PDMS chip has been published elsewhere (Martinez et al. 2010).

7.4 Contact Imaging Chip

7.4.1 Fabrication of Benzophenone-8 Filter

The benzophenone-8 filter was fabricated using polyvinyl acetate (PVAc) **(Fig. 7.4A)**. PVAc was chosen as the base due to its (1) biocompatible nature, (2) inexpensive cost, (3) ability to form a uniform thin film as a coating, (4) optically transparent properties, (5) ability to be dissolved easily by methanol. Next, benzophenone-8 was chosen due to its well characterized property of being a UV absorber in the 300-400 nm range. Benzophenone-8 dye was mixed with PVAc in a methanol solution at a concentration of 0.1 g/mL. The mixture was kept in a dissolved liquid form by sealing the solution in an air-tight container to prevent the methanol from drying (Blockstein et al. 2012).

7.4.2 Preparation of imager for use with benzophenone-8 filter and SiO_2 deposition

The imager or light detector used was an Aptina MT9V032 image sensor, which has low light detection abilities (below 0.1 lux) and a monochrome design. The image sensor was mounted to a field-programmable gate array (FPGA) board (part number UI-1222LE-M-GL, 1stVision Inc.) with size dimensions of 36x36x8mm (HxWxD) **(Fig. 7.4B)**. The original glass covering on the image sensor was mechanically removed to allow direct access to the image sensor. To protect the exposed bond wires, a silicon rubber (InterTechnology Inc.) was applied to the wires and allowed to dry for 24 hours. Next, the PVAc/benzophenone-8/methanol mixture was applied to the chip surface and spin coated at 800 rpm to produce a 20 µm thick layer of filter and allowed to dry for another 24 hours. A 20 µm thick filter was shown to produce the optimal balance between filter, reproducibility, thinness to allow concentrated emission light to pass to the image sensor (Blockstein et al. 2012). Finally a sputtering device (Lesker CMS-18) was used to coat the filter with an addition layer of 100nm SiO_2 **(Fig. 7.4C)**. The layer was added to mimic the typical glass slide culture conditions used in our cultures of *Lymnaea* neurons. This specific step improved cell adhesion and subsequent growth, in addition to fura-2 dye loading. Similar to previous culture surfaces, poly-L-lysine adsorption treatment was performed as described in previous sections.

Figure 7.1

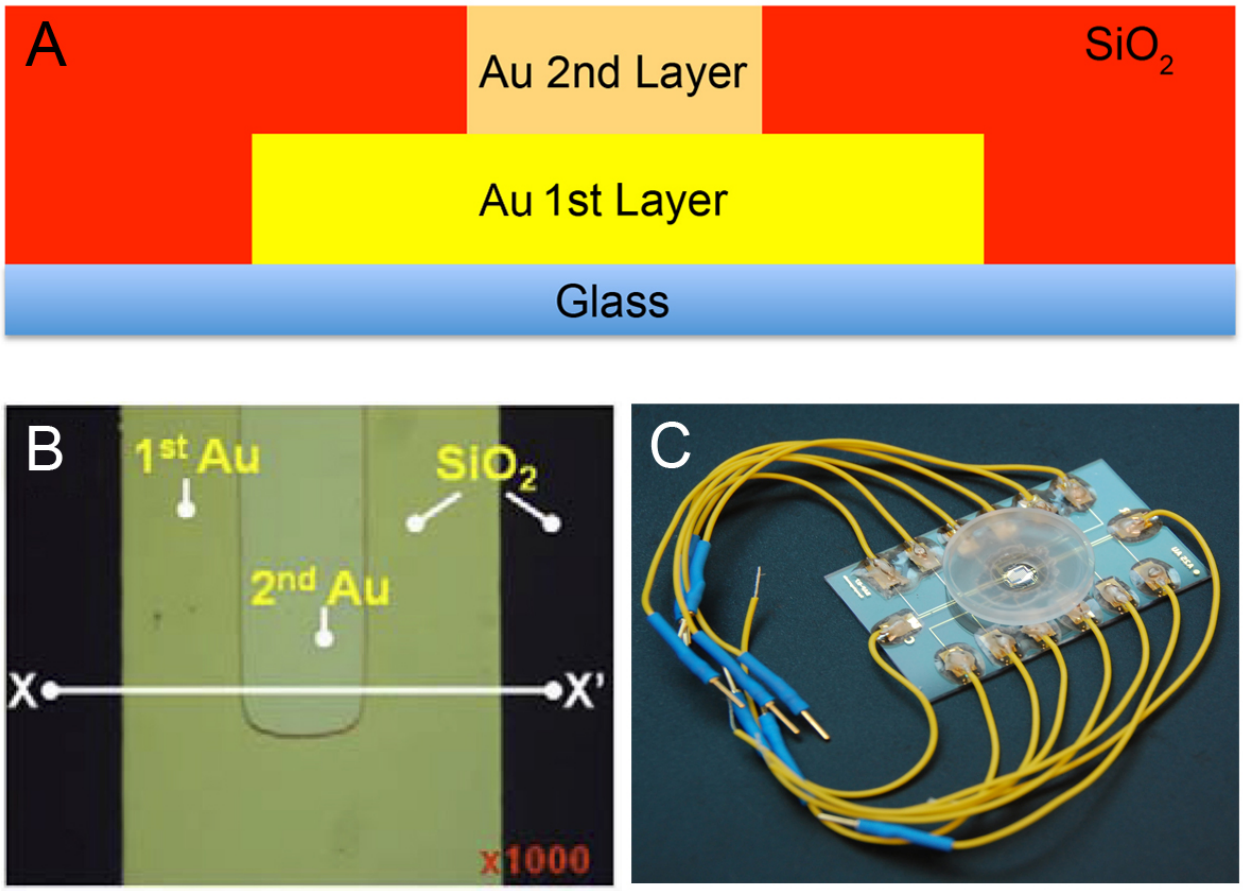
A
Au 2nd Layer
SiO2
Au 1st Layer
Glass
B
1st Au
SiO2
2nd Au
X
X'
x1000
C

Figure 7.1: Planar amperometry microelectrode array

(A) A cross sectional schematic showing the glass layer, the two Au layers and the SiO_2 layer following planarization. The second Au layer forms the electrochemical sensing area while the first Au layer forms the electrical contact between the second Au layer and the external wires. **(B)** A high magnification (1000x zoom) image of a single electrode. The two distinct Au layers are shown with a SiO_2 layer on the same planar level as the second Au layer. **(C)** A photograph showing the final assembled device. Electrical wires are soldered to the gold connection pads allowing for individual interrogation of the different sensor pads. A machined plastic dish is adhered to the chip surface with medical silicone adhesive to form a culture media well.

Figure 7.2

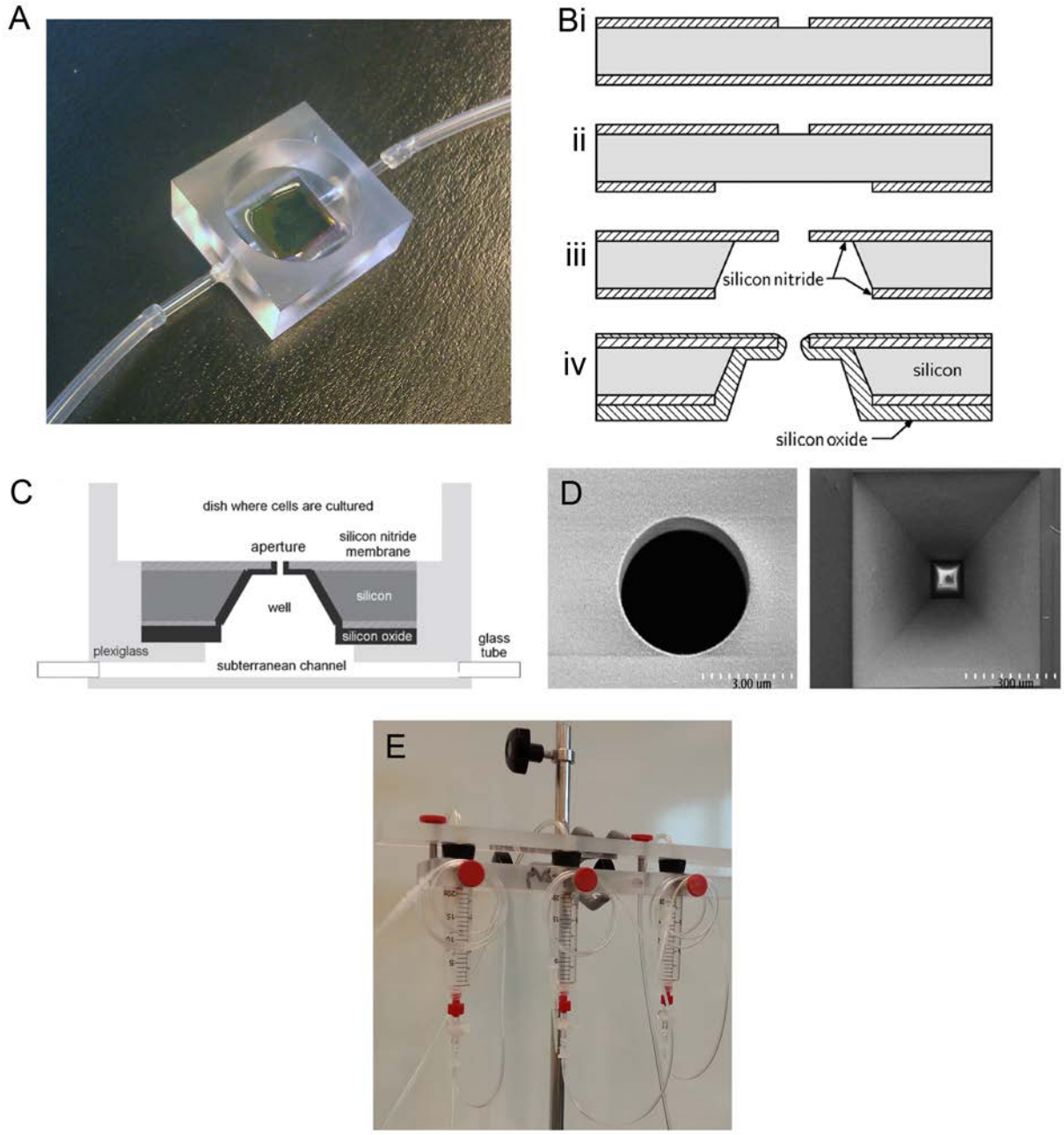
A
Bi
ii
iii
silicon nitride
iv
silicon
silicon oxide
C
dish where cells are cultured
aperture
silicon nitride membrane
silicon
well
silicon oxide
plexiglass
glass tube
subterranean channel
D
3.00 um
3.00 um
E

Figure 7.2: One-hole silicon nitride planar patch clamp chip

(A) A photograph of the packaged and assembled one-hole silicon nitride planar patch clamp chip. **(Bi)** To fabricate the silicon suface, a 3 or 6 inch double-side polished silicon wafer was coated on both sides with a 1 µm silicon nitride layer using a low-pressure chemical vapor deposition process. On one side of the chip, a 3 to 4 µm aperture (forming the patch clamp opening) was opened in the silicon nitride using a reactive ion etching process with a photoresist mask. **(Bii)** A larger 600 x 600 µm window was opened through the silicon nitride layer on the opposite side in alignment with the aperture on the front. **(Biii)** The silicon bulk material was then etched in a 30% KOH solution resulting in a truncated pyramid that allows direct passage from the large window on one side to the small aperture on the other side. **(Biv)** A layer of silicon dioxide was deposited on the backside to passivate the bare silicon walls and on the front side to facilitate surface functionalization. **(C)** The silicon surface was then assembled and fixed with silicon glue into a machined Plexiglas culture chamber. Glass tubes were also attach to the subterranean channel to facilitate connection with the patch amplifier. **(D)** SEM images of the surface (left) of the 4 µm aperture chip prior to the passivation step and the underside (right) inverted pyramid side of the aperture chip. **(E)** A 1atm pressurized filling apparatus was used to fill the subterranean channel with pipette solution.

Figure 7.3

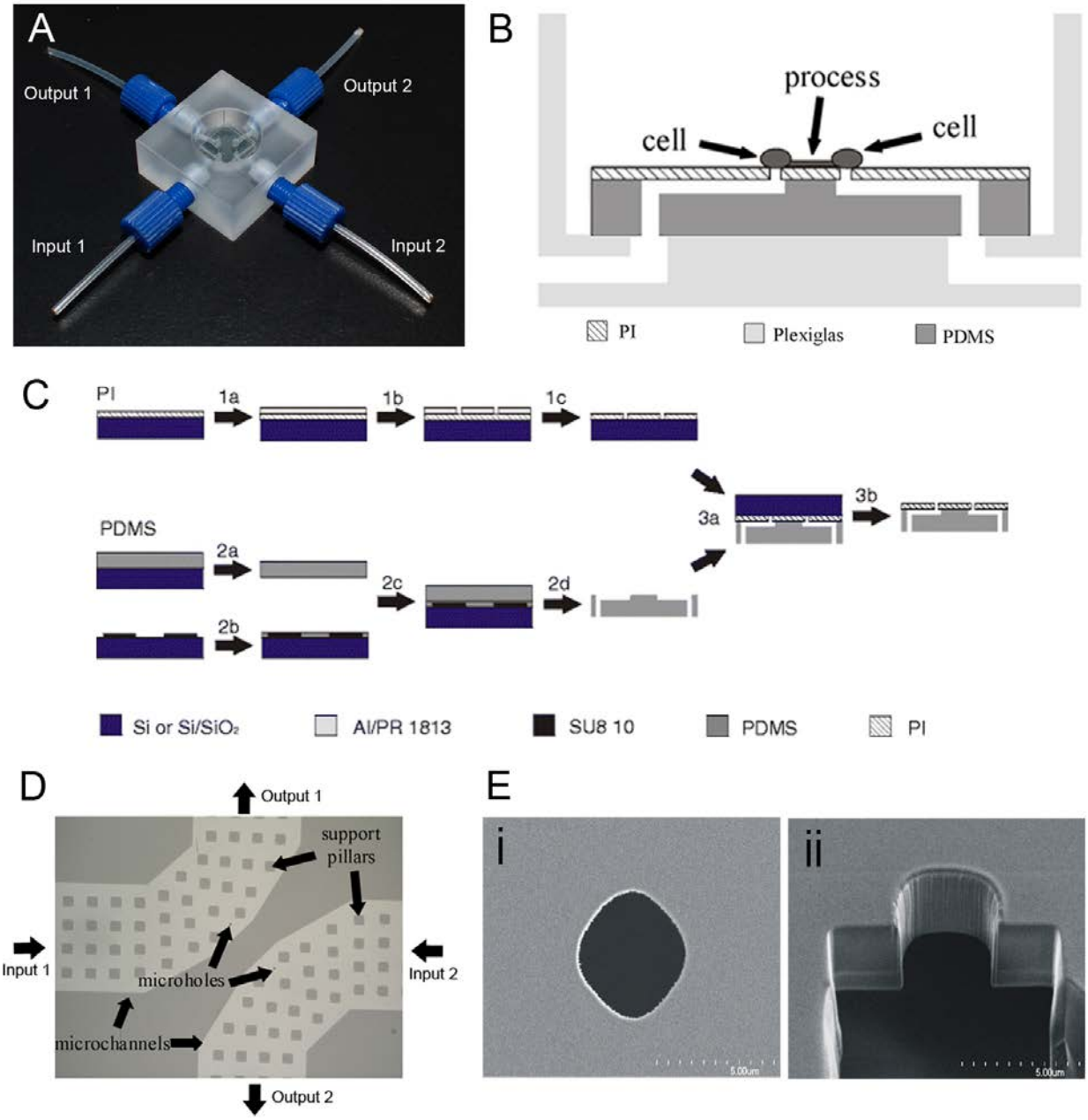
A
Output 1
Output 2
Input 1
Input 2
B
process
cell
cell
PI
Plexiglas
PDMS
C
PI
1a
1b
1c
PDMS
2a
2b
2c
2d
3a
3b
Si or Si/SiO2
Al/PR 1813
SU8 10
PDMS
PI
D
Output 1
support pillars
Input 1
Input 2
microholes
microchannels
Output 2
E
i
ii

Figure 7.3: Two-hole polyimide planar patch clamp chip

(A) An Image of the packaged and fully assembled two-hole polyimide planar patch clamp chip. **(B)** A schematic depicting the polyimide (PI) membrane with two apertures aligned and adhered to a polydimethylsiloxane (PDMS) microchannel structure. The entire assembly is then mounted onto a Plexiglas culture chamber containing microfluidic channels. **(C)** The PI and PDMS layers are individually fabricated and then assembled to form the final top layer apertures and microfluidic channels. To fabricate the PI layer, a PI is formed on a two inch wafer. Next, a 50 nm aluminum mask and photoresist layer is deposited on top of the PI layer (step 1a). Next, lithography and wet etching expose the areas in the aluminum layer that is to form the apertures on the PI (step 1b). A reactive ion etching step creates the apertures on the PI layer (step 1c). To fabricate the PDMS layer, a PDMS layer is created by pouring it onto a blank silicon wafer to create the base support structure (step 2a). A second PDMS layer is created by spin-coating into an SU8-on-silicon mold at 3700rpm and curing on a hot plate (step 2b). The two PDMS layers are surface treated and then covalently bonded (step 2c) and released to form the final top layer (step 2d). Finally, the PI and PDMS layer are surface treated and then aligned and bonded (step 3a and 3b). **(D)** A light microscopy image of the culture surface showing the location of the apertures from two independent channels, the support pillars formed by the PDMS layer to support the PI layer, and the individual micro-channels. **(E)** A scanning electron micrograph depicting the PI aperture. (i) The aperture from a top view and (ii) the aperture in a cross sectional view. The apertures are 4 μm in diameter and the thickness of the PI layer is 3.3 μm.

Figure 7.4

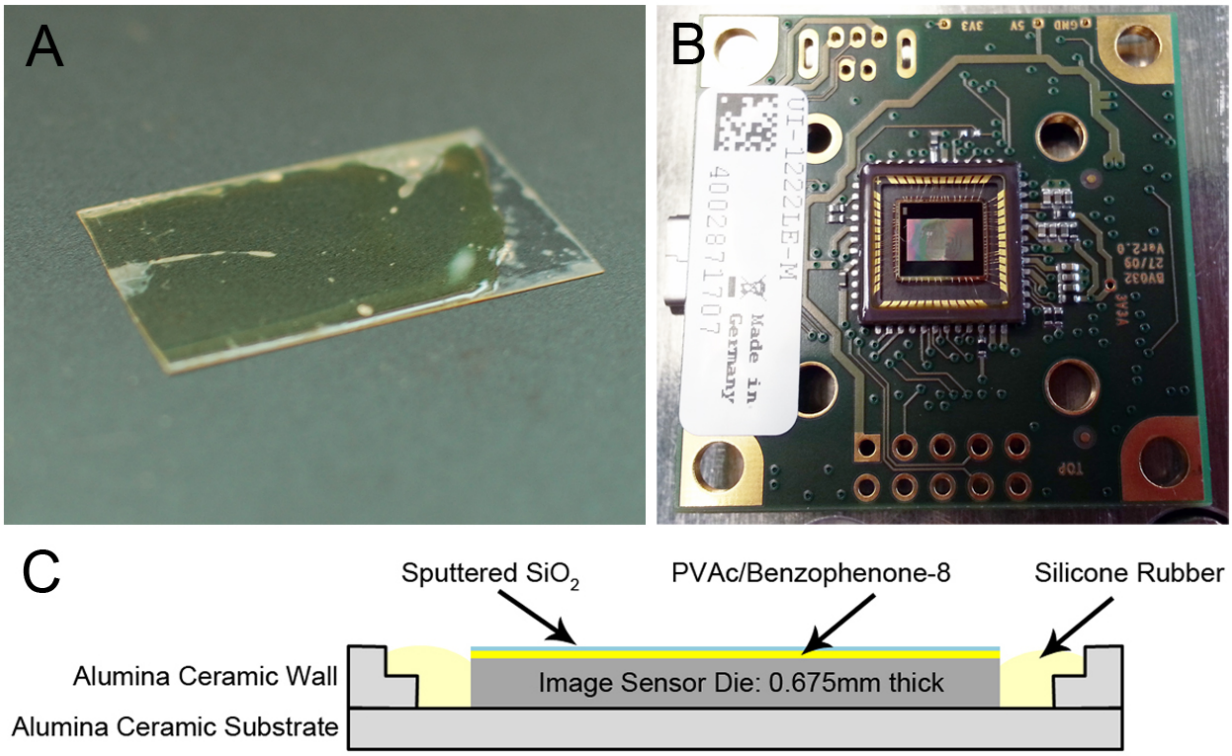
A
B
UI-122LE-M
4002871707
Made in Germany
C
Sputtered SiO_2
PVAc/Benzophenone-8
Silicone Rubber
Alumina Ceramic Wall
Image Sensor Die: 0.675mm thick
Alumina Ceramic Substrate

Figure 7.4: Contact Imaging Chip

A) The polyvinyl acetate benzophenone-8 filter was initially coated onto glass coverslips to facilitate testing of their optical properties. A thin layer of the filter can be seen in the image. **(B)** A photograph of the Aptina MT9V032 image sensor. **(C)** A cross sectional schematic of the image sensor with the spin-coated polyvinyl acetate benzophenone-8 filter layer and a sputtered SiO_2 layer. Silicone rubber was used to insulate the wire bonding.

Appendix II – Contributions

Chapter 3 (Full Manuscripts)

Luk C.C., Schmold N.M., Lee T.K. and Syed N.I. (2010) A novel approach reveals temporal patterns of synaptogenesis between the isolated growth cones of *Lymnaea* neurons." European Journal of Neuroscience **32**(9): 1442-1451.

Luk CC and Schmold NM wrote the manuscript. Luk CC and Schmold NM analyzed the data. Luk CC, Lee TK, Syed NI carried out the experiments. Luk CC, Syed NI, Lee TK designed the experiments.

Chapter 5 (Full Manuscripts)

Luk C.C., Naruo H., Prince D., Hassan A., Doran S.A., Goldberg J.I. and Syed N.I. (2011). "A novel form of presynaptic CaMKII-dependent short-term potentiation between Lymnaea neurons." European Journal of Neuroscience. 34(4):569-577.

Luk CC and Syed NI wrote the manuscript. Luk CC and Prince D analyzed the data. Luk CC, Naruo H, Prince D, Hassan A, Doran SA, Goldberg JI carried out the experiments. Luk CC, Syed NI, Naruo H designed the experiments.

Chapter 3 (Figures)

Patel B.A., **Luk C.C.**, Leow P.L., Zaidi W., Lee A.J., Syed N.I. (2013) A planar microelectrode array for simultaneous detection of electrically evoked dopamine release from distinct locations of a single isolated neuron. Analyst. **138**(10):2833-2839.

Patel BA, Luk CC, Syed NI wrote the manuscript. Luk CC, Syed NI, Patel BA designed the experiments. Luk CC, Patel BA, Lee AJ carried out the experiments. Patel BA, Leow PL designed the chip.

Chapter 4 (Figures)

Martina, M., **Luk C.,** Py C., Martinez D., Comas T., Monette T., Denhoff M., Syed N. and Mealing G.A. (2011). "Recordings of cultured neurons and synaptic activity using patch-clamp chips." Journal of Neural Engineering 8(3): 034002. *–Reproduced with permission from IOP Publishing Limited.*

Martina M, Luk C, Syed NI, Mealing GA wrote the manuscript. Luk C, Syed NI, Martina M designed the experiments. Luk C, Martina M, Comas T, Monette T carried out the experiments. PyC, Martinez D, Denhoff M, Mealing GA designed the chips.

Mudraboyina A.K., Blockstein L., **Luk C.C.**, Syed N.I., Yadid-Pecht O. (2014) A novel lensless miniature contact imaging system for monitoring calcium changes in live neurons. IEEE Photonics Journal. **6**(1):1-15. – *Reproduced with permission from IEEE.*

Contributed figure 6, figure 7, figure 8. Luk CC and Blockstein L wrote the manuscript.

Appendix I (Figures):

Py C., Denhoff M.W., Martina M., Monette R., Comas T., Ahuja T., Martinez D., Wingar S., Caballero J., Laframboise S., Mielke J., Bogdanov A., **Luk C.**, Syed N. and Mealing G. (2010). "A novel silicon patch-clamp chip permits high-fidelity recording of ion channel activity from functionally defined neurons." Biotechnology and Bioengineering **107**(4): 593-600.

Contributed figure 5.

Martinez D., Py C., Denhoff M.W., Martina M., Monette R., Comas T., **Luk C.**, Syed N. and Mealing G. (2010). "High-fidelity patch-clamp recordings from neurons cultured on a polymer microchip." Biomedical Microdevices **12**(6): 977-985.

Contributed figure 4, figure 6.

8. References

Ackman, J. B. and M. C. Crair (2014). "Role of emergent neural activity in visual map development." Curr Opin Neurobiol **24**(1): 166-175.

Ahmari, S. E., J. Buchanan and S. J. Smith (2000). "Assembly of presynaptic active zones from cytoplasmic transport packets." Nat Neurosci **3**(5): 445-451.

Ahmed, Z., P. S. Walker and R. E. Fellows (1983). "Properties of neurons from dissociated fetal rat brain in serum-free culture." J Neurosci **3**(12): 2448-2462.

Akaneya, Y., T. Tsumoto, S. Kinoshita and H. Hatanaka (1997). "Brain-derived neurotrophic factor enhances long-term potentiation in rat visual cortex." J Neurosci **17**(17): 6707-6716.

Alberts, P., R. Rudge, T. Irinopoulou, L. Danglot, C. Gauthier-Rouviere and T. Galli (2006). "Cdc42 and actin control polarized expression of TI-VAMP vesicles to neuronal growth cones and their fusion with the plasma membrane." Mol Biol Cell **17**(3): 1194-1203.

Allen, S. J. and D. Dawbarn (2006). "Clinical relevance of the neurotrophins and their receptors." Clin Sci (Lond) **110**(2): 175-191.

Allison, D. W., A. S. Chervin, V. I. Gelfand and A. M. Craig (2000). "Postsynaptic scaffolds of excitatory and inhibitory synapses in hippocampal neurons: maintenance of core components independent of actin filaments and microtubules." J Neurosci **20**(12): 4545-4554.

Allison, D. W., V. I. Gelfand, I. Spector and A. M. Craig (1998). "Role of actin in anchoring postsynaptic receptors in cultured hippocampal neurons: differential attachment of NMDA versus AMPA receptors." J Neurosci **18**(7): 2423-2436.

Assali, A., P. Gaspar and A. Rebsam (2014). "Activity dependent mechanisms of visual map formation--from retinal waves to molecular regulators." Semin Cell Dev Biol **35**: 136-146.

Atluri, P. P. and W. G. Regehr (1996). "Determinants of the time course of facilitation at the granule cell to Purkinje cell synapse." J Neurosci **16**(18): 5661-5671.

Atwood, H. L. and S. Karunanithi (2002). "Diversification of synaptic strength: presynaptic elements." Nat Rev Neurosci **3**(7): 497-516.

Baaken, G., M. Sondermann, C. Schlemmer, J. Ruhe and J. C. Behrends (2008). "Planar microelectrode-cavity array for high-resolution and parallel electrical recording of membrane ionic currents." Lab Chip **8**(6): 938-944.

Baddeley, A. (1992). "Working memory." Science **255**(5044): 556-559.

Bao, J. X., E. R. Kandel and R. D. Hawkins (1997). "Involvement of pre- and postsynaptic mechanisms in posttetanic potentiation at Aplysia synapses." Science **275**(5302): 969-973.

Barak, O. and M. Tsodyks (2014). "Working models of working memory." Curr Opin Neurobiol **25**: 20-24.

Basarsky, T. A., V. Parpura and P. G. Haydon (1994). "Hippocampal synaptogenesis in cell culture: developmental time course of synapse formation, calcium influx, and synaptic protein distribution." J Neurosci **14**(11 Pt 1): 6402-6411.

Bayazitov, I. T., R. J. Richardson, R. G. Fricke and S. S. Zakharenko (2007). "Slow presynaptic and fast postsynaptic components of compound long-term potentiation." J Neurosci **27**(43): 11510-11521.

Beierlein, M., D. Fioravante and W. G. Regehr (2007). "Differential expression of posttetanic potentiation and retrograde signaling mediate target-dependent short-term synaptic plasticity." Neuron **54**(6): 949-959.

Berglund, K., M. Midorikawa and M. Tachibana (2002). "Increase in the pool size of releasable synaptic vesicles by the activation of protein kinase C in goldfish retinal bipolar cells." J Neurosci **22**(12): 4776-4785.

Bertram, R., A. Sherman and E. F. Stanley (1996). "Single-domain/bound calcium hypothesis of transmitter release and facilitation." J Neurophysiol **75**(5): 1919-1931.

Betz, W. J. (1970). "Depression of transmitter release at the neuromuscular junction of the frog." J Physiol **206**(3): 629-644.

Biederer, T., Y. Sara, M. Mozhayeva, D. Atasoy, X. Liu, E. T. Kavalali and T. C. Sudhof (2002). "SynCAM, a synaptic adhesion molecule that drives synapse assembly." Science **297**(5586): 1525-1531.

Bliss, T. V. and A. R. Gardner-Medwin (1973). "Long-lasting potentiation of synaptic transmission in the dentate area of the unanaestetized rabbit following stimulation of the perforant path." J Physiol **232**(2): 357-374.

Bliss, T. V. and T. Lomo (1973). "Long-lasting potentiation of synaptic transmission in the dentate area of the anaesthetized rabbit following stimulation of the perforant path." J Physiol **232**(2): 331-356.

Blockstein, L., C. C. Luk, Mudraboyina A.K., S. N.I. and O. Yadid-Pecht (2012). "A PVAc-Based Benzophenone-8 Filter as an Alternative to Commercially Available Dichroic Filters for Monitoring Calcium Activity in Live Neurons via Fura-2 AM." IEEE Photonics Journal **4**(3): 1005-1012.

Blockstein, L., C. C. Luk, A. K. Mudraboyina, N. I. Syed and O. Yadid-Pecht (2012). "A PVAc based benzophenone-8 filter as an alternative to commercially available dichroic filters for monitoring calcium activity in live neurons via Fura-2 AM." IEEE Photonics Journal **4**(3): 1004-1012.

Borodinsky, L. N., Y. H. Belgacem and I. Swapna (2012). "Electrical activity as a developmental regulator in the formation of spinal cord circuits." Curr Opin Neurobiol **22**(4): 624-630.

Borodinsky, L. N., C. M. Root, J. A. Cronin, S. B. Sann, X. Gu and N. C. Spitzer (2004). "Activity-dependent homeostatic specification of transmitter expression in embryonic neurons." Nature **429**(6991): 523-530.

Borodinsky, L. N. and N. C. Spitzer (2007). "Activity-dependent neurotransmitter-receptor matching at the neuromuscular junction." Proc Natl Acad Sci U S A **104**(1): 335-340.

Bose, C. M., D. Qiu, A. Bergamaschi, B. Gravante, M. Bossi, A. Villa, F. Rupp and A. Malgaroli (2000). "Agrin controls synaptic differentiation in hippocampal neurons." J Neurosci **20**(24): 9086-9095.

Boulanger, L. M. and M. M. Poo (1999). "Presynaptic depolarization facilitates neurotrophin-induced synaptic potentiation." Nat Neurosci **2**(4): 346-351.

Bradke, F., J. W. Fawcett and M. E. Spira (2012). "Assembly of a new growth cone after axotomy: the precursor to axon regeneration." Nat Rev Neurosci **13**(3): 183-193.

Brager, D. H., X. Cai and S. M. Thompson (2003). "Activity-dependent activation of presynaptic protein kinase C mediates post-tetanic potentiation." Nat Neurosci **6**(6): 551-552.

Brenner, H. R. and M. Akaaboune (2014). "Recycling of acetylcholine receptors at ectopic postsynaptic clusters induced by exogenous agrin in living rats." Dev Biol **394**(1): 122-128.

Brosenitsch, T. A. and D. M. Katz (2001). "Physiological patterns of electrical stimulation can induce neuronal gene expression by activating N-type calcium channels." J Neurosci **21**(8): 2571-2579.

Brunet, I., C. Weinl, M. Piper, A. Trembleau, M. Volovitch, W. Harris, A. Prochiantz and C. Holt (2005). "The transcription factor Engrailed-2 guides retinal axons." Nature **438**(7064): 94-98.

Buonanno, A. and R. D. Fields (1999). "Gene regulation by patterned electrical activity during neural and skeletal muscle development." Curr Opin Neurobiol **9**(1): 110-120.

Burden, S. J., N. Yumoto and W. Zhang (2013). "The role of MuSK in synapse formation and neuromuscular disease." Cold Spring Harb Perspect Biol **5**(5): a009167.

Burnette, D. T., L. Ji, A. W. Schaefer, N. A. Medeiros, G. Danuser and P. Forscher (2008). "Myosin II activity facilitates microtubule bundling in the neuronal growth cone neck." Dev Cell **15**(1): 163-169.

Burrone, J., M. O'Byrne and V. N. Murthy (2002). "Multiple forms of synaptic plasticity triggered by selective suppression of activity in individual neurons." Nature **420**(6914): 414-418.

Bury, L. A. and S. L. Sabo (2014). "Dynamic mechanisms of neuroligin-dependent presynaptic terminal assembly in living cortical neurons." Neural Dev **9**(1): 13.

Butler, S. J. and G. Tear (2007). "Getting axons onto the right path: the role of transcription factors in axon guidance." Development **134**(3): 439-448.

Carabelli, V., S. Gosso, A. Marcantoni, Y. Xu, E. Colombo, Z. Gao, E. Vittone, E. Kohn, A. Pasquarelli and E. Carbone (2010). "Nanocrystalline diamond microelectrode arrays

fabricated on sapphire technology for high-time resolution of quantal catecholamine secretion from chromaffin cells." Biosens Bioelectron **26**(1): 92-98.

Carmignoto, G., T. Pizzorusso, S. Tia and S. Vicini (1997). "Brain-derived neurotrophic factor and nerve growth factor potentiate excitatory synaptic transmission in the rat visual cortex." J Physiol **498 (Pt 1)**: 153-164.

Carrasco, M. A., P. Castro, F. J. Sepulveda, J. C. Tapia, K. Gatica, M. I. Davis and L. G. Aguayo (2007). "Regulation of glycinergic and GABAergic synaptogenesis by brain-derived neurotrophic factor in developing spinal neurons." Neuroscience **145**(2): 484-494.

Chapman, P. F., B. G. Frenguelli, A. Smith, C. M. Chen and A. J. Silva (1995). "The alpha-Ca2+/calmodulin kinase II: a bidirectional modulator of presynaptic plasticity." Neuron **14**(3): 591-597.

Charrier, C., M. V. Ehrensperger, M. Dahan, S. Levi and A. Triller (2006). "Cytoskeleton regulation of glycine receptor number at synapses and diffusion in the plasma membrane." J Neurosci **26**(33): 8502-8511.

Chavis, P. and G. Westbrook (2001). "Integrins mediate functional pre- and postsynaptic maturation at a hippocampal synapse." Nature **411**(6835): 317-321.

Chilton, J. K. (2006). "Molecular mechanisms of axon guidance." Dev Biol **292**(1): 13-24.

Chow, I. and M. M. Poo (1985). "Release of acetylcholine from embryonic neurons upon contact with muscle cell." J Neurosci **5**(4): 1076-1082.

Chu, Y., D. Fioravante, M. Leitges and W. G. Regehr (2014). "Calcium-dependent PKC isoforms have specialized roles in short-term synaptic plasticity." Neuron **82**(4): 859-871.

Cohen-Cory, S. (2002). "The developing synapse: construction and modulation of synaptic structures and circuits." Science **298**(5594): 770-776.

Colbran, R. J. (2004). "Protein phosphatases and calcium/calmodulin-dependent protein kinase II-dependent synaptic plasticity." J Neurosci **24**(39): 8404-8409.

Constantine-Paton, M., H. T. Cline and E. Debski (1990). "Patterned activity, synaptic convergence, and the NMDA receptor in developing visual pathways." Annu Rev Neurosci **13**: 129-154.

Cottrell, J. R., G. R. Dube, C. Egles and G. Liu (2000). "Distribution, density, and clustering of functional glutamate receptors before and after synaptogenesis in hippocampal neurons." J Neurophysiol **84**(3): 1573-1587.

Coultrap, S. J., R. K. Freund, H. O'Leary, J. L. Sanderson, K. W. Roche, M. L. Dell'Acqua and K. U. Bayer (2014). "Autonomous CaMKII mediates both LTP and LTD using a mechanism for differential substrate site selection." Cell Rep **6**(3): 431-437.

Crabtree, G. W. and J. A. Gogos (2014). "Synaptic plasticity, neural circuits, and the emerging role of altered short-term information processing in schizophrenia." Front Synaptic Neurosci **6**: 28.

Craig, A. M., C. D. Blackstone, R. L. Huganir and G. Banker (1994). "Selective clustering of glutamate and gamma-aminobutyric acid receptors opposite terminals releasing the corresponding neurotransmitters." Proc Natl Acad Sci U S A **91**(26): 12373-12377.

Craig, A. M. and H. Boudin (2001). "Molecular heterogeneity of central synapses: afferent and target regulation." Nat Neurosci **4**(6): 569-578.

Craig, A. M., E. R. Graf and M. W. Linhoff (2006). "How to build a central synapse: clues from cell culture." Trends Neurosci **29**(1): 8-20.

Crispino, M., J. T. Chun, C. Cefaliello, C. Perrone Capano and A. Giuditta (2014). "Local gene expression in nerve endings." Dev Neurobiol **74**(3): 279-291.

Crozier, R. A., C. Bi, Y. R. Han and M. R. Plummer (2008). "BDNF modulation of NMDA receptors is activity dependent." J Neurophysiol **100**(6): 3264-3274.

Dai, Z. and H. B. Peng (1993). "Elevation in presynaptic Ca2+ level accompanying initial nerve-muscle contact in tissue culture." Neuron **10**(5): 827-837.

Dallman, J. E., A. K. Davis and W. J. Moody (1998). "Spontaneous activity regulates calcium-dependent K+ current expression in developing ascidian muscle." J Physiol **511 (Pt 3)**: 683-693.

David, G. and E. F. Barrett (2003). "Mitochondrial Ca2+ uptake prevents desynchronization of quantal release and minimizes depletion during repetitive stimulation of mouse motor nerve terminals." J Physiol **548**(Pt 2): 425-438.

Davis-Lopez de Carrizosa, M. A., C. J. Morado-Diaz, S. Morcuende, R. R. de la Cruz and A. M. Pastor (2010). "Nerve growth factor regulates the firing patterns and synaptic composition of motoneurons." J Neurosci **30**(24): 8308-8319.

Davis, L., P. Dou, M. DeWit and S. B. Kater (1992). "Protein synthesis within neuronal growth cones." J Neurosci **12**(12): 4867-4877.

de Jong, A. P. and D. Fioravante (2014). "Translating neuronal activity at the synapse: presynaptic calcium sensors in short-term plasticity." Front Cell Neurosci **8**: 356.

Debski, E. A. and H. T. Cline (2002). "Activity-dependent mapping in the retinotectal projection." Curr Opin Neurobiol **12**(1): 93-99.

Delaney, K. R., R. S. Zucker and D. W. Tank (1989). "Calcium in motor nerve terminals associated with posttetanic potentiation." J Neurosci **9**(10): 3558-3567.

Desarmenien, M. G. and N. C. Spitzer (1991). "Role of calcium and protein kinase C in development of the delayed rectifier potassium current in Xenopus spinal neurons." Neuron **7**(5): 797-805.

Dickson, B. J. (2002). "Molecular mechanisms of axon guidance." Science **298**(5600): 1959-1964.

Diefenbach, T. J., P. B. Guthrie, H. Stier, B. Billups and S. B. Kater (1999). "Membrane recycling in the neuronal growth cone revealed by FM1-43 labeling." J Neurosci **19**(21): 9436-9444.

Doran, S. A. and J. I. Goldberg (2006). "Roles of Ca2+ and protein kinase C in the excitatory response to serotonin in embryonic molluscan ciliary cells." Can J Physiol Pharmacol **84**(6): 635-646.

Drachman, D. A. (2005). "Do we have brain to spare?" Neurology **64**(12): 2004-2005.

Du, J., L. Feng, F. Yang and B. Lu (2000). "Activity- and Ca(2+)-dependent modulation of surface expression of brain-derived neurotrophic factor receptors in hippocampal neurons." J Cell Biol **150**(6): 1423-1434.

Dulcis, D. and N. C. Spitzer (2012). "Reserve pool neuron transmitter respecification: Novel neuroplasticity." Dev Neurobiol **72**(4): 465-474.

Faas, G. C., S. Raghavachari, J. E. Lisman and I. Mody (2011). "Calmodulin as a direct detector of Ca2+ signals." Nat Neurosci **14**(3): 301-304.

Fainzilber, M., A. B. Smit, N. I. Syed, W. C. Wildering, Hermann, R. C. van der Schors, C. Jimenez, K. W. Li, J. van Minnen, A. G. Bulloch, C. F. Ibanez and W. P. Geraerts (1996). "CRNF, a molluscan neurotrophic factor that interacts with the p75 neurotrophin receptor." Science **274**(5292): 1540-1543.

Farrar, N. R. and G. E. Spencer (2008). "Pursuing a 'turning point' in growth cone research." Dev Biol **318**(1): 102-111.

Feldman, D. E. (2009). "Synaptic mechanisms for plasticity in neocortex." Annu Rev Neurosci **32**: 33-55.

Feller, M. B. (1999). "Spontaneous correlated activity in developing neural circuits." Neuron **22**(4): 653-656.

Feng, Z. P., N. Grigoriev, D. Munno, K. Lukowiak, B. A. MacVicar, J. I. Goldberg and N. I. Syed (2002). "Development of Ca2+ hotspots between Lymnaea neurons during synaptogenesis." J Physiol **539**(Pt 1): 53-65.

Feng, Z. P., J. Klumperman, K. Lukowiak and N. I. Syed (1997). "In vitro synaptogenesis between the somata of identified Lymnaea neurons requires protein synthesis but not extrinsic growth factors or substrate adhesion molecules." J Neurosci **17**(20): 7839-7849.

Fertig, N., R. H. Blick and J. C. Behrends (2002). "Whole cell patch clamp recording performed on a planar glass chip." Biophys J **82**(6): 3056-3062.

Fields, R. D., F. Eshete, B. Stevens and K. Itoh (1997). "Action potential-dependent regulation of gene expression: temporal specificity in ca2+, cAMP-responsive element binding proteins, and mitogen-activated protein kinase signaling." J Neurosci **17**(19): 7252-7266.

Fields, R. D., E. A. Neale and P. G. Nelson (1990). "Effects of patterned electrical activity on neurite outgrowth from mouse sensory neurons." J Neurosci **10**(9): 2950-2964.

Fink, C. C. and T. Meyer (2002). "Molecular mechanisms of CaMKII activation in neuronal plasticity." Curr Opin Neurobiol **12**(3): 293-299.

Fioravante, D., Y. Chu, A. P. de Jong, M. Leitges, P. S. Kaeser and W. G. Regehr (2014). "Protein kinase C is a calcium sensor for presynaptic short-term plasticity." Elife **3**: e03011.

Fioravante, D. and W. G. Regehr (2011). "Short-term forms of presynaptic plasticity." Curr Opin Neurobiol **21**(2): 269-274.

Fisher, S. A., T. M. Fischer and T. J. Carew (1997). "Multiple overlapping processes underlying short-term synaptic enhancement." Trends Neurosci **20**(4): 170-177.

Fiumara, F., G. Leitinger, C. Milanese, P. G. Montarolo and M. Ghirardi (2005). "In vitro formation and activity-dependent plasticity of synapses between Helix neurons involved in the neural control of feeding and withdrawal behaviors." Neuroscience **134**(4): 1133-1151.

Fiumara, F., C. Milanese, A. Corradi, S. Giovedi, G. Leitinger, A. Menegon, P. G. Montarolo, F. Benfenati and M. Ghirardi (2007). "Phosphorylation of synapsin domain A is required for post-tetanic potentiation." J Cell Sci **120**(Pt 18): 3228-3237.

Flanagan-Steet, H., M. A. Fox, D. Meyer and J. R. Sanes (2005). "Neuromuscular synapses can form in vivo by incorporation of initially aneural postsynaptic specializations." Development **132**(20): 4471-4481.

Flores-Otero, J., H. Z. Xue and R. L. Davis (2007). "Reciprocal regulation of presynaptic and postsynaptic proteins in bipolar spiral ganglion neurons by neurotrophins." J Neurosci **27**(51): 14023-14034.

Florio, M. and W. B. Huttner (2014). "Neural progenitors, neurogenesis and the evolution of the neocortex." Development **141**(11): 2182-2194.

Flynn, N., A. Getz, F. Visser, T. A. Janes and N. I. Syed (2014). "Menin: a tumor suppressor that mediates postsynaptic receptor expression and synaptogenesis between central neurons of Lymnaea stagnalis." PLoS One **9**(10): e111103.

Fossier, P., G. Baux and L. Tauc (1990). "Activation of protein kinase C by presynaptic FLRFamide receptors facilitates transmitter release at an aplysia cholinergic synapse." Neuron **5**(4): 479-486.

Fox, L. E. and P. E. Lloyd (2001). "Evidence that post-tetanic potentiation is mediated by neuropeptide release in Aplysia." J Neurophysiol **86**(6): 2845-2855.

Friedman, H. V., T. Bresler, C. C. Garner and N. E. Ziv (2000). "Assembly of new individual excitatory synapses: time course and temporal order of synaptic molecule recruitment." Neuron **27**(1): 57-69.

Gao, X. B. and A. N. van den Pol (2000). "GABA release from mouse axonal growth cones." J Physiol **523 Pt 3**: 629-637.

Gaze, R. M., M. J. Keating and S. H. Chung (1974). "The evolution of the retinotectal map during development in Xenopus." Proc R Soc Lond B Biol Sci **185**(80): 301-330.

Ghirardi, M., F. Benfenati, S. Giovedi, F. Fiumara, C. Milanese and P. G. Montarolo (2004). "Inhibition of neurotransmitter release by a nonphysiological target requires protein synthesis and involves cAMP-dependent and mitogen-activated protein kinases." J Neurosci **24**(21): 5054-5062.

Giachello, C. N., F. Fiumara, C. Giacomini, A. Corradi, C. Milanese, M. Ghirardi, F. Benfenati and P. G. Montarolo (2010). "MAPK/Erk-dependent phosphorylation of synapsin mediates formation of functional synapses and short-term homosynaptic plasticity." J Cell Sci **123**(Pt 6): 881-893.

Giese, K. P. and K. Mizuno (2013). "The roles of protein kinases in learning and memory." Learn Mem **20**(10): 540-552.

Gilly, W. F., R. Gillette and M. McFarlane (1997). "Fast and slow activation kinetics of voltage-gated sodium channels in molluscan neurons." J Neurophysiol **77**(5): 2373-2384.

Glass, D. J., D. C. Bowen, T. N. Stitt, C. Radziejewski, J. Bruno, T. E. Ryan, D. R. Gies, S. Shah, K. Mattsson, S. J. Burden, P. S. DiStefano, D. M. Valenzuela, T. M. DeChiara and G. D. Yancopoulos (1996). "Agrin acts via a MuSK receptor complex." Cell **85**(4): 513-523.

Gonzalez-Islas, C. and P. Wenner (2006). "Spontaneous network activity in the embryonic spinal cord regulates AMPAergic and GABAergic synaptic strength." Neuron **49**(4): 563-575.

Graf, R. A., S. B. Kater and H. Gordon (1999). "Prolonged cytosolic calcium elevations in growth cones contacting muscle." Dev Neurosci **21**(6): 409-416.

Granger, A. J. and R. A. Nicoll (2014). "Expression mechanisms underlying long-term potentiation: a postsynaptic view, 10 years on." Philos Trans R Soc Lond B Biol Sci **369**(1633): 20130136.

Greig, L. C., M. B. Woodworth, M. J. Galazo, H. Padmanabhan and J. D. Macklis (2013). "Molecular logic of neocortical projection neuron specification, development and diversity." Nat Rev Neurosci **14**(11): 755-769.

Gu, X. and N. C. Spitzer (1995). "Distinct aspects of neuronal differentiation encoded by frequency of spontaneous Ca2+ transients." Nature **375**(6534): 784-787.

Guemez-Gamboa, A., L. Xu, D. Meng and N. C. Spitzer (2014). "Non-cell-autonomous mechanism of activity-dependent neurotransmitter switching." Neuron **82**(5): 1004-1016.

Guillin, O., N. Griffon, E. Bezard, L. Leriche, J. Diaz, C. Gross and P. Sokoloff (2003). "Brain-derived neurotrophic factor controls dopamine D3 receptor expression: therapeutic implications in Parkinson's disease." Eur J Pharmacol **480**(1-3): 89-95.

Gundersen, R. W. and J. N. Barrett (1979). "Neuronal chemotaxis: chick dorsal-root axons turn toward high concentrations of nerve growth factor." Science **206**(4422): 1079-1080.

Guo, J. and E. S. Anton (2014). "Decision making during interneuron migration in the developing cerebral cortex." Trends Cell Biol **24**(6): 342-351.

Guthrie, P. B., R. E. Lee and S. B. Kater (1989). "A comparison of neuronal growth cone and cell body membrane: electrophysiological and ultrastructural properties." J Neurosci **9**(10): 3596-3605.

Guthrie, P. B., R. E. Lee, V. Rehder, M. F. Schmidt and S. B. Kater (1994). "Self-recognition: a constraint on the formation of electrical coupling in neurons." J Neurosci **14**(3 Pt 2): 1477-1485.

Habets, R. L. and J. G. Borst (2006). "An increase in calcium influx contributes to post-tetanic potentiation at the rat calyx of Held synapse." J Neurophysiol **96**(6): 2868-2876.

Hamakawa, T., M. A. Woodin, M. C. Bjorgum, S. D. Painter, M. Takasaki, K. Lukowiak, G. T. Nagle and N. I. Syed (1999). "Excitatory synaptogenesis between identified Lymnaea neurons requires extrinsic trophic factors and is mediated by receptor tyrosine kinases." J Neurosci **19**(21): 9306-9312.

Hanley, J. G. (2014). "Actin-dependent mechanisms in AMPA receptor trafficking." Front Cell Neurosci **8**: 381.

Hanson, M. G. and L. T. Landmesser (2003). "Characterization of the circuits that generate spontaneous episodes of activity in the early embryonic mouse spinal cord." J Neurosci **23**(2): 587-600.

Harris, A. J. (1981). "Embryonic growth and innervation of rat skeletal muscles. III. Neural regulation of junctional and extra-junctional acetylcholine receptor clusters." Philos Trans R Soc Lond B Biol Sci **293**(1065): 287-314.

Haydon, P. G., C. S. Cohan, D. P. McCobb, H. R. Miller and S. B. Kater (1985). "Neuron-specific growth cone properties as seen in identified neurons of Helisoma." J Neurosci Res **13**(1-2): 135-147.

Haydon, P. G. and P. Drapeau (1995). "From contact to connection: early events during synaptogenesis." Trends Neurosci **18**(4): 196-201.

Haydon, P. G. and P. Drapeau (1995). "From contact to connection: Early events during synaptogenesis." Trends in Neurosciences **18**: 196-201.

Haydon, P. G., D. P. McCobb and S. B. Kater (1984). "Serotonin selectively inhibits growth cone motility and synaptogenesis of specific identified neurons." Science **226**(4674): 561-564.

Haydon, P. G. and M. J. Zoran (1989). "Formation and modulation of chemical connections: evoked acetylcholine release from growth cones and neurites of specific identified neurons." Neuron **2**(5): 1483-1490.

Hebb, D. O. (1949). The Organization of Behavior. New York, John Wiley.

Herculano-Houzel, S. (2009). "The human brain in numbers: a linearly scaled-up primate brain." Front Hum Neurosci **3**: 31.

Hodge, J. J., P. Mullasseril and L. C. Griffith (2006). "Activity-dependent gating of CaMKII autonomous activity by Drosophila CASK." Neuron **51**(3): 327-337.

Holt, C. E. and W. A. Harris (1983). "Order in the initial retinotectal map in Xenopus: a new technique for labelling growing nerve fibres." Nature **301**(5896): 150-152.

Hubel, D. H. and T. N. Wiesel (1963). "Shape and arrangement of columns in cat's striate cortex." J Physiol **165**: 559-568.

Hubener, M. and T. Bonhoeffer (2014). "Neuronal plasticity: beyond the critical period." Cell **159**(4): 727-737.

Huberman, A. D., M. B. Feller and B. Chapman (2008). "Mechanisms underlying development of visual maps and receptive fields." Annu Rev Neurosci **31**: 479-509.

Hume, R. I., L. W. Role and G. D. Fischbach (1983). "Acetylcholine release from growth cones detected with patches of acetylcholine receptor-rich membranes." Nature **305**(5935): 632-634.

Humeau, Y., F. Doussau, F. Vitiello, P. Greengard, F. Benfenati and B. Poulain (2001). "Synapsin controls both reserve and releasable synaptic vesicle pools during neuronal activity and short-term plasticity in Aplysia." J Neurosci **21**(12): 4195-4206.

Hur, E. M., Saijilafu and F. Q. Zhou (2012). "Growing the growth cone: remodeling the cytoskeleton to promote axon regeneration." Trends Neurosci **35**(3): 164-174.

Hynes, R. O. (2002). "Integrins: bidirectional, allosteric signaling machines." Cell **110**(6): 673-687.

Ivgy-May, N., H. Tamir and M. D. Gershon (1994). "Synaptic properties of serotonergic growth cones in developing rat brain." J Neurosci **14**(3 Pt 1): 1011-1029.

Jacobi, S., J. Soriano, M. Segal and E. Moses (2009). "BDNF and NT-3 increase excitatory input connectivity in rat hippocampal cultures." Eur J Neurosci **30**(6): 998-1010.

Ji, S. J. and S. R. Jaffrey (2014). "Axonal transcription factors: novel regulators of growth cone-to-nucleus signaling." Dev Neurobiol **74**(3): 245-258.

Jin, I. and R. D. Hawkins (2003). "Presynaptic and postsynaptic mechanisms of a novel form of homosynaptic potentiation at aplysia sensory-motor neuron synapses." J Neurosci **23**(19): 7288-7297.

Kalashnikova, E., R. A. Lorca, I. Kaur, G. A. Barisone, B. Li, T. Ishimaru, J. S. Trimmer, D. P. Mohapatra and E. Diaz (2010). "SynDIG1: an activity-regulated, AMPA- receptor-interacting transmembrane protein that regulates excitatory synapse development." Neuron **65**(1): 80-93.

Kandel, E. R., Y. Dudai and M. R. Mayford (2014). "The molecular and systems biology of memory." Cell **157**(1): 163-186.

Kandel, E. R., J. H. Schwartz and T. M. Jessell (2000). Principles of Neural Science, McGraw-Hill.

Kandler, K., A. Clause and J. Noh (2009). "Tonotopic reorganization of developing auditory brainstem circuits." Nat Neurosci **12**(6): 711-717.

Kang, H. and E. M. Schuman (1995). "Long-lasting neurotrophin-induced enhancement of synaptic transmission in the adult hippocampus." Science **267**(5204): 1658-1662.

Kao, J. P. (1994). "Practical aspects of measuring [Ca2+] with fluorescent indicators." Methods Cell Biol **40**: 155-181.

Katz, B. and R. Miledi (1968). "The role of calcium in neuromuscular facilitation." J Physiol **195**(2): 481-492.

Katz, L. C. and C. J. Shatz (1996). "Synaptic activity and the construction of cortical circuits." Science **274**(5290): 1133-1138.

Kay, L., L. Humphreys, B. J. Eickholt and J. Burrone (2011). "Neuronal activity drives matching of pre- and postsynaptic function during synapse maturation." Nat Neurosci **14**(6): 688-690.

Kerr, J. N. and A. Nimmerjahn (2012). "Functional imaging in freely moving animals." Curr Opin Neurobiol **22**(1): 45-53.

Kerrisk, M. E., C. A. Greer and A. J. Koleske (2013). "Integrin alpha3 is required for late postnatal stability of dendrite arbors, dendritic spines and synapses, and mouse behavior." J Neurosci **33**(16): 6742-6752.

Kerschensteiner, D. (2013). "Spontaneous Network Activity and Synaptic Development." Neuroscientist **20**(3): 272-290.

Kilman, V., M. C. van Rossum and G. G. Turrigiano (2002). "Activity deprivation reduces miniature IPSC amplitude by decreasing the number of postsynaptic GABA(A) receptors clustered at neocortical synapses." J Neurosci **22**(4): 1328-1337.

Kim, N. and S. J. Burden (2008). "MuSK controls where motor axons grow and form synapses." Nat Neurosci **11**(1): 19-27.

Kim, Y. I., H. J. Choi and C. S. Colwell (2006). "Brain-derived neurotrophic factor regulation of N-methyl-D-aspartate receptor-mediated synaptic currents in suprachiasmatic nucleus neurons." J Neurosci Res **84**(7): 1512-1520.

Kirkby, L. A., G. S. Sack, A. Firl and M. B. Feller (2013). "A role for correlated spontaneous activity in the assembly of neural circuits." Neuron **80**(5): 1129-1144.

Klein, J. P., E. A. Tendi, S. D. Dib-Hajj, R. D. Fields and S. G. Waxman (2003). "Patterned electrical activity modulates sodium channel expression in sensory neurons." J Neurosci Res **74**(2): 192-198.

Korogod, N., X. Lou and R. Schneggenburger (2005). "Presynaptic Ca2+ requirements and developmental regulation of posttetanic potentiation at the calyx of Held." J Neurosci **25**(21): 5127-5137.

Korogod, N., X. Lou and R. Schneggenburger (2007). "Posttetanic potentiation critically depends on an enhanced Ca(2+) sensitivity of vesicle fusion mediated by presynaptic PKC." Proc Natl Acad Sci U S A **104**(40): 15923-15928.

Kroger, S. and J. E. Schroder (2002). "Agrin in the developing CNS: new roles for a synapse organizer." News Physiol Sci **17**: 207-212.

Kumamoto, T. and C. Hanashima (2014). "Neuronal subtype specification in establishing mammalian neocortical circuits." Neurosci Res **86C**: 37-49.

Kummer, T. T., T. Misgeld and J. R. Sanes (2006). "Assembly of the postsynaptic membrane at the neuromuscular junction: paradigm lost." Curr Opin Neurobiol **16**(1): 74-82.

Lacour, S. P., S. Benmerah, E. Tarte, J. FitzGerald, J. Serra, S. McMahon, J. Fawcett, O. Graudejus, Z. Yu and B. Morrison, 3rd (2010). "Flexible and stretchable micro-electrodes for in vitro and in vivo neural interfaces." Med Biol Eng Comput **48**(10): 945-954.

Lankford, K. L., F. G. DeMello and W. L. Klein (1988). "D1-type dopamine receptors inhibit growth cone motility in cultured retina neurons: evidence that neurotransmitters act as morphogenic growth regulators in the developing central nervous system." Proc Natl Acad Sci U S A **85**(8): 2839-2843.

Lee, S. J., Y. Escobedo-Lozoya, E. M. Szatmari and R. Yasuda (2009). "Activation of CaMKII in single dendritic spines during long-term potentiation." Nature **458**(7236): 299-304.

Lessmann, V. (1998). "Neurotrophin-dependent modulation of glutamatergic synaptic transmission in the mammalian CNS." Gen Pharmacol **31**(5): 667-674.

Lessmann, V., K. Gottmann and R. Heumann (1994). "BDNF and NT-4/5 enhance glutamatergic synaptic transmission in cultured hippocampal neurones." Neuroreport **6**(1): 21-25.

Lessmann, V. and R. Heumann (1998). "Modulation of unitary glutamatergic synapses by neurotrophin-4/5 or brain-derived neurotrophic factor in hippocampal microcultures: presynaptic enhancement depends on pre-established paired-pulse facilitation." Neuroscience **86**(2): 399-413.

Li, Z., L. G. Hilgenberg, D. K. O'Dowd and M. A. Smith (1999). "Formation of functional synaptic connections between cultured cortical neurons from agrin-deficient mice." J Neurobiol **39**(4): 547-557.

Lin, S., L. Landmann, M. A. Ruegg and H. R. Brenner (2008). "The role of nerve- versus muscle-derived factors in mammalian neuromuscular junction formation." J Neurosci **28**(13): 3333-3340.

Lin, W., R. W. Burgess, B. Dominguez, S. L. Pfaff, J. R. Sanes and K. F. Lee (2001). "Distinct roles of nerve and muscle in postsynaptic differentiation of the neuromuscular synapse." Nature **410**(6832): 1057-1064.

Lin, W., B. Dominguez, J. Yang, P. Aryal, E. P. Brandon, F. H. Gage and K. F. Lee (2005). "Neurotransmitter acetylcholine negatively regulates neuromuscular synapse formation by a Cdk5-dependent mechanism." Neuron **46**(4): 569-579.

Lin, Y., R. Trouillon, M. I. Svensson, J. D. Keighron, A. S. Cans and A. G. Ewing (2012). "Carbon-ring microelectrode arrays for electrochemical imaging of single cell exocytosis: fabrication and characterization." Anal Chem **84**(6): 2949-2954.

Liou, J. C., Y. H. Chen and W. M. Fu (1999). "Target-dependent regulation of acetylcholine secretion at developing motoneurons in Xenopus cell cultures." J Physiol **517 (Pt 3)**: 721-730.

Lipski, J., R. Nistico, N. Berretta, E. Guatteo, G. Bernardi and N. B. Mercuri (2011). "L-DOPA: a scapegoat for accelerated neurodegeneration in Parkinson's disease?" Prog Neurobiol **94**(4): 389-407.

Lissin, D. V., S. N. Gomperts, R. C. Carroll, C. W. Christine, D. Kalman, M. Kitamura, S. Hardy, R. A. Nicoll, R. C. Malenka and M. von Zastrow (1998). "Activity differentially regulates the surface expression of synaptic AMPA and NMDA glutamate receptors." Proc Natl Acad Sci U S A **95**(12): 7097-7102.

Lonart, G. and F. Simsek-Duran (2006). "Deletion of synapsins I and II genes alters the size of vesicular pools and rabphilin phosphorylation." Brain Res **1107**(1): 42-51.

Lovell, P., B. McMahon and N. I. Syed (2002). "Synaptic precedence during synapse formation between reciprocally connected neurons involves transmitter-receptor interactions and AA metabolites." J Neurophysiol **88**(3): 1328-1338.

Lowery, L. A. and D. Van Vactor (2009). "The trip of the tip: understanding the growth cone machinery." Nat Rev Mol Cell Biol **10**(5): 332-343.

Lu, B., P. T. Pang and N. H. Woo (2005). "The yin and yang of neurotrophin action." Nat Rev Neurosci **6**(8): 603-614.

Lu, J. T., Y. J. Son, J. Lee, T. L. Jetton, M. Shiota, L. Moscoso, K. D. Niswender, A. D. Loewy, M. A. Magnuson, J. R. Sanes and R. B. Emeson (1999). "Mice lacking alpha-calcitonin gene-related peptide exhibit normal cardiovascular regulation and neuromuscular development." Mol Cell Neurosci **14**(2): 99-120.

Luk, C. C., H. Naruo, D. Prince, A. Hassan, S. A. Doran, J. I. Goldberg and N. I. Syed (2011). "A novel form of presynaptic CaMKII-dependent short-term potentiation between Lymnaea neurons." Eur J Neurosci **34**(4): 569-577.

Luthi, A., L. Schwyzer, J. M. Mateos, B. H. Gahwiler and R. A. McKinney (2001). "NMDA receptor activation limits the number of synaptic connections during hippocampal development." Nat Neurosci **4**(11): 1102-1107.

Ma, L., T. Harada, C. Harada, M. Romero, J. M. Hebert, S. K. McConnell and L. F. Parada (2002). "Neurotrophin-3 is required for appropriate establishment of thalamocortical connections." Neuron **36**(4): 623-634.

Malenka, R. C., J. A. Kauer, D. J. Perkel, M. D. Mauk, P. T. Kelly, R. A. Nicoll and M. N. Waxham (1989). "An essential role for postsynaptic calmodulin and protein kinase activity in long-term potentiation." Nature **340**(6234): 554-557.

Malinow, R., H. Schulman and R. W. Tsien (1989). "Inhibition of postsynaptic PKC or CaMKII blocks induction but not expression of LTP." Science **245**(4920): 862-866.

Mammen, A. L., R. L. Huganir and R. J. O'Brien (1997). "Redistribution and stabilization of cell surface glutamate receptors during synapse formation." J Neurosci **17**(19): 7351-7358.

Marek, K. W., L. M. Kurtz and N. C. Spitzer (2010). "cJun integrates calcium activity and tlx3 expression to regulate neurotransmitter specification." Nat Neurosci **13**(8): 944-950.

Marler, K. J., E. Becker-Barroso, A. Martinez, M. Llovera, C. Wentzel, S. Poopalasundaram, R. Hindges, E. Soriano, J. Comella and U. Drescher (2008). "A TrkB/EphrinA interaction controls retinal axon branching and synaptogenesis." J Neurosci **28**(48): 12700-12712.

Marom, S. and D. Dagan (1987). "Calcium current in growth balls from isolated Helix aspersa neuronal growth cones." Pflugers Arch **409**(6): 578-581.

Martina, M., C. Luk, C. Py, D. Martinez, T. Comas, R. Monette, M. Denhoff, N. Syed and G. A. Mealing (2011). "Recordings of cultured neurons and synaptic activity using patch-clamp chips." J Neural Eng **8**(3): 034002.

Martinez, A., S. Alcantara, V. Borrell, J. A. Del Rio, J. Blasi, R. Otal, N. Campos, A. Boronat, M. Barbacid, I. Silos-Santiago and E. Soriano (1998). "TrkB and TrkC signaling are required for maturation and synaptogenesis of hippocampal connections." J Neurosci **18**(18): 7336-7350.

Martinez, D., C. Py, M. W. Denhoff, M. Martina, R. Monette, T. Comas, C. Luk, N. Syed and G. Mealing (2010). "High-fidelity patch-clamp recordings from neurons cultured on a polymer microchip." Biomed Microdevices **12**(6): 977-985.

Mattson, M. P., P. Dou and S. B. Kater (1988). "Outgrowth-regulating actions of glutamate in isolated hippocampal pyramidal neurons." J Neurosci **8**(6): 2087-2100.

Mayford, M., J. Wang, E. R. Kandel and T. J. O'Dell (1995). "CaMKII regulates the frequency-response function of hippocampal synapses for the production of both LTD and LTP." Cell **81**(6): 891-904.

McAllister, A. K., L. C. Katz and D. C. Lo (1996). "Neurotrophin regulation of cortical dendritic growth requires activity." Neuron **17**(6): 1057-1064.

McCobb, D. P., P. M. Best and K. G. Beam (1990). "The differentiation of excitability in embryonic chick limb motoneurons." J Neurosci **10**(9): 2974-2984.

McCobb, D. P. and S. B. Kater (1988). "Membrane voltage and neurotransmitter regulation of neuronal growth cone motility." Dev Biol **130**(2): 599-609.

McCroskery, S., A. Bailey, L. Lin and M. P. Daniels (2009). "Transmembrane agrin regulates dendritic filopodia and synapse formation in mature hippocampal neuron cultures." Neuroscience **163**(1): 168-179.

Medeiros, N. A., D. T. Burnette and P. Forscher (2006). "Myosin II functions in actin-bundle turnover in neuronal growth cones." Nat Cell Biol **8**(3): 215-226.

Meems, R., D. Munno, J. van Minnen and N. I. Syed (2003). "Synapse formation between isolated axons requires presynaptic soma and redistribution of postsynaptic AChRs." J Neurophysiol **89**(5): 2611-2619.

Mehta, A., J. M. Luck, C. C. Luk and N. I. Syed (2013). "Synaptic metaplasticity underlies tetanic potentiation in lymnaea: a novel paradigm." PLoS One **8**(10): e78056.

Merlie, J. P., K. E. Isenberg, S. D. Russell and J. R. Sanes (1984). "Denervation supersensitivity in skeletal muscle: analysis with a cloned cDNA probe." J Cell Biol **99**(1 Pt 1): 332-335.

Meyer-Franke, A., M. R. Kaplan, F. W. Pfrieger and B. A. Barres (1995). "Characterization of the signaling interactions that promote the survival and growth of developing retinal ganglion cells in culture." Neuron **15**(4): 805-819.

Misgeld, T., T. T. Kummer, J. W. Lichtman and J. R. Sanes (2005). "Agrin promotes synaptic differentiation by counteracting an inhibitory effect of neurotransmitter." Proc Natl Acad Sci U S A **102**(31): 11088-11093.

Mudraboyina, A. K., L. Blockstein, C. C. Luk, N. I. Syed and O. Yadid-Pecht (2014). "A novel lensless miniature contact imaging system for monitoring calcium changes in live neurons." IEEE Photonics Journal **6**(1): 1-15.

Mulkey, R. M., C. E. Herron and R. C. Malenka (1993). "An essential role for protein phosphatases in hippocampal long-term depression." Science **261**(5124): 1051-1055.

Munno, D. W. and N. I. Syed (2003). "Synaptogenesis in the CNS: An odyssey from wiring together to firing together." Journal of Physiology **552**: 1-11.

Munno, D. W. and N. I. Syed (2003). "Synaptogenesis in the CNS: an odyssey from wiring together to firing together." J Physiol **552**(Pt 1): 1-11.

Munno, D. W., M. A. Woodin, K. Lukowiak, N. I. Syed and P. S. Dickinson (2000). "Different extrinsic trophic factors regulate neurite outgrowth and synapse formation between identified Lymnaea neurons." J Neurobiol **44**(1): 20-30.

Murray, P. S. and P. V. Holmes (2011). "An overview of brain-derived neurotrophic factor and implications for excitotoxic vulnerability in the hippocampus." Int J Pept **2011**: 654085.

Myers, J. P., M. Santiago-Medina and T. M. Gomez (2011). "Regulation of axonal outgrowth and pathfinding by integrin-ECM interactions." Dev Neurobiol **71**(11): 901-923.

Nagahara, A. H., D. A. Merrill, G. Coppola, S. Tsukada, B. E. Schroeder, G. M. Shaked, L. Wang, A. Blesch, A. Kim, J. M. Conner, E. Rockenstein, M. V. Chao, E. H. Koo, D. Geschwind, E. Masliah, A. A. Chiba and M. H. Tuszynski (2009). "Neuroprotective effects of brain-derived neurotrophic factor in rodent and primate models of Alzheimer's disease." Nat Med **15**(3): 331-337.

Naruo, H., S. Onizuka, D. Prince, M. Takasaki and N. I. Syed (2005). "Sevoflurane blocks cholinergic synaptic transmission postsynaptically but does not affect short-term potentiation." Anesthesiology **102**(5): 920-928.

Neher, E., B. Sakmann and J. H. Steinbach (1978). "The extracellular patch clamp: a method for resolving currents through individual open channels in biological membranes." Pflugers Arch **375**(2): 219-228.

Nerbonne, J. M. and A. M. Gurney (1989). "Development of excitable membrane properties in mammalian sympathetic neurons." J Neurosci **9**(9): 3272-3286.

O'Brien, R. J., S. Kamboj, M. D. Ehlers, K. R. Rosen, G. D. Fischbach and R. L. Huganir (1998). "Activity-dependent modulation of synaptic AMPA receptor accumulation." Neuron **21**(5): 1067-1078.

Okabe, S. (2013). "Fluorescence imaging of synapse formation and remodeling." Microscopy (Oxf) **62**(1): 51-62.

Okabe, S., H. D. Kim, A. Miwa, T. Kuriu and H. Okado (1999). "Continual remodeling of postsynaptic density and its regulation by synaptic activity." Nat Neurosci **2**(9): 804-811.

Padamsey, Z. and N. Emptage (2014). "Two sides to long-term potentiation: a view towards reconciliation." Philos Trans R Soc Lond B Biol Sci **369**(1633): 20130154.

Panzer, J. A., Y. Song and R. J. Balice-Gordon (2006). "In vivo imaging of preferential motor axon outgrowth to and synaptogenesis at prepatterned acetylcholine receptor clusters in embryonic zebrafish skeletal muscle." J Neurosci **26**(3): 934-947.

Paridaen, J. T. and W. B. Huttner (2014). "Neurogenesis during development of the vertebrate central nervous system." EMBO Rep **15**(4): 351-364.

Park, H. and M. M. Poo (2013). "Neurotrophin regulation of neural circuit development and function." Nat Rev Neurosci **14**(1): 7-23.

Patel, B. A., C. C. Luk, P. L. Leow, A. J. Lee, W. Zaidi and N. I. Syed (2013). "A planar microelectrode array for simultaneous detection of electrically evoked dopamine release from distinct locations of a single isolated neuron." Analyst **138**(10): 2833-2839.

Pinkstaff, J. K., J. Detterich, G. Lynch and C. Gall (1999). "Integrin subunit gene expression is regionally differentiated in adult brain." J Neurosci **19**(5): 1541-1556.

Pivovarov, A. S. and E. I. Drozdova (2002). "Ca-dependent regulation of the Na-K-pump by post-tetanic sensitization of extrasynaptic cholinoreceptors in common snail neurons." Neurosci Behav Physiol **32**(3): 223-229.

Py, C., M. W. Denhoff, M. Martina, R. Monette, T. Comas, T. Ahuja, D. Martinez, S. Wingar, J. Caballero, S. Laframboise, J. Mielke, A. Bogdanov, C. Luk, N. Syed and G. Mealing (2010). "A novel silicon patch-clamp chip permits high-fidelity recording of ion channel activity from functionally defined neurons." Biotechnol Bioeng **107**(4): 593-600.

Py, C., M. Martina, R. Monette, T. Comas, M. W. Denhoff, C. Luk, N. I. Syed and G. Mealing (2012). "Culturing and electrophysiology of cells on NRCC patch-clamp chips." J Vis Exp(60).

Rajan, I. and H. T. Cline (1998). "Glutamate receptor activity is required for normal development of tectal cell dendrites in vivo." J Neurosci **18**(19): 7836-7846.

Rajan, I., S. Witte and H. T. Cline (1999). "NMDA receptor activity stabilizes presynaptic retinotectal axons and postsynaptic optic tectal cell dendrites in vivo." J Neurobiol **38**(3): 357-368.

Ramón y Cajal, S. (1909). Histologie du System Nerveux de l'Homme et des Vertebres. Paris: Malonine.

Raper, J. and C. Mason (2010). "Cellular strategies of axonal pathfinding." Cold Spring Harb Perspect Biol **2**(9): a001933.

Regehr, W. G. (2012). "Short-term presynaptic plasticity." Cold Spring Harb Perspect Biol **4**(7): a005702.

Rehder, V., J. R. Jensen, P. Dou and S. B. Kater (1991). "A comparison of calcium homeostasis in isolated and attached growth cones of the snail Helisoma." J Neurobiol **22**(5): 499-511.

Rico, B., B. Xu and L. F. Reichardt (2002). "TrkB receptor signaling is required for establishment of GABAergic synapses in the cerebellum." Nat Neurosci **5**(3): 225-233.

Ridgway, R. L., N. I. Syed, K. Lukowiak and A. G. Bulloch (1991). "Nerve growth factor (NGF) induces sprouting of specific neurons of the snail, Lymnaea stagnalis." J Neurobiol **22**(4): 377-390.

Robichaux, M. A. and C. W. Cowan (2014). "Signaling mechanisms of axon guidance and early synaptogenesis." Curr Top Behav Neurosci **16**: 19-48.

Rodriguez, O. C., A. W. Schaefer, C. A. Mandato, P. Forscher, W. M. Bement and C. M. Waterman-Storer (2003). "Conserved microtubule-actin interactions in cell movement and morphogenesis." Nat Cell Biol **5**(7): 599-609.

Rosenegger, D. and K. Lukowiak (2010). "The participation of NMDA receptors, PKC, and MAPK in the formation of memory following operant conditioning in Lymnaea." Mol Brain **3**: 24.

Sabo, S. L., R. A. Gomes and A. K. McAllister (2006). "Formation of presynaptic terminals at predefined sites along axons." J Neurosci **26**(42): 10813-10825.

Sabo, S. L. and A. K. McAllister (2003). "Mobility and cycling of synaptic protein-containing vesicles in axonal growth cone filopodia." Nat Neurosci **6**(12): 1264-1269.

Sadanandappa, M. K., B. Blanco Redondo, B. Michels, V. Rodrigues, B. Gerber, K. VijayRaghavan, E. Buchner and M. Ramaswami (2013). "Synapsin function in GABA-ergic interneurons is required for short-term olfactory habituation." J Neurosci **33**(42): 16576-16585.

Sanford, S. D., J. C. Gatlin, T. Hokfelt and K. H. Pfenninger (2008). "Growth cone responses to growth and chemotropic factors." Eur J Neurosci **28**(2): 268-278.

Schaffhausen, J. H., T. M. Fischer and T. J. Carew (2001). "Contribution of postsynaptic Ca2+ to the induction of post-tetanic potentiation in the neural circuit for siphon withdrawal in Aplysia." J Neurosci **21**(5): 1739-1749.

Scharfman, H. E. (1997). "Hyperexcitability in combined entorhinal/hippocampal slices of adult rat after exposure to brain-derived neurotrophic factor." J Neurophysiol **78**(2): 1082-1095.

Scheiffele, P., J. Fan, J. Choih, R. Fetter and T. Serafini (2000). "Neuroligin expressed in nonneuronal cells triggers presynaptic development in contacting axons." Cell **101**(6): 657-669.

Schindowski, K., K. Belarbi and L. Buee (2008). "Neurotrophic factors in Alzheimer's disease: role of axonal transport." Genes Brain Behav **7 Suppl 1**: 43-56.

Schmold, N. and N. I. Syed (2012). "Molluscan neurons in culture: shedding light on synapse formation and plasticity." J Mol Histol **43**(4): 383-399.

Schulman, H. (1993). "The multifunctional Ca2+/calmodulin-dependent protein kinases." Curr Opin Cell Biol **5**(2): 247-253.

Schwabe, T., H. Neuert and T. R. Clandinin (2013). "A network of cadherin-mediated interactions polarizes growth cones to determine targeting specificity." Cell **154**(2): 351-364.

Serpinskaya, A. S., G. Feng, J. R. Sanes and A. M. Craig (1999). "Synapse formation by hippocampal neurons from agrin-deficient mice." Dev Biol **205**(1): 65-78.

Sharma, N., C. D. Deppmann, A. W. Harrington, C. St Hillaire, Z. Y. Chen, F. S. Lee and D. D. Ginty (2010). "Long-distance control of synapse assembly by target-derived NGF." Neuron **67**(3): 422-434.

Shen, R. Y., C. A. Altar and L. A. Chiodo (1994). "Brain-derived neurotrophic factor increases the electrical activity of pars compacta dopamine neurons in vivo." Proc Natl Acad Sci U S A **91**(19): 8920-8924.

Sheng, H. Z., R. D. Fields and P. G. Nelson (1993). "Specific regulation of immediate early genes by patterned neuronal activity." J Neurosci Res **35**(5): 459-467.

Shi, L., A. K. Fu and N. Y. Ip (2012). "Molecular mechanisms underlying maturation and maintenance of the vertebrate neuromuscular junction." Trends Neurosci **35**(7): 441-453.

Shonesy, B. C., N. Jalan-Sakrikar, V. S. Cavener and R. J. Colbran (2014). "CaMKII: a molecular substrate for synaptic plasticity and memory." Prog Mol Biol Transl Sci **122**: 61-87.

Sigworth, F. J. and K. G. Klemic (2005). "Microchip technology in ion-channel research." IEEE Trans Nanobioscience **4**(1): 121-127.

Soto, F., X. Ma, J. L. Cecil, B. Q. Vo, S. M. Culican and D. Kerschensteiner (2012). "Spontaneous activity promotes synapse formation in a cell-type-dependent manner in the developing retina." J Neurosci **32**(16): 5426-5439.

Spafford, J. D., T. Dunn, A. B. Smit, N. I. Syed and G. W. Zamponi (2006). "In vitro characterization of L-type calcium channels and their contribution to firing behavior in invertebrate respiratory neurons." J Neurophysiol **95**(1): 42-52.

Spencer, G. E., J. Klumperman and N. I. Syed (1998). "Neurotransmitters and neurodevelopment. Role of dopamine in neurite outgrowth, target selection and specific synapse formation." Perspect Dev Neurobiol **5**(4): 451-467.

Spencer, G. E., K. Lukowiak and N. I. Syed (2000). "Transmitter-receptor interactions between growth cones of identified Lymnaea neurons determine target cell selection in vitro." J Neurosci **20**(21): 8077-8086.

Spitzer, N. C. (2012). "Activity-dependent neurotransmitter respecification." Nat Rev Neurosci **13**(2): 94-106.

Stanton, P. K., J. Winterer, C. P. Bailey, A. Kyrozis, I. Raginov, G. Laube, R. W. Veh, C. Q. Nguyen and W. Muller (2003). "Long-term depression of presynaptic release from the readily releasable vesicle pool induced by NMDA receptor-dependent retrograde nitric oxide." J Neurosci **23**(13): 5936-5944.

Stevens, C. F. and J. M. Sullivan (1998). "Regulation of the readily releasable vesicle pool by protein kinase C." Neuron **21**(4): 885-893.

Stevens, C. F. and Y. Wang (1994). "Changes in reliability of synaptic function as a mechanism for plasticity." Nature **371**(6499): 704-707.

Suter, D. M. and P. Forscher (1998). "An emerging link between cytoskeletal dynamics and cell adhesion molecules in growth cone guidance." Curr Opin Neurobiol **8**(1): 106-116.

Sutherland, D. J., Z. Pujic and G. J. Goodhill (2014). "Calcium signaling in axon guidance." Trends Neurosci **37**(8): 424-432.

Syed, N., P. Richardson and A. Bulloch (1996). "Ciliary neurotrophic factor, unlike nerve growth factor, supports neurite outgrowth but not synapse formation by adult Lymnaea neurons." J Neurobiol **29**(3): 293-303.

Syed, N. I. (2006). Molecular Mechanisms of Synaptogenesis, Springer.

Syed, N. I. and G. E. Spencer (1994). "Target cell selection and specific synapse formation by identified *Lymnaea* neurons *in vitro*." Neth J Zool **44**(3-4): 327-338.

Syed, N. I., H. Zaidi and P. Lovell (1999). In vitro reconstruction of neuronal circuits: a simple model system approach. Modern Techniques in Neuroscience Research. U. Windhurst and H. Johansson. Berlin, Springer.

Takada, N., Y. Yanagawa and Y. Komatsu (2005). "Activity-dependent maturation of excitatory synaptic connections in solitary neuron cultures of mouse neocortex." Eur J Neurosci **21**(2): 422-430.

Takeuchi, T., A. J. Duszkiewicz and R. G. Morris (2014). "The synaptic plasticity and memory hypothesis: encoding, storage and persistence." Philos Trans R Soc Lond B Biol Sci **369**(1633): 20130288.

Talauliker, P. M., D. A. Price, J. J. Burmeister, S. Nagari, J. E. Quintero, F. Pomerleau, P. Huettl, J. T. Hastings and G. A. Gerhardt (2011). "Ceramic-based microelectrode arrays: recording surface characteristics and topographical analysis." J Neurosci Methods **198**(2): 222-229.

Tang, Y. and R. S. Zucker (1997). "Mitochondrial involvement in post-tetanic potentiation of synaptic transmission." Neuron **18**(3): 483-491.

Tao, H. W. and M. M. Poo (2005). "Activity-dependent matching of excitatory and inhibitory inputs during refinement of visual receptive fields." Neuron **45**(6): 829-836.

Tomita, S., V. Stein, T. J. Stocker, R. A. Nicoll and D. S. Bredt (2005). "Bidirectional synaptic plasticity regulated by phosphorylation of stargazin-like TARPs." Neuron **45**(2): 269-277.

Trouillon, R., C. Cheung, B. A. Patel and D. O'Hare (2010). "Electrochemical study of the intracellular transduction of vascular endothelial growth factor induced nitric oxide synthase activity using a multi-channel biocompatible microelectrode array." Biochim Biophys Acta **1800**(9): 929-936.

Tsay, H. J. and J. Schmidt (1989). "Skeletal muscle denervation activates acetylcholine receptor genes." J Cell Biol **108**(4): 1523-1526.

Turner, M. B., T. M. Szabo-Maas, J. C. Poyer and M. J. Zoran (2011). "Regulation and restoration of motoneuronal synaptic transmission during neuromuscular regeneration in the pulmonate snail Helisoma trivolvis." Biol Bull **221**(1): 110-125.

Uesaka, N., S. Hirai, T. Maruyama, E. S. Ruthazer and N. Yamamoto (2005). "Activity dependence of cortical axon branch formation: a morphological and electrophysiological study using organotypic slice cultures." J Neurosci **25**(1): 1-9.

van Kesteren, R. E., J. S. Gagatek, A. Hagendorf, Y. Gouwenberg, A. B. Smit and N. I. Syed (2008). "Postsynaptic expression of an epidermal growth factor receptor regulates cholinergic synapse formation between identified molluscan neurons." Eur J Neurosci **27**(8): 2043-2056.

van Kesteren, R. E., N. I. Syed, D. W. Munno, J. Bouwman, Z. P. Feng, W. P. Geraerts and A. B. Smit (2001). "Synapse formation between central neurons requires postsynaptic expression of the MEN1 tumor suppressor gene." J Neurosci **21**(16): RC161.

van Nierop, P., S. Bertrand, D. W. Munno, Y. Gouwenberg, J. van Minnen, J. D. Spafford, N. I. Syed, D. Bertrand and A. B. Smit (2006). "Identification and functional expression of a family of nicotinic acetylcholine receptor subunits in the central nervous system of the mollusc Lymnaea stagnalis." J Biol Chem **281**(3): 1680-1691.

van Nierop, P., A. Keramidas, S. Bertrand, J. van Minnen, Y. Gouwenberg, D. Bertrand and A. B. Smit (2005). "Identification of molluscan nicotinic acetylcholine receptor (nAChR) subunits involved in formation of cation- and anion-selective nAChRs." J Neurosci **25**(46): 10617-10626.

Verderio, C., S. Coco, G. Fumagalli and M. Matteoli (1994). "Spatial changes in calcium signaling during the establishment of neuronal polarity and synaptogenesis." J Cell Biol **126**(6): 1527-1536.

Verhage, M., A. S. Maia, J. J. Plomp, A. B. Brussaard, J. H. Heeroma, H. Vermeer, R. F. Toonen, R. E. Hammer, T. K. van den Berg, M. Missler, H. J. Geuze and T. C. Sudhof (2000). "Synaptic assembly of the brain in the absence of neurotransmitter secretion." Science **287**(5454): 864-869.

Vicario-Abejon, C., C. Collin, R. D. McKay and M. Segal (1998). "Neurotrophins induce formation of functional excitatory and inhibitory synapses between cultured hippocampal neurons." J Neurosci **18**(18): 7256-7271.

Vitureira, N., M. Letellier and Y. Goda (2012). "Homeostatic synaptic plasticity: from single synapses to neural circuits." Curr Opin Neurobiol **22**(3): 516-521.

Volianskis, A. and M. S. Jensen (2003). "Transient and sustained types of long-term potentiation in the CA1 area of the rat hippocampus." J Physiol **550**(Pt 2): 459-492.

Waites, C. L., A. M. Craig and C. C. Garner (2005). "Mechanisms of vertebrate synaptogenesis." Annu Rev Neurosci **28**: 251-274.

Wan, G., M. E. Gomez-Casati, A. R. Gigliello, M. C. Liberman and G. Corfas (2014). "Neurotrophin-3 regulates ribbon synapse density in the cochlea and induces synapse regeneration after acoustic trauma." Elife **3**.

Wang, X., Y. Li, K. L. Engisch, S. T. Nakanishi, S. E. Dodson, G. W. Miller, T. C. Cope, M. J. Pinter and M. M. Rich (2005). "Activity-dependent presynaptic regulation of quantal size at the mammalian neuromuscular junction in vivo." J Neurosci **25**(2): 343-351.

Wang, Y., H. Markram, P. H. Goodman, T. K. Berger, J. Ma and P. S. Goldman-Rakic (2006). "Heterogeneity in the pyramidal network of the medial prefrontal cortex." Nat Neurosci **9**(4): 534-542.

Wang, Y. Y., H. I. Wu, W. L. Hsu, H. W. Chung, P. H. Yang, Y. C. Chang and W. Y. Chow (2014). "In vitro growth conditions and development affect differential distributions of RNA in axonal growth cones and shafts of cultured rat hippocampal neurons." Mol Cell Neurosci **61**: 141-151.

Washbourne, P., J. E. Bennett and A. K. McAllister (2002). "Rapid recruitment of NMDA receptor transport packets to nascent synapses." Nat Neurosci **5**(8): 751-759.

Wayman, G. A., Y. S. Lee, H. Tokumitsu, A. Silva and T. R. Soderling (2008). "Calmodulin-kinases: modulators of neuronal development and plasticity." Neuron **59**(6): 914-931.

West, A. E. and M. E. Greenberg (2011). "Neuronal activity-regulated gene transcription in synapse development and cognitive function." Cold Spring Harb Perspect Biol **3**(6).

Westerink, R. H. (2004). "Exocytosis: using amperometry to study presynaptic mechanisms of neurotoxicity." Neurotoxicology **25**(3): 461-470.

Weston, C., C. Gordon, G. Teressa, E. Hod, X. D. Ren and J. Prives (2003). "Cooperative regulation by Rac and Rho of agrin-induced acetylcholine receptor clustering in muscle cells." J Biol Chem **278**(8): 6450-6455.

Weston, C., B. Yee, E. Hod and J. Prives (2000). "Agrin-induced acetylcholine receptor clustering is mediated by the small guanosine triphosphatases Rac and Cdc42." J Cell Biol **150**(1): 205-212.

Wiersma-Meems, R., J. Van Minnen and N. I. Syed (2005). "Synapse formation and plasticity: the roles of local protein synthesis." Neuroscientist **11**(3): 228-237.

Wiesel, T. N. and D. H. Hubel (1963). "Single-Cell Responses in Striate Cortex of Kittens Deprived of Vision in One Eye." J Neurophysiol **26**: 1003-1017.

Williams, M. E., S. A. Wilke, A. Daggett, E. Davis, S. Otto, D. Ravi, B. Ripley, E. A. Bushong, M. H. Ellisman, G. Klein and A. Ghosh (2011). "Cadherin-9 regulates synapse-specific differentiation in the developing hippocampus." Neuron **71**(4): 640-655.

Winlow, W., P. G. Haydon and P. R. Benjamin (1981). "Multiple Postsynaptic Actions of the Giant Dopamine-Containing Neurone RPeD1 of Lymnaea stagnalis." J Exp Biol **94**: 137-148.

Witzemann, V. (2006). "Development of the neuromuscular junction." Cell Tissue Res **326**(2): 263-271.

Woodin, M. A., T. Hamakawa, M. Takasaki, K. Lukowiak and N. I. Syed (1999). "Trophic factor-induced plasticity of synaptic connections between identified Lymnaea neurons." Learn Mem **6**(3): 307-316.

Woodin, M. A., D. W. Munno and N. I. Syed (2002). "Trophic factor-induced excitatory synaptogenesis involves postsynaptic modulation of nicotinic acetylcholine receptors." J Neurosci **22**(2): 505-514.

Wu, H., W. C. Xiong and L. Mei (2010). "To build a synapse: signaling pathways in neuromuscular junction assembly." Development **137**(7): 1017-1033.

Xia, Z. and D. R. Storm (2005). "The role of calmodulin as a signal integrator for synaptic plasticity." Nat Rev Neurosci **6**(4): 267-276.

Xu, F., D. A. Hennessy, T. K. Lee and N. I. Syed (2009). "Trophic factor-induced intracellular calcium oscillations are required for the expression of postsynaptic acetylcholine receptors during synapse formation between Lymnaea neurons." J Neurosci **29**(7): 2167-2176.

Xu, F., C. C. Luk, R. Wiersma-Meems, K. Baehre, C. Herman, W. Zaidi, N. Wong and N. I. Syed (2014). "Neuronal somata and extrasomal compartments play distinct roles during synapse formation between Lymnaea neurons." J Neurosci **34**(34): 11304-11315.

Xu, J., L. He and L. G. Wu (2007). "Role of Ca(2+) channels in short-term synaptic plasticity." Curr Opin Neurobiol **17**(3): 352-359.

Yagi, T. and M. Takeichi (2000). "Cadherin superfamily genes: functions, genomic organization, and neurologic diversity." Genes Dev **14**(10): 1169-1180.

Yamasaki, N., M. Maekawa, K. Kobayashi, Y. Kajii, J. Maeda, M. Soma, K. Takao, K. Tanda, K. Ohira, K. Toyama, K. Kanzaki, K. Fukunaga, Y. Sudo, H. Ichinose, M. Ikeda, N. Iwata, N. Ozaki, H. Suzuki, M. Higuchi, T. Suhara, S. Yuasa and T. Miyakawa (2008). "Alpha-CaMKII deficiency causes immature dentate gyrus, a novel candidate endophenotype of psychiatric disorders." Mol Brain **1**(1): 6.

Yang, X., S. Arber, C. William, L. Li, Y. Tanabe, T. M. Jessell, C. Birchmeier and S. J. Burden (2001). "Patterning of muscle acetylcholine receptor gene expression in the absence of motor innervation." Neuron **30**(2): 399-410.

Yang, Y. and N. Calakos (2013). "Presynaptic long-term plasticity." Front Synaptic Neurosci **5**: 8.

Yao, W. D., J. Rusch, M. Poo and C. F. Wu (2000). "Spontaneous acetylcholine secretion from developing growth cones of Drosophila central neurons in culture: effects of cAMP-pathway mutations." J Neurosci **20**(7): 2626-2637.

Young, S. H. and M. M. Poo (1983). "Spontaneous release of transmitter from growth cones of embryonic neurones." Nature **305**(5935): 634-637.

Zachek, M. K., J. Park, P. Takmakov, R. M. Wightman and G. S. McCarty (2010). "Microfabricated FSCV-compatible microelectrode array for real-time monitoring of heterogeneous dopamine release." Analyst **135**(7): 1556-1563.

Zachek, M. K., P. Takmakov, B. Moody, R. M. Wightman and G. S. McCarty (2009). "Simultaneous decoupled detection of dopamine and oxygen using pyrolyzed carbon microarrays and fast-scan cyclic voltammetry." Anal Chem **81**(15): 6258-6265.

Zhang, B., K. L. Adams, S. J. Luber, D. J. Eves, M. L. Heien and A. G. Ewing (2008). "Spatially and temporally resolved single-cell exocytosis utilizing individually addressable carbon microelectrode arrays." Anal Chem **80**(5): 1394-1400.

Zhang, B., M. L. Heien, M. F. Santillo, L. Mellander and A. G. Ewing (2011). "Temporal resolution in electrochemical imaging on single PC12 cells using amperometry and voltammetry at microelectrode arrays." Anal Chem **83**(2): 571-577.

Zhang, B., S. Luo, Q. Wang, T. Suzuki, W. C. Xiong and L. Mei (2008). "LRP4 serves as a coreceptor of agrin." Neuron **60**(2): 285-297.

Zhang, L. I. and M. M. Poo (2001). "Electrical activity and development of neural circuits." Nat Neurosci **4 Suppl**: 1207-1214.

Zhang, W. and D. L. Benson (2001). "Stages of synapse development defined by dependence on F-actin." J Neurosci **21**(14): 5169-5181.

Zhang, Y. H., X. X. Chi and G. D. Nicol (2008). "Brain-derived neurotrophic factor enhances the excitability of rat sensory neurons through activation of the p75 neurotrophin receptor and the sphingomyelin pathway." J Physiol **586**(13): 3113-3127.

Zheng, J. Q., M. Felder, J. A. Connor and M. M. Poo (1994). "Turning of nerve growth cones induced by neurotransmitters." Nature **368**(6467): 140-144.

Zhong, L. R., S. Estes, L. Artinian and V. Rehder (2013). "Acetylcholine elongates neuronal growth cone filopodia via activation of nicotinic acetylcholine receptors." Dev Neurobiol **73**(7): 487-501.

Ziv, N. E. and C. C. Garner (2004). "Cellular and molecular mechanisms of presynaptic assembly." Nat Rev Neurosci **5**(5): 385-399.

Zong, Y. and R. Jin (2013). "Structural mechanisms of the agrin-LRP4-MuSK signaling pathway in neuromuscular junction differentiation." Cell Mol Life Sci **70**(17): 3077-3088.

Zoran, M. J., R. T. Doyle and P. G. Haydon (1991). "Target contact regulates the calcium responsiveness of the secretory machinery during synaptogenesis." Neuron **6**(1): 145-151.

Zoran, M. J., L. R. Funte, S. B. Kater and P. G. Haydon (1993). "Neuron-muscle contact changes presynaptic resting calcium set-point." Dev Biol **158**(1): 163-171.

Zou, Y. and A. I. Lyuksyutova (2007). "Morphogens as conserved axon guidance cues." Curr Opin Neurobiol **17**(1): 22-28.

Zucker, R. S. and L. Lando (1986). "Mechanism of transmitter release: voltage hypothesis and calcium hypothesis." Science **231**(4738): 574-579.

Zucker, R. S. and W. G. Regehr (2002). "Short-term synaptic plasticity." Annu Rev Physiol **64**: 355-405.